Institut für Nutzpflanzenwissenschaften und Ressourcenschutz
Lehrstuhl für Pflanzenzüchtung

Genetic variations in root architecture traits for water and nitrogen use efficiency in wheat and barley

Dissertation

zur Erlangung des Grades

Doktor der Agrarwissenschaften (Dr. agr.)

an der Landwirtschaftlichen Fakultät

der Rheinischen Friedrich-Wilhelms-Universität Bonn

Md. Nurealam Siddiqui

aus

Kurigram, Bangladesh

Bonn, 2022

Printed and/or published with the support of the German Academic Exchange Service (DAAD)

Referent	:	Prof. Dr. Jens Léon
Koreferent	:	Prof. Dr. Frank Hochholdinger
Fachnahes Mitglied	:	Dr. Thomas Gaiser
Vorsitzender	:	Prof. Dr. Florian M. W. Grundler
Tag der mündlichen Prüfung	:	05.10.2022

Angefertigt mit Genehmigung der Landwirtschaftlichen Fakultät der Universität Bonn

This glorious achievement is dedicated to my beloved father *Md Abdul Hamid Bepari*, who passed away in 2013.

Abstract

The soil edaphic resources such as water and nitrogen are essential for crop production because they are required by plants for proper growth and tissue development. The global crop production is vulnerable due to rapid climatic changes and scarcity of natural resources. Insufficient water availability in the soil swiftly translates to water deficiency in plant systems, which in turn affects metabolism and developmental processes, ultimately arresting plant growth and yield stability. Yield reduction caused by drought typically ranges between 30 to 90% in the field. In the majority of agricultural regions, nitrogen (N) availability is the most limiting factor for crop production. However, excess N fertilization affects soil acidification processes, thereby reducing soil fertility. Additionally, rapid pollution of ground and surface water is caused by nitrate leaching, a direct consequence of excess/inadequate N fertilization. This may affect biodiversity and promotes harmful climatic changes as well as reduced air quality. Therefore, developing cultivars with high water and nitrogen use efficiency (WUE and NUE) is crucial for economic cereal production and the protection of ecosystems.

The root is the foremost plant organ responsible for extracting soil resources in water- and nutrient-limited conditions. When plants sense a water shortage, roots continue to grow into deep soil layers to facilitate the uptake of available water and nutrients. To this end, identifying genetic factors and candidate genes affecting root architecture and characterizing their roles in adaptation to water and N deficiency should be addressed. Therefore, this thesis employs genetic and molecular approaches to explore natural variations in root phenotype, anatomy and transcriptomic profiles to study the underlying genetic architecture of candidate genes associated with WUE and NUE.

To decipher the genetic control mechanisms for root phenotypic adaptation to water availability, root system architecture traits of a diverse set of 200 winter wheat genotypes, grown with and without water in the field, were evaluated. Water stress differentially modulated root architecture and plasticity traits. A total of 25 marker-trait associations connected to natural variations in root architecture and plasticity were identified by GWAS. They were distributed on chromosomes 1A, 1B, 2A, 2B, 3A, 3B, 4B, 5A, 5D, 7A and 7B. In total, 396 putative candidate genes associated with root plasticity were detected using linkage disequilibrium analysis. Interestingly, these genes were directly involved in water transport and channel activity, cellular response to water deprivation, scavenging reactive oxygen species, root growth and development as well as hormone-activated signaling pathway-transmembrane transport; biological processes essential to regulate WUE. Transcript expression analysis revealed that the candidate genes were highly expressed in roots at multiple root growth stages and during drought treatments. We found that traits affecting root phenotypic plasticity were highly quantitative, and the associated loci were involved in WUE pathways.

Next, we were curious how root architecture traits contribute to NUE by regulating nitrate transport systems in wheat and barley. To achieve this, we performed a comparative genome-wide scan using wheat and barley datasets characterized under high and low N input. We identified several candidate genes involved in NUE, including *NPF2.12,* a convergently selected low-affinity nitrate transporter gene. Phylogenetic analysis revealed that *NPF2.12* encodes a highly convergent MAJOR FACILITATOR SUPERFAMILY domain-containing protein with nitrate transporter activity. In response to low nitrate availability, we observed that variations in the *NPF2.12* promoter resulted in higher root growth and root-to-shoot nitrate transport by decreasing its transcript expression in both wheat and barley. Further, a loss-of-function *npf2.12* allele transactivated *NIA1*, a gene encoding for a nitrate reductase, that enhanced nitric oxide production under low nitrate conditions and led to competent root growth and nitrate transport comparable to the wild-type. Importantly, multiple field trials showed that the *TaNPF2.12*^{TT} allele significantly enhanced N uptake, N transport in leaves and grains and subsequently NUE under low N supply. Thus, we identified *NPF2.12* as a convergently selected nitrate transporter and an *NPF2.12-NIA1* signaling cascade that can be exploited to improve NUE or rather root growth at low N availability.

In summary, this thesis provides genetic and molecular mechanisms underlying root architectural adaptation to water- and N-deficit conditions. The identified root architecture traits, syntenic loci and transporter genes can be targeted in breeding programs for high-resolution gene trait analyses to develop cultivars with improved WUE and NUE.

Zusammenfassung

Die edaphischen Ressourcen des Bodens wie Wasser und Stickstoff sind für die pflanzliche Erzeugung von entscheidender Bedeutung, da sie von den Pflanzen für ein ordentliches Wachstum und eine gute Gewebeentwicklung benötigt werden. Die weltweite pflanzliche Produktion ist aufgrund der raschen klimatischen Veränderungen und der Verknappung der natürlichen Ressourcen gefährdet. Eine unzureichende Wasserverfügbarkeit im Boden führt schnell zu Wassermangel in den Pflanzensystemen, was wiederum den Stoffwechsel und die Entwicklungsprozesse beeinträchtigt und letztlich das Pflanzenwachstum und die Ertragsstabilität stoppt. Die durch Trockenheit verursachten Ertragseinbußen liegen in der Regel zwischen 30 und 90 % auf dem Feld. In den meisten landwirtschaftlichen Regionen ist die Verfügbarkeit von Stickstoff (N) der wichtigste limitierende Faktor für die Pflanzenproduktion. Eine übermäßige N-Düngung führt jedoch zu einer Versauerung des Bodens aus und verringert so die Bodenfruchtbarkeit. Darüber hinaus wird die Qualität des Grund- und Oberflächenwassers durch Nitratauswaschung sukzessive beeinträchtigt, was die direkte Folge einer übermäßigen/unangemessenen N-Düngung ist. Dies kann die biologische Vielfalt verringern und schädliche klimatische Veränderungen sowie eine Verschlechterung der Luftqualität fördern. Daher ist die Entwicklung von Sorten mit hoher Wasser- und Stickstoffnutzungseffizienz (WUE und NUE) von entscheidender Bedeutung für eine wirtschaftliche Getreideproduktion und den Schutz der Ökosysteme.

Die Wurzel ist das wichtigste Pflanzenorgan, das für die Gewinnung von Bodenressourcen unter wasser- und nährstoffarmen Bedingungen verantwortlich ist. Wenn Pflanzen einen Wassermangel bemerken, wachsen die Wurzeln weiter in tiefere Bodenschichten, um die Aufnahme von verfügbarem Wasser und Nährstoffen zu erleichtern. Zu diesem Zweck sollen genetische Faktoren und Kandidatengene identifiziert werden, die die Wurzelarchitektur beeinflussen, und ihre Rolle bei der Anpassung an Wasser- und Stickstoffmangel untersucht werden. In dieser Arbeit werden daher genetische und molekulare Ansätze zur Erforschung natürlicher Variationen des Wurzelphänotyps, der Anatomie und der transkriptomischen Profile verwendet, um die zugrunde liegende genetische Architektur von Kandidatengenen zu untersuchen, die mit WUE und NUE in Verbindung stehen.

Um die genetischen Kontrollmechanismen für die phänotypische Anpassung der Wurzeln an die Wasserverfügbarkeit zu entschlüsseln, wurden die Merkmale der Wurzelsystemarchitektur einer Reihe von 200 Winterweizengenotypen bewertet, die natürlich im Feld bzw. ohne Bewässerung im Rainout-Shelter angebaut wurden. Wasserstress modulierte die Wurzelarchitektur und die Plastizitätseigenschaften auf unterschiedliche Weise. Durch GWAS wurden insgesamt 25 Marker-Merkmals-Assoziationen identifiziert, die mit natürlichen Variationen in der Wurzelarchitektur und -plastizität verbunden sind. Sie waren auf den

Chromosomen 1A, 1B, 2A, 2B, 3A, 3B, 4B, 5A, 5D, 7A und 7B verteilt. Insgesamt wurden 396 mutmaßliche Kandidatengene, die mit der Wurzelplastizität in Verbindung stehen, durch eine Kopplungsungleichgewichtsanalyse ermittelt. Interessanterweise waren diese Gene direkt am Wassertransport und der Leitungsbahnenaktivität, der zellulären Reaktion auf Wasserentzug, dem Abfangen reaktiver Sauerstoffspezies, dem Wurzelwachstum und der Wurzelentwicklung sowie dem hormonaktivierten Signalweg-Transmembrantransport beteiligt; biologische Prozesse, die für die Regulierung der WUE von wesentlicher Bedeutung sind. Die Analyse der Transkriptionsausprägung zeigte, dass die Kandidatengene in den Wurzeln in verschiedenen Phasen des Wurzelwachstums und während der Behandlung mit Trockenheit stark ausgeprägt waren. Wir stellten fest, dass die Merkmale, die die phänotypische Plastizität der Wurzeln beeinflussen, in hohem Maße quantitativ sind, und dass die zugehörigen Loci in die WUE-Verläufe eingebunden sind.

Als Nächstes wollten wir wissen, wie Merkmale der Wurzelarchitektur zu NUE beitragen, indem sie die Nitrat-Transportsysteme in Weizen und Gerste regulieren. Zu diesem Zweck führten wir einen vergleichenden genomweiten Scan mit Weizen- und Gerstendaten durch, die unter hohem und niedrigem N-Input charakterisiert wurden. Wir identifizierten mehrere Kandidatengene, die an NUE beteiligt sind, darunter *NPF2.12*, ein konvergent ausgewähltes Nitrat-Transporter-Gen mit niedriger Affinität. Eine phylogenetische Analyse ergab, dass *NPF2.12* für ein hochkonvergentes, eine MAJOR FACILITATOR SUPERFAMILY-Domäne enthaltendes Protein mit Nitrat-Transporter-Aktivität kodiert. Als Reaktion auf eine geringe Nitratverfügbarkeit beobachteten wir, dass Variationen des *NPF2.12*-Promotors zu einem höheren Wurzelwachstum und Nitrat-Transport von der Wurzel zum Spross führten, indem die Expression des Transkripts sowohl in Weizen als auch in Gerste verringert wurde. Darüber hinaus wurde das Gen *NIA1* durch ein *NPF2.12*-Allel mit Funktionsverlust transaktiviert. *NIA1* kodiert für eine Nitratreduktase, welche die Stickoxidproduktion unter nitratarmen Bedingungen erhöht und damit zu einem kompetenten Wurzelwachstum und einem mit dem Wildtyp vergleichbaren Nitrattransport führte. Wichtig ist, dass mehrere Feldversuche zeigten, dass das *TaNPF2.12TT*-Allel die N-Aufnahme, den N-Transport in Blättern und Körnern und in der Folge die NUE bei geringer N-Versorgung signifikant verbesserte. Somit haben wir NPF2.12 als einen konvergent selektierten Nitrat-Transporter und eine *NPF2.12-NIA1*-Signalkaskade identifiziert, die zur Verbesserung der NUE bzw. des Wurzelwachstums bei geringer N-Verfügbarkeit genutzt werden kann.

Zusammenfassend lässt sich sagen, dass diese Arbeit genetische und molekulare Mechanismen aufzeigt, die der Anpassung der Wurzelarchitektur an Bedingungen mit Wasser- und Stickstoffmangel zugrunde liegen. Die identifizierten Wurzelarchitekturmerkmale, genetischen Loci und Transportergene können in Züchtungsprogrammen für hochauflösende

Genmerkmalanalysen gezielt eingesetzt werden, um Sorten mit hoher WUE und NUE zu entwickeln.

List of Abbreviations

ANOVA	Analysis of variance
ALMT	Aluminum-activated malate transporters
CLC	Chloride channel
CRISPR	Clustered regularly interspaced palindromic repeats
CV	Coefficient of variation
DATS	dual-affinity transport system
DEG	Differentially expressed gene
DRO1	DEEPER ROOTING 1
EMS	Ethyl methanesulfonate
FAO	Food Agriculture Organization
FDR	False discovery rate
GO	Gene ontology
GS2	Second isoform
GWAS	Genome-wide association study
h^2	Broad-sense heritability
HATS	High-affinity transport system
HN	High nitrogen
LATS	Low-affinity transport system
LD	Linkage disequilibrium
LN	Low nitrogen
MAF	Minor allele frequencies
MAS	Marker-assisted selection
MFS	Major facilitator superfamily
MLM	Mixed linear model
MTA	Marker-trait association
mSDP	Main shoot nodal root cross section occupied by stele
N	Nitrogen
Nitrate	NO_3^-
NIA1	Nitrate reductase 1
NGS	Next-generation sequencing
NO	Nitric oxide
NPF	Nitrate transporter 1/peptide transporter
NR	Nitrate reductase
NRC	Number of root crossings
NRF	Number of root forks

NRT	Number of root tips
NRT2	Nitrate transporter 2
NUE	Nitrogen use efficiency
NUpE	Nitrogen uptake efficiency
NUtE	Nitrogen utilization efficiency
P	Stress plasticity
PC	Principal component
PCA	principal component analysis
PTR	Peptide transfer
Q-Q	Quantile-quantile
QRO1	QUICK ROOTING 1
QTL	Quantitative trait loci
RA	Root angle
RAD	Root average diameter
RD	Rooting depth
RSA	Root system architecture
RCBD	Randomized complete block design
RIL	Recombinant inbred line
RSA	Root surface area
RV	Root volume
SD	Standard deviation
SLC/SLAH	slow anion associated channel homolog
SNP	Single nucleotide polymorphisms
STI	Stress tolerance index
TRL	Total root length
tSDP	Tiller nodal root cross section occupied by stele
WT	Wild-type
WUE	Water use efficiency

Table of Contents

List of Figures

List of Tables

List of Supplementary Data: Chapter 3

List of Supplementary Data: Chapter 4

General Introduction

1.1 Cereals are important crops worldwide

For millennia, cereal grains have been a vital source of nourishment for humankind, covering approximately 95% of the global food demand (Awika 2011; Asgari et al. 2017). The major cereal grains are vital nutrient sources and provide more than 50% of the average person's daily energy intake (Chandler and Brendel 2002; FAO 2014). In addition, maize, barley and sorghum serve as the prime sources of livestock feed, while rice and barley are important resources for the brewing industry (Chopra and Prakash 2002). Cereals are diversely used to produce various types of oils, syrup, malt, processed foods, gluten, alcoholic beverages and more importantly renewable energy (Pomeranz and Munck 1981).

The UN expects the world population to gain about one third of its current size and reach nine billion by 2050. To meet the food demand of our growing population, an estimated 70% higher food production is necessary (FAO 2017). For that, global cereal cultivation needs to rise by about 40% or approximately 900 million tons (Perniola et al. 2015).

1.1.1 Wheat

With an estimated annual yield of 694 metric tons, wheat (*Triticum aestivum L.)* is the second most popular and economically important cereal crop. It serves as staple food for over 30% of the world population and is a major source of energy and protein in the human diet (Shewry and Hey 2015; Lositska 2019). However, water stress due to the occurrence of unpredictable climate change is endangering the global wheat production (Shah et al. 2017). This is critical considering that over 840 million tonnes of wheat would be needed to feed the world population in future years (McMahon 2017).

Wheat farming and domestication began 10,000 years ago. Diploid einkorn (2n=2x=14, AA) and tetraploid emmer (2n=4x=28, AABB) were the first cultivated varieties of wheat (Heun et al. 1997; Dubcovsky and Dvorak 2007). Over time, common or bread wheat (2n=6x=42, AABBDD), classified as a member of the genus *Triticum* in the family of Poaceae (grasses), prevailed as the predominant species (Tadesse et al. 2016). After decades of intensive research, it is now considered a cross between *T. turgidum* (2n=4x=28, AABB) and *Aegilops tauchii* var. (2n=2x=14, DD) (Riley et al. 1958; Dvorak et al. 1998) (Figure 1.1). As stated by Shewry (2009) bread wheat cultivation then spread to the near east by about 9000 years ago. Nowadays, it is grown and cultivated in a wide range of agro-ecological zones spanning the southern UK and northeastern France, which offer ideal growing conditions, and the dry lands of Australia and Mexico (Cracknell 2015). During winter in the northern hemisphere, wheat plants undergo vernalization; after being sown in autumn they lay dormant under the snow,

protected from adverse weather conditions, and continue growing at warmer spring temperatures to complete their life cycle (Cracknell 2015; Tadesse et al. 2016).

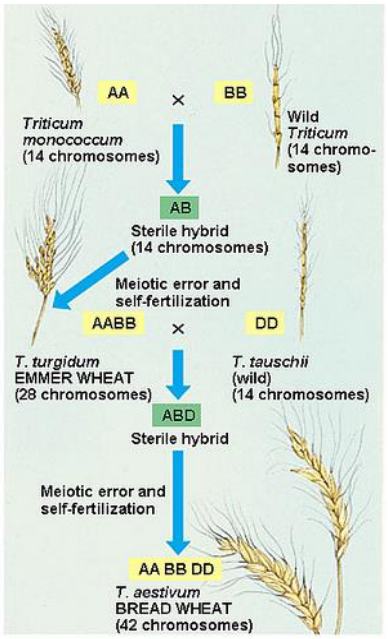

Figure 1.1. Hybridisations schemes involved in the evolution of bread wheat, *Triticum aestivum*. (https://sites.google.com/site/selectivebreedingcrops).

1.1.2 Barley

Barley (*Hordeum vulgare*) is another domesticated cereal crop, thought to be cultivated about 17,000 years ago in ancient Mesopotamia and Egypt (Morrell et al. 2007; Zhou 2009). Like the small-grain cereals wheat and rye, it is a self-pollinating, annual, monocotyledonous, flowering plant that belongs to the family of Poaceae. However, while these two are part of the Triticeae tribe, barley is evolutionary distinct (Friedt et al. 2010). A phylogenetic analysis revealed that wheat and barley shared a common ancestor approximately 3 to 4 million years BC. Further back in time, between 40 and 54 million years BC, was the common ancestor of wheat, rice and barley (Figure 1.2).

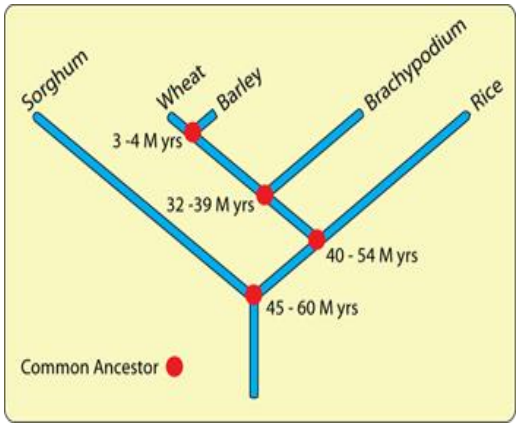

Figure 1.2. Phylogenetic tree explaining the evolutionary relationship between some of the major cereal grasses. Barley is a small grass species that is often utilized in genetic studies due to its small and relatively simple genome (www.cerealsdb.uk.net).

In terms of area of cultivation as well as total annual production, barley ranks fourth after maize, wheat and rice. It can be grown either as a spring or winter crop, with winter annuals being planted in autumn and requiring a period of cold weather before they will flower. Germination sets in at a minimum temperature of 1 to 2°C but the optimal temperature ranges from 12 to 25°C (Tiwari 1998). Barley is widely cultivated in temperate climates but due to its versatility and adaptability it can be grown in a variety of agro-ecological conditions (Zhou 2009). Therefore, barley has been an important food crop in many arid and semi-arid regions where other cereal grains like wheat might struggle (Tricase et al. 2018).

In the past centuries, barley was cultivated mainly for human consumption (Cowan and Mollgaard 1988; Baik et al. 2011), but is now grown primarily for animal feed and fodder. As reported by FAO (2018), only about 6% of the total world production are eaten by people, mainly in some developing countries where it remains a staple food. 70% are intended to feed livestock (Langridge 2018; Tricase et al. 2018). Malted barley is also of significant industrial value for breweries and distilleries (Schwar and Li 2011; Arendt and Zannini 2013). They use approximately 21% of the total world production. More recently, barley garnered worldwide interest for the production of biofuel, an important source of renewable energy (Tricase et al. 2018).

Interestingly, barley has emerged as a very well-known model cereal crop in some research disciplines including plant breeding, genetics, pathology, physiology and biotechnology (Saisho and Takeda 2011; Holubová et al. 2018; Harwood 2019). Barley possesses several beneficial attributes for experimental studies. These include its diploid genome, low chromosome number (2n=14), ease of cultivation, adaptability in a wide range of climatic conditions and extensive genetic resources (Mochida 2010; Harwood 2016). Compared to other corps, barley naturally exhibits a wide range of diversity and adaptive capacity in stressful

environments (Dresselhaus and Hückelhoven 2018; Harwood 2019). As a result, this crop has been extensively used to investigate abiotic stress responses of plants (Harwood 2016), aiding in the identification and characterization of stress responsive genes (Gürel et al. 2016; Harwood 2019).

1.2 Effects of drought on cereal growth and survivability

Drought events are globally on the rise and a major hindrance to crop production (Iqbal et al. 2020; Siddiqui et al. 2021a). The effects of limited water supply on plants have been reported at the morphological, biochemical, molecular and physiological levels and are obvious at all phenological growth stages (Cattivelli et al. 2008; Kadam et al. 2012). For instance, photosynthesis and biomass production are some of the major metabolic processes that are directly affected by drought (Kulkarni et al. 2017). Drought stress fundamentally changes plant water relations and eventually hampers water use efficiency (WUE), relative water content and leaf water content, promoting the production of active oxygen species, which are destructive to useful biological macromolecules (Farooq et al. 2009; Carmo et al. 2012). This restricts the growth of crop plants by disturbing the affinity with water soluble nutrients, consequently decreasing photosynthetic activity and eventually resulting in substantial yield loss (Iqbal et al. 2020). The induction of various plant morphological, physiological and molecular attributes is elemental to support survival under water-deficit stress conditions (Figure 1.3).

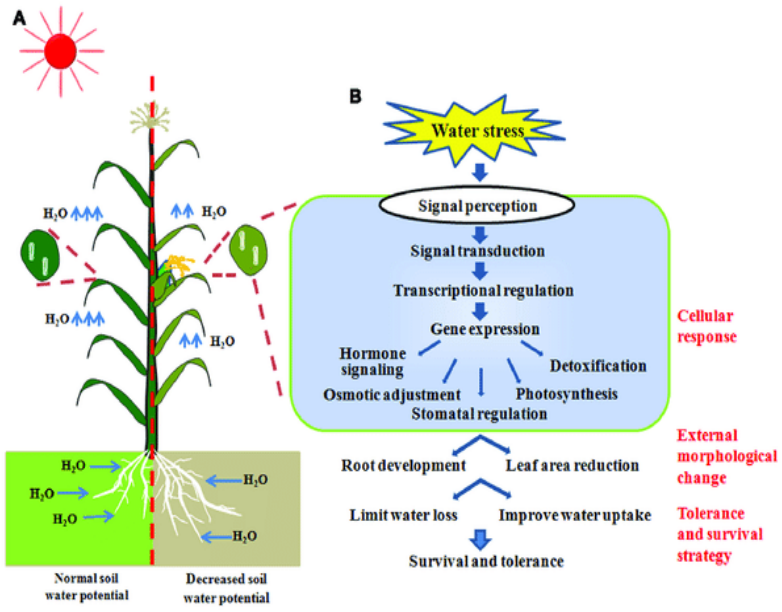

Figure 1.3: Effect of water-deficit stress on crop plants. (A) The physiological and morphological adaptations of plants grown under water-deficit conditions. (B) Cellular response to drought stress, including signaling transduction and physiological alterations to optimize survival (adapted from Wang and Qin 2017).

Tolerance, escape and avoidance are the three major categories of plant stress response mechanisms during limited water availability (Basu et al. 2016). Drought tolerance covers mechanisms that improve the crop's ability to tolerate low rainfall patterns and help it carry on at low tissue water potential. In this context, plants defy drought stress by osmotic adjustments to preserve turgor, increase elasticity or diminish cell size (Morgan 1984; Basu et al. 2016). Drought escape allows plants to complete their normal life cycle before they are affected by serious stress. This involves strategies like early maturity and flowering (Shavrukov et al. 2017). Finally, drought avoidance is the ability of plants to continue growing within the restricted downfall patterns, as to maintain a better water standing. Plants mitigate water loss from transpiration by reducing their leaf size and surface area, while water uptake may be increased by improved liquid conductance and higher root density and length (Nada and Abogadallah 2018). All these strategies, which can optimize plant growth and survivability under water limited conditions, are defined as drought resistance (Wang and Qin 2017). The biochemical and physiological processes that contribute to acquired drought tolerance and survival actions, including hormone biosynthesis and transport, adjusted osmotic status, photosynthesis, stomatal regulation and detoxification of plant cells, are modulated by the expression of drought-responsive genes.

1.3 Nitrogen in agriculture

Plants are dependent on inorganic nitrogen (N) and about 85–90 million metric tonnes of N fertilizers are applied to the soil per year globally (Good et al. 2004). The capacity of a plant to acquire N from the soil depends on three important factors: soil type, environment and species. Generally, soil N availability can vary largely in both space and time owing to factors like precipitation, wind, temperature, soil type and pH. Therefore, the adopted form in which N is taken up relies on the plant’s adaptive capability to soil conditions. In general, plants adjusted to low pH and reduced soils, mostly found in mature forests or the arctic tundra, favour ammonium or amino acids as N sources, while plants grown in basic and more aerobic soils prefer nitrate (Maathuis 2009).

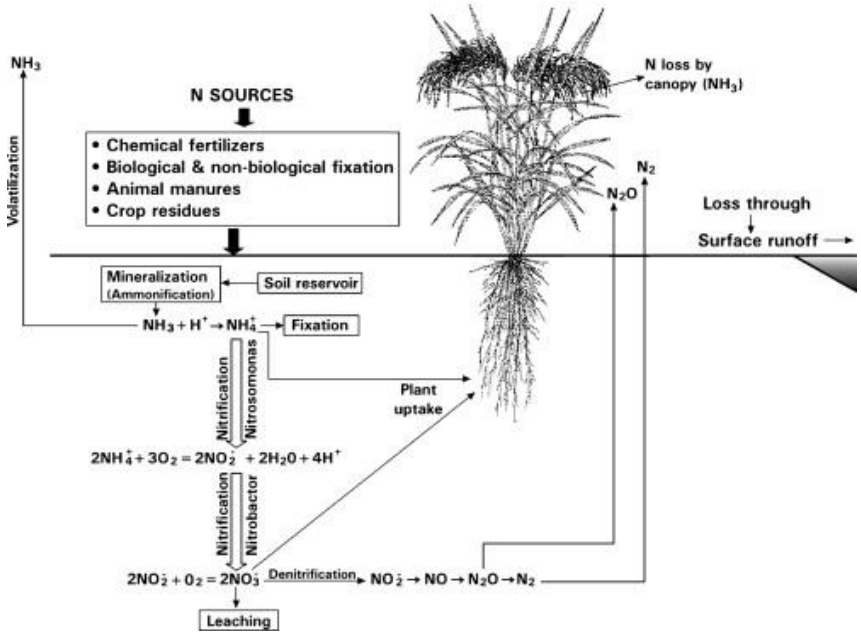

Figure 1.4: Simplified illustration of the nitrogen cycle in soil-plant systems (Fageria and Baligar 2005).

The impact of N on crop plants is substantial. Therefore, expanding our knowledge on crop growth responses to this essential element is crucial. To illustrate this point, appropriate doses of N fertilizer accelerate photosynthetic efficiency in both rice pants (Hussain et al. 2016) and oilseed rape (Hu et al. 2007), promote tolerance to biotic stress (Guo et al. 2009), enhance dry matter accumulation, nutrient uptake and use efficiency (Barłóg and Grzebisz 2004) and subsequently improve grain yield (Juan et al. 2009).

Although N serves as a primary driving force for plant development, excessive N input is known to cause yield losses by limiting the N use efficiency (NUE) (Wang et al. 2004; Vitousek et al. 2009). Additionally, N is regarded as one of the most expensive nutrients. In 2016, a worldwide total of 140 million tons of N were manufactured for around 60 billion US$ (FAO 2018). Despite this enormous cost and input, only 33-40% of the applied N can be transformed into grain yield. The remaining N is lost through nitrate leaching into the environment, thereby causing serious environmental threats like acidification of the soil and water bodies, surface and groundwater contamination, increased greenhouse gases due to excess N_2O emissions, loss of biodiversity and increased airborne particulate substances (Figure 1.4; Hirel et al. 2011; Dhital and Raun 2016). Over-fertilization has become a major constraint for sustainable intensive agriculture in many developed parts of the world, including China (Meng et al. 2013). In contrast, low N availability is one of the limiting factors for crop yield in many developing countries of the world, including sub-Saharan Africa and Latin America (Gibbon et al. 2007). Therefore, reducing the extreme use of N fertilizers without hampering productivity is critical. The adaptive responses of N-efficient cultivars to low N supply are of special interest for this.

1.4 Importance of improving water and nitrogen use efficiency in cereals

It has been recorded that agriculture consumes 80–90% of all freshwater utilized for human purposes; the majority of that is used in crop production (Morison et al. 2008; D'Odorico et al. 2020). Globally, this amounts to 70% of the freshwater withdrawn from water resources and contributes greatly to its scarcity (FAO 2002; WRI 2005). Still, water is essential for plant survivability, growth, development and reproduction and ultimately yield and nutritional quality. Its availability greatly affects major metabolic processes and pathways, such as photosynthesis, respiration as well as absorption, translocation and utilization of minerals (McElrone et al. 2013). Transpiration and evaporation processes are regulated through the plant's stomata and pull water from the soil, through the roots, into the whole aboveground plant (Morison et al. 2008). That water carries with it mineral and nutrients from the soil that are critical for plant growth and productivity. Within the plant, water functions as key molecules for all metabolic activities and mediates the transport of metabolites from source to sink. As a result, water shortages are one of the leading constraints for plant growth and productivity worldwide. Hence, we demand to develop appropriate cropping systems to cultivate crops best suited to the environmental conditions, with minimal use of water, either in irrigated or rainfed production. In particular, we need to design crops that require a minimum amount of water to produce maximum yield. This can be achieved through an integrated understanding of the physiological, biochemical and molecular mechanisms that determine growth, water loss and plant response to reduced water availability.

N is the most limiting nutrient for crop production and its efficient application is critical for the environmental and economic sustainability of cropping systems. It plays a decisive role by regulating multiple biochemical and physiological mechanisms in plants, as it is an indispensable constituent of proteins, nucleic acids, chlorophyll and growth hormones (de Bang et al. 2021). Moreover, the dynamic nature of N and its tendency for loss from soil-plant systems creates threatening environmental issues and an urgent need for its competent management. Crop response to applied N, its uptake and use efficiency are critical factors determining crop N requirements for ultimate economic yield. Recovery of N in crop plants is generally lower than 50%. Low recovery of N is not only associated with higher cost of production, but also environmental pollution. Hence, improving NUE is imperative to increase crop yield, minimize production costs and balance environmental stability as well as quality (Fageria and Baligar 2005). To improve NUE in crop plants, integrated N management practices that take improved fertilizer along with soil and crop management practices into consideration are necessary.

1.5 Root system architecture in cereal crops

Roots are the crucial plant organ for survival and productivity under adverse environmental conditions. They perform a wide range of functions like providing anchorage, supplying the upper plant parts with nutrients from the soil, and developing symbiotic interactions with microorganism in the rhizosphere. The diverse association of a root with its soil environment underlies on its shape and configuration, from the cellular to whole-plant system (Khan et al. 2016).

Root system architecture (RSA) differs from species to species and depends on the availability of soil water, root growth, physiology and architectural components (Corre-Hellou et al. 2007). There are mainly two categories of cereal roots, the primary roots also termed seminal roots, emerging from the scutellar and epiblast nodes of the germinating caryopsis embryo (Lucas et al. 2000; Manske and Vlek 2002; Smith and Smet 2012), and the secondary roots, which are coined adventitious, nodal or crown roots and emerge from the coleoptile nodes at the base of the apical culm and tiller. The number of primary roots in cereals usually ranges from 5 to 7, sometimes extends up to 10. For instance, in wheat, seminal root formation is regulated genetically and numbers range from 3 to 6, which constitutes about 1-14% of the whole root system (Akman et al. 2011). The number of adventitious roots is commonly correlated with tiller number (Reynolds et al. 2001). Usually, primary or seminal roots penetrate the deeper soil layer more promptly than secondary or nodal roots. Hence, they are recognized as the more important avenue for utilizing deep soil moisture, despite both major root types functioning in a complementary pattern (Tang et al. 2011). In addition to primary and secondary roots, another type of roots called lateral roots (or branch roots) emerges on the primary and adventitious roots when wheat roots develop until a certain stage (Hochholdinger and Tuberosa et al. 2009). Consequently, first and second order lateral roots emerge on the primary and adventitious roots at a particular interval. In summary, the whole root system of cereals consists of primary roots, adventitious roots and several orders of lateral roots (Tang et al. 2011). Additionally, shoot-born roots emerge from the hypocotyl in response to stress (Koevoets et al. 2016; Wasaya et al. 2018). RSA traits like root growth angle, seminal root number and length, which adapt in response to water deficits, are determined at the early growth stage in the soil (Figure 1.5; Zhu et al. 2019).

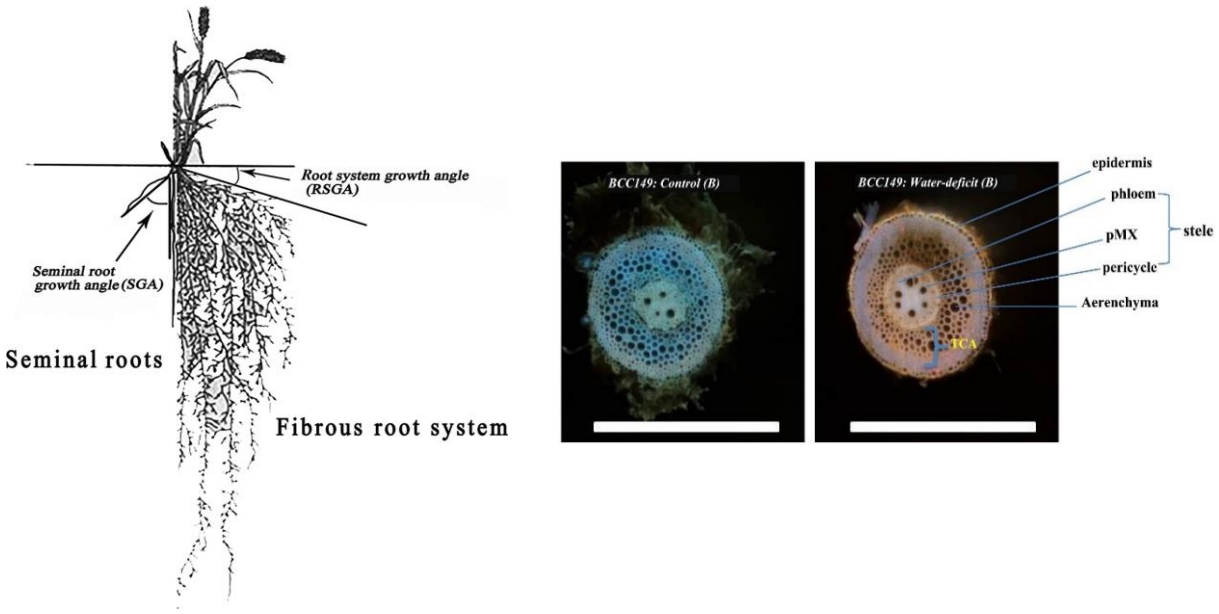

Figure 1.5: Cereal root system architecture showing root growth angle in the seminal and fibrous roots (left side; adapted from Zhu et al. 2019) and root anatomical structures under control and water-deficit stress (right side; adapted from Oyiga et al. 2020).

The cereal root system architecture (RSA) consists of multiple embryonic (primary and seminal) and postembryonic (lateral, crown and brace) roots (Lehmensiek et al. 2009). This parts of RSA have own significance such as primary and seminal roots which are produced at the basal limit of embryo they help for healthy growth and also to search for nutrient and water in the soil (Khan et al. 2016). In wheat also RSA like root growth angle, seminal root number, and length which are help for adaptation of plant during water deficit, and they determined at the early growth stage in soil (Figure 1.5; Zhu et al. 2019). Other RSA parts also formed aboveground and underground of shoot node known as crown and brace roots (nodal roots) which are used for loading resistance and also have a role for water and nutrient uptake (Ahmed et al. 2018). Lateral roots also emerged in all parts of roots within the soil and it has a critical role in water and nutrient uptake (Rogers and Benfey 2015).

1.6 Root architecture traits confer water stress tolerance

Roots evolved to be responsive and intensely accommodative to their native surroundings, so their morphology, growth, and physiology are closely associated with plant genotype and growth medium properties. For example, the elongation rate and number of lateral roots may decrease due to high soil water content or soil density (Bengough et al. 2011). In contrast, water-deficit environments prompt plants to increase their root surface area by growing lateral roots and root hairs directionally to acquire soil moisture (Dietrich 2018; Siddiqui et al. 2021b). As such, the root system is crucial to improve plant adaptation to various environmental stress conditions like drought, salinity, water logging, and nutrient deficiencies (Chen et al. 2020).

The wheat root system displays drought adaptations, such as lateral roots, which emerge from primary and nodal roots and are used to absorb water and nutrients (Zarebanadkouki et al. 2013). Each root trait has specific functions that contribute to the adaptation to drought stress (Table 1-1; Wasaya et al. 2018). For example, when the primary roots have a narrow vertical growth angle, they can reach deeper soil layers to access receding ground water, which consequently increases yield (Trachsel et al. 2013; Nguyen and Stangoulis 2019). Thus, deep root systems are beneficial for the adaptation of crops to water stress conditions (Figure 1.6; Wasson et al. 2012). In this context, deep rooting improves root vigor (Comas et al. 2013). The required rapid root growth is accomplished by a high number of cell divisions and extensions that occur within the root tip (Rahni and Birnbaum 2019). There are other factors that affect root vigor, such as the amount of water at the root tip (Colombi et al. 2017), photo assimilation (Hauer-Jákli and Tränkner 2019) or shoot growth, tiller number and branching (Ito et al. 2018). The reduction of the tiller number in wheat also causes the root to become deeper and longer (Slack et al. 2018). Root density contributes to plant adaptation during drought stress by easily penetrating the compact soil layer for better absorption of water (Friedli et al. 2019). The nodal root and its lateral roots also spread in the deep soil to maximize water uptake and nutrient acquisition (Ehdaie et al. 2012). This is amplified by a high number of root hairs, which helps increase the contact surface area between the plant and the moist soil (Choi and Cho 2019). Besides that, the plasticity of the cortical, stele and total cross-sectional areas of the roots affect a plant's ability to grow in harsh environmental conditions (Kadam et al. 2017; Oyiga et al. 2020). All in all, root anatomical phenes related to deep rooting, root density and a smaller central metaxylem may enhance water uptake-efficiency and improve tolerance to water stress (Kulkarni et al. 2017). It is evident that root anatomical traits are highly determined by environmental factors and a combination of the genotype and environment interactions (Dorlodot et al. 2007). Therefore, it is important to examine them in the soil and evaluate their relation with the genetic variations that influence crop yield during drought stress (Fleury et al. 2010). This warrants the re-thinking of root trait-based breeding and genetic dissection of root anatomical phenes for drought-adaptive mechanisms.

Table 1-1: List of root system architectural traits which facilitates plant adaptation to water-deficit stress (Wasaya et al. 2018).

Traits	**Functions**	**References**
Fine roots	Water absorption and nutrients uptake from the soil.	(Baesso et al. 2018)
Coarse roots	Attach the plant to the soil, form RSA, control the depth of the root system, enhance the ability of the plant to grow on the surface of the soil	(Marden et al. 2018; Montagnoli et al. 2020)
Nodal roots	Anchor the plant to the soil and resource uptake	(Shorinola et al. 2019)
Root diameter	Controls root length, absorption of water and surface area during water deficit conditions	(Hazman and Brown 2018)
Root hairs	Manage the root attachment to the soil particle for the uptake of water and nutrients	(Zhang et al. 2020)
Root angle	Assists deep root growth during drought and affects which roots contain or absorb water and nutrients	(Wasaya et al. 2018)
Root tissue density	Affects the root length during drought and increases the surface area for improved plant growth	(Comas et al. 2013)
Root length density	Involved in the efficient extraction of subsoil water	(Fan et al. 2017)
Number of root forks and crossing	Play crucial roles for better adaptation to water-deficit conditions by increasing water absorption rate	(Ibrahim et al. 2012)
Xylem vessel	Reduced xylem vessel increase axial resistance to conserve more water	(Richards and Passioura 1989)
Root cortical aerenchyma, cell size and file number	Assist to minimize nutrient and carbon costs for soil exploration	(Lynch 2013)

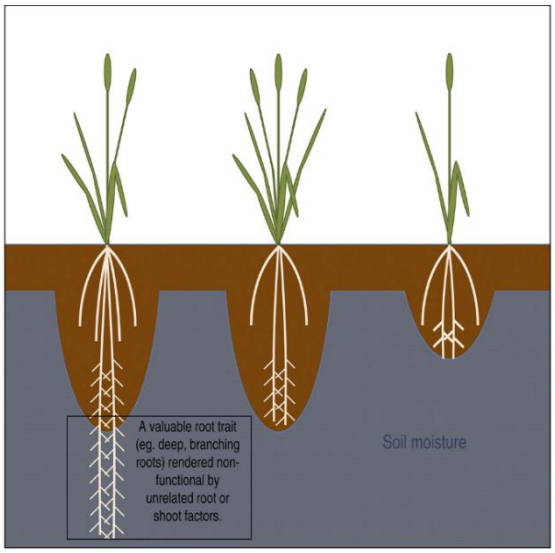

Figure 1.6: Cartoon illustrating the role of different root lengths penetrate different soil layers. The plant on the left carries the better root traits (here assumed to be deep, highly branched roots), but an unrelated root or shoot restraint negates the advantage. Instead, the non-functional roots are an energetic burden for the plant. Hence, in an indirect assessment, the plant on the left may not compete as well as the plant in the middle that has a completely functional root system; even though it does not have the superior trait (deep, highly branched roots). On the basis of superior and functional root traits, the middle plant will also outperform the right plant with a shallow root system (adapted from Wasson et al. 2012).

1.7 Root architecture contributes to nitrogen-use efficiency

Plant growth and yield heavily depends on N availability and multiple physiological processes (Figure 1.7). Based on these aspects, it is effective to apply the productivity index and the component traits of this index (Barraclough et al. 2010). NUE may be scrutinized as the top category trait and in wheat is the yield of grain produced per unit of N supply to the crop; it is defined as kg yield per kg of N supply; it is also the combination of the two second level traits, N uptake efficiency (NUpE) and N utilization efficiency (NUtE). Analytically, NUE is the output of NUpE x NUtE (Figure 1.7).

Increasing NUE and minimizing N use is challenging but crucial to protect the environment and boost a viable and productive agriculture. Roots are the principal organ of the plants, responsible for the acquisition of soil-based resources and their competence at soil exploring is regarded as the crucial benchmark for NUE (Li et al. 2016). Addressing the demand for yield increases in major cereal crops like wheat, without compromising the environment and ecosystem health through excessive N fertilization, necessitates breeding modern cultivars with improved root system traits.

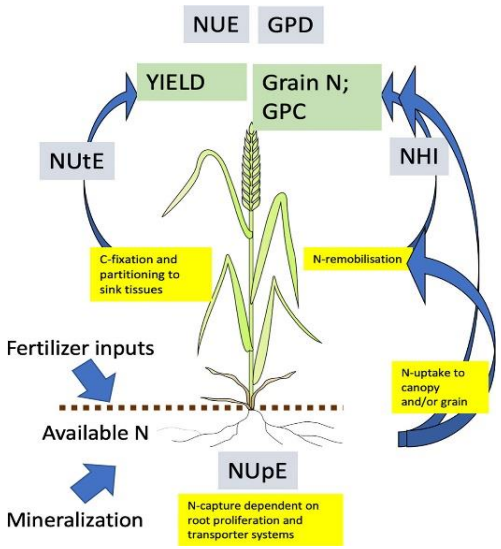

Figure 1.7: Processes involving to and measuring nitrogen use efficiency (NUE) in wheat. NUE-related traits express in grey boxes; primary traits indicate green boxes; physiological system express in yellow boxes. Arrows express movement of N (Adapted from Hawkesford 2011).

Several studies documented that root architectural characteristics are intimately associated with N uptake. RSA comprises traits like rooting depth, root diameter, surface area, length, density, dry weight etc. that play a paramount role during N acquisition under both field and controlled conditions (Liu et al. 2012; Li et al. 2016). For instance, the root growth angle determines root distribution and depth in the soil domain, thereby affecting performance under N deficit conditions (Trachsel et al. 2013; York and Lynch 2015; Dathe et al. 2016). Narrow vertical root growth angles, facilitate steep and deeper rooting, which boosts absorption of mobile nutrients, such as N, from deep soil strata (Lynch 2013; Trachsel et al. 2013; Zhan and Lynch 2015). In some crop species, greater root length and density are viable root architectural characteristics that can enhance N acquisition by increasing the root surface area without hampering carbon allocation to the roots (Kage 1997). Anatomical traits corresponding to reduced metabolic cost per segment, such as larger aerenchyma and lesser cortical cell file numbers, could facilitate deeper rooting (Lynch 2013, 2018). So, designing an adaptive root system architecture that integrates various beneficial traits (length, density, dry weight, branching, thickness and volume) might be an effective solution to the problem of inefficient nutrient uptake, especially of N (Figure 1.8).

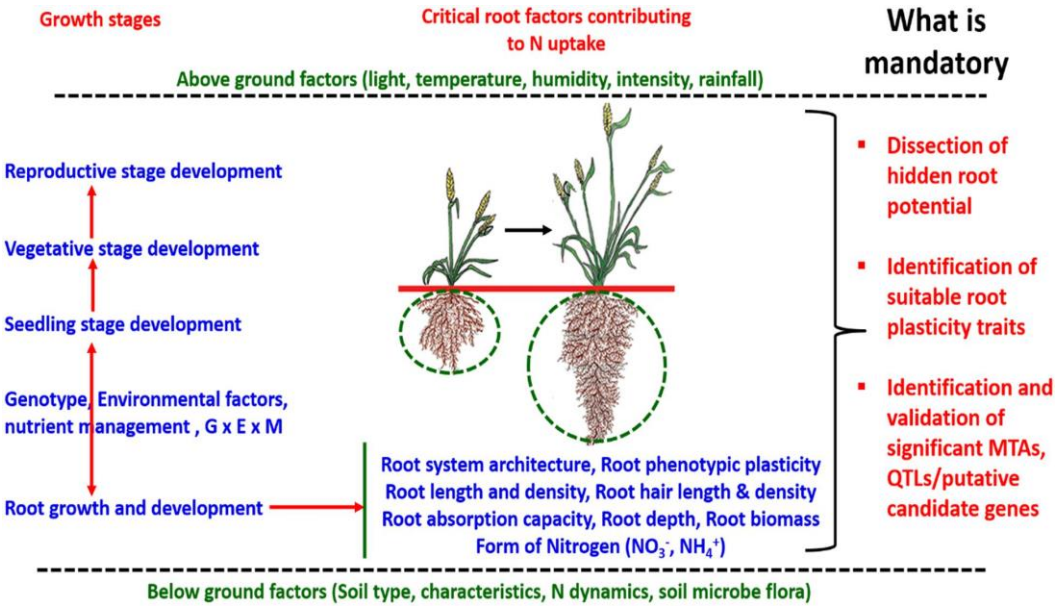

Figure 1.8: Schematic illustration of the role of above and below ground factors as well as genotype-environment-nutrient interactions in establishing root architecture at multiple growth and development stages for better N uptake in cereal crops (adapted from Sandhu et al. 2021).

Adaptation of root anatomy in response to stress has been poorly examined when compared with other root architectural and morphological traits (Yang et al. 2019). Recently several studies of root trait-based phenotyping and breeding particularly addressed methods and candidate gene discovery concerning root morphology and architecture (Cobb et al. 2013; Fiorani and Schurr 2013; Meister et al. 2014; Paez-Garcia et al. 2015). Given the significance of root system traits for improving grain yield, uptake and utilization of N under drought stress, however, it has been also established that N is directly involved in signaling mechanisms that collectively control the growth and shape of root architecture (Garnett et al. 2009b; Mohd-Radzman et al. 2013). Overall, N-uptake capability of the plants depends on root proliferation and transporter systems (Figure1.7; Hawkesford 2011; O'Brien et al. 2016).

1.8 Challenges and opportunities of field-based root phenotyping

Due to complexity of root phenotyping, genome-wide mapping for root traits has not been hugely explored so far. The great pitfall in deciphering genomic regions for root architectural characteristics is the difficulty in analyzing root characteristics of plants grown in soil, particularly when exploring a large number of mapping populations. To date, most of the root phenotyping has been performed hydroponic systems or sand culture to identify quantitative trait loci (QTL). This may create bottlenecks for the measurements of root growth characteristics since the interface of container and growth medium is a highly artificial environment (Ye et al. 2018). Therefore, high throughput root phenotyping under natural conditions or directly in the field would be desirable. An underground root assessment facility

or simultaneous root-shoot phenotyping would be effective ways to observe beneficial traits and speed up genetic gain underlying root improvement programs (Tracy et al. 2020).

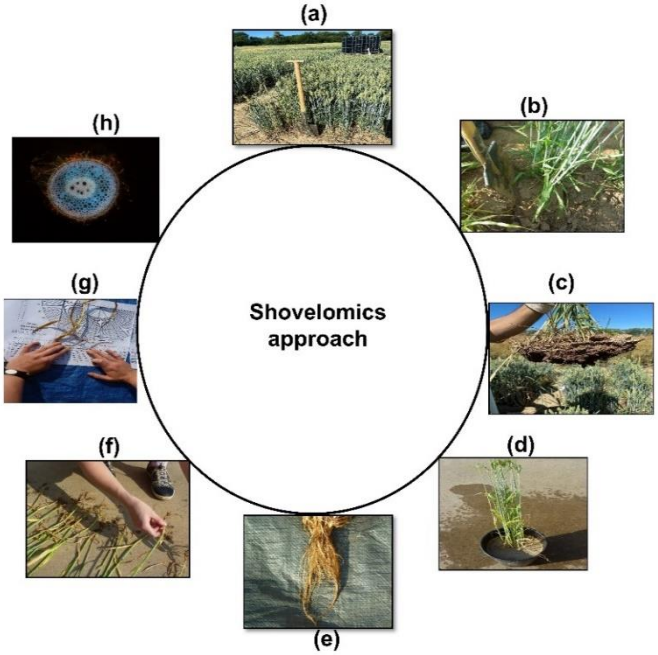

Figure 1.9. Flow diagram of "Shovelomics" protocol in phenotyping root system architectural traits of cereal crops. (a) working station and adult wheat plant in the field (b) roots are excavated by a shovel 20 cm away from the plant base and at a depth of ~25 cm (c) the lumps of excavated soil containing root systems are shaken briefly to remove most of the soil (d) remaining soil and debris are removed by rinsing with clean water (e) the clean root sample after soaking, washing and rinsing (f) manual scoring of root length, number and branching (g) placing clean roots on scoring board to measure root growth angle and (h) phenotyping of nodal root anatomical structures using laser ablation tomography.

Nowadays, routine phenotyping of crop roots to identify genotypes with desirable traits associated with yield, quality and disease resistance is either invasive, minimally invasive or non-invasive (Tracy et al. 2020; Wasson et al. 2020). Invasive or destructive methods entail coring or shovelling to extract the entire root system and high throughput digital image analysis platforms (Trachsel et al. 2011; Das et al. 2015; Wasson et al. 2020). The "shovelomics" approach introduced by Trachsel et al. (2011) is a field-based excavation process followed by manual phenotyping of basic root characteristics (Figure 1.9). A detailed description of "shovelomics" is provided in Figure 1.9. As quantitative genetic and genomic studies need precise, rapid and robust phenotyping tools, "shovelomics" is popular as a relatively high throughput technique for field-grown plants (Trachsel et al. 2011). Recently, "shovelomics" has been adopted for mapping large sets of cereal germplasms in field-based trials with maize (Schneider et al. 2020) and barley (Oyiga et al. 2020). Minirhizotrons and transparent imaging windows inserted into the soil are minimally invasive, non-destructive options to monitor root

growth and turnover, thus, allowing repeated measurements. Unlike coring tools, Minirhizotrons have great limitations because the artificial plane between soil and tube can affect root growth negatively (Rytter and Rytter 2012). Finally, the non-invasive or indirect root phenotyping method allows simultaneous measurements of root system architecture, structures and functions without damaging the roots within the soil environment and rhizosphere (Wasson et al. 2020). In order to accelerate root breeding potential, “shovelomics” as well as non-invasive whole-plant phenotyping and automated robotics for root phenotyping and analysis need to be introduced for mapping large sets of germplasms.

1.9 Genetic factors involved in water and nitrogen use efficiency

The traits related to WUE and NUE in cereal crops are polygenic in nature. Therefore, it is complicated to unravel their physiological and molecular mechanisms (Yang et al. 2017). Recently, a number of cutting-edge genetic and genomic approaches such as QTL mapping, genome-wide association study (GWAS), marker assisted breeding and introgression from the wild gene pool are being exploited to dissect the complexity of quantitative traits (Sun et al. 2012; Mwadzingeni et al. 2016 and 2017). Advancements in QTL and association mapping methods in cereals were an important first step for fine mapping and discovery of QTL allele’s improving WUE and NUE (Gupta et al. 2017).

The detection of traits related to nutrient and WUE and the progress of next-generation sequencing are useful to establish a genomic footing for cereal crops, especially for complex genomes like wheat (Guo et al. 2011). With the current advancements in high-throughput phenotyping and genotyping methods, approaches like genomic selection that enables the analysis of the architecture of complex traits improved. They may provide valuable prospects for accurate genomic selection, characterization, molecular marker investigation, QTL mapping and candidate gene profiling (Mwadzingeni et al. 2017). Several state-of-the-art techniques to increase WUE and NUE have been established, such as exploring root architecture (Foulkes et al. 2009). Therefore, detection and validation of the allelic variants of genes that are interlinked with various root system phenes in wheat and barley may serve as valuable resources for the future genetic gain in cereal crops.

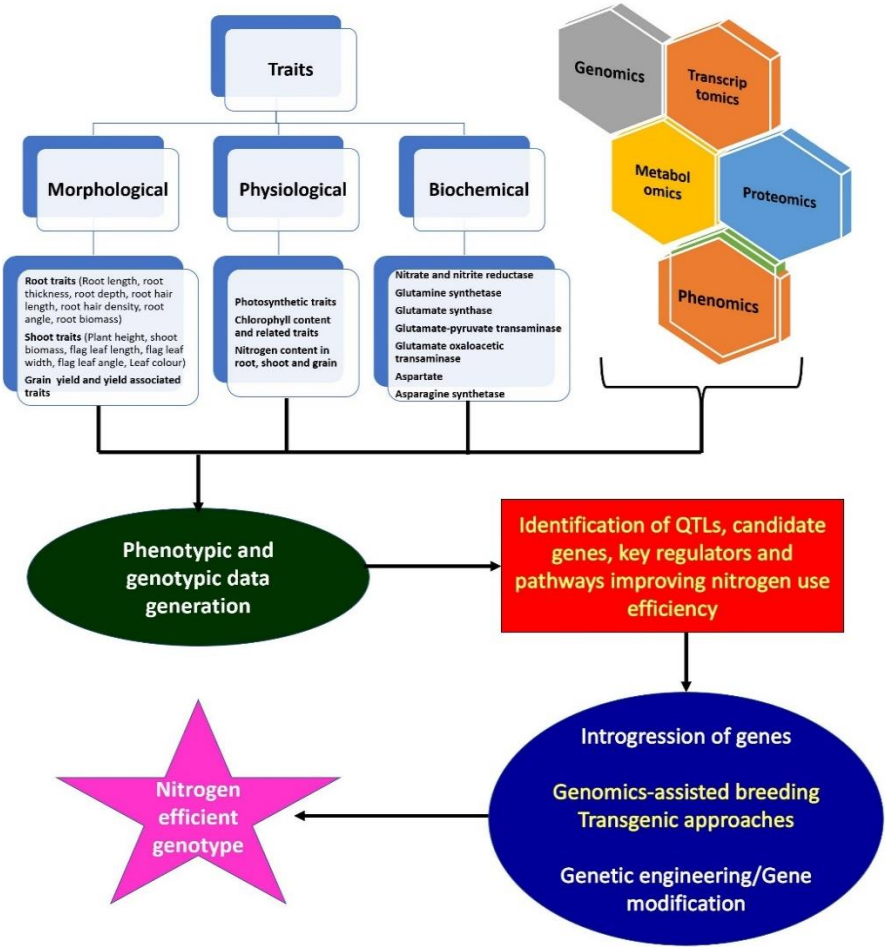

Figure 1.10. Graphical representation of the different traits (morphological, physiological and biochemical), QTLs, and candidate genes targeted to improve nutrient efficient cultivars (adapted from Sandhu et al. 2021).

The identification of genomic regions (QTL/SNP) associated with WUE and NUE would be vital sources for selection of more efficient cultivars (Cormier et al. 2016). This technique enables plant breeders to successfully screen genetic resources and markers involved in water and N responses, aiding in the improvement of cultivars with high WUE and NUE. Several studies have been conducted in cereals to determine novel traits, genes/QTL, alleles, tolerant breeding lines, landraces and wild relatives to augment WUE and NUE (Siddiqui et al. 2021; Sandhu et al. 2021). Alahmad et al. (2019) reported on association mapping wheat lines together with well-conditioned wheat cultivars using 102 simple sequence repeat markers to identify the genetic markers that are related to QTLs for root traits. The results indicated the presence of two novel QTLs that are related to water stress tolerance. Candidate genes/SNPs/QTLs controlling N acquisition have been identified in wheat in response to various doses of fertilization using biparental populations (An et al. 2006; Xu et al. 2013; Mahjourimajd et al. 2016). In rice, the genetic loci for nutrient uptake have been co-located with loci for root hair length (Sandhu et al. 2015), grain yield and root plasticity traits (Sandhu et al. 2016). Several

genomic regions for phenotypic traits linked to N use and grain yield have been dissected in the chromosomal regions harbouring second isoform (GS2) in wheat and rice (Obara et al., 2001; Yamaya et al. 2002; Habash et al. 2007; Fontaine et al. 2009; Yamaya 2011), indicating the power of the genetic factors neighbouring GS2 shows higher phenotypic performances underlying nutrient use efficiency. Moreover, comparative genome-wide mapping is employed to discover highly conserved genetic architecture, new candidate genes, and regulatory components for traits of interest across related species and genera. These inter-genome regulatory mechanisms can establish new hypotheses about closely related species (Sandhu et al. 2021).

1.10 Molecular identification and functional characterization of NO_3^- transporters

N uptake and accumulation by plant roots is a dynamic process controlled by a distinct form of transport protein family. In the rhizosphere, inorganic N is mostly available as NO_3^-; the concentration of NH_4^+ is significantly lower in comparison (Nieder et al. 2010). The molecular detection and functional characterization of NO_3^- transporter genes has been an active research topic since the mid-1990s and brought up a multitude of candidates. Five transporter families facilitate the NO_3^- uptake and transport by crop plants: i) the nitrate transporter 1/peptide transporter (NPF) (Léran et al. 2014), ii) the nitrate transporter 2 (NRT2), iii) the chloride channel (CLC), iv) the slow anion associated channel homolog (SLC/SLAH) and v) the aluminum-activated malate transporter (ALMT) family (Li et al. 2017). Among these five families, only NPF and NRT2 are well studied and have been identified on a large scale in cereal crops. The primary uptake of NO_3^- and NH_4^+ to the root apoplast occurrs by mass flow and diffusion, respectively (Mandal et al. 2018). *NPF* and *NRT2* gene families are involved in transporting NO_3^- to the root cells (Nacry et al. 2013).

Different types of plasma membrane mediated transporter proteins associated with active transport processes have been reported; they are grouped as high- or low-affinity transporters (Loqué and Wirén 2004; Glass 2009; Dechorgnat et al. 2011). Due to the nature of the affinity and availability of NO_3^- near the rhizosphere, three categories of transport systems have been identified: a high-affinity transport system (HATS), a low-affinity transport system (LATS) and a dual-affinity transport system (DATS). The LATS and HATS basically facilitate NO_3^- transport at high (>1 mmol) and low concentration (<1 mmol L^{-1} NO_3^-), respectively, while the DATS mediates NO_3^- transport at both high and low concentration (Dechorgnat et al. 2011). The above mentioned three NO_3^- transporter protein families are generally encoded by genes of the *NPF* family (Morere-Le Paven et al. 2011; Wen et al. 2017).

Until now, NPF proteins have been demonstrated to mediate transport activities not only for NO_3^- but also for peptides (Komarova et al. 2008), amino acids (Zhou et al. 1998), nitrite

(Sugiura et al. 2007), glucosinolates (Nour-Eldin et al. 2012), auxin (Krouk et al. 2010), abscisic acid and gibberelins (Kanno et al. 2012, Tal et al. 2016).

CHL1 (also named *NRT1.1* and now *NPF6.3*) was the first NO_3^- transporter gene characterized in *Arabidopsis*. It was was discovered in a screening using T-DNA insertion mutants with chloride resistance (Tsay et al. 1993). *NPF6.3* (*CHL1/NRT1.1*) encodes a 590-amino-acid protein that contains 12 membrane-spanning domains. It belongs to the family of NPF (*NRT1/PTR* Family; Leran et al. 2014) genes (formerly known as *NRT1/PTR* family) that contais 53 genes in *Arabidopsis*. Phylogenetic analyses have shown that NPF families comprise a high number of genes classified into 8-10 subfamilies in higher plants (Leran et al. 2014, von Wittgenstein et al. 2014). *NPF6.3* (*CHL1/NRT1.1*) was originally validated as a LATS associated with NO_3^- uptake by plant roots and later shown to be a dual-affinity transporter, demonstrating either low or high affinity for NO_3^- (Liu and Tsay 2003). Apart from this, other NPF transporters in *Arabidopsis* (listed by O'Brien et al. 2016) were characterized as strict LATS involved in root NO_3^- uptake.

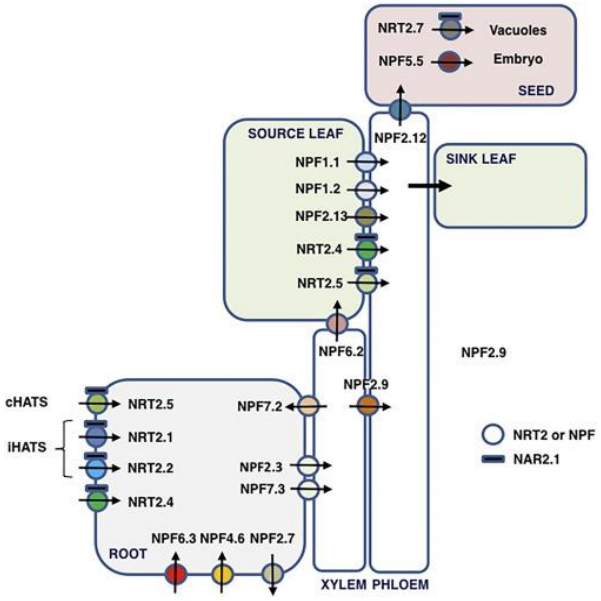

Figure 1.11. Localization and function of the *Arabidopsis* nitrate transporters, especially of the *NRT2* and *NPF* families.

Notably, *NPF4.6* (*NRT1.2/AIT1*) is a constitutive LATS involved in NO_3^- influx (Huang et al. 1999), whereas *NPF2.7* (*NAXT1*) mediates NO_3^- efflux to the external medium (Segonzac et al. 2007). All other listed *AtNPFs* validated to date are involved in internal transport processes (Figure 1.11; O'Brien et al. 2016). Importantly, *AtNPF2.12* (*NRT1.6*) was shown to be involved in NO_3^- transport processes to the developing seeds (Almagro et al. 2008). Finally, several other NPF proteins have been reported to be involved in NO_3^- transport (reviewed in Leran et al. 2014) but their detailed functions in the NO_3^- uptake and transport by modulating

root architecture traits has yet to be determined. Until now, *NPF2.12*, a NO_3^- transporter that coordinates root growth under NO_3^- limited conditions, has not been identified and characterized in cereal crops.

1.11 Research hypothesis and objectives

1.11.1 Research hypothesis

The adaptation of cereal crop species to water and N limited conditions are associated with root architectural traits regulated by genomic loci.

1.11.2 Research objectives

Water and N both are essential resources for crop growth and productivity. Water scarcity and excess application of N in the field are associated with yield loss and cost penalties. To reduce the negative impact on the environment of increasing yield by raising the input of natural resources, enhancing resource use efficiency is crucial. Root architecture is evidently a very promising avenue to enhance water- and nutrient-use efficiency. Harnessing genetic variations in root architecture, discovering candidate genes associated with water and nitrate transport systems and their functional characterization is prerequisite to develop novel water and N-use efficient cultivars. Therefore, the major goal of this study was to estimate genetic variations among wheat and barley germplasms and identification of traits and candidate genes related to WUE and NUE.

The following specific objectives in this were pursued:

1. Summarize the updated knowledge on genetics and genomics of root system variations and identify major effect QTLs including their syntenic relationship for drought adaptation in major cereal crops.
2. Genetic dissection of root phenotypic plasticity traits and underlying candidate genes in adaptation to drought in wheat.
   - 2.1 Assess the root phenotypic diversity of winter bread wheat cultivars grown under drought and control conditions.
   - 2.2 Identify drought-responsive loci and underlying candidate genes associated with root architecture plasticity responses using GWAS.
   - 2.3 Determine transcript expression levels of plasticity associated genes in roots under drought conditions.
3. Uncover a convergently selected nitrate transporter in wheat and barley that coordinates root growth and nitrate-use efficiency.
   - 3.1 Conduct a comparative genome-wide scan using diverse panels of winter wheat and spring barley to analyze root architectural dynamics under high and low N input levels in field and controlled conditions.

3.2 Identify marker-trait associations and underlying candidate genes involved in N transport and metabolisms and prioritize a convergently selected nitrate transporter, *NPF2.12,* between wheat and barley.

3.3 Compare allelic variations of *NPF2.12* in wheat and barley and examine their involvement with root growth and nitrate transport.

3.4 Root transcriptome analysis to obtain an insight into *NPF2.12* regulatory networks and underlying signaling cascades.

1.12 References

Ahmed, M.A., Zarebanadkouki, M., Meunier, F., Javaux, M., Kaestner, A., Carminati, A. Root type matters: measurement of water uptake by seminal, crown, and lateral roots in maize. J Exp Bot 69, 1199–1206 (2018).
Akman, H., Giroux, M., Bruckner, P., Topal, A. Wheat root systems, genetics and methodology for evaluation of root characteristics: a review. Selçuk Tarım ve Gıda Bilimleri Dergisi 25 (4), 109-117 (2011).
Alahmad, S., El Hassouni, K., Bassi, F.M., Dinglasan, E., Youssef, C., Quarry, G., Aksoy, A., Mazzucotelli, E., Juhász, A., Able, J.A. and Christopher, J. A major root architecture QTL responding to water limitation in durum wheat. Front Plant Sci 10, p.436 (2019).

Almagro, A., Lin, S. H., Tsay, Y. F. Characterization of the Arabidopsis nitrate transporter NRT1. 6 reveals a role of nitrate in early embryo development. The Plant Cell 20(12), 3289-3299 (2008).

An, D., Su, J., Liu, Q., Zhu, Y., Tong, Y., Li, J. et al. Mapping QTLs for nitrogen uptake in relation to the early growth of wheat (*Triticum aestivum* L.). Plant Soil 284, 73–84 (2006).

Arendt, E.K., Zannini, E. Cereal Grains for the Food and Beverage Industries. Cambridge: Woodhead Publishing; p. 485 (2013).

Asgari, M. J., Gharineh, M. H., Ziaiyan, A. H., Asoudar, M. A. Effects of water stress on wheat nitrogen use under minimum and conventional tillage system. Crop Res 52 (6), 209-217 (2017).

Awika, J.M. Major Cereal Grains Production and Use around the World. Advances in Cereal Science: Implications to Food Processing and Health Promotion ACS Symposium Series; American Chemical Society: Washington, DC (2011).

Baesso, B., Chiatante, D., Terzaghi, M., Zenga, D., Nieminen, K., Mahonen, A.P., Siligato, R., Helariutta, Y., Scippa, G.S., Montagnoli, A. Transcription factors PRE3 and WOX11 are involved in the formation of new lateral roots from secondary growth taproot in *A. thaliana*. Plant Biol 20, 426–432 (2018).

Baik, B.K., Newman, C.W., Newman, R.K., Ullrich, S.E. Food uses of barley. In: Ullrich SE, editor. Barley: Production, Improvement, and Uses. Oxford: Wiley-Blackwell; 2011. pp. 532-562 (2011).

Barłóg, P., Grzebisz, W. Effect of timing and nitrogen fertilizer application on winter oilseed rape (Brassica napus L.). II. Nitrogen uptake dynamics and fertilizer efficiency. J Agron Crop Sci 190, 314–323 (2004).

Barraclough, P. B., Howarth, J. R., Jones, J., Lopez-Bellido, R., Parmar, S., Shepherd, C. E., et al. Nitrogen efficiency of wheat: Genotypic and environmental variation and prospects for improvement. Eur J Agron 33, 1–11 (2010).

Basu, S., Ramegowda, V., Kumar, A. and Pereira, A. Plant adaptation to drought stress. F1000Res 5, 1554 (2016).

Bengough, A.G., McKenzie, B.M., Hallett, P.D., Valentine, T.A. Root elongation, water stress, and mechanical impedance: a review of limiting stresses and beneficial root tip traits. J. Exp. Bot. 62, 59–68 (2011).

Carmo, B., Zanelato, F., Almei, A.F. Regulation of Gene Expression in Response to Abiotic Stress in Plants, in: Bubulya, P. (Ed.), *Cell Metabolism - Cell Homeostasis and Stress Response*. InTech (2012).

Cattivelli, L., Rizza, F., Badeck, F.W., Mazzucotelli, E., Mastrangelo, A.M., Francia, E., Marè, C., Tondelli, A., Stanca, A.M., Drought tolerance improvement in crop plants: an integrated view from breeding to genomics. Field Crops Res 105 (1-2), 1-14 (2008).

Chandler, V. L., Brendel, V. The maize genome sequencing project. Plant Physiol 130, 1594–1597 (2002).

Chen, Y., Palta, J., Prasad, P.V.V., Siddique, K.H.M. Phenotypic variability in bread wheat root systems at the early vegetative stage. BMC Plant Biol 20, 185 (2020).

Choi, H.-S., Cho, H.-T. Root hairs enhance Arabidopsis seedling survival upon soil disruption. Sci Rep 9, 11181 (2019).

Chopra, V.L., S. Prakash, eds. Evolution and Adaptation of Cereal Crops. Science Publishers Inc, NH, USA. (Gramene Reference ID 8381) (2002).

Cobb, J. N., DeClerck, G., Greenberg, A., Clark, R., McCouch, S. Next-generation phenotyping: requirements and strategies for enhancing our understanding of genotype–phenotype relationships and its relevance to crop improvement. Theor Appl Genet 126(4), 867-887 (2013).

Colombi, T., Kirchgessner, N., Walter, A., Keller, T. Root tip shape governs root elongation rate under increased soil strength. Plant Physiol 174, 2289–2301 (2017).

Comas, L.H., Becker, S.R., Cruz, V.M.V., Byrne, P.F., Dierig, D.A. Root traits contributing to plant productivity under drought. Front Plant Sci 4 (2013).

Cormier, F., Foulkes, J., Hirel, B., Gouache, D., Moenne-Loccoz, Y. Le Gouis, J. Breeding for increased nitrogen-use efficiency: a review for wheat (*T. aestivum* L.). Plant Breed 135, 255–278 (2016).

Corre-Hellou, G., Brisson, N., Launay, M., Fustec, J., Crozat, Y. Effect of root depth penetration on soil nitrogen competitive interactions and dry mater production in pea–barley intercrops given different soil nitrogen supplies. Field Crops Res 103(1), 76–85 (2007).

Cowan, W.D., Mollgaard, A. Alternative uses of barley components in the food and feed industries. In: Sparrow R C M, Lance, Henry R J (eds.) Alternative End Uses of Barley. DHB (1988).

Cracknell. Encyclopedia of Food and Health - 1st Edition (2015).

D'Odorico, P., Chiarelli, D. D., Rosa, L., Bini, A., Zilberman, D., Rulli, M. C. The global value of water in agriculture. Proc Natl Acad Sci 117, 21985–21993 (2020).

Das A, Schneider H, Burridge J, Ascanio AKM, Wojciechowski T, Topp CN, Bucksch A. Digital imaging of root traits (DIRT): a high-throughput computing and collaboration platform for field-based root phenomics. Plant Methods 11, 51 (2015).

Dathe A, Postma JA, Postma-Blaauw MB, Lynch JP. 2016. Impact of axial root growth angles on nitrogen acquisition in maize depends on environmental conditions. Ann Bot 118, 401–414.

de Bang, T. C., Husted, S., Laursen, K. H., Persson, D. P., Schjoerring, J. K. The molecular–physiological functions of mineral macronutrients and their consequences for deficiency symptoms in plants. New Phytol 229(5), 2446-2469 (2021).

Dechorgnat, J., Nguyen, C. T., Armengaud, P., Jossier, M., Diatloff, E., Filleur, S., Daniel-Vedele, F. From the soil to the seeds: the long journey of nitrate in plants. J Expt Bot 62(4), 1349-1359 (2011).

Dhital, S., Raun, W.R. Variability in optimum nitrogen rates for maize. Agron J 108, 2165–2173 (2016).

Dietrich, D. Hydrotropism: how roots search for water. J Expt Bot 69, 2759–2771 (2018).

Dresselhaus, T. Hückelhoven, R. Biotic and abiotic stress responses in crop plants. Agron 8 (11), 267 (2018).

Dubcovsky, J., Dvorak, J. Genome plasticity a key factor in the success of polyploid wheat under domestication. Sci 316 (5833), 1862-1866 (2007).

Dvorak, J., Luo, M.C., Yang, Z.L., Zhang, H.B. The structure of the *Aegilops tauschii* gene pool and the evolution of hexaploid wheat. Theor Appl Genet 97(4), 657-670 (1998).

Ehdaie, B., Layne, A.P., Waines, J.G. Root system plasticity to drought influences grain yield in bread wheat. Euphytica 186, 219–232 (2012).

Fageria, N.K., Baligar, V.C. Enhancing nitrogen use efficiency in crop plants. Adv Agron 88, 97-185 (2005).

Fan, Y., Miguez-Macho, G., Jobbágy, E.G., Jackson, R.B., Otero-Casal, C. Hydrologic regulation of plant rooting depth. Proc Natl Acad Sci 114 10572–10577 (2017).

FAO. Crops and drops: making the best use of water for agriculture, p. 28. Rome, Italy: FAO. Information brochure (2002).

FAO (Retrieved 2020-08-03). Countries - Select All; Regions - World + (Total); Elements - Production Quantity; Items - Barley; Years - 2018. FAO STAT. http://www.fao.org/faostat/en/#home

Farooq, M., Wahid, A., Kobayashi, N., Fujita, D., Basra, S.M.A. Plant drought stress: effects, mechanisms and management. Agron Sustain Dev 29, 185–212 (2009).

Fiorani, F., Schurr, U. Future scenarios for plant phenotyping. Ann Rev Plant Biol 64, 267–291 (2013).

Fleury, D., Jefferies, S., Kuchel, H., Langridge, P. Genetic and genomic tools to improve drought tolerance in wheat. J Expt Bot 61, 3211–3222 (2010).

Food and Agricultural Organization (FAO). The future of food and agriculture – Trends and challenges. Rome (2017).

Food and Agricultural Organization (FAO). Statistical book. www.fao.org/economic (2014).

Foulkes, M., Hawkesford, M., Barraclough, P., Holdsworth, M., Kerr, S., Kightley, S. et al. Identifying traits to improve the nitrogen economy of wheat: Recent advances and future prospects. Field Crops Res 114, 329–342 (2009).

Friedli, C.N., Abiven, S., Fossati, D., Hund, A. Modern wheat semi-dwarfs root deep on demand: response of rooting depth to drought in a set of Swiss era wheats covering 100 years of breeding. Euphytica 215, 85 (2019).

Friedt, W., Horsley, R. D., Harvey, B. L., Poulsen, D. M. E., Lance, R. C. M., Ceccarelli, S. et al. Barley Breeding History, Progress, Objectives, and Technology. In S.E. Ullrich (Hrsg.), *Barley* (1. Auflage, S. 160–220). Wiley. doi:10.1002/9780470958636 (2010).

Garnett, T., Conn, V., Kaiser, B.N. Root based approaches to improving nitrogen use efficiency in plants. Plant Cell Environ 32(9), 1272-83 (2009).

Gibbon, D., Dixon, J., Velazquez, D. Beyond drought tolerant maize: study of additional priorities in maize. Report to Generation Challenge Program. 1–42 (2007).

Glass, A.D. Nitrate uptake by plant roots. Bot 87, 659–667 (2009).

Good, A.G., Shrawat, A.K., Muench, D.G. Can less yield more? Is reducing nutrient input into the environment compatible with maintaining crop production? Trend Plant Sci 9, 597-605 (2004).

Guo, T.T., Wang, D.F., Fang, J., Zhao, J. F., Yuan, S. J., Xiao, L. T. et al. Mutations in the rice OsCHR4 gene, encoding a CHD3 family chromatin remodeler, induce narrow and rolled leaves with increased cuticular wax. Int J Mol Sci 20: 2567 (2019).

Guo, X., Sun, W., Wei, W., Yang, J., Kang, Y., Wu, J. et al. Effects of NPK on physiological and biochemical characteristics of winter rapaseed in northwest cold and drought region. Acta Agric Boreali-Occident Sin 2, 027 (2009).

Gupta, P.K., Balyan, H.S., Gahlaut, V. QTL analysis for drought tolerance in wheat: present status and future possibilities. Agron 7: 5 (2017).

Gürel, F., Öztürk, Z. N., Uçarlı, C., Rosellini, D. Barley genes as tools to confer abiotic stress tolerance in crops. Front Plant Sci *7*. doi:10.3389/fpls.2016.01137 (2016).

Harwood, W. Barley as a cereal model for biotechnology applications. In: Jones HD (ed) Biotechnology of major cereals. CABI, Wallingford, 80–87 (2016).

Harwood, W.A. An Introduction to Barley: The crop and the model. In W.A. Harwood (Hrsg.), *Barley* (Band 1900, S. 1–5). New York, NY: Springer New York. doi: 10.1007/978-1-4939-8944-7_1 (2019).

Hauer-Jákli, M., Tränkner, M. Critical leaf magnesium thresholds and the impact of magnesium on plant growth and photo-oxidative defense: A systematic review and meta-analysis from 70 years of research. Front Plant Sci 10, 766 (2019).

Hawkesford, M.J. “Improving nutrient use efficiency in crops,” in eLS (Chichester, UK: John Wiley & Sons, Ltd.) (2011).

Hazman, M., Brown, K.M. Progressive drought alters architectural and anatomical traits of rice roots. Rice 11, 62 (2018).

Heun, M., Schäfer-Pregl, R., Klawan, D., Castagna, R., Accerbi, M., Borghi, B., Salamini, F. Site of einkorn wheat domestication identified by DNA fingerprinting. Sci 278 (5341), 1312-1314 (1997).

Hirel, B., Tétu, T., Lea, P.J., Dubois, F. Improving nitrogen use efficiency in crops for sustainable agriculture. Sustainability 3, 1452–1485 (2011).

Hochholdinger, F., Tuberosa, R. Genetic and genomic dissection of maize root development and architecture. Curr Opin. Plant Biol. 12(2): 172-177 (2009).

Holubová, K., Hensel, G., Vojta, P., Tarkowski, P., Bergougnoux, V., Galuszka, P. Modification of barley plant productivity through regulation of cytokinin content by reverse-genetics approaches. Front Plant Sci 9, 1676 (2018).

Hu, L., Cheng, H., Zhou, G., Fu, T. “Effect of different nitrogen nutrition on the quality of rapeseed (Brassica napus L.) stressed by drought,” in The 12th International Rapeseed Congress Proceedings Wuhan (2007).

Huang, N.C., Liu, K.H., Lo, H.J., Tsay, Y.F. Cloning and functional characterization of an Arabidopsis nitrate transporter gene that encodes a constitutive component of low-affinity uptake. The Plant Cell 11(8), 1381-1392 (1999).

Hussain, S., khan, F., Cao, W., Wu, L., Geng, M. Seed priming alters the production and detoxification of reactive oxygen intermediates in rice seedlings grown under sub-optimal temperature and nutrient supply. Front Plant Sci 7, 439 (2016).

Ibrahim SE, Schubert A, Pillen K, Léon J (2012) QTL analysis of drought tolerance for seedling root morphological traits in an advanced backcross population of spring wheat. Int J Agric Sci 2: 619-629.

Iqbal M.S., Singh A.K., Ansari M.I. Effect of Drought Stress on Crop Production. In: Rakshit A., Singh H., Singh A., Singh U., Fraceto L. (eds) New Frontiers in Stress Management for Durable Agriculture. Springer, Singapore (2020).

Ito, S., Yamagami, D., Asami, T. Effects of gibberellin and strigolactone on rice tiller bud growth. J Pestic Sci 43, 220–223 (2018).

Juan, Z., Jianwei, L., Fang, C., Yinshui, L. Effect of nitrogen, phosphorus, potassium, and boron fertilizers on yield and profit of rapeseed (*Brassica napus* L.) in the Yangtze River Basin. Acta Agron Sin 35, 87–92 (2009).

Kadam, N.N., Tamilselvan, A., Lawas, L.M., Quinones, C., Bahuguna, R.N., Thomson, M.J. et al. Genetic control of plasticity in root morphology and anatomy of rice in response to water deficit. Plant Physiol 174(4), 2302-2315 (2017).

Kadam, S., Singh, K., Shukla, S., Goel, S., Vikram, P., Pawar, V., Gaikwad, K., Khanna-Chopra, R., Singh, N. Genomic associations for drought tolerance on the short arm of wheat chromosome 4B. Funct Integr Genomics 12(3), 447-464 (2012).

Kage, H. Is low rooting density of faba beans a cause of high residual nitrate content of soil at harvest? Plant Soil 190, 47–60 (1997).

Kanno, Y., Hanada, A., Chiba, Y., Ichikawa, T., Nakazawa, M., Matsui, M. et al. Identification of an abscisic acid transporter by functional screening using the receptor complex as a sensor. Proc Natl Acad Sci 109(24), 9653-9658 (2012).

Khan, M.A., Gemenet, D.C., Villordon, A. Root system architecture and abiotic stress tolerance: current knowledge in root and tuber crops. Front Plant Sci 7, 1584 (2016).

Koevoets, I.T., Venema, J.H., Elzenga, J.Theo.M., Testerink, C. Roots withstanding their environment: exploiting root system architecture responses to abiotic stress to improve crop tolerance. Front Plant Sci 07 (2016).

Komarova, N.Y., Thor, K., Gubler, A., Meier, S., Dietrich, D., Weichert, A. et al. AtPTR1 and AtPTR5 transport dipeptides in planta. Plant Physiol 148(2), 856-869 (2008).

Krouk, G., Lacombe, B., Bielach, A., Perrine-Walker, F., Malinska, K., Mounier, E. et al. Nitrate-regulated auxin transport by NRT1. 1 defines a mechanism for nutrient sensing in plants. Dev Cell, 18(6), 927-937 (2010).

Kulkarni, M., Soolanayakanahally, R., Ogawa, S., Uga, Y., Selvaraj, M.G., Kagale, S., Drought response in wheat: key genes and regulatory mechanisms controlling root system architecture and transpiration efficiency. Front Chem *5*, 06 (2017).

Langridge, P. Economic and Academic Importance of Barley. In N. Stein & G.J. Muehlbauer (Hrsg.), *The Barley Genome* (S. 1–10). Cham: Springer International Publishing. doi:10.1007/978-3-319-92528-8 (2018).

Lehmensiek, A., Bovill, W., Wenzl, P., Langridge, P., Appels, R. Genetic mapping in the Triticeae, in: Muehlbauer, G.J., Feuillet, C. (Eds.), Genetics and genomics of the Triticeae. Springer US, New York, NY, pp. 201–235 (2009).

Léran, S., Varala, K., Boyer, J. C., Chiurazzi, M., Crawford, N., Daniel-Vedele, F. et al. A unified nomenclature of NITRATE TRANSPORTER 1/PEPTIDE TRANSPORTER family members in plants. Trends Plant Sci 19(1), 5-9 (2014).

Li, P., Zhuang, Z., Cai, H., Cheng, S., Soomro, A.A., Liu, Z., Gu, R., Mi, G., Yuan, L., Chen, F. Use of genotype–environment interactions to elucidate the pattern of maize root plasticity to nitrogen deficiency. J Integr Plant Biol 58, 242–253 (2016).

Li, H., Hu, B., and Chu, C. Nitrogen use efficiency in crops: Lessons from *Arabidopsis* and rice. J Exp Bot 68, 2477–2488 (2017).

Liu, S., Song, F., Zhu, X., Xu, H. Dynamics of root growth and distribution in maize from the black soil region of NE China. J Agri Sci 4, 21–30 (2012).

Liu, K. H., Tsay, Y.F. (2003). Switching between the two actions modes of the dual-affinity nitrate transporter CHL1 by phosphorylation. EMBO J *22*(5), 1005-1013.

Loqué, D., von Wirén, N. Regulatory levels for the transport of ammonium in plant roots. J. Exp Bot 55, 1293–1305 (2004).

Lositska, T. Methodical aspects of determining the efficiency of grain production in modern conditions. EES 3(3), 44-52 (2019).

Lucas, M.E., Hoad, S.P., Russel, G., Bingham, I.J. Management of cereal root systems. The Home-Grown Cereals Authority (HGCA) Research Review Workshop. Research Review No. 43 (2000).

Lynch, J.P. Steep, cheap and deep: an ideotype to optimize water and N acquisition by maize root systems. Annals of Botany 112, 347–357 (2013).

Lynch, J.P. Rightsizing root phenotypes for drought resistance. J Exp Bot 69, 3279–3292 (2018).

Maathuis, F. J. Physiological functions of mineral macronutrients. Curr Opin Plant Biol 12(3), 250-258 (2009).

Mahjourimajd, S., Kuchel, H., Langridge, P., Okamoto, M. Evaluation of Australian wheat genotypes for response to variable nitrogen application. Plant Soil 399, 247–255 (2016).

Mandal, V.K., Sharma, N., Raghuram, N. "Molecular targets for improvement of crop nitrogen use efficiency: current and emerging options," in *Engineering Nitrogen Utilization in Crop Plants*, eds A. Shrawat, A. Zayed, and D. Lightfoot (Cham: Springer). doi: 10.1007/978-3-319-92958-3_577 (2018).

Manske, G.G.B., Vlek, P.L.G. Root architecture –Wheat as a model plant. p. 249 – 260. In: Waisel, Y., Eshel, A., Kafkafi, U. (ed.): Plant roots: The hidden half. Marcel Dekker Inc., New York, 1120 p (2002).

Marden, M., Lambie, S., Rowan, D. Root system attributes of 12 juvenile indigenous early colonising shrub and tree species with potential for mitigating erosion in New Zealand. N. Z. J. For Sci 48, 11 (2018).

McElrone, A.J., Choat, B., Gambetta, G.A., and Brodersen, C.R. Water uptake and transport in vascular plants. Nat Educ Knowl 4 (2013).
McMahon, P. Feeding frenzy: the new politics of food. Profile Books (2017).

Meister, R., Rajani, M.S., Ruzicka, D., Schachtman, D.P. Challenges of modifying root traits in crops for agriculture. Trends Plant Sci 19, 779–788 (2014).

Meng, Q., Yue, S., Chen, X., Cui, Z., Ye, Y., Ma, W., et al. Understanding dry matter and nitrogen accumulation with time-course for high-yielding wheat production in China. PLoS ONE 8:e68783 (2013).

Mohd-Radzman, N. A., Djordjevic, M. A., & Imin, N. Nitrogen modulation of legume root architecture signaling pathways involves phytohormones and small regulatory molecules. Front Plant Sci 4, 385 (2013).

Montagnoli, A., Lasserre, B., Sferra, G., Chiatante, D., Scippa, G.S., Terzaghi, M., Dumroese, R.K. Formation of annual ring eccentricity in coarse roots within the root cage of pinus ponderosa growing on slopes. Plants 9, 181 (2020).

Morere-Le Paven, M.C., Viau, L., Hamon, A., Vandecasteele, C., Pellizzaro, A., Bourdin, C. et al. Characterization of a dual-affinity nitrate transporter MtNRT1. 3 in the model legume Medicago truncatula. J Exp Bot 62(15), 5595-5605 (2011).

Morgan, J.M. Osmoregulation and water stress in higher plants. Ann Rev Plant Physiol 35(1), 299-319 (1984).

Morrell, P.L., Clegg, M.T. Genetic evidence for a second domestication of barley (Hordeum vulgare) east of the Fertile Crescent. Proc Natl Acad Sci 104: 3289–94 (2007).

Mwadzingeni L, Figlan S, Shimelis H, Mondal S, Tsilo TJ. 2017. Genetic resources and breeding methodologies for improving drought tolerance in wheat. J Crop Improv 31: 5, 648-672

Mwadzingeni, L., Shimelis, H., Dube, E., Laing, M.D., Tsilo, T.J. Breeding wheat for drought tolerance: Progress and technologies. J Integr Agric 15: 935–943 (2016).

Nacry, P., Bouguyon, E., Gojon, A. Nitrogen acquisition by roots: physiological and developmental mechanisms ensuring plant adaptation to a fluctuating resource. *Plant Soil*, *370*(1), 1-29 (2013).

Nada, R.M. and Abogadallah, G.M., Root-favored biomass allocation improves growth and yield of field-grown rice (*Oryza sativa* L.) plants only when the shoot sink is expandable. Acta Physiol Plant 40(6), p.123 (2018).

Nguyen, V.L., Stangoulis, J. Variation in root system architecture and morphology of two wheat genotypes is a predictor of their tolerance to phosphorus deficiency. Acta Physiol Plant 41, 109 (2019).

Nieder, R., Benbi, D. K., Scherer, H. W. Fixation and defixation of ammonium in soils: a review. Biol Fert Soils 47, 1–14 (2010).

Nour-Eldin, H. H., Andersen, T. G., Burow, M., Madsen, S. R., Jørgensen, M. E., Olsen, C., et al. NRT/PTR transporters are essential for translocation of glucosinolate defence compounds to seeds. Nature 488 (7412), 531-534 (2012).

Obara, M., Kajiura, M., Fukuta, Y., Yano, M., Hayashi, M., Yamaya, T., et al. Mapping of QTLs associated with cytosolic glutamine synthetase and NADH-glutamate synthase in rice (*Oryza sativa L*.). J Exp Bot 52, 1209–1217 (2001).

O'Brien, J. A., Vega, A., Bouguyon, E., Krouk, G., Gojon, A., Coruzzi, G., et al. (2016). Nitrate transport, sensing, and responses in plants. Mol Plant 9(6), 837-856.

Oyiga, B.C., Palczak, J., Wojciechowski, T., Lynnch, J.P., Naz, A.A., Leon, J., Ballvora, A. Genetic components of root architecture and anatomy adjustments to water-deficit stress in spring barley. Plant Cell Environ 1–20 (2020).

Paez-Garcia, A., Motes, C., Scheible, W.R., Chen, R., Blancaflor, E., Monteros, M. Root traits and phenotyping strategies for plant improvement. Plants 4, 334–355 (2015).

Perniola, M., Lovelli, S., Arcieri, M., Amato, M. Sustainability in cereal crop production in Mediterranean environments. Vastola (ed.), The sustainability of agro-food and natural resource systems in the mediterranean basin, doi. 10.1007/978-3-319-16357-4_2 (2015).

Pomeranz, Y and L. Munck, eds., Cereals: A renewable resource. American association of cereal chemists, St. Paul, MN. (Gramene Reference ID 8387) (1981).

Rahni, R., Birnbaum, K.D. Week-long imaging of cell divisions in the Arabidopsis root meristem. Plant Methods 15, 30 (2019).

Reynolds MP, Ortiz-Monasterio JI, McNab A. Application of physiology in wheat breeding. D.F. CIMMYT. Mexico (2001).

Richards, RA., Passioura, JB. A breeding program to reduce the diameter of the major xylem vessel in the seminal roots of wheat and its effect on grain yield in rain-fed environments. Aust J Agric Res 40(5), 943-950 (1989).

Riley, R., Unrau, J., Chapman, V. Evidence on the origin of the B genome of wheat. *J. Hered.*, *49*(3), 91-98 (1958).

Rytter, R.M., Rytter, L. Quantitative estimates of root densities at minirhizotrons differ from those in the bulk soil. Plant Soil 350, 205–220 (2012).

Saisho, D., Takeda, K. Barley: Emergence as a new research material of crop science. Plant Cell Physiol 52 (5), 724–727 (2011).

Sandhu, N., Raman, K. A., Torres, R. O., Audebert, A., Dardou, A., Kumar, A., et al. Rice root architectural plasticity traits and genetic regions for adaptability to variable cultivation and stress conditions. Plant Physiol 171, 2562–2576 (2016).

Sandhu, N., Sethi, M., Kumar, A., Dang, D., Singh, J., Chhuneja, P. Biochemical and genetic approaches improving nitrogen use efficiency in cereal crops: A review. Front Plant Sci 12, 657629 (2021).

Sandhu, N., Torres, R. O., Sta Cruz, M. T., et al. Traits and QTLs for development of dry direct-seeded rainfed rice varieties. J Exp Bot 66, 225–244 (2015).

Schneider, H.M., Klein, S.P., Hanlon, M.T., Nord, E.A., Kaeppler, S., Brown, K.M., et al. Genetic control of root architectural plasticity in maize. J Exp Bot 71, 3185–3197 (2020).

Schwar, P., Li, Y. Malting and brewing uses of barley. In: Ullrich SE, editor. Barley: Production, Improvement, and Uses. Oxford: Wiley-Blackwell; 2011. pp. 478-521 (2011).

Segonzac, C., Boyer, J. C., Ipotesi, E., Szponarski, W., Tillard, P., et al. Nitrate efflux at the root plasma membrane: identification of an Arabidopsis excretion transporter. The Plant Cell 19(11), 3760-3777 (2007).

Shah, A.A., Salgotra, R.K., Wani, S.A., Mondal, S.K. Breeding and genomics approaches to increase crop yield under drought stress in climate change scenario. Eur J Exp Biol 7(4), pp.1-7 (2017).

Shavrukov, Y., Kurishbayev, A., Jatayev, S., Shvidchenko, V., Zotova, L., Koekemoer, F., de Groot, S., et al. Early flowering as a drought escape mechanism in plants: How can it aid wheat production?. Front Plant Sci 8, 1950 (2017).

Shewry, P.R. and Hey, S.J. The contribution of wheat to human diet and health. Food Eenergy Secur 4(3), 178-202 (2015).

Shewry, P.R., Wheat. J Exp Bot 60(6), 1537-1553 (2009).

Shorinola, O., Kaye, R., Golan, G., Peleg, Z., Kepinski, S., Uauy, C. Genetic screening for mutants with altered seminal root numbers in hexaploid wheat using a high-throughput root phenotyping platform. G3amp58 GenesGenomesGenetics 9, 2799–2809 (2019).

Siddiqui, M.N., Léon, J., Naz, A.A., Ballvora, A. Genetics and genomics of root system variation in adaptation to drought stress in cereal crops. J Exp Bot 72(4), 1007-1019 (2021b).

Siddiqui, M.N., Teferi, T.J., Ambaw, A.M., Gabi, M.T., Koua, P., Léon, J., Ballvora, A. New drought-adaptive loci underlying candidate genes on wheat chromosome 4B with improved photosynthesis and yield responses. Physiol Plant 173(4), 2166-2180 (2021a).

Slack, S., York, L.M., Roghazai, Y., Lynch, J., Bennett, M., Foulkes, J., Wheat shovelomics II: Revealing relationships between root crown traits and crop growth (preprint). Plant Biol https://doi.org/10.1101/280917 (2018).

Smith, S., De Smet, I. Root system architecture: insights from Arabidopsis and cereal crops. Philos Trans R Soc B 367, 1441–1452 (2012).

Sugiura, M., Georgescu, M. N., Takahashi, M. A. nitrite transporter associated with nitrite uptake by higher plant chloroplasts. Plant Cell Physiol 48(7), 1022-1035 (2007).

Sun, J., Guo, Y., Zhang, G., Gao, M., Zhang, G., Kong, F., et al. QTL mapping for seedling traits under different nitrogen forms in wheat. Euphyt 191, 317–331 (2012).

Tadesse, W., Amri, A., Ogbonnaya, F.C., Sanchez-Garcia, M., Sohail, Q., Baum, M. Wheat. In *Genetic and Genomic Resources for Grain Cereals Improvement* (pp. 81-124). Elsevier, Academic Press (2016).

Tal, I., Zhang, Y., Jørgensen, M. E., Pisanty, O., Barbosa, I. C., Zourelidou, M., et al. The Arabidopsis NPF3 protein is a GA transporter. Nat Commun 7(1), 1-11 (2016).

Tang, L, Tan, F., Jiang, H., Lei, X., Cao, W., Zhu, Y. Root architecture modeling and visualization in wheat. Part II, International Federation for Information Processing (IFIP) AICT 345, 479–490 (2011).

Tiwari, V. Growth and Production of Barley, 9 (1998).

Trachsel, S., Kaeppler, S.M., Brown, K.M., Lynch, J.P. Shovelomics: high throughput phenotyping of maize (*Zea mays* L.) root architecture in the field. Plant Soil 341, 75-87. (2011).

Trachsel S, Kaeppler SM, Brown KM, Lynch JP. 2013. Maize root growth angles become steeper under low N conditions. Field Crops Res 140, 18–31 (2013).

Tracy, S.R., Nagel, K.A., Postma, J.A., Fassbender, H., Wasson, A., Watt, M. Crop improvement from phenotyping roots: highlights reveal expanding opportunities. Trends Plant Sci 25, 105-118 (2020).

Tricase, C., Amicarelli, V., Lamonaca, E., Leonardo Rana, R. Economic Analysis of the Barley Market and Related Uses. In Z. Tadele (Hrsg.), *Grasses as Food and Feed*. IntechOpen. doi:10.5772/intechopen.78967 (2018).

Tsay, Y.F., Schroeder, J.I., Feldmann, K.A., Crawford, N.M. The herbicide sensitivity gene CHL1 of Arabidopsis encodes a nitrate-inducible nitrate transporter. Cell 72(5), 705-713 (1993).

Vitousek, P.M., Naylor, R., Crews, T., David, M.B., Drinkwater, L. E., et al. Nutrient imbalances in agricultural development. Sci 324(5934), 1519-1520 (2009).

Von Wittgenstein, N.J., Le, C.H., Hawkins, B. J., Ehlting, J. Evolutionary classification of ammonium, nitrate, and peptide transporters in land plants. BMC Evol Biol 14(1), 1-17 (2014).

Wang, H., Qin, F. Genome-wide association study reveals natural variations contributing to drought resistance in crops. Front Plant Sci 8, 1110 (2017).

Wang, S. et al. Characterization of polyploid wheat genomic diversity using a high-density 90,000 single nucleotide polymorphism array. Plant Biotechnol J 12, 787–796 (2014).

Wasaya, A., Zhang, X., Fang, Q., Yan, Z. Root phenotyping for drought tolerance: A review. Agron 8, 241 (2018).

Wasson, A.P., Nagel, K.A., Tracy, S., Watt, M. Beyond digging: Noninvasive root and rhizosphere phenotyping. Trend Plant Sci 25, 119-120 (2020).

Wasson, A.P., Richards, R.A., Chatrath, R., Misra, S.C., Prasad, S.V.S., Rebetzke, G.J., et al. Traits and selection strategies to improve root systems and water uptake in water-limited wheat crops. J Exp Bot 63, 3485–3498 (2012).

Wen, Z., Tyerman, S.D., Dechorgnat, J., Ovchinnikova, E., Dhugga, K. S., et al. Maize NPF6 proteins are homologs of Arabidopsis CHL1 that are selective for both nitrate and chloride. The Plant Cell 29(10), 2581-2596 (2017).

Xu, Y., Wang, R., Tong, Y., Zhao, H., Xie, Q., Liu, D., et al. Mapping QTLs for yield and nitrogen-related traits in wheat: Influence of nitrogen and phosphorus fertilization on QTL expression. Theor App Genet 127, 59–72 (2013).

Yamaya, T., Obara, M., Nakajima, H., Sasaki, S., Hayakawa, T., and Sato, T. Genetic manipulation and quantitative−trait loci mapping for nitrogen recycling in rice. J Exp Bot 53, 917–925 (2002).

Yang, J.T., Schneider, H.M., Brown, K.M., Lynch, J.P. (2019). Genotypic variation and nitrogen stress effects on root anatomy in maize are node specific. J Exp Bot 70(19), 5311-5325.

Yang, X., Xia, X., Zhang, Z., Nong, B., Zeng, Y., Xiong, F., et al. (2017). QTL mapping by whole genome re-sequencing and analysis of candidate genes for nitrogen use efficiency in rice. Front Plant Sci 8, 1634.

Ye, H., Roorkiwal, M., Valliyodan, B., Zhou, L., Chen, P., Varshney, R.K., Nguyen, H.T. Genetic diversity of root system architecture in response to drought stress in grain legumes. J Exp Bot 69(13), 3267-3277 (2018).

York LM, Lynch JP. 2015. Intensive field phenotyping of maize (*Zea mays* L.) root crowns identifies phenes and phene integration associated with plant growth and nitrogen acquisition. J Exp Bot 66, 5493–5505.

Zarebanadkouki, M., Kim, Y.X., Carminati, A. Where do roots take up water? Neutron radiography of water flow into the roots of transpiring plants growing in soil. New Phytol 199, 1034–1044 (2013).

Zhan, A., Lynch, J.P. Reduced frequency of lateral root branching improves N capture from low-N soils in maize. J Exp Bot 66, 2055–2065 (2015).

Zhang, X., Mi, Y., Mao, H., Liu, S., Chen, L., Qin, F. Genetic variation in *ZmTIP1* contributes to root hair elongation and drought tolerance in maize. Plant Biotechnol J 18, 1271–1283 (2020).

Zhou, J.J., Theodoulou, F.L., Muldin, I., Ingemarsson, B., Miller, A.J. Cloning and functional characterization of a Brassica napus transporter that is able to transport nitrate and histidine. J Biol Chem 273(20), 12017-12023 (1998).

Zhou, M. X. Barley production and consumption. In G. Zhang & C. Li (Hrsg.), *Genetics and Improvement of Barley Malt Quality* (S. 1–17). Berlin, Heidelberg: Springer Berlin Heidelberg. doi: 10.1007/978-3-642-01279-2 (2009).

Zhu, Y., Weiner, J., Yu, M., Li, F. Evolutionary agroecology: Trends in root architecture during wheat breeding. Evol. Appl. 12, 733–743 (2019).

Journal of Experimental Botany, Vol. 72, No. 4 pp. 1007–1019, 2021
doi:10.1093/jxb/eraa487 Advance Access Publication 23 October 2020
This paper is available online free of all access charges (see https://academic.oup.com/jxb/pages/openaccess for further details)

REVIEW PAPER

Genetics and genomics of root system variation in adaptation to drought stress in cereal crops

Md. Nurealam Siddiqui[1,2], Jens Léon[1], Ali A. Naz[1,*] and Agim Ballvora[1,*]
[1] Institute of Crop Science and Resource Conservation (INRES) – Plant Breeding and Biotechnology, University of Bonn, Bonn, Germany
[2] Department of Biochemistry and Molecular Biology, Bangabandhu Sheikh Mujibur Rahman Agricultural University, Gazipur 1706, Bangladesh

* Correspondence: a.naz@uni-bonn.de or ballvora@uni-bonn.de

Received 18 March 2020; Editorial decision 9 October 2020; Accepted 19 October 2020

Editor: Miriam Gifford, University of Warwick, UK

Abstract

Cereals are important crops worldwide that help meet food demands and nutritional needs. In recent years, cereal production has been challenged globally by frequent droughts and hot spells. A plant's root is the most relevant organ for the plant adaptation to stress conditions, playing pivotal roles in anchorage and the acquisition of soil-based resources. Thus, dissecting root system variations and trait selection for enhancing yield and sustainability under drought stress conditions should aid in future global food security. This review highlights the variations in root system attributes and their interplay with shoot architecture features to face water scarcity and maintain thus yield of major cereal crops. Further, we compile the root-related drought responsive quantitative trait loci/genes in cereal crops including their interspecies relationships using microsynteny to facilitate comparative genomic analyses. We then discuss the potential of an integrated strategy combining genomics and phenomics at genetic and epigenetic levels to explore natural genetic diversity as a basis for knowledge-based genome editing. Finally, we present an outline to establish innovative breeding leads for the rapid and optimized selection of root traits necessary to develop resilient crop varieties.

Keywords: Cereals, comparative genomics, drought stress adaptation, genetic variations, molecular breeding, root system attributes.

Introduction

The adverse impacts of abiotic stresses are increasing owing to the rapid increase in climatic unpredictability and successive degradation of arable lands. This is negatively affectingthe overall homeostasis of plants, and limiting crop expan- sion and, ultimately, crop production worldwide (Bray *et al.*, 2000; Checker *et al.*, 2012; Fahad *et al.*, 2017). Approximately 50–70% of the crop yield reduction is the direct consequenceof abiotic stresses (Francini and Sebastiani, 2019). Drought is a major abiotic stress factor, significantly affecting crop yields by negatively affecting plant growth, physiology, and reproduction (Fahad *et al.*, 2017; Lamaoui *et al.*, 2018). For instance, a meta-study based on data published from 1980 to 2015 reported that up to 21% and 40% of yield losses on a global scale in wheat (*Triticum aestivum* L.) and maize (*Zea mays* L.), respectively, result from the negative effects of drought stress (Daryanto *et al.*, 2016).

Natural populations of crop plants, in terms of landraces and wild relatives, have established stunning levels of variation in developmental and adaptive traits.This has occurred through the continuous process of evolution and by-passing the bottlenecks of natural selection over an extremely protracted time span. These unique variations are essential sources of new traits that can be used to overcome yield stagnancy, improve climatic adaptation, and increase the narrow genetic diversity of cultivated varieties (Govindaraj *et al.*, 2015). Thus, the systematic genetic and molecular determination of natural genetic resources for crops across varied environments is essential. It will help to identify and incorporate new breeding targets for yield and sustainability that will help meet the current and future challenges of crop production and climate change. The power of quantitative genetics and genomics has increased considerably in the last decade after the advent of state-of-the-art molecular genome analyses methods, such as next-generation sequencing (NGS) and high-throughput genotyping (Mwadzingeni *et al.*, 2016, 2017). These methods have allowed the rapid identification of the hidden genetic footprints of com- plex traits, such as root system variation, with great pre- cision (Shelden and Roessner, 2013; Naz *et al.*, 2014). In addition, phenomics is emerging as a new way to investigate plant traits at morphological and physiological levels under given environmental conditions using modern sensing and quantification techniques. Recently, newer methods, such as transcriptomics, proteomics, metabolomics, and ionomics ('molecular phenotyping'), have been employed to determine trait inheritance at the physiological level. Similarly, non-invasive phenotyping methods are available to record system views of plant development, the energy dynamics of yield and yield components, and drought fitness from the cellular to whole-plant levels (Rascher *et al.*, 2011).

A plant's root is the fundamental organ that plays critical roles in extracting soil resources under water-limited conditions. When plants sense a water shortage, roots continue growing and enter deep soil layers (Maeght *et al.*, 2013; Koevoets *et al.*, 2016; Fan *et al.*, 2017;Vyver and Peters, 2017). Root architecture and morphological attributes are crucial in the dehydration avoidance through efficient uptake of water and nutrients and favorable gas exchange, which facilitate carbon assimilation and yield potential under a drought stress scenario (Gewin, 2010; Kell, 2011; Lopes *et al.*, 2011; Palta *et al.*, 2011). Many studies have focused on the genetics of root system variations and its role in drought stress adaptation and yield stability (de Dorlodot *et al.*, 2007; Lynch, 2011; Uga *et al.*, 2015; Koevoets *et al.*, 2016; Polania *et al.*, 2017).The global genetic diversity may be readily exploited using marker-assisted selection (MAS) and genomic selection tools to produce elite cultivars able to face environmental extremes (Tron *et al.*, 2015;Valliyodan *et al.*, 2017).While numerous comprehensive reviews have highlighted the genetic diversity of root system architecture under drought conditions in legumes (Valliyodan *et al.*, 2017; Ye *et al.*, 2018), root crops, and tuber crops (Khan *et al.*, 2016), we focused on root system genomics and their utility in drought stress adaptation in cereal crops. In this review, we address the importance of harnessing the genetic variation in root system traits to promote adaptations to drought stress. It will be useful to address the following questions related to root system genetics and genomics involved in drought stress adaptation. (i) How do root system traits confer tolerance to drought stress by maintaining root–shoot balance? (ii) What is the current progress in genetic studies to identify genetic variations and genomic loci in response to drought stress? (iii) Which specific loci and syntenic regions are related to stress adaptation for resilience breeding? (iv) Which strategies will hasten the development of resilient cereal varieties through the employment of newly established techniques of phenomics, genomics, molecular breeding, and genome editing?

Cereal productivity is threatened by drought stress worldwide

In recent years, drought stress has become the most vital cause of crop yield reductions (Lamaoui *et al.*, 2018; Webber *et al.*, 2018).Whole agroecosystems may suffer from frequent drought risks as the consequence of the global increase in temperature (Leng and Hall, 2019). According to the FAO (2018), >60%of the global population will inhabit areas with water deficiencies by 2025, and currently 70% of the world's freshwater withdrawals are for agricultural purposes. With the dramatic increase in the global population, water requirements are rising at an alarming rate, resulting in an increasing need to breed water-efficient crops (Ruggiero *et al.*, 2017; Blankenagel *et al.*, 2018).The breeding of drought-tolerant cultivars requires improved root system architectural attributes as a necessity for the crops to cope with the changing climatic conditions.

Plants experience drought stress either when the water availability near the root zone is limited or when there is an imbalance between water uptake and loss through transpiration that hinders plant growth and development during the plant life cycle (Ji *et al.*, 2010; Anjum *et al.*, 2011). Under drought stress conditions, plants exhibit a wide variety of disorganization that may result in an alteration from high sensitivity to viable tolerance (Joshi *et al.*, 2016). Drought restricts various crucial physiological processes, including growth performance, correlations between nutrients and water, photosynthesis, and assimilate partitioning, which consequently results in significant reductions in biomass production and yield (Daryanto *et al.*, 2017; Hussain *et al.*, 2018). A lower absorption rate of photosynthetically active radiation, a decreased radiation use efficiency, and a decline in the harvest index are leading factors of yield reduction under limited soil moisture conditions (Earl and Davis, 2003; Randhawa *et al.*, 2017). Evolution has shaped the inherent potential of plant populations for morphological and physiological adjustments that mitigate the detrimental impacts of drought stress (Farooq *et al.*, 2009; Basu *et al.*, 2016).

Drought tolerance has been defined as the ability of cer- tain genotypes to perform better than others under drought stress conditions. The underlying mechanisms may involve dehydration tolerance or avoidance, as well as drought escape (Levitt, 1972; Turner, 1979; Blum, 2005). Therefore, the extent and combination of these adaptive mechanisms need to be explored to understand the utility levels of different traits in enhancing the tolerance to water scarcity of crop varieties. Plant physiologists have explored several emerging root–shoot system traits that might trigger plant adaptation to drought stress by improving the water use efficiency, as well as a limited number of traits that may help optimize soil water acquisition (Choat *et al.*, 2018; Rosa *et al.*, 2019).

Interplay of root and shoot attributes in increasing cereal yield and sustainability under drought stress conditions

Roots and shoots are two fundamental axes of plant development. Although roots and shoots develop and grow at different locations, there is an active communication between the two organs that determines the specific plant architecture (Fig. 1). Interconnected hormonal circuits, as chemical signaling pathways, dominated by auxin and cytokinins play fundamental roles in the coordinated development of these organs (Puig *et al.*, 2012; Naz *et al.*, 2013).There exists a rootwards auxin flow from the shoot and a shootwards cytokinin flow from the root (Ko *et al.*, 2014). The auxin transported from shoot to root activates strigolactones in the roots that then move upwards through the xylem and suppress axillary shoot branching (tillering). Additionally, shoot biomass is heavily influenced by aboveground environmental factors (such as photoperiod, rainfall, and temperature). Similarly, roots show a great plasticity in responses to available soil moisture and nutrients, as well as in their interactions with biota in the rhizosphere (Zhu *et al.*, 2011; Chen *et al.*, 2019). The root, shoot, and atmospheric factors combine to influence plant adapative systematic responses, including stomatal closure, to diverse environmental stimuli, including drought stress (Jia and Zhang, 2008). Interestingly, shoot growth is reduced under drought stress conditions but root growth continues through essential reserve translocation from the shoot using long-distance chemical and hydraulic signal transduction (Fig. 1; Davies *et al.*, 2002; Schachtman and Goodger, 2008).

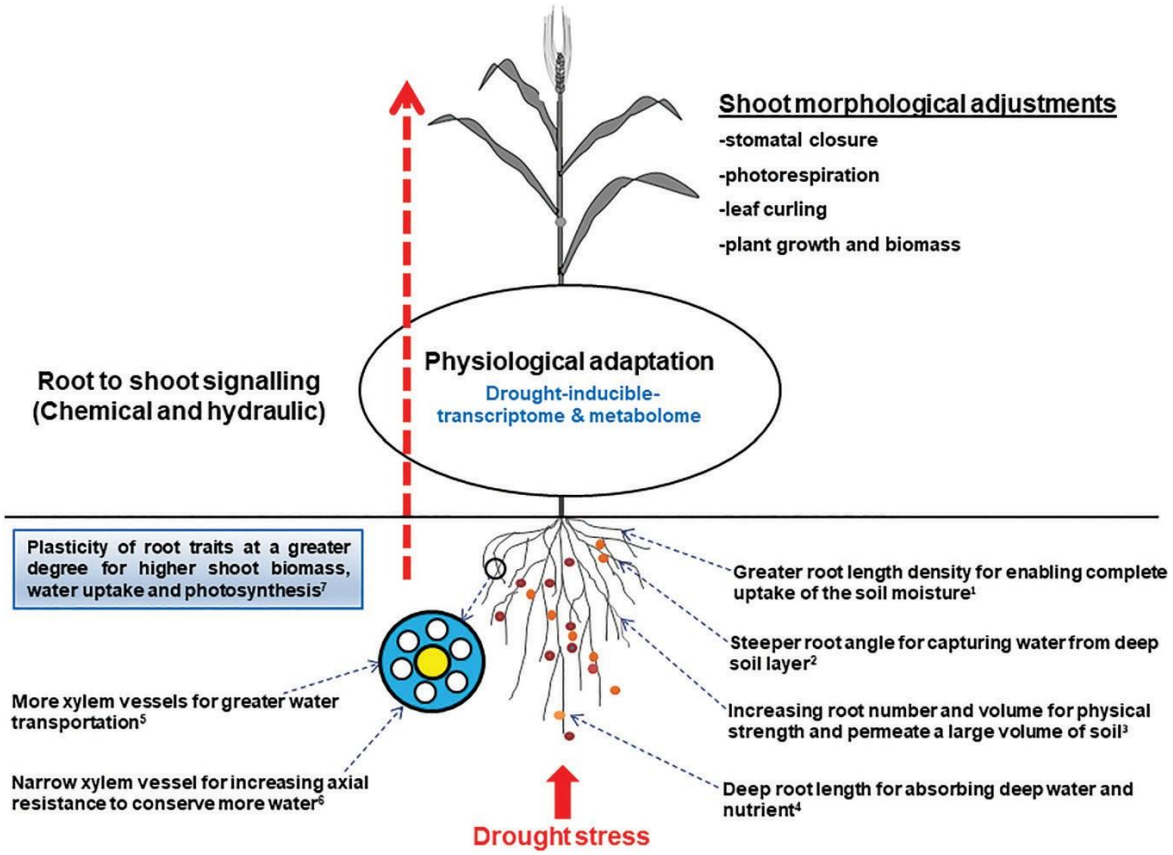

Fig. 1. Diagram of plant root–shoot system revealed functions of root system attributes to improve shoot morphological adjustment through root–shoot signaling under drought stress conditions (modified from Reinert *et al.*, 2019). ([1]Lynch, 2013; [2]Uga *et al.*, 2011; [3]Sharma *et al.*, 2011; [4]Wasson *et al.*, 2014; [5]Wasson *et al.*, 2012; [6]Richards and Passioura, 1989; [7]Kano-Nakata *et al.*, 2011).

Unlike the tap root system in dicots, major cereal crops establish a fibrous root system that comprises two components, seminal and nodal roots (Lucas *et al.*, 2000; Manske and Vlek, 2002; Smith and Smet, 2012). Seminal roots develop during post-embryogenesis from embryo radicals, while nodal roots are initiated at the base of each established tiller during ontogeny (Wahbi, 1995). The development of each tiller above ground consequently increases the number of nodal roots below ground because of their location close to the soil. The development of nodal roots in turn enhances the uptake of water and nutrients, as well as favorable gas exchanges, which facilitate the initiationof new tillers and shoot growth (Naz *et al.*, 2014). A direct positive correlation has been reported between root and shoot traits in barley (Arifuzzaman *et al.*, 2014; Naz *et al.*, 2014). However, it is still largely unknown whether shoots facilitate the production of more nodal roots or the increase in rooting influences tillering and additional shoot attributes positively. The answer to this question is of fundamental importance in understanding the interplay between root and shoot attributes to establish desirable plant architectures of cereal crops and to use potentially positive genetic and environmental interactions to increase yield and sustainability.

How do root system traits mediate tolerance to drought stress?

Roots form indispensable biological plant structures that largely contribute to the plant's ability to recover from drought stress. A 'deep, wide-spreading, much-branched root system' is a crucial landmark of drought tolerance as stated by Kramer (1969). The depth and spreading natureof root systems are recognized as the key components that allow plants to access available soil water (Blum, 2011; Fenta*et al.*, 2014), and their advantageous effects on adaption to drought stress have been determined in many economically important cereal crops.

Root angle is considered an important drought-adaptive trait that determines the horizontal and vertical distributions of roots into the soil (Christopher *et al.*, 2013; Uga *et al.*, 2013a). Root angle has been intimately linked with the deep rooting reported in rice (Kato *et al.*, 2006), wheat (Slack *et al.*, 2018, Preprint), and sorghum (Singh *et al.*, 2011). Narrower root angles may decrease the energy supplied during root penetration into the deeper soil horizons to optimize water uptake under limited rainfall conditions (Fig. 1; Wasson *et al.*, 2012; Meister *et al.*, 2014; Oyiga *et al.*, 2019). Deep rooting in thinner root systems, compared with thick or shallow root systems, has the potential to adjust to the soil components, particularly in the water-limited dry land soils (Lynch, 2014). Therefore, cultivars possessing greater primary root elongation, a lower lateral root branching tendency, and extensive root hairs are more likely to access soil moisture from deep soil layers under water shortage conditions (Wasson *et al.*, 2012; Uga *et al.*, 2013a; Akman and Topal, 2014; Lynch *et al.*, 2014). Root architectural traits are also characterized by proliferative roots developed through lateral root initiation and elongation, and these characteristics include lateral root number/volume, root length density, and root surface area, which aid in water uptake from water-limited soils (Fig. 1;Ye *et al.*, 2018). Greater root masses and root length densities improve yield performances by enhancing the water uptake rate when the subsoil layers have limited water, but they are negatively associated with grain yield when present in topsoil layers (Fang *et al.*, 2017). Another important component of a proliferative root system is root surface area, which represents the total area of the root system that is in contact with the soil, and an increase in area improves drought stress tolerance (Sharma *et al.*, 2011; Wasson *et al.*, 2012).

In addition to root architectural traits, a wide range of root anatomical traits, such as cell size, number, configuration, and density, determine the pathways through which water and nutrients enter and are transported (Marschner, 1995; Burton*et al.*, 2013). Other crucial anatomical traits, such as cell wall thickness and cell density, provide mechanical strength to the root system during severe environmental stresses (Justin and Armstrong,1987; Striker *et al.*,2007).A modification of the root anatomy, such as aerenchymal development in maize (Lynch, 2011; Burton *et al.*, 2013), may store the energy supply to accelerate soil exploration and penetration during water stress conditions (Addington *et al.*, 2006; Maseda and Fernández, 2006). The size of the root xylem vessels is correlated with drought tolerance in cereals, and a reduction in the diameters of xylem vessels increases the amount of water extracted per unit of root length (Fig. 1; Giuliani *et al.*, 2005; Comas *et al.*, 2013).The diameters and distribution of the xylem vessels, especially metaxylem that regulates root axial hydraulic conductivity, have been reported to affect drought stress tolerance in cereal crops (Kadam *et al.*, 2015, 2017). Importantly, useful anatomical traits, such as root cortical aerenchymae, cortical cell size, and the cortical cell file number, help limit the nutrient and carbon costs of soil exploration by altering root cortical tissues to air spaces (Lynch, 2013).

To cope with drought stress, cereal species tend to be plastic (Kadam *et al.*, 2017). The phenotypic plasticity of a genotype against rapid climatic fluctuations and severe drought stress requires an integrated response by different drought stress-adaptive mechanisms, such as dehydration resistance and dehydration escape or avoidance (Levit, 1972; Kadam *et al.*, 2017). Recently, several studies have shown that plasticity of root traits is mostly advantageous for the effective adaptation to drought stress (Kadam *et al.*, 2015; Sandhu *et al.*, 2016; Schneider *et al.*, 2020a, b). For instance, under drought stress conditions, the plasticity of different root traits, such as root length density and total root length (Kano *et al.*, 2011; Kano-Nakata *et al.*, 2011, 2013; Tran *et al.*, 2015), contributed to a greater shoot

biomass and increased water use and photosynthetic efficiency levels (Fig. 1). The plasticity of root system responses also induces tolerance to drought stress by increasing the number of fibrous roots, and minimizing the lateral root diameters and root biomass fluctuations (Osmont *et al.*, 2007; Meister *et al.*, 2014; Salazar-Henao *et al.*, 2016). Recently, the genomic loci regulating root phenotypic plasticity under drought stress conditions in cereal crop species (Sandhu *et al.*, 2016; Kadam *et al.*, 2017; Schneider *et al.*, 2020a, b) revealed that the plasticity of root systems might be an excellent source of genetic variation for stress adaptation (Schneider and Lynch, 2020).

Genetics of root system variation and drought stress adaptation in cereal crops

Modifications of the root system resulting from natural domestication and breeding have led to differing root architectural spatial configurations (de Dorlodot *et al.*, 2007). Therefore, the identification of novel quantitative trait loci (QTLs) is a fundamental research platform in the dissecting of the large genetic variabilities of root system attributes. Genome-wide mapping has been employed to identify novel genetic loci for root architectural traits using different mapping populations, such as introgression and recombinant inbred lines (RILs), biparental populations, and global core collections. In the following sections, we summarize the identification of essen- tial QTLs/genes for root-related drought stress adaptation in selected cereal species.

Rice

Rice is widely cultivated on lowland rainfed and irrigated areas in Asia and Africa as an essential component of subsistence farming. Rice is highly susceptible to drought stress, and even moderate drought stress may cause significant yield losses in rice (O'Toole, 1982; Centritto *et al.*, 2009). In cereals in general, but especially in rice, deep rooting is determined by the distribution of wide root growth angles and root lengths (Uga *et al.*, 2015). An enormous genetic variation in root angle distribution has been identified in two root system categories; group A has shallow rooting and group B has shallow to deep rooting on the basis of the characterization of 97 rice accessions (Tomita *et al.*, 2017). Six major effect QTLs for deep rooting were unraveled (Uga *et al.*, 2011, 2012, 2013*b*, 2015; Kitomi *et al.*, 2018) using RILs derived from a cross between 'IR64', a lowland cultivar possessing a shallow rooting system with an inactive *DEEPER ROOTING 1* (*DRO1*) allele, and 'Kinandang Patnog',an upland cultivar possessing a deep rooting system with an active *DRO1* allele, implying the involvement

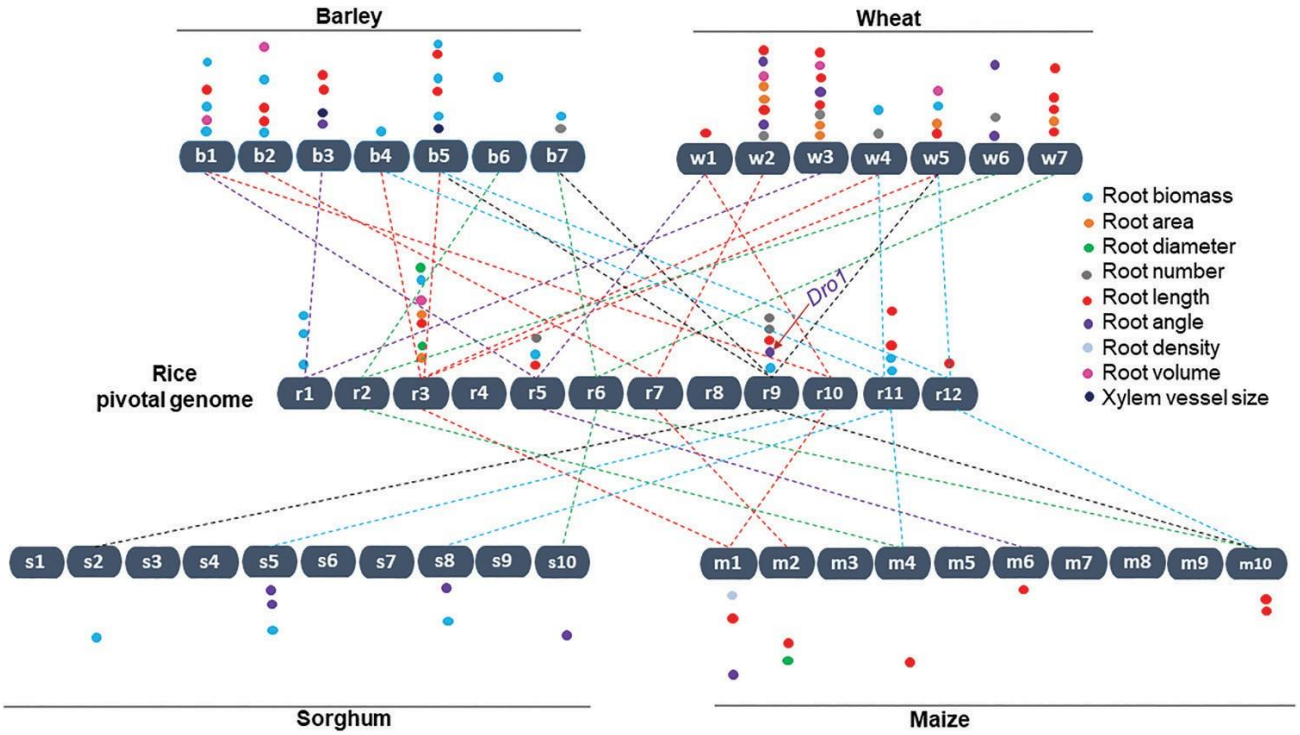

Fig. 2. Schematic representation of the cereal genome-wide microsynteny map showing the effect of major QTLs for root system attributes identified between rice chromosomes (r1–r12) adopted as a reference, and the wheat (w1–w7), barley (b1–b7), maize (m1–m10), and sorghum (s1–s10) genomes in response to drought stress. The microsynteny map was constructed based on Salse *et al.* (2009). Each line represents an orthologous locus for root-related drought-adaptive traits highlighted across the genomes. The approximate chromosomal locations of the QTLs are represented by different colors based on published reports. Detailed information and accurate positions of the QTLs are provided in Supplementary Table S1.

of the locus in the deep root phenotype (Uga *et al.*, 2011; Kitomi *et al.*, 2018). Similarly, another study identified a key QTL for root growth angle (*DRO2*) on chromosome 4 using three F_2 populations derived from crosses between each of three shallow rooting cultivars ('ARC5955', 'Pinulupot1', and 'Tupa729') and 'Kinandang Patong' (Uga *et al.*, 2013*b*). On the basis of their findings, we concluded that 'Kinandang Patong' has contributory *DRO1* and *DRO2* alleles that direct down- ward rice root growth. Kitomi *et al.* (2018) also identified two major QTLs for root length, *QUICK ROOTING 1* (*QRO1*)on chromosome 2 and *QRO2* on chromosome 6, using the same parents. High-throughput phenotyping and genotyping of a rice-mapping population of 361 diverse lines derived from a cross between 'Moroberekan' and 'Swarna' were carriedout to map QTLs for drought tolerance traits, including root architecture. The identified drought yield QTL, *qDTY3.2*, for deeper root growth contributes to sustaining the entire plant's water status by interacting with shoot-related drought toler- ance traits (Grondin *et al.*, 2018).

The genetic mapping of rice germplasms in response to drought stress has identified genomic loci associated with root traits (Fig. 2; see Supplementary Table S1 at *JXB* on- line). A meta-study resulted in the identification of a valuable genomic region, the 'QTL hotspot', harboring meta-QTLs associated with root architectural traits, such as root density, maximum root elongation and thickness, root/shoot ratio, andthe root penetration index, as well as drought tolerance traits.The 'QTL hotspot' is a demarcated segment of 5 Mb that en- compasses only a few stress-related candidate genes (Courtois*et al.*, 2009). Another study which investigated root traits of the seedlings of 162 F_{12} RILs derived from a cross between 'Milyang23' and 'Tong88-7' identified five major QTLs relatedto important root traits, such as root length, root dry weight, and dry weight (Fig. 2; Han *et al.*, 2018). The alleles for the QTLs donated by 'Tong88-7' contributed to the improvement in the root traits.The QTLs involved in drought tolerance and root architecture-related traits have been mapped using com- posite interval mapping of a cross of 'IR55419-04' and 'Super Basmati'. Three QTLs on chromosomes 3, 9, and 11 for deep rooting length, and four QTLs on chromosome 3 for deep root surface area and diameter, were identified under water deficit conditions, explaining 3.8–32.09% of the genetic vari- ance.These three QTLs (*qDRL3*, *-9*, and *-11)* for deep rooting length have donor alleles from 'IR55419-04' (Fig. 2; Sabar *et al.*, 2019). Moreover, to harness the genetic variations in root archi- tectural traits under drought conditions, an in-depth genome- wide association study (GWAS) identified 106 significant loci from a diverse panel of 274 *indica* genotypes. This included *a priori* candidate genes for regulating the water deficit stress plasticity of root architectural and anatomical characteristics (Kadam *et al.*, 2017). More recently, another study identified 143 loci contributing to 21 root traits, such as maximum root length, root volume, and root dry weight, under drought con- ditions. In total, root-related candidate genes, including *DRO1*, *WOX11*, and *OsPID* co-located with the associated loci, were identified (Li *et al.*, 2017).

Wheat

As the second most economically important grain crop, wheat has been investigated in depth for root system variation.Recently, several advanced spring wheat accessions screenedfrom the Cultivated Wheat Collection germplasms showed ef- ficient root systems for extensive deep rooting and large root biomasses (Narayanan *et al.*, 2014). The geographic area from which wheat genotypes were collected had significant influ- ences on rooting depth. The wheat subsets originating from Australia, the Mediterranean, and western Asia have greater rooting depths in comparison with subsets collected from south Asia, Latin America, Mexico, and Canada. The increased rooting length might be attributed to the adaptive traits of genotypes cultivated in the relatively drier environments of the western USA to enhance water acquisition. In a biparental RIL population derived from a cross between Chinese winterwheat varieties 'Xiaoyan 54' and 'Jing 411', two major QTLswere identified for primary root length and maximum root length, with the donor alleles being contributed by the older cultivar 'Xiaoyan 54', which has a larger and deeper root system(Ren *et al.*, 2012). A study by Ma *et al.* (2017) detected 15 QTLs on eight chromosomes related to root traits, including maximum root length and total root length, in a population of 'Q1028' and 'ZM9023'. The positive QTL alleles were con- tributed from the semi-wild parent 'Q1028', which possesses a longer root system.

Genetic studies to explore the major QTL effects on root architectural traits under different water regimes have been carried out in wheat mapping populations. Liu *et al.* (2013) mapped seven consistently expressed QTLs that were asso- ciated with seminal root traits, including total root length, seminal root number, project root area, root surface area, and seminal root angle, and the individual QTLs manifested phenotypic variations ranging from 4.98% to 24.31% under different water regimes. This study importantly noticed that one chromosomal region at the interval *Xgwm644.2–P6901.2*on chromosome 3B harbored nine QTLs affecting most ofthe root morphological traits. Recently, favorable alleles of eight QTLs linked to root length were mapped to the wheat RILs derived from a cross between 'W7984' (synthetic) and 'Opata 85' under hydroponic conditions, with two of the eight QTLs being contributed from the drought-resistant parent 'W7984' (Fig. 2; Supplementary Table S1; Ayalew *et al.*, 2017).A GWAS of 91 phenotypically diverse genotypes across 21 countries displayed two significant drought induced major al-leles that cause long root lengths under polyethylene glycol (PEG)- induced water stress. The GWAS approach also iden- tified three drought-responsive pleiotropic single nucleo- tide polymorphism (SNP) markers associated with root dry biomass in a panel of 100 bread wheat genotypes selected

on the basis of their breeding history for drought tolerance (Mathew *et al.*, 2019). Another study identified five significant markers causing extended rooting lengths under drought stress conditions using a mapping population consisting of two introgressed populations (Bhatta *et al.*, 2018).

Barley

Drought stress is a detrimental limiting factor for barley that causes up to 50% yield reductions (Jenks and Hasegawa, 2005; Samarah, 2005). Roots of 301 'BC2DH' populations derived from a cross between exotic accessions of *Hordeum vulgare* ssp. *spontaneum* C. Koch (ISR42-8) from Israel and the spring barley cultivar 'Scarlett' (*H. vulgare* ssp. *vulgare*) from Germany were sampled from the drought-induced tunnels at the mature stage and analyzed for root and other important physiological traits, including yield. When investigating favorable drought-responsive QTLs, Sayed (2011) found that the wild parent donated the favorable alleles to 27 (34.1%) of the 79 QTLs that influenced root and physiological traits. These novel exotic alleles contribute to drought-adaptive traits, such as root length and proline content. For instance, the presence of exotic alleles at marker locus *VrnH1* resulted in an extension of the root length by 9.17% under drought stress conditions. This result im- plied that the introgression from wild barley promoted longerroot lengths in the 'S42' population. Using these introgression lines, other studies identified seven QTLs associated with root architectural traits, with the introgression of exotic alleles at the *QRl.S42.5H* loci accounting for a 9% increase in root length (Fig. 2; Supplementary Table S1; Arifuzzaman *et al.*, 2014). Naz *et al.* (2014) reported six major QTLs for root length, eight for root dry weight, and five for root volume, and all the beneficial QTL alleles of wild origin have been fixed in the 'Scarlett' cultivar background (Fig. 2). Moreover, high-throughput GWAS mapping for detecting QTLs associated with root architectural traits has been reported in barley recently. An association mapping study by Reinert *et al.* (2016) using 179 diverse genotypes, comprising 48 wild accessions and 131 cultivars, across 38 countries identified two drought-adaptive QTLs for root dry biomass on chromosomes 2H and 5H. By comparing their relative performances, a potential QTL (*QRdw.2H*) was identified on chromosome 5H at 95 cM, where the homozygous major allele produced the greatest variability on the phenotype (R^2=24.93%) (Fig. 2; Supplementary Table S1; Reinert *et al.*, 2016). A panel of 233 barley genotypes containing a majority of the lines (223) from a worldwide broad genetic and phenotypic diversity panel, in which 58% of the genotypes were two rowed and 42% were six rowed, were analyzed for root architecture traits under drought stress conditions using a recently developed high-throughput phenotyping method. This study precisely identified a catalog of QTL-harboring 'hotspots' and four QTLs for drought-inducing root traits (Fig. 2; Supplementary Table S1; Abdel-Ghani *et al.*, 2019). Another recent study performed a comprehensive GWAS across three cropping seasons using a 192 diverse spring barley panel to characterize both root morphological and anatomical traits under water deficit stress. Three to four QTL intervals showed strong effects across growing seasons for both root morphological and anatomical traits in response to water deficit stress (Fig. 2; Supplementary Table S1; Oyiga *et al.*, 2019).

Maize

Maize originated in a semi-arid area, where it grew in less fertile soil that lacked sufficient irrigation and fertilizers. Thus, improving the stress resilience of maize is necessary for continued crop production in these less cultivable areas. Large genetic diversity and heritability levels were found for maize root system traits (Burton *et al.*, 2014), ranging from small and compact to large and exploratory patterns, in a RIL nested association mapping (NAM) subpopulation derived from a cross between 'B73' (compact root system) and 'Ki3' (exploratory root system) (Zurek *et al.*, 2015). Clusters of QTLs for both root depth and average root width were mapped on chromosomes 2, 9, and 10, with the large additive effects on root depth and average root width originating from the 'Ki3' allele. QTL mapping using 187 'BC_4F_3' maize lines derived from an interspecific cross between a larger root system donor parental line ('Ye478') and a small root system recurrent parental line ('Wu312') revealed 30 QTLs for root architectural traits, with 80.6% carrying a favorable allele originating from the donor parent 'Ye478' (Cai *et al.*, 2012). A single QTL was detected for drought-related traits using two inbred parents from drought-tolerant and -sensitive populations, and root density contributed 24% of the phenotypic variation (Fig. 2; Supplementary Table S1; Rahman *et al.*, 2011). Recently, a study identified major QTL effects for crown root angle (*CRA2*) and crown root length (*CRL1*) under drought conditions using a RIL population comprising 204 F_8 lines derived from a cross between two inbred lines, 'DH1M' and 'T877' (Fig. 2; Supplementary Table S1; Li *et al.*, 2018). The 'T877' allele contributed a major effect on root angle at an SNP marker (288.8 cM), whereas the favorable allele for primary root length was from 'DH1M'. Additionally, an in-depth GWAS was performed to identify SNPs for the most important root functional and structural traits, including rooting depth, root length, and root length density, related to drought-adaptive mechanisms using the CIMMYT Asia association mapping panel, consisting of 396 diverse inbred maize lines derived from tropical and subtropical pools and populations from the Latin American, African, and Asian maize programs. The CIMMYT lines were drought tolerant. In total, 18 SNPs were identified from manually and digitally scored root functional and structural traits that showed common associations with more than one trait. Of these, 12 SNPs were observed within or near the various gene functional regions (Zaidi *et al.*, 2016). A few recent field-based GWAS approaches pinpointed candidate genes for drought stress and environmental plasticity of root architectural and anatomical

phenes using a large association panel comprised of maize inbred lines. The report showed that root phenotypic plasticity was highly quantitative, and plasticity loci were distinct from the loci that govern trait expression under water deficit and environmental stress conditions (Schneider *et al.*, 2020a, b).

Sorghum

Sorghum is widely cultivated in tropical and subtropical semi-arid regions, mostly under natural soil moisture conditions. Large genetic diversity levels in root and shoot traits associated with drought stress were observed in 141 F_6 RILs from a cross between two parents possessing a narrow and a wide angle for the first flush of nodal roots (Mace *et al.*, 2012). In this study, nodal root angle was significantly correlated with shoot traits, and four major QTLs for nodal root angle (*qRA*) were also successfully identified, which together explained 58.2% of the phenotypic variation (Fig. 2; Supplementary Table S1).

Comparative genomics of root-related drought stress adaptation using microsynteny among cereal crop species

Evolving from a common ancestor, cereal crops revealed a significant genetic conservation among themselves (Salse *et al.*, 2008).This genetic conservation can be traced among the species using molecular (genomic) data and full-length genome sequence data for cereal crops. This concept also led to the establishment of inter-specific hybrid genome maps to identify syntenic chromosomal regions precisely across genomes as well as their interspecies variation. Here, we showed a comparative genomic map of cereal crops that revealed their genetic synteny of genome-wide QTLs/loci for root attributes related to drought stress adaptation (Fig. 2).

To date, 23, 31, 24, 9, and 7 major QTL effects on the different root traits in response to drought stress have been identified across the chromosomes of rice, wheat, barley, maize, and sorghum, respectively (Fig. 2; Supplementary Table S1). Interestingly, rice chromosomes r6, r9, and r11 were found to be syntenic with wheat chromosomes w7, w5, and w4, respectively, and barley chromosomes b7, b5, and b4, respectively, and they also had syntenic relationships with maize chromosomes m10, m10, and m4, respectively, and sorghum chromosomes s10, s2, and s8, respectively (Fig. 2). These syntenic regions revealed drought-adaptive QTLs for various root system attributes (Fig. 2), predicting a conserved genetic regulation among cereal genomes. Such synteny may facilitate an understanding of genome-wide relationships among QTLs/genes related to stress adaptation. More importantly, the unique cloned and characterized drought-adaptive rice gene *DRO1*, which regulates root growth angle, showed a high-yield performance under drought stress conditions (Uga *et al.*, 2013a). This gene lies on rice chromosome r9, which showed a syntenic relationship with wheat chromosome w5, barley chromosomes b5 and b7, maize chromosome m10, and sorghum chromosome s2, and all the syntenic chromosomal regions revealed associations with root-related drought stress adaptation (Fig. 2). This genome-wide syntenic relationship implies that other economically important cereal crops, such as wheat, barley, maize, and sorghum, contain *DRO1* homologs that might be useful for promoting root-related drought stress adaptations in cereals using comparative genomics. Furthermore, it will aid in the utilization of the genetic potential of crop species for particular adaptive responses to alter a specific mechanism in another species using natural genetic variations. However, the number of commonalities does not correspond to the genetic conservation. Such gaps may result from limited studies in one or the other cereal species because of large root phenotyping. Therefore, based on this microsynteny map, new studies should focus on root system characterization and genomics that may provide distinct genetic loci or genetic mechanisms among cereal crop species.

Directions of future research on root system variations in drought stress adaptation and their introduction into breeding programs

Roots and shoots evolved together for nearly 3.5 million years. However, owing to directional selection for yield in the past century, root attributes were completely neglected in breeding programs, unless the improvement was indirect. Therefore, a future breeding dimension should focus simultaneously on the recruitment of lost root system variations for yield and sustainability.

Several studies reported that root system attributes enhance shoot architecture for yield and drought fitness in cereals, reflecting that roots should be the foremost breeding target of the future (Naz *et al.*, 2014; Sandhu *et al.*, 2016; Li *et al.*, 2018). The natural genetic diversity in differential root system architecture may be useful to understand drought adaptation mechanisms and improve cultivars by generating beneficial root architecture.To date, studies have reported and validated QTLs associated with root system traits, such as root length, biomass, number, angle, volume, diameter, density, and xylem vessel size, under drought stress conditions (Fig. 2; Supplementary Table S1). More importantly, the diversity of the wild relatives of crops showed remarkable root system variations that have great potential in drought stress adaptation (Naz *et al.*, 2014; Reinert *et al.*, 2016). Here, we summarized a considerable amount of donor genotypes, including wild relatives (Supplementary Table S1), but very limited strategies have been undertaken to exploit these lines in resilient breeding programs. These promising donor parents need to be introgressed into elite backgrounds to enhance the stress-adaptive potential of the cultivated gene pool.

The enhancement of root-related drought stress adaptation by applying classical breeding is difficult owing to the complexity levels of these traits (Witcombe *et al.*, 2007;Van Oosten *et al.*, 2016). Genomic and phenomic approaches are gaining popularly as important tools that allow in-depth analyses of crops to increase our understanding of the complexity of the mechanisms underlying stress adaptation. Although both *cis*- and *trans*-genetic components, along with epigenetics, are involved directly in trait complexity, the role of *cis*-genetic modules appears to be more influential on the quantitative divergence in expression of genes controlling polygenic traits across dynamic environments (Signor and Nuzhdin, 2018). Therefore, genotype×environment interactions form the biggest challenge in the precise genetic determination of these traits under field conditions.This scenario demands an expression QTL analysis as a high-resolution genomics approach for the precise dissection of traits at morphological and physiological levels across varying environments. In addition, over the last decades, NGS and bioinformatics tools have been rapidly advancing, allowing the discovery of new genes and regulatory sequences controlling diverse complex traits (Taunk *et al.*, 2019).

Comparative genomics is another reliable cutting-edge avenue that has increased the amount of available genomic information. Comparative genomic analyses characterize genomic structural alterations, gene structures, and genome synteny, as well as induced functions among cereal crop species. Using comparative genomics tools, stress-responsive differentially expressed genes regulating root system architectural traits have been identified in rice (Lou *et al.*, 2017), wheat (Dalal *et al.*, 2018; Hu *et al.*, 2018), maize (Li *et al.*, 2017), and barley (Kwasniewski *et al.*, 2016). For example, transcriptome profiling in rice identified 49 candidate differentially expressed genes, and a weighted gene co-expression network analysis confirmed 18 hub genes, all of which were more highly expressed in deep roots than in shallow roots (Lou *et al.*, 2017). Genetic modifications represent another viable option for crop advancement (Hussain, 2015; Mwadzingeni *et al.*, 2017). They provide the unique opportunity to edit the targeted genome sequences for particular breeding aims. Genome editing was recently revolutionized by CRISPR/Cas9 [clustered regularly interspaced palindromic repeats (CRISPR)/CRISPR-associated protein 9]-based approaches. As an advanced breeding tool, the CRISPR/Cas9 system has been successfully utilized to develop novel variants of *ARGOS8* by editing its promoter sequences to increase expression, which enhanced maize yield potentials under natural field drought stress conditions (Shi *et al.*, 2017). The above high-resolution geneticsand genomic approaches may help dissect trait complexity and target selection in breeding (such as genomic selection), as well as functional analyses of genes controlling root-borne shoot dynamics and crosstalk in the determination of yield potentials in cereals.

In summary, we propose to implement the following multistep root breeding strategies to establish drought stress adaptations in cereals: (i) screening global genetic diversity levels using diverse natural populations to identify morphological and physiological novelties for root–shoot attributes related to yield and sustainability; (ii) establishing state-of-the-art populations for the high-resolution and quantitative dissection of traits; (iii) using high-throughput non-invasive and automated tools for root phenotyping under field conditions; (iv) combining high-resolution phenotypic trait data with genome-wide molecular data to identify QTL epistasis and gene×environment interactions using state-of-the-art computing models; (v) analyzing sequences of wild, landraces, and donor lines to dissect allelic variations associated with root-related drought stress adaptations using comparative genomics; (vi) deploying stably expressed major QTL effects and 'QTL hotspot' re- gions, as well as genomic selection tools, that integrate phenotype, genotype, and environment to improve breeding stocks; (vii) forwarding large effect QTLs both individually and by pyramiding QTLs for the functional characterization of the underlying genes; (viii) characterizing genetic synteny across the cereal genomes and developing interspecies hybrid genetic maps for gene isolation, comparative analyses, and interspecies introgression; (ix) employing expression QTL analyses based on RNA-sequencing as molecular phenotypes for high-resolution gene trait analyses; (x) manipulating and editing gene functions using technologies such as CRISPR/Cas9; (xi) establishing a link between quantitative traits and epigenetic signatures to reveal major roles in drought stress adaptation; and (xii) establishing an interdisciplinary research platform among geneticists, breeders, biotechnologists, agronomists, and crop physiologists to combine knowledge on root system variation. These efforts will allow us to focus on the most relevant traits,their combinations, and interplay in breeding programs to develop resilient crops and to secure sustainable cereal production under changing climatic conditions.

Supplementary data

The following supplementary data are available at *JXB* online.

Table S1. List of recently identified major effect QTLs/genes associated with root system attributes to drought stress in major cereal crops.

Acknowledgements

The authors would like to gratefully acknowledge the German Academic Exchange Service (DAAD) for providing a PhD fellowship to MNS and German Federal Ministry of Education and Research (BMBF) and PTJ for funding with the grant 031A354 the project BRIWECS.

Author contributions

MNS: conceptualization, data curation, writing—original draft preparation, writing-review and editing; JL: supervision and validation; AAN: conceptualization, writing—review and editing, and validation,AB: supervision, conceptualization, writing—review and editing, and validation.

Conflict of interest

The authors declare no conflict of interest.

References

Abdel-Ghani AH, Sharma R, Wabila C, *et al.* 2019. Genome-wide association mapping in a diverse spring barley collection reveals the presence of QTL hotspots and candidate genes for root and shoot architecture traits at seedling stage. BMC Plant Biology **19**, 216.

Addington RN, Donovan LA, Mitchell RJ, Vose JM, Pecot SD, Jack SB, Hacke UG, Sperry JS, Oren R. 2006. Adjustments in hydraulic architecture of *Pinus palustris* maintain similar stomatal conductance in xeric and mesic habitats. Plant, Cell & Environment **29**, 535–545.

Akman H, Topal A. 2014. Distribution of root biomass in different growth stages of wheat grown under field conditions. In: International Conference on Plant Biology and Biotechnology. Session 3. Plant Physiology and Biochemistry, Almaty, Kazakhstan.

Anjum SA, Wang LC, Farooq M, Hussain M, Xue LL, Zou CM. 2011. Brassinolide application improves the drought tolerance in maize through modulation of enzymatic antioxidants and leaf gas exchange. Journal of Agronomy and Crop Science **197**, 177–185.

Arifuzzaman M, Sayed MA, Muzammil S, Pillen K, Schumann H, Naz AA, Léon J. 2014. Detection and validation of novel QTL for shoot and root traits in barley (*Hordeum vulgare* L.). Molecular Breeding **34**, 1373–1387.

Ayalew H, Liu H, Yan G. 2017. Identification and validation of root length QTLs for water stress resistance in hexaploid wheat (*Titicum aestivum* L.). Euphytica **213**,126.

Basu S, Ramegowda V, Kumar A, Pereira A. 2016. Plant adaptation to drought stress. F1000Research **5**, F1000 Faculty Rev-1554.

Bhatta M, Morgounov A, Belamkar V, Baenziger PS. 2018. Genome-wide association study reveals novel genomic regions for grain yield and yield-related traits in drought-stressed synthetic hexaploid wheat. International Journal of Molecular Science **19**, 3011.

Blankenagel S, Yang Z, Avramova V, Schön CC, Grill E. 2018. Generating plants with improved water use efficiency. Agronomy **8**, 194.

Blum A. 2005. Drought resistance, water-use efficiency, and yield potential—are they compatible, dissonant, or mutually exclusive? Crop Pasture Science **56**, 1159–1168.

Blum A. 2011. Plant breeding for water-limited environments. New York: Springer.

Bray EA, Bailey-Serres J, Weretilnyk K. 2000. Responses to abiotic stresses. In: Buchanan BB, Gruissem W, Jones RL, eds. Biochemistry and molecular biology of plants. Rockville, MD: American Society of Plant Physiologists, 1158–1203.

Burton AL, Johnson JM, Foerster JM, Hirsch CN, Buell CR, Hanlon MT, Kaeppler SM, Brown KM, Lynch JP. 2014. QTL mapping and phenotypic variation for root architectural traits in maize (*Zea mays* L.). Theoretical and Applied Genetics **127**, 2293–2311.

Burton AL, Lynch JP, Brown KM. 2013. Spatial distribution and phenotypic variation in root cortical aerenchyma of maize (*Zea mays* L.). Plant and Soil **367**, 263–274.

Cai H, Chen F, Mi G, Zhang F, Maurer HP, Liu W, Reif JC, Yuan L. 2012. Mapping QTLs for root system architecture of maize (*Zea mays* L.) in the field at different developmental stages. Theoretical and Applied Genetics **125**, 1313–1324.

Centritto M, Lauteri M, Monteverdi MC, Serraj R. 2009. Leaf gas exchange, carbon isotope discrimination, and grain yield in contrasting rice genotypes subjected to water deficits during the reproductive stage. Journal of Experimental Botany **60**, 2325–2339.

Checker VG, Chhibbar AK, Khurana P. 2012. Stress-inducible expression of barley *Hva1* gene in transgenic mulberry displays enhanced tolerance against drought, salinity and cold stress. Transgenic Research **21**, 939–957.

Chen Y, Palta JA, Wu P. Siddique KHM. 2019. Crop root systems and rhizosphere interactions. Plant and Soil **439**, 1–5.

Choat B, Brodribb TJ, Brodersen CR, Duursma RA, López R, Medlyn BE. 2018. Triggers of tree mortality under drought. Nature **558**, 531–539.

Christopher J, Christopher M, Jennings R, Jones S, Fletcher S, Borrell A, Manschadi AM, Jordan D, Mace E, Hammer G. 2013. QTL for root angle and number in a population developed from bread wheat (*Triticum aestivum*) with contrasting adaptation to water-limited environments. Theoretical and Applied Genetics **126**, 1563–1574.

Comas LH, Becker SR, Cruz VM, Byrne PF, Dierig DA. 2013. Root traits contributing to plant productivity under drought. Frontiers in Plant Science **4**, 442.

Courtois B, Ahmadi N, Khowaja F, Price AH, Rami J, Frouin J, Hamelin C, Ruiz M. 2009. Rice root genetic architecture: meta-analysis from a drought QTL database. Rice **2**, 115.

Dalal M, Sahu S, Tiwari S, Rao AR, Gaikwad K. 2018. Transcriptome analysis reveals interplay between hormones, ROS metabolism and cell wall biosynthesis for drought-induced root growth in wheat. Plant Physiology and Biochemistry **130**, 482–492.

Daryanto S, Wang L, Jacinthe PA. 2016. Global synthesis of drought effects on maize and wheat production. PLoS One **11**, e0156362.

Daryanto S, Wang L, Jacinthe P. 2017. Global synthesis of drought effects on cereal, legume, tuber and root crops production: a review. Agricultural Water Management **179**, 18–33.

Davies WJ, Wilkinson S, Loveys B. 2002. Stomatal control by chemical signalling and the exploitation of this mechanism to increase water use efficiency in agriculture. New Phytologist **153**, 449–460.

de Dorlodot S, Forster B, Pagès L, Price A, Tuberosa R, Draye X. 2007. Root system architecture: opportunities and constraints for genetic improvement of crops. Trends in Plant Science **12**, 474–481.

Earl H, Davis RF. 2003. Effect of drought stress on leaf and whole canopy radiation use efficiency and yield of maize. Agronomy Journal **95**, 688–696.

Fahad S, Bajwa AA, Nazir U, *et al.* 2017. Crop production under drought and heat stress: plant responses and management options. Frontiers in Plant Science **8**, 1147.

Fan Y, Miguez-Macho G, Jobbágy EG, Jackson RB, Otero-Casal C. 2017. Hydrologic regulation of plant rooting depth. Proceedings of the National Academy of Sciences, USA **114**, 10572–10577.

Fang Y, Du Y, Wang J, Wu A, Qiao S, Xu B, Zhang S, Siddique KHM, Chen Y. 2017. Moderate drought stress affected root growth and grain yield in old, modern and newly released cultivars of winter wheat. Frontiers in Plant Science **8**, 672.

FAO. 2018. The future of food and agriculture– alternative pathways to 2050. Rome: Food and Agriculture Organization.

Farooq M, Wahid A, Kobayashi N, Fujita D, Basra SMA. 2009. Plant drought stress: effects, mechanisms and management. Agronomy for Sustainable Development **29**, 185–212.

Fenta BA, Beebe SE, Kunert KJ, Burridge JD, Barlow KM, Lynch PJ. 2014. Field phenotyping of soybean roots for drought stress tolerance. Agronomy **4**, 418–435.

Francini A, Sebastiani L. 2019. Abiotic stress effects on performance of horticultural crops. Horticulturae **5**, 67.

Gewin V. 2010. Food: an underground revolution. Nature **466**, 552–553.

Giuliani S, Sanguineti MC, Tuberosa R, Bellotti M, Salvi S, Landi P. 2005. Root-ABA1, a major constitutive QTL, affects maize root architecture and leaf ABA concentration at different water regimes. Journal of Experimental Botany **56**, 3061–3070.

Govindaraj M, Vetriventhan M, Srinivasan M. 2015. Importance of genetic diversity assessment in crop plants and its recent advances: an overview of its analytical perspectives. Genetics Research International **2015**, 431487.

Grondin A, Dixit S, Torres R, Venkateshwarlu C, Rogers E, Mitchell-Olds T, Benfey PN, Kumar A, Henry A. 2018. Physiological mechanisms contributing to the QTL qDTY$_{3.2}$ effects on improved performance of rice Moroberekan×Swarna BC2F$_{3:4}$ lines under drought. Rice **11**, 43.

Han J, Shin N, Jang S, Yu Y, Chin JH, Yoo S. 2018. Identification of quantitative trait loci for vigorous root development under water-deficiency conditions in rice. Plant Breeding and Biotechnology **6**, 147–158.

Hu L, Xie Y, Fan S, Wang Z, Wang F, Zhang B, Li H, Song J, Kong L. 2018. Comparative analysis of root transcriptome profiles between drought-tolerant and susceptible wheat genotypes in response to water stress. Plant Science **272**, 276–293.

Hussain B. 2015. Modernization in plant breeding approaches for improving biotic stress resistance in crop plants. Turkish Journal of Agriculture and Forestry **39**, doi: 10.3906/tar-1406-176.

Hussain HA, Hussain S, Khaliq A, Ashraf U, Anjum SA, Men S, Wang L. 2018. Chilling and drought stresses in crop plants: implications, cross talk, and potential management opportunities. Frontiers in Plant Science **9**, 393.

Ibrahim SE, Schubert A, Pillen K, Léon, J. 2012. QTL analysis of drought tolerance for seedling root morphological traits in an advanced backcross population of spring wheat. International Journal of Agricultural Science **2**, 619–629.

Jenks MA, Hasegawa PM. 2005. Plant abiotic stress. Oxford, UK: Blackwell Publishers.

Ji X, Shiran B, Wan J, Lewis DC, Jenkins CL, Condon AG, Richards RA, Dolferus R. 2010. Importance of pre-anthesis anther sinkstrength for maintenance of grain number during reproductive stage waterstress in wheat. Plant, Cell & Environment **33**, 926–942.

Jia W, Zhang J. 2008. Stomatal movements and long-distance signaling in plants. Plant Signaling & Behavior **3**, 772–777.

Joshi R, Wani SH, Singh B, Bohra A, Dar ZA, Lone AA, Pareek A, Singla-Pareek SL. 2016. Transcription factors and plants response to drought stress: current understanding and future directions. Frontiers in Plant Science **7**, 1029.

Justin SHFW, Armstrong W. 1987. The anatomical characteristics of roots and plant response to soil flooding. New Phytologist **106**, 465–495.

Kadam NN, Tamilselvan A, Lawas LMF, *et al.* 2017. Genetic control of plasticity in root morphology and anatomy of rice in response to water deficit. Plant Physiology **174**, 2302–2315.

Kadam NN, Yin X, Bindraban PS, Struik PC, Jagadish KS. 2015. Does morphological and anatomical plasticity during the vegetative stage make wheat more tolerant of water deficit stress than rice? Plant Physiology **167**, 1389–1401.

Kano M, Inukai Y, Kitano H, Yamauchi A. 2011. Root plasticity as the key root trait for adaptation to various intensities of drought stress in rice. Plant and Soil **342**, 117–128.

Kano-Nakata M, Gowda VR, Henry A, Serraj R, Inukai Y, Fujita D, Yamauchi A. 2013. Functional roles of the plasticity of root system development in biomass production and water uptake under rainfed lowland conditions. Field Crops Research **144**, 288–296.

Kano-Nakata M, Inukai Y, Wade LJ, Siopongco JDLC, Yamauchi A. 2011. Root development, water uptake, and shoot dry matter productionunder water deficit conditions in two CSSLs of rice: functional roles of root plasticity. Plant Production Science **14**, 307–317.

Kato Y, Abe J, Kamoshita A, Yamagishi J. 2006. Genotypic variation in root growth angle in rice (*Oryza sativa* L.) and its association with deep root development in upland fields with different water regimes. Plant and Soil **287**, 117–129.

Kell DB. 2011. Breeding crop plants with deep roots: their role in sustainable carbon, nutrient and water sequestration. Annals of Botany **108**, 407–418.

Khan MA, Gemenet DC, Villordon A. 2016. Root system architecture and abiotic stress tolerance: current knowledge in root and tuber crops. Frontiers in Plant Science **7**, 1584.

Kitomi Y, Nakao E, Kawai S, Kanno N, Ando T, Fukuoka S, Irie K, Uga Y. 2018. Fine mapping of *QUICK ROOTING 1* and *2*, quantitative trait loci increasing root length in rice. G3 **8**, 727–735.

Ko D, Kang J, Kiba T, *et al.* 2014. Arabidopsis ABCG14 is essential for the root-to-shoot translocation of cytokinin. Proceedings of the National Academy of Sciences, USA **111**, 7150–7155.

Koevoets IT, Venema JH, Elzenga JT, Testerink C. 2016. Roots withstanding their environment: exploiting root system architecture responses to abiotic stress to improve crop tolerance. Frontiers in Plant Science **7**, 1335.

Kramer PJ. 1969. Plant and soil water relationships: a modern synthesis. New York: McGrawHill.

Kwasniewski M, Daszkowska-Golec A, Janiak A, Chwialkowska K, Nowakowska U, Sablok G, Szarejko I. 2016. Transcriptome analysis reveals the role of the root hairs as environmental sensors to maintain plant functions under water-deficiency conditions. Journal of Experimental Botany **67**, 1079–1094.

Lamaoui M, Jemo M, Datla R, Bekkaoui F. 2018. Heat and drought stresses in crops and approaches for their mitigation. Frontiers in Chemistry **6**, 26.

Leng G, Hall J. 2019. Crop yield sensitivity of global major agricultural countries to droughts and the projected changes in the future. The Science of the Total Environment **654**, 811–821.

Levitt J. 1972. Responses of plants to environmental stresses. New York: Academic Press.

Li P, Zhang Y, Yin S, *et al.* 2018. QTL-by-environment interaction in the response of maize root and shoot traits to different water regimes. Frontiers in Plant Science **9**, 229.

Li T, Yang H, Zhang W, Xu D, Dong Q, Wang F, Lei Y, Liu G, Zhou Y, Chen H, Li C. 2017. Comparative transcriptome analysis of root hairs proliferation induced by water deficiency in maize. Journal of Plant Biology **60**, 26–34.

Liu X, Li R, Chang X, Jing R. 2013. Mapping QTLs for seedling root traits in a doubled haploid wheat population under different water regimes. Euphytica **189**, 51–66.

Lopes MS, Araus JL, van Heerden PD, Foyer CH. 2011. Enhancing drought tolerance in C$_4$ crops. Journal of Experimental Botany **62**, 3135–3153.

Lou Q, Chen L, Mei H, *et al.* 2017. Root transcriptomic analysis revealing the importance of energy metabolism to the development of deep roots in rice (*Oryza sativa* L.). Frontiers in Plant Science **8**, 1314.

Lucas ME, Hoad SP, Russel G, Bingham IJ. 2000. Management of cereal root systems. The Home-Grown Cereals Authority (HGCA) Research Review Workshop. Research Review No. 43.

Lynch JP. 2011. Root phenes for enhanced soil exploration and phosphorus acquisition: tools for future crops. Plant Physiology **156**, 1041–1049.

Lynch JP. 2013. Steep, cheap and deep: an ideotype to optimize water and N acquisition by maize root systems. Annals of Botany **112**, 347–357.

Lynch JP. 2014. Root phenes that reduce the metabolic costs of soil exploration: opportunities for 21st century agriculture. Plant, Cell & Environment **38**, 1775–1784.

Lynch JP, Chimungu JG, Brown KM. 2014. Root anatomical phenes associated with water acquisition from drying soil: targets for crop improvement. Journal of Experimental Botany **65**, 6155–6166.

Ma J, Luo W, Zhang H, *et al.* 2017. Identification of quantitative trait loci for seedling root traits from Tibetan semi-wild wheat (*Triticum aestivum* ssp. *tibetanum*). Genome **25**, 1–8.

Mace ES, Singh V, Van Oosterom EJ, Hammer GL, Hunt CH, Jordan DR. 2012. QTL for nodal root angle in sorghum (*Sorghum bicolor*

L. Moench) co-locate with QTL for traits associated with drought adaptation. Theoretical and Applied Genetics **124**, 97–109.

Maeght JL, Rewald B, Pierret A. 2013. How to study deep roots—and why it matters. Frontiers in Plant Science **4**, 299.

Manske GGB, Vlek PLG. 2002. Root architecture—wheat as a model plant. In: Waisel Y, Eshel A, Kafkafi U, eds. Plant roots: the hidden half. New York: Marcel Dekker Inc., 249–260.

Marschner H. 1995. Mineral nutrition of higher plants, 2nd edn. New York: Academic Press.

Maseda PH, Fernández RJ. 2006. Stay wet or else: three ways in which plants can adjust hydraulically to their environment. Journal of Experimental Botany **57**, 3963–3977.

Mathew I, Shimelis H, Shayanowako AIT, Laing M, Chaplot V. 2019. Genome-wide association study of drought tolerance and biomass allocation in wheat. PLoS One **14**, e0225383.

Meister R, Rajani MS, Ruzicka D, Schachtman DP. 2014. Challenges of modifying root traits in crops for agriculture. Trends in Plant Science **19**, 779–788.

Mwadzingeni L, Figlan S, Shimelis H, Mondal S, Tsilo TJ. 2017. Genetic resources and breeding methodologies for improving drought tolerance in wheat. Journal of Crop Improvement **31**, 648–672.

Mwadzingeni L, Shimelis H, Dube E, Laing MD, Tsilo TJ. 2016. Breeding wheat for drought tolerance: progress and technologies. Journal of Integrative Agriculture **15**, 935–943.

Narayanan S, Mohan A, Gill KS, Prasad PV. 2014. Variability of root traits in spring wheat germplasm. PLoS One **9**, e100317.

Naz AA, Arifuzzaman M, Muzammil S, Pillen K, Léon J. 2014. Wild barley introgression lines revealed novel QTL alleles for root and related shoot traits in the cultivated barley (*Hordeum vulgare* L.). BMC Genetics **15**, 107.

Naz AA, Raman S, Martinez CC, Sinha NR, Schmitz G, Theres K. 2013. Trifoliate encodes an MYB transcription factor that modulates leaf and shoot architecture in tomato. Proceedings of the National Academy of Sciences, USA **110**, 2401–2406.

Osmont KS, Sibout R, Hardtke CS. 2007. Hidden branches: developments in root system architecture. Annual Review of Plant Biology **58**, 93–113.

O'Toole JC. 1982. Adaptation of rice to drought prone environments. In: Drought resistance in crops with emphasis on rice. Los Baños, Philippines: IRRI, 195–213.

Oyiga BC, Palczak J, Wojciechowski T, Lynch JP, Naz AA, Léon J, Ballvora A. 2019. Genetic components of root architecture and anatomy adjustments to water-deficit stress in spring barley. Plant, Cell & Environment **43**, 692–711.

Palta JA, Chen X, Milroy SP, Rebetzke GJ, Dreccer MF, Watt M. 2011. Large root systems: are they useful in adapting wheat to dry environments? Functional Plant Biology **38**, 347–354.

Polania J, Poschenrieder C, Rao I, Beebe S. 2017. Root traits and their potential links to plant ideotypes to improve drought resistance in common bean. Theoretical and Experimental Plant Physiology **29**, 143–154.

Puig J, Pauluzzi G, Guiderdoni E, Gantet P. 2012. Regulation of shoot and root development through mutual signaling. Molecular Plant **5**, 974–983.

Rahman H, Pekic S, Lazic-Jancic V, Quarrie SA, Shah SM, Pervez A, Shah MM. 2011. Molecular mapping of quantitative trait loci for drought tolerance in maize plants. Genetics and Molecular Research **10**, 889–901.

Randhawa M, Maqsood M, Shehzad M, *et al.* 2017. Light interception, radiation use efficiency and biomass accumulation response of maize to integrated nutrient management under drought stress conditions. Turkish Journal of Field Crops **22**, 134–142.

Rascher U, Blossfeld S, Fiorani F, *et al.* 2011. Non-invasive approaches for phenotyping of enhanced performance traits in bean. Functional Plant Biology **38**, 968–983.

Reinert S, Kortz A, Léon J, Naz AA. 2016. Genome-wide association mapping in the global diversity set reveals new QTL controlling root system and related shoot variation in barley. Frontiers in Plant Science **7**, 1061.

Reinert S, Osthoff A, Léon J, Naz AA. 2019. Population genetics revealed a new locus that underwent positive selection in barley. International Journal of Molecular Sciences **20**, 202.

Ren Y, He X, Liu D, Li J, Zhao X, Li B, Tong Y, Zhang A, Li Z. 2012. Major quantitative trait loci for seminal root morphology of wheat seedlings. Molecular Breeding **30**, 139–148.

Richards RA, Passioura JB. 1989. A breeding program to reduce the diameter of the major xylem vessel in the seminal roots of wheat and its effect on grain yield in rain-fed environments. Australian Journal of Agricultural Research **40**, 943–950.

Rosa NM, Lin CW, Kang YJ, Dhondt S, Gonzalez N, Inzé D, Falter-Braun P. 2019. Drought resistance is mediated by divergent strategies in closely related Brassicaceae. New Phytologist **223**, 783–797.

Ruggiero A, Punzo P, Landi S, Costa A, Van Oosten MJ, Grillo S. 2017. Improving plant water use efficiency through molecular genetics. Horticulturae **3**, 31.

Sabar M, Shabir G, Shah SM, Aslam K, Naveed SA, Arif M. 2019. Identification and mapping of QTLs associated with drought tolerance traits in rice by a cross between Super Basmati and IR55419-04. Breeding Science **69**, 169–178.

Salazar-Henao JE, Vélez-Bermúdez IC, Schmidt W. 2016. The regulation and plasticity of root hair patterning and morphogenesis. Development **143**, 1848–1858.

Salse J, Abrouk M, Bolot S, Guilhot N, Courcelle E, Faraut T, Waugh R, Close TJ, Messing J, Feuillet C. 2009. Reconstruction of monocotelydoneous proto-chromosomes reveals faster evolution in plants than in animals. Proceedings of the National Academy of Sciences, USA **106**, 14908–14913.

Salse J, Bolot S, Throude M, Jouffe V, Piegu B, Quraishi UM, Calcagno T, Cooke R, Delseny M, Feuillet C. 2008. Identification and characterization of shared duplications between rice and wheat provide new insight into grass genome evolution. The Plant Cell **20**, 11–24.

Samarah NH. 2005. Effects of drought stress on growth and yield of barley. Agronomy for Sustainable Development **25**, 145–149.

Sandhu N, Raman KA, Torres RO, Audebert A, Dardou A, Kumar A, Henry A. 2016. Rice root architectural plasticity traits and genetic regions for adaptability to variable cultivation and stress conditions. Plant Physiology **171**, 2562–2576.

Sayed MAA. 2011. QTL analysis for drought tolerance related to root and shoot traits in barley (*Hordeum vulgare* L.). PhD thesis, Plant Breeding, Institute of Crop Science and Resources Conservation, University of Bonn, Germany.

Schachtman DP, Goodger JQ. 2008. Chemical root to shoot signaling under drought. Trends in Plant Science **13**, 281–287.

Schneider HM, Klein SP, Hanlon MT, Kaeppler S, Brown KM, Lynch JP. 2020*b*. Genetic control of root anatomical plasticity in maize. The Plant Genome **13**, e20003.

Schneider HM, Klein SP, Hanlon MT, Nord EA, Kaeppler S, Brown KM, Warry A, Bhosale R, Lynch JP. 2020*a*. Genetic control of root architectural plasticity in maize. Journal of Experimental Botany **71**, 3185–3197.

Schneider HM, Lynch JP. 2020. Should root plasticity be a crop breeding target? Frontiers in Plant Science **11**, 546.

Sharma S, Xu S, Ehdaie B, Hoops A, Close TJ, Lukaszewski AJ, Waines JG. 2011. Dissection of QTL effects for root traits using a chromosome arm-specific mapping population in bread wheat. Theoretical and Applied Genetics **122**, 759–769.

Shelden MC, Roessner U. 2013. Advances in functional genomics for investigating salinity stress tolerance mechanisms in cereals. Frontiers in Plant Science **4**, 123.

Shi J, Gao H, Wang H, Lafitte HR, Archibald RL, Yang M, Hakimi SM, Mo H, Habben JE. 2017. ARGOS8 variants generated by CRISPR-Cas9 improve maize grain yield under field drought stress conditions. Plant Biotechnology Journal **15**, 207–216.

Signor SA, Nuzhdin SV. 2018. The evolution of gene expression in cis and trans. Trends in Genetics **34**, 532–544.

Singh V, van Oosterom EJ, Jordan DR, Hunt CH, Hammer GL. 2011. Genetic variability and control of nodal root angle in sorghum. Crop Science **51**, 2011–2020.

Slack S, York LM, Roghazai Y, Lynch J, Bennett M, Foulkes J. 2018. Wheat shovelomics II: revealing relationships between root crown traits and crop growth. bioRxiv **280917**, doi: 10.1101/280917. [Preprint].

Smith S, De Smet I. 2012. Root system architecture: insights from Arabidopsis and cereal crops. Philosophical Transactions of the Royal Society B: Biological Sciences **367**, 1441–1452.

Striker GG, Insausti P, Grimoldi AA, Vega AS. 2007. Trade-off between root porosity and mechanical strength in species with different types of aerenchyma. Plant, Cell & Environment **30**, 580–589.

Taunk J, Rani A, Singh R, Yadav NR, Yadav RC. 2019. Genomic strategies for improving abiotic stress tolerance in crop plants. In: Rajpal V, Sehgal D, Kumar A, Raina S, eds. Genetic enhancement of crops for tolerance to abiotic stress: mechanisms and approaches, Vol. I. Cham: Springer, 205–230.

Tomita A, Sato T, Uga Y, Obara M, Fukuta Y. 2017. Genetic variation of root angle distribution in rice (*Oryza sativa* L.) seedlings. Breeding Science **67**, 181–190.

Tran TT, Kano-Nakata M, Suralta RR, Menge D, Mitsuya S, Inukai Y, Yamauchi A. 2015. Root plasticity and its functional roles were triggered by water deficit but not by the resulting changes in the forms of soil N in rice. Plant and Soil **386**, 65–76.

Tron S, Bodner G, Laio F, Ridolfi L, Leitner D. 2015. Can diversity in root architecture explain plant water use efficiency? A modeling study. Ecological Modelling **312**, 200–210.

Turner NC. 1979. Drought resistance and adaptation to water deficits in crop plants. In: Mussell H, Staples CR, eds. Stress physiology in crop plants. New York: John Wiley & Sons, 343–372.

Uga Y, Hanzawa E, Nagai S, Sasaki K, Yano M, Sato T. 2012. Identification of *qSOR1*, a major rice QTL involved in soil-surface rooting in paddy fields. Theoretical and Applied Genetics **124**, 75–86.

Uga Y, Kitomi Y, Yamamoto E, Kanno N, Kawai S, Mizubayashi T, Fukuoka S. 2015. A QTL for root growth angle on rice chromosome 7 is involved in the genetic pathway of DEEPER ROOTING 1. Rice **8**, 8.

Uga Y, Okuno K, Yano M. 2011. *Dro1*, a major QTL involved in deep rooting of rice under upland field conditions. Journal of Experimental Botany **62**, 2485–2494.

Uga Y, Sugimoto K, Ogawa S, *et al.* 2013*a*. Control of root system architecture by *DEEPER ROOTING 1* increases rice yield under drought conditions. Nature Genetics **45**, 1097–1102.

Uga Y, Yamamoto E, Kanno N, Kawai S, Mizubayashi T, Fukuoka S. 2013*b*. A major QTL controlling deep rooting on rice chromosome 4. Scientific Reports **3**, 3040.

Valliyodan B, Ye H, Song L, Murphy M, Shannon JG, Nguyen HT. 2017. Genetic diversity and genomic strategies for improving drought and waterlogging tolerance in soybeans. Journal of Experimental Botany **68**, 1835–1849.

Van Oosten MJ, Costa A, Punzo P, Landi S, Ruggiero A, Batelli A, Grillo S. 2016. Genetics of drought stress tolerance in crop plants. In: Hossain M, Wani S, Bhattacharjee S, Burritt D, Tran LS, eds. Drought stress tolerance in plants, Vol. II. Cham: Springer, 39–70.

Vyver C, Peters S. 2017. How do plants deal with dry days? Frontiers for Young Minds **5**, 58.

Wahbi A, Gregory PJ. 1995. Growth and development of young roots of barley (*Hordeum vulgare* L.) genotypes. Annals of Botany **75**, 533–539.

Wasson AP, Rebetzke GJ, Kirkegaard JA, Christopher J, Richards RA, Watt M. 2014. Soil coring at multiple field environments can directly quantify variation in deep root traits to select wheat genotypes for breeding. Journal of Experimental Botany **65**, 6231–6249.

Wasson AP, Richards RA, Chatrath R, Misra SC, Prasad SV, Rebetzke GJ, Kirkegaard JA, Christopher J, Watt M. 2012. Traits and selection strategies to improve root systems and water uptake in water-limited wheat crops. Journal of Experimental Botany **63**, 3485–3498.

Webber H, Ewert F, Olesen JE, *et al.* 2018. Diverging import- ance of drought stress for maize and winter wheat in Europe. Nature Communications **9**, 4249.

Witcombe JR, Hollington PA, Howarth CJ, Reader S, Steele KA. 2007. Breeding for abiotic stresses for sustainable agriculture. Philosophical Transactions of the Royal Society B: Biological Sciences **363**, 703–716.

Ye H, Roorkiwal M, Valliyodan B, Zhou L, Chen P, Varshney RK, Nguyen HT. 2018. Genetic diversity of root system architecture in response to drought stress in grain legumes. Journal of Experimental Botany **69**, 3267–3277.

Zaidi PH, Seetharam K, Krishna G, Krishnamurthy L, Gajanan S, Babu R, Zerka M, Vinayan MT, Vivek BS. 2016. Genomic regions associated with root traits under drought stress in tropical maize (*Zea mays* L.). PLoS One **11**, e0164340.

Zhu J, Ingram PA, Benfey PN, Elich T. 2011. From lab to field, new approaches to phenotyping root system architecture. Current Opinion in Plant Biology **14**, 310–317.

Zurek PR, Topp CN, Benfey PN. 2015. Quantitative trait locus mapping reveals regions of the maize genome controlling root system architecture. Plant Physiology **167**, 1487–1496.

Title: Genetic dissection of root architectural plasticity underlying candidate genes for drought adaptation in bread wheat

Md. Nurealam Siddiqui[1], Melesech T. Gabi[1], Abebaw M. Ambaw[1], Tesfaye J. Teferi[1], Said Dadshani[2], Jens Léon[1,3], Agim Ballvora[1*]

[1]Institute of Crop Science and Resource Conservation (INRES)-Plant Breeding, University of Bonn, 53115 Bonn, Germany

[2]INRES-Plant Nutrition, University of Bonn, 53115 Bonn, Germany

[3]Field Lab Campus Klein-Altendorf, University of Bonn, Klein-Altendorf 2, 53359 Rheinbach, Germany

[*]**Corresponding author**: Dr. Agim Ballvora: ballvora@uni-bonn.de

Manuscript under revision (Planta)

Key message: Genome-wide associated study in bread wheat reveals root phenotypic plasticity is highly quantitative and associated loci are responsive to drought.

Abstract

The frequency of droughts has dramatically increased over the last 50 years (Alizadeh et al. 2020), causing yield declines in cereals, including wheat. Wheat varieties with efficient root systems show great potential for plant adaptation to drought stress, however; genetic control of root systems under field conditions is not yet fully understood. Here, the natural variation in root architecture plasticity (phenotypic switching due to changing environments) was dissected under field-based control (well-irrigated) and drought (rain-out shelter) conditions by a genome-wide association study using 200 diverse wheat cultivars. Root architecture and plasticity traits differentially responded to drought stress. A total of 25 marker-trait associations underlying natural variations in root architectural plasticity were identified in response to drought stress. They were abundantly distributed on chromosomes 1A, 1B, 2A, 2B, 3A, 3B, 4B, 5A, 5D, 7A and 7B of the wheat genome. Gene ontology annotation showed that many candidate genes associated with plasticity were involved in water-transport and water channel activity, cellular response to water deprivation, scavenging reactive oxygen species, root growth and development and hormone-activated signaling pathway-transmembrane transport, which indicating their responsiveness to drought stress. Further, *in silico* transcript abundance analysis demonstrated that plasticity candidate genes were highly expressed in roots across different root growth stages and under drought treatments. Collectively, our results suggests that root phenotypic plasticity is highly quantitative, and the corresponding loci are associated with drought stress that may provide novel ways to enable root trait breeding.

Keywords: Candidate genes, Drought stress, GWAS, Root phenotypic plasticity, Single nucleotide polymorphisms, Wheat.

Introduction

Globally, 90-95% of the produced wheat is the hexapody common or bread wheat (*Triticum aestivum* L.), an important stable source of nutrients and fodder for 40% of the world's population (Giraldo et al. 2019a; Sallam et al. 2019). As the global population is rapidly growing, the demand for wheat will also be high; thus, wheat production will increase to 70% by 2050 (Ray et al. 2012). Although the demand for wheat is becoming high, its production is being constrained by various abiotic factors, with drought being the main factor reducing wheat production by 20% (Daryanto et al. 2016), including the following main climatic factors: water scarcity, flooding, high and low-temperature stress, making wheat vulnerable to yield losses during the grain-filling period.

Drought stress is the absence or lack of water in a given environment that could alter the biochemical, physiological and molecular systems of a plant. It is the main factor affecting the broad spectrum of agro-climatic production and productivity of wheat (Sallam et al. 2019). Several biological processes regulate the drought tolerance of plants, which in turn affects the grain yield (Zhu et al. 2019). The root system architecture is a major factor for the plant adaptation during different climatic conditions, including water stress conditions (Khan et al. 2016a; Siddiqui et al. 2021a). Wheat is categorised as a monocot root system possessing both seminal and adventurous roots (Nguyen and Stangoulis 2019). Root architectural traits of wheat contributing to water-deficit adaptation are root length, root surface area, root volume, root number, and root diameter (Ahmed et al. 2018; Siddiqui et al. 2021a). The root traits of wheat, particularly during water scarcity, are important for water absorption and are also essential for nutrient uptake, such as nitrogen and phosphorus (Alahmad et al. 2019). During water-deficit stress, plants tend to change their root architectural structure, e.g. branched roots, increased root length and increased root biomass, to meet their water needs (Fenta et al. 2014). Therefore, rooting depth is considered an essential trait that may enhance the plant's ability to minimise reduced productivity, especially when insufficient soil moisture is available. In deep soils with water reserves, a deep root system is crucial in drought resistance (Christopher et al. 2013; Siddiqui et al. 2021a). Root architectural traits that help improve the water uptake during drought stress conditions are proliferative rooting, such as lateral root number, length density, surface area and volume (Jaganathan et al. 2015). The plant also adapts to drought stress by modulating the fibrous root systems, decreasing lateral root diameter, and altering its root biomass (Salazar-Henao et al. 2016). Moreover, cereal roots show plasticity to adapt to drought. Plasticity is the phenotypic changes due to variable environments might be for short or long periods. Plasticity in root phenotypes can be beneficial for drought adaptation (Kano-Nakata et al. 2013; Prince et al. 2017). Recently, genetic basis

of root plasticity in enhancing drought adaptation has been successfully uncovered by genome-wide association study (GWAS) (Kadam et al. 2017; Schneider et al. 2020).

In the past few decades, the grain yield and quality of bread wheat have greatly focused on breeding. Due to population growth and climate changes, wheat adaptation to environmental extreme conditions should be further improved. Using state-of-the-art phenotyping and sequencing methods, deep genetic and molecular bases of drought stress tolerance in wheat should be analysed and applied (Crespo-Herrera et al. 2017; Sukumaran et al. 2018). Although the roots play an important role in plant tolerance to abiotic stresses and productivity, plant breeders mostly focus on above-ground traits because of the difficulty in investing below-ground traits due to precise phenotyping, especially in large population (Oyiga et al. 2020). Field-based genetic dissection of the root phenotypic traits in wheat, particularly at the flowering stage, is limited compared to other crops due to its genetic complexity and extensive root phenotyping. Due to limitations of field-based root phenotyping, rapid phenotyping strategies should be utilised to better understand genetic responses and rapid selection of root traits and associated genetic components to develop resilient wheat varieties through molecular breeding, showing the necessity of ensuring future food security (Mwadzingeni et al. 2016, Siddiqui et al. 2021a). Nowadays, however, a rapid and popular root phenotyping method, known as Shovelomics" is being used by digging up the upper part of the root systems in the field to phenotype the plant root system and/or root architectural traits (Trachsel et al. 2011; York et al. 2018).

Association mapping or GWAS is a powerful tool that uses both phenotypic and genotypic data to identify a specific location of a gene responsible for trait variability (Qaseem et al. 2018). It is associated with genetic markers linked to a particular trait based on linkage disequilibrium (LD) (Lehmensiek et al. 2009; Ye et al. 2018). A GWAS applying a diverse association mapping panel with higher allelic diversity and historical recombination has a higher resolution than biparental quantitative trait loci (QTL) studies (Khan and Korban 2012). High-density single nucleotide polymorphisms (SNPs) are a prerequisite for a successful GWAS (Cui et al. 2017; Cericola et al. 2017). Furthermore, using the drought tolerance index and plasticity in GWAS provides valuable information for marker-assisted selection in wheat (Ballesta et al. 2020; Schneider et al., 2020). Therefore, GWAS has popularly become an essential tool in identifying SNPs/alleles associated with complex traits, such as root-related traits in bread wheat, that provides a genetic basis for identifying causal genes (Li et al. 2019).

Here, we hypothesise that bread wheat tolerance to drought stress is associated with root architectural plasticity regulated by genomic loci. To address this hypothesis, we formulated the following objectives: (i) to assess the root phenotypic diversity of winter bread wheat cultivars grown under drought and control conditions, (ii) to identify drought-responsive loci

underlying candidate genes associated with root phenotypic plasticity responses and (iii) to determine transcript expression levels of plasticity-associated genes in comparing different organs, including roots and drought stress conditions, as they showed involvement in drought stress.

Materials and Methods

Plant materials

In this study, a total of 200 diverse wheat cultivars were used to assess the genetic diversity of root architecture traits as described by Voss-Fels et al. (2019) and Siddiqui et al. (2021b). Among these 200 cultivars, 60% were obtained from Germany and the others from different countries.

Field experiment

The field experiment was conducted in the 2019-2020 wheat growing season under natural rain-fed (control) and rain-out shelter (drought stress) conditions, as previously described by Siddiqui et al. (2021b). The experiment was designed as a split-plot design with treatments (control and drought) defined as main plots. The experiment layout was followed by split-plot design, where treatments (control and drought) were considered as main plots. The 200 wheat cultivars were sown in a randomised complete block design with three repetitions, each plot contained one cultivar in a single row length of 0.5 m and a between-row distance of 0.21 m. Each plot contained four rows flanked by two border rows to avoid edge effects. Each plot was irrigated by movable sprinklers that deliver ~5.00 L/m^2 water per day. Then, drought was induced by closing the roof cover. Drought treatment is applied from the tillering initiation phase (BBCH21, Biologische Bundesanstalt, Bundessortenamt und Chemische Industrie) to the complete flowering phase (BBCH65). Details of fertilizer application, management practices and soil moisture levels under control and drought treatment were described by Siddiqui et al. (2021b).

Root phenotyping using the ‘Shovelomics’ approach

The wheat root system was phenotyped by “Shovelomics” protocol, i.e. digging out the upper part of the wheat root and determining the root architectural traits (Trachsel et al. 2011; York et al. 2018). The root systems from three individual plants per plot were excavated at BBCH65 using a shovel to maintain a distinct depth of 27 cm (distance from the cutting edge to the shoulder of a shovel) at a distance of ~0.2 m away from the plant base to avoid root destruction from both the control and drought-stressed plants (Oyiga et al. 2020). The lumps of excavated

soil containing the roots were dissolved by submerging in a freshwater bucket until soil was removed from the roots. Thereafter, the roots were gently washed to remove the remaining soil particles and rinsed with clean water. The clean and fresh roots were preserved with 50% alcohol in a plastic pot. Then, the preserved roots were scanned using an Epson scanner (Perfection LA24000) with a resolution of 600 dots per inch and root images were analysed using the WinRhizo software (Regent Instruments Inc., Quebec, Canada) to record the root architectural traits (Kadam et al. 2017).

Statistical analysis

The collected phenotypic data on root system traits were analysed using the R software version 3.6.1 (R Core Team 2018). . Before analysis, extreme outliers we removed based on the following criteria of mean of all accessions ±3 standard deviation (SD), as described by Ueda et al. (2015). Then, data normality was tested following the histogram evaluation, Shapiro-Wilk test and box plot in the R studio. For the descriptive study, a two-way analysis of variance (ANOVA) for root system traits such as; total root length (TRL), root average diameter (RAD), root surface area (RSA), number of root tips (NRT), number of root crossings (NRC), number of root forks (NRF) and root volume (RV), was conducted. During the ANOVA analysis, cultivar and treatment effects were considered as fixed effects with the interaction, whereas block was considered as a random effects (Siddiqui et al. 2021b). Descriptive statistics such as the mean, median, mode, min, max, coefficient of variation, and SD, were analysed. Besides, Pearson's pairwise correlations (r) were calculated for all RSA traits to determine the correlation between phenotypes using statgraphics version 18.1.13 software. Heritability was estimated using broad-sense heritability (H^2) and calculated using the following formula (Gitonga et al. 2014): $H^2= V_G/(V_G+V_E/r)$, where V_G is the estimation of genetic variance, V_E is the estimation of error variance for each treatment and r is the number of replication of each cultivar. Stress plasticity of the root system architectural traits was calculated using the following equation: (P)= (WW-WS)/WW, where WS is water stress and WW is well-watered as described by Schneider et al. (2020). Moreover, the stress tolerance index (STI) of root traits of all cultivars is estimated by taking the phenotypic value under water stress and well-watered conditions using the following equation: $STI= (WS \times WW)/(\text{mean } WW)^2$ where, WS is water stress and WW is well-watered, following Nouraein et al. (2013).

Genome-wide association study

The GWAS was conducted for seven root architectural traits (TRL, RAD, RSA, NRT, NRC, NRF, and RV) under water-deficit stress environmental conditions. A total of 24,216 SNP markers were obtained employing the genomic DNA extraction process (Dadshani et al. 2021), which were used to evaluate the genetic variation of the root traits. The association mapping

was performed using the TASSEL software 5.2.54 (Waples et al. 2019), following the mixed linear model (MLM) including five principal components (PC) and a kinship matrix (Siddiqui et al. 2021b). To set the significant threshold, a 5% false discovery rate (FDR) was calculated using the '*q*value' package of the R software (Chen et al. 2019). The quantile-quantile (Q-Q) plot and rectangular Manhattan plots were prepared using the CM plot package of R (Nkambule 2020). Significant SNP markers were defined based on the FDR threshold and satisfy the requirements of FDR *q*-value <5% considered as true positive (Siddiqui et al. 2021b).

Candidate gene selection and expression analysis

For each root trait, the Plink formats of the data and LD were analysed using Haploview 4.2 to identify the candidate loci (Barrett et al. 2005). The defined LD block heat-map was determined based on the D´ value in the upper confidence bounds exceeded 0.98 and lower bounds of >0.7 (Gabriel 2002). To compare the haplotype belonging to a block with significant SNP markers, the Student's t-test (two samples assuming equal variances) and Tukey's test >2 haplotypes comparisons were performed. LD blocks with highly significant SNP markers were expected to carry putative candidate loci. Significant SNPs that did not establish haplotype blocks, i.e. the genes close to these loci (1 Mbp from both sides) were considered putative candidate genes as stated by Begum et al. (2020). The gene annotation and ontology were conducted in the wheat URGI database (Alaux et al. 2018). To locate significant SNPs on various chromosomes, a map chart was generated following Voorrips (2002). Further, expression profiles of the drought-associated candidate genes were curated using the publicly available RNA-seq data (Zhang et al. 2020).

Results

Root phenotypic diversity and correlation analysis in response to drought stress

Root architecture-related traits in wheat cultivars were evaluated under both control and water-deficit stress conditions at the complete flowering stage (BBCH65) to identify the drought-responsive loci underlying candidate genes by employing a GWAS. The analysis of two-way ANOVA showed that the effects of genotypes were highly significant ($P < 0.001$) among all phenotypic traits, whereas RAD showed a moderate significant differences ($P < 0.05$) (Table 1). Moreover, treatment effects revealed highly significant differences for all studied traits. Interaction between the genotype and treatment demonstrated highly significant differences among all analysed traits ($P > 0.05$) (Table 1). The heritability calculation demonstrated a high broad-sense heritability (H^2) for all studied traits, such as TRL, RSA, RAD, NRT, NRF, NRC

and RV with ranges from 0.73 to 0.87, indicating that the wheat association panel may contain substantial genetic diversity to confer to drought stress response. The highest STI was observed for TRL, NRT, NRF and NRC and compared to other traits (Table 1), implying that those traits might largely contribute to adjusting roots to the water-deficit environment.

However, the calculated stress plasticity for TRL (+44.22), NRT (+91.52), NRF (+52.27) and NRC (+219.73) showed increasing trends, whereas the RSA (-0.86), RAD (-34.3) and RV (-32.05) were reduced under water-deficit stress than control conditions, respectively (Table 1). Further, ANOVA revealed significant genotypic differences ($P > 0.05$) for all of the calculated plasticity traits (Table 1). Pearson's product-moment correlation shows that TRL is highly and significantly correlated with NRF (0.92) and NRT (0.94), NRC with NRF (0.95) and RV with RSA (0.96), suggesting that RSA traits maintain an interconnection to accommodate the plant root system to drought stress. However, RSA with NRF and TRL did not show any significant correlations (Fig. S1).

Association mapping and identification of candidate plasticity loci for drought tolerance

To identify SNPs, the association mapping was conducted based on RSA-related traits in response to drought stress and plasticity as a trait. Based on the calculated drought stress plasticity, all evaluated traits, e.g. plasticity of the total root length (pTRL), plasticity of the average root diameter (pRAD) and plasticity of the number of root tips (pNRT), demonstrated a significant association with SNPs (Figs. 1-3). To minimise the false-positive results of the markers to trait association, an MLM used with five PC and kinship matrices, as previously described by Siddiqui et al. (2021b). Based on FDR-adjusted threshold level ($-\log_{10} P > 4.0$), a total of 25 SNPs were identified for plasticity traits (pTRL, pRAD and pNRT) and RSA, NRF and RV traits in response to drought stress (Table 2). For other traits, very weak associations was observed as revealed by $-\log_{10}$ *p*-values and Q–Q plots (Figs. S1-S3). Next, LD analysis was performed based on significant SNPs to define a region containing plausible candidate genes. A total of 38 blocks harbouring 235 putative genes were defined (Table 3, Table S1). Significant markers and SNP positions were located on chromosomes 1A, 2A and 5A that were more likely associated with the RSA response during drought conditions, such as those responsible for water deprivation, root hair, and root cell differentiation (chromosome 1A), in response to environmental stress (chromosome 2A), and phenotypic switching and cellular response to heat (chromosome 5A) (Table S1; Fig. S4). Interestingly, candidate genes were found to be related to plasticity responses showing involvement to drought stress tolerance mechanisms (Table 4); therefore prioritised the plasticity traits in detail.

Table 1: Descriptive statistics and analysis of variance (ANOVA) results for phenotypic root architectural traits of wheat under natural field-based control and water-deficit stress environments.

Traits and unit	Control					Drought					STI	H^2	P (%)	ANOVA			P
	Min	Max	Mean	SD	CV	Min	Max	G	SD	CV				G	T	G×T	G
TRL (cm)	24.29	242.3	106.5	49.72	46.67	40.27	273.14	133.14	52.07	39.11	1.27	0.76	44.22	***	***	***	***
RSA (cm^2)	6.52	77.59	32.01	16.37	51.12	5.35	58.56	25.64	11.54	45.00	0.84	0.87	-0.86	***	***	***	***
RAD (mm)	0.51	1.38	0.94	0.18	18.95	0.27	0.96	0.61	0.13	22.28	0.65	0.70	-34.30	*	***	***	***
NRT (count)	43.00	558.0	234.8	118.9	50.65	58.00	943.0	404.11	198.49	49.12	1.69	0.74	91.52	***	***	***	***
NRF (count)	90.00	1082	462.4	230.3	49.81	108.0	1460.0	603.31	313.70	52.00	1.28	0.76	52.27	***	***	***	***
NRC (count)	1.00	71.00	28.32	16.27	57.43	3.00	202.0	74.63	48.51	65.00	2.62	0.73	219.73	***	***	***	***
RV (cm^3)	0.08	1.96	0.76	0.43	56.77	0.04	1.00	0.40	0.22	53.36	0.54	0.76	-32.05	***	***	***	***

NB; the phenotypic value of all root phenotypic traits represents the mean of all accessions.*, $p<0.05$;***, $p<0.001$. The abbreviations: Min, minimum; Max, maximum; SD, standard deviation; CV, coefficient of variation; NS, non-significant; TRL, total root length; RSA, root surface area; RAD, root average diameter; NRT, number of root tips; NRF, number of root forks; NRC, number of root crossings, RV, root volume; H^2, broad-sense heritability; STI, stress tolerance index and P, stress plasticity.

Table 2: Summary of all significant single nucleotide polymorphic (SNP) markers identified by GWAS in response to drought stress and plasticity.

Trait	SNP markers	Chr.	MAF	Alleles	-log$_{10}$ *p*-value	r^2
pTRL	AX-490522663	1A	0.422	C:A	5.389180199	0.135
	AX-476020090	1B	0.283	G:T	4.308803537	0.088
	AX-473530929	1B	0.185	C:T	4.023214569	0.080
	AX-89768547	2A	0.19	C:T	4.015337694	0.098
	AX-585941635	2B	0.195	T:G	5.44267329	0.136
	AX-20836050	3A	0.132	T:G	5.525885763	0.138
	AX-526932489	4B	0.213	A:G	5.520611864	0.138
	AX-704835640	5A	0.458	A:G	5.391580949	0.134
pRAD	AX-690934270	2A	0.075	C:T	4.724088353	0.077
	AX-31875912	7A	0.111	T:G	5.737552483	0.084
	AX-700388976	7B	0.167	T:C	5.412450212	0.077
RSA	AX-814183606	3B	0.276	T:C	4.98699415	0.105
	AX-814356941	3B	0.166	G:T	4.337157206	0.089
	AX-479202697	5A	0.438	T:C	4.667440359	0.119
	AX-549850407	5D	0.4	A:G	4.012664497	0.082
NRF	AX-65417557	2B	0.464	C:T	4.016279017	0.081
	AX-243102306	2B	0.176	A:C	4.039619611	0.099
pNRT	AX-490522663	1A	0.422	C:A	4.870631037	0.233
	AX-579774126	2B	0.214	T:G	4.341900688	0.233
	AX-20836050	3A	0.132	T:G	5.611405107	0.239
	AX-527283513	4B	0.198	A:G	5.424745099	0.234
	AX-705374739	5A	0.458	A:G	4.674389488	0.233
RV	AX-695555707	3B	0.37	A:G	4.522651694	0.083
	AX-814183606	3B	0.276	T:C	4.529192156	0.086

The SNPs with –log$_{10}$ (*P*-value) ≥4.0 (threshold set by 5% FDR correction) are listed together with the corresponding trait. Abbreviation: Chr., chromosome; MAF, minor allele frequency; r^2, marker r^2 values; A, adenine; G, guanine; T, thymine; C, cytosine; TRL, total root length, RAD, root average diameter; RSA, root surface area; NRF, number of root forks; NRT, number of root tips and RV, root volume.

Plasticity of the total root length

The association mapping of the pTRL was performed from TRL mean values, yielding significant marker-trait associations (MTAs) (Fig. 1). The log-transformed TRL data demonstrated the normal distribution with equal mean and median values (Fig. 1A). The Q-Q plot showed that the observed *P*-value of pTRL deviated from the expected *P*-value (Fig. 1B). Manhattan plot revealed that nine SNPs passed the threshold level at 5% FDR. Those MTAs occurred on chromosome 1B, one consistent peak consisted of three significant SNPs and on

other chromosomes 1A, 2A, 3A, 4B and 5A, each peak containing only one SNP (Fig. 1C). The LD block heat-map indicated that significant SNP markers of chromosome 1A (AX-490522663) grouped with other 11 SNP markers on a major LD block (Figs. 1D, E).

Table 3. List of single nucleotide polymorphisms (SNPs) and candidate genes identified by GWAS based on significant marker-trait associations (MTAs) and linkage disequilibrium (LD) block recognized from the putative regions in response to drought stress and plasticity.

Trait	Chr.	LD block	Number of SNPs	Putative Region (bp)		Number of genes
				Start	End	
pTRL	1A	Block 2	12	4.89E+08	491149320	19
	1B	Block 1	31	4.72E+08	478722611	35
	2A	Block 1	7	89597473	90425823	5
	2B	Block 3	8	5.82E+08	587815112	8
	3A	Block 3	7	20741217	21069728	10
	4B	Block 1	18	5.27E+08	529334216	3
	5A	Block 1	19	7.05E+08	705565704	3
pRAD	2A	Block 2	9	6.91E+08	691181098	8
	7A	no block	1	30875862	32875862	6
RSA	3B	Block 3	11	8.14E+08	815504335	12
	5A	Block 2	9	4.79E+08	479203284	4
	5D	Block 3	3	5.5E+08	549852162	1
NRF	2B	Block 1	10	65225853	65808631	4
	2B	Block 1	21	2.38E+08	244534860	24
pNRT	1A	Block 2	12	4.89E+08	491149320	20
	2B	Block 2	4	5.79E+08	580020356	9
	3A	Block 3	7	20741217	20955640	9
	4B	Block 2	17	5.27E+08	529334216	14
	5A	Block 1	19	7.05E+08	705565704	9
RV	3B	Block 1	15	6.94E+08	696288703	14
	3B	Block 3	11	8.14E+08	815504335	18

The significant single nucleotide polymorphisms (SNPs) which does not belong to an LD block, a 1Mbp window on either side of significant SNP was considered to search putative candidate genes. The same chromosome with the same colour shade represents their common sharing of the same putative region for different traits. Abbreviation: pTRL, plasticity of total root length; pRAD; plasticity of root average diameter; RSA, root surface area; NRF, number of root forks; pNRT, plasticity of number of root tips; RV, root volume; Chr, chromosome and bp, base pair.

The significant SNP of chromosome 2A (AX-89768547) was grouped with other six SNPs on a major LD block (Fig. 1F). The major LD block of chromosome 3A with significant SNP was grouped with six other SNPs (Fig. 1G).

The LD block on chromosome 1A contained two main haplotypes, CTGTCAGCACGG and TCACTCATGTAT, which belonged to 71 and 88 cultivars, respectively. For both haplotypes, no significant differences were observed for pTRL based on Student's *t*-test (Figs. 1D, E). The LD block of chromosome 2A contained three main haplotypes, 32 cultivars possessing ACAGTGGC, 10 containing GTGACAAT and 149 harbouring ATGACAAT and all three haplotypes did not differ from each other in their association values with pTRL (Figs. 1F, G). Another LD block on chromosome 3A also formed two main haplotypes, TAGACTCGGCCG within 27 genotypes and TCGACTCAGCCG 128 cultivars, and also showed non-significant difference for pTRL trait (Figs. 1H, I).

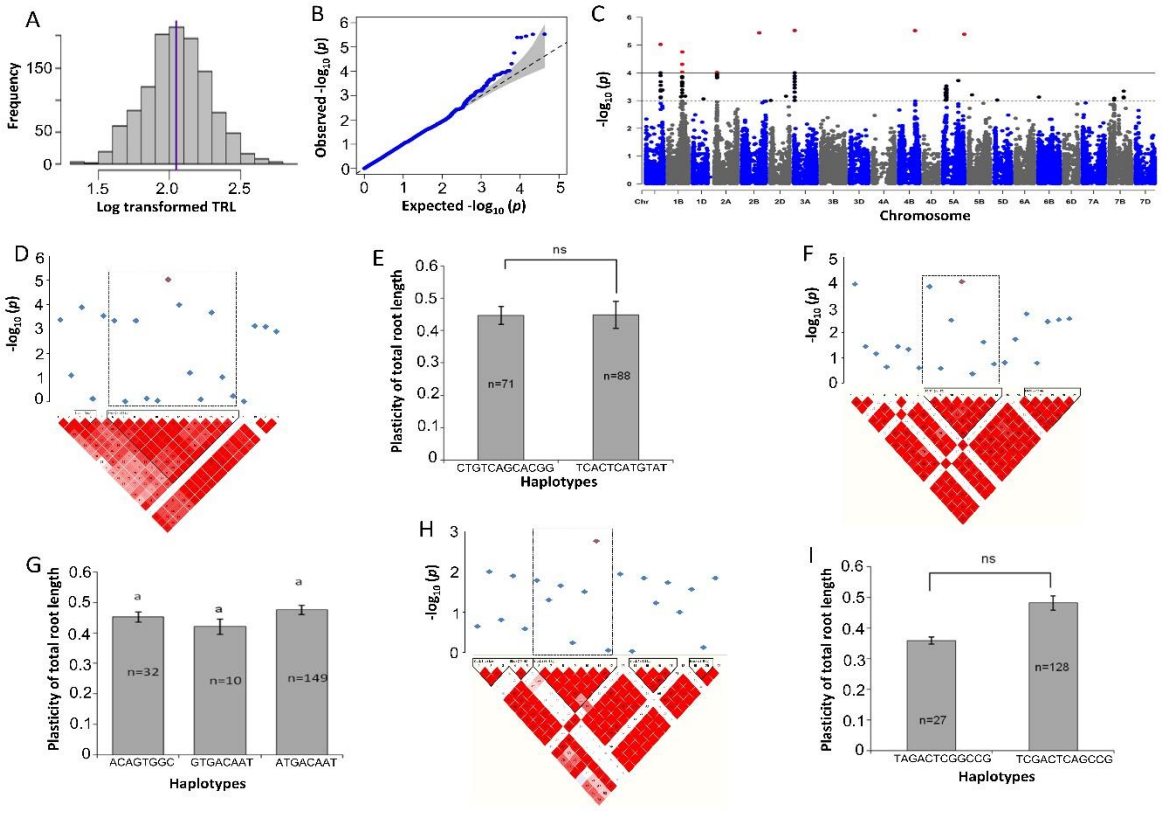

Fig. 1: Marker-trait associations (MTAs) for the plasticity of total root length (pTRL). **A.** Histogram plot highlighted the frequency distribution of log-transformed data of total root length (TRL). The blue and red colour lines in the middle of plot indicate mean and median of the data set, respectively. **B.** Quantile-Quantile (Q-Q) plot indicate the efficiency of GWAS *P*-values of PRL, Y-axis: observed -$\log_{10}$ (*P*-value) and X-axis expected –$\log_{10}$ (*P*-value). **C.** Rectangular Manhattan plot from association mapping of pTRL with a mixed linear model (MLM) considered the kinship and population structure matrix, Y-axis: -$\log_{10}$ (*P*-value) and X-axis: the entire 21 chromosomes of the wheat genome**.** The red SNPs above the black line indicated the significant SNPs which passed the threshold level at $P \leq 0.0001$. The black SNPs above the dotted black line represented all the SNPs that did not reach the threshold level. **D, F and H.** The

linkage disequilibrium (LD) map expressing the peak region on chromosome 1A, 2A and 3A, respectively. Pair-wise LD map between SNP markers is denoted by *D'* values, dark red represent 1, whereas white for 0. The region surrounded by the dark dotted line represents LD block that harbour significant SNPs. **E, G and I.** Phenotypic comparison of the haplotype groups established for the significant SNPs as detected by LD block. Different letters indicate statistical difference at $P < 0.05$, n indicates the number of genotypes represents each specific haplotype.

The major LD blocks for the pTRL contained putative candidate genes with annotation in multiple biological processes, such as response to the heat and reactive oxygen species, water deprivation, responses to environmental stress and abiotic stimulus, cellular response to auxin signalling pathway, root hair elongation and lateral root development (Table 4).

Plasticity of the average root diameter

The association mapping conducted on pRAD has shown significant MTAs (Fig. 2). The log-transformed data revealed a normal distribution with equal mean and median values (Fig. 2A). The Q-Q plot indicated the observed *P*-value of pRAD that deviated from the expected *P*-value (Fig. 2B). Manhattan plot suggested that three SNPs satisfied the threshold level at 5% FDR, which all relied on chromosomes 2A, 7A and 7B (Fig. 2C). The LD block heat-map indicated significant SNP markers of chromosome 7B (AX-700388976) lineage with their four neighbour SNP markers on a major LD block (Fig. 2D). The LD block on chromosome 7B established four main haplotypes, in which ACCGG belonged to 33 cultivars, ATTAG carried 23 cultivars, GTTAA belonged to 51 cultivars and GTTAG possessed 90 cultivars for pRAD traits (Fig. 2E). The Student's *t*-test analysis for these four haplotypes showed that ACCGG and GTTAA haplotypes had significant differences for the trait, and when compared to the haplotypes, both showed non-significant differences for pRAD (Fig. 2E).

The LD block for pRAD with significant SNP markers harboured candidate genes associated with biological processes, such as cellular response to auxin stimulus, jasmonic acid-mediated signalling pathway, potassium ion transmembrane transport, stabilised membrane potential and response to the light intensity with the molecular activity of hydrolysis (Table 4).

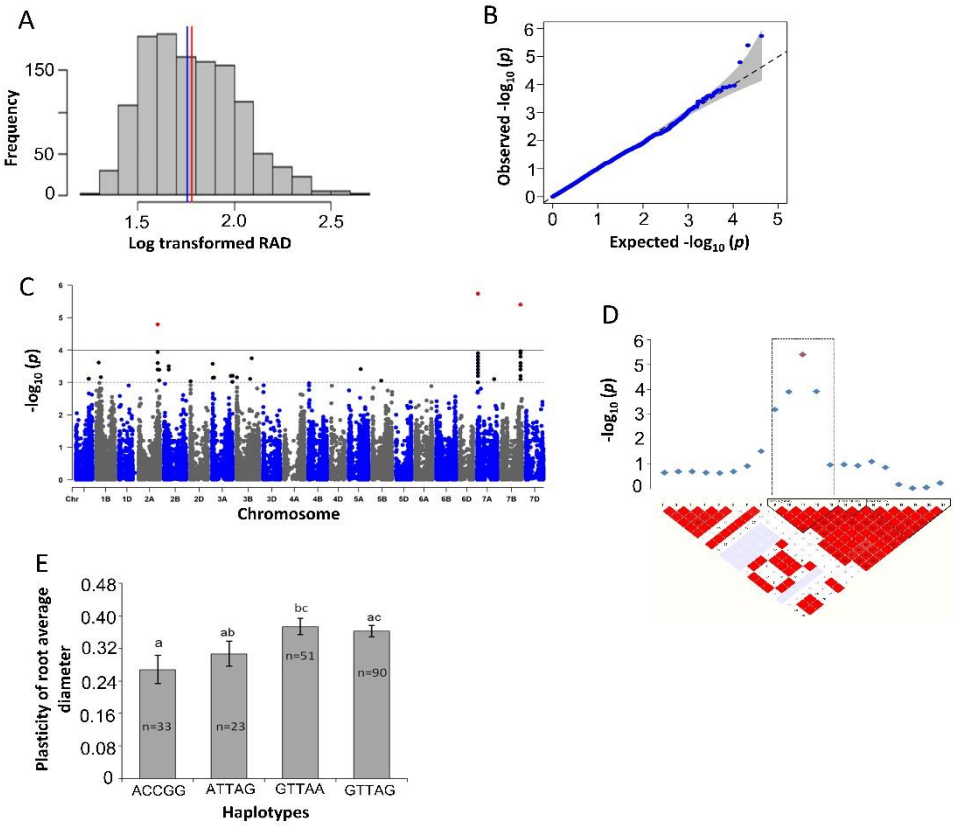

Fig. 2: Marker-trait associations (MTAs) for the plasticity of root average diameter (pRAD). **A.** Histogram plot highlighted the frequency distribution of log-transformed data of root average diameter (RAD). The blue and red colour lines in the middle of plot indicate mean and median of the data set, respectively. **B.** Quantile- Quantile (Q-Q) plot indicate the efficiency of GWAS *P*-values of RAD, Y-axis: observed -$\log_{10}$ (*P*-value) and X-axis expected –$\log_{10}$ (*P*-value). **C.** Rectangular Manhattan plot from association mapping of pRAD with a mixed linear model (MLM) considered the kinship and population structure matrix, Y-axis: -$\log_{10}$ (*P*-value) and X-axis: the entire 21 chromosomes of the wheat genome**.** The red SNPs above the black line indicated the significant SNPs which passed the threshold level at $P \leq 0.0001$. The black SNPs above the dotted black line represented all the SNPs that did not reach the threshold level. **D.** The linkage disequilibrium (LD) map expressing the peak region on chromosome 7B. Pair-wise LD map between SNP markers is denoted by *D'* values, dark red represent 1, whereas white for 0. The region surrounded by the dark dotted line represents LD block that harbour significant SNPs. **E.** Phenotypic comparison of the haplotype groups established for the significant SNPs as detected by LD block. Different letters indicate statistical difference at $P < 0.05$, n indicates the number of genotypes represents each specific haplotype.

Plasticity of the number of root tips

To perform the association mapping, stress plasticity was calculated using the NRT values, which revealed significant MTAs (Fig. 3). The normality distribution of NRT displayed by the log-transformed data contained exactly equal mean and median values (Fig. 3A). The Q-Q plot revealed the observed *P*-value of pNRT that deviated from the expected *P*-value (Fig. 3B). The

Manhattan plot implied that five SNPs confirmed the threshold level at 5% FDR. These five SNPs were found on chromosomes 1A, 2A, 3A, 4B and 5A (Fig. 3C). Significant SNP markers on chromosome 1A (AX-490522663) established an LD block by linkage with the other 11 SNP markers (Fig. 3D). The LD block of significant SNP markers on chromosome 5A (AX-705374739) formed a linkage with the other 18 neighbour SNPs (Fig. 3E). The LD block on chromosome 1A contained two main haplotypes, 88 cultivars carrying CTGTCAGCACG, whereas 71 cultivars possessed TCACTCATGTT and the Student's *t*-test analysis showed that both haplotypes had non-significant differences for the pNRT (Fig. 3D). The LD block on chromosome 5A contained three main haplotypes, with ACCTGGGGATGCTTAGTGC belongs to 21 cultivars, ACCTGGGGATGCTTCGTGC on 18 cultivars, and GTTCAAAAGCATCGCAGAT on 39 cultivars, which all exhibited non-significant differences for pNRT (Fig. 3D).

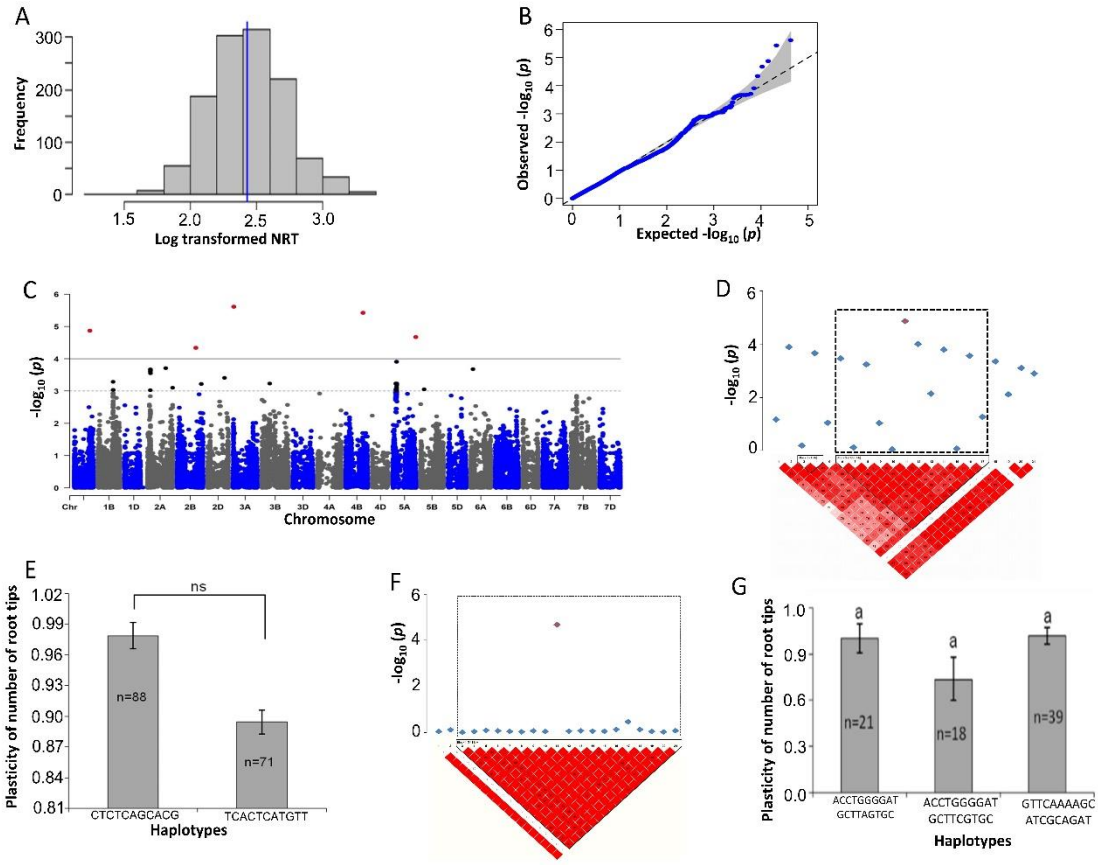

Fig. 3: Marker-trait associations (MTAs) for the plasticity of number of root tips (pNRT). **A.** Histogram plot highlighted the frequency distribution of log-transformed data of number of root tips (NRT). The blue and red colour lines in the middle of plot indicate mean and median of the data set, respectively. **B.** Quantile- Quantile (Q-Q) plot indicate the efficiency of GWAS *P*-values of RAD, Y-axis: observed -$\log_{10}$ (*P*-value) and X-axis expected –$\log_{10}$ (*P*-value). **C.** Rectangular Manhattan plot from association mapping of pNRT with a mixed linear model (MLM) considered the kinship and population structure matrix, Y-axis: -$\log_{10}$ (*P*-value) and X-axis: the entire 21 chromosomes of the wheat genome**.** The red SNPs above the black line indicated the significant SNPs which passed the threshold level at *P*≤0.0001.

The black SNPs above the dotted black line represented all the SNPs that did not reach the threshold level. **D, and F.** The linkage disequilibrium (LD) map expressing the peak region on chromosome 1A and 5A, respectively. Pair-wise LD map between SNP markers is denoted by *D′* values, dark red represent 1, whereas white for 0. The region surrounded by the dark dotted line represents LD block that harbour significant SNPs. **E and G.** Phenotypic comparison of the haplotype groups established for the significant SNPs as detected by LD block. Different letters indicate statistical difference at $P < 0.05$, n indicates the number of genotypes represents each specific haplotype.

The LD block for pNRT containing candidate genes showed functional associations in different biological functions, such as responses to water deprivation, response to heat, response to reactive oxygen species, root hair cell differentiation, root hair elongation, lateral root development, response to auxin and other hormones, phenotypic switching, hyperosmotic salinity response and also molecular activity, such as water channel, hydrolysis and ATPase (Table 4).

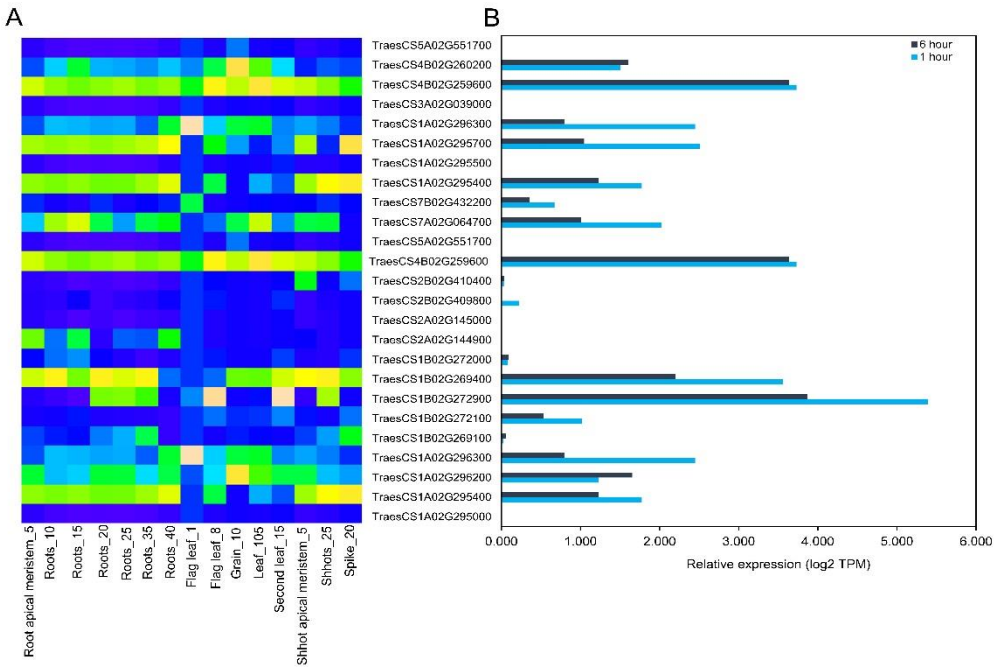

Fig. 4: Transcript expression patterns of selected plasticity responsive candidate genes for root growth and drought tolerance. A. Expression within different tissues of wheat represented as root apical meristem_5 (tillering stage), roots_10 (flag leaf stage), roots_15 (30% spike), roots_20 (14-days old), roots_25 (seven leaf stage), roots_30, roots_35 and roots_40 (fifth leaf stage), flag leaf_1 (milk grain stage), flag leaf_8 (12 dpa), grain_10 (ripening stage), leaf_105 (9-days old), second leaf_15 (17-days old), shoot apical meristem_5 (tillering stage), shoots_25 (2-days old) and spike_20 (flag leaf stage). Deep blue color indicates lower and deep coral color indicates higher expression values (log2 TPM). B. Expression patterns of candidate genes under 1 hour (deep sky blue color bar) and 6 hours (black color bar) of drought treatments. RNA-seq data were curated from the WheatGmap database and are

represented by heat-map of transcripts per kilobase million (TPM) values. The expression data is also provided in Supplementary Table S2 and S3.

Expression analysis of candidate genes under drought stress

Expression levels of identified plasticity candidate genes involving drought tolerance mechanisms were determined using the WheatGmap browser (https://www.wheatgmap.org; Zhang et al. 2020). We observed a wide range of transcript expression for candidate genes in different developmental stages, including multiple root growth stages (Fig. 4A). Among the top 25 short-listed plasticity candidate genes based on their functional annotations in drought (Table 4), the majority of candidate genes were found to be highly expressed in roots at different developmental stages (Fig. 4A, Table S2), indicating that they might be involved in root growth and development. Next, their expression levels were determined using the above-mentioned WheatGmap database after 1 and 6 h of drought imposition (Fig. 4B). Varying expression levels were observed among selected candidate genes, whereas eight genes were stably and largely expressed in response to both 1 and 6 h of drought treatments (Fig. 4B, Table S3). Interestingly, these eight genes were particularly expressed in the roots and simultaneously under drought, predicting that these genes play vital roles in root developmental plasticity to better withstand plants' to drought stress.

Discussion

In wheat, root architectural traits are crucial in water and nutrient acquisition, and root growth patterns have been reported to be highly affected by soil water availability (Liu et al. 2018). Importantly, root architectural traits are plastic in response to drought crucial for water and nutrient acquisition, anchorage and storage (Schneider et al. 2020; Kevei et al. 2022). Therefore, expanding our knowledge on the genetic control of root architectural trait plasticity and uncovering their associated candidate genes will be useful to improve wheat productivity to water limited areas.

To analyse the genetic components of root architectural plasticity to water availability, root system traits were phenotyped under normal watering and drought conditions by withdrawing water supply from tillering to the flowering stage of the wheat growth to identify natural genetic variations and putative genes associated with RSA plasticity underlying the drought adaptation. As a result of drought imposition, wheat cultivars showed significant phenotypic variations of root traits, including TRL, RAD, NRF, NRC and NRF, indicating that these traits are more responsive during water-deficit stress (Table 1; Ye et al. 2018).

Table 4: Short-list of plasticity responsive candidate genes based on their functional involvement in drought tolerance mechanisms.

Traits	Chr.	Gene ID	Gene size	Gene annotation	
				Molecular function	**Biological function**
pTRL	1A	TraesCS1A02G295000	1,549	protein self-association-unfolded protein binding (GO:0006950), abscisic acid binding-signaling receptor activity (GO:0009725),	response to heat- response to reactive oxygen species-response to salt stress (GO:0006950), abscisic acid-activated signaling pathway (GO:0009725)
		TraesCS1A02G295400	629	water channel activity (GO:0009414), hydrolase activity(GO:0005886)	response to water deprivation (GO:0009414), carbohydrate metabolic process(GO:0005886)
		TraesCS1A02G296200	4,331	structural molecule activity (GO:0006888)	response to freezing (GO:0050826), intracellular protein transport-vesicle-mediated transport (GO:0006888)
		TraesCS1A02G296300	5,040	potassium ion leak channel activity(GO:0016021), actin filament binding-ATP binding(GO:0048765)	root hair elongation-vesicle transport along actin filament- root hair cell differentiation (GO:0048765) **,** lateral root development (GO:0048527)
	1B	TraesCS1B02G269100	1,321	protein self-association-unfolded protein binding (GO:0006979), growth factor activity-growth hormone receptor binding-hormone activity(GO:0060416)	response to heat -response to reactive oxygen species -response to salt stress (GO:0006979), lateral root development (GO:0048527), positive regulation of growth-response to growth hormone **(**GO:0060416)
		TraesCS1B02G272100	3,720	water channel activity- (GO:0006833), cellular response to water deprivation (GO:0042631), hydrolase activity (GO:0048046)	Transport-water transport (GO:0006833), apoplast (GO:0048046)
		TraesCS1B02G272900	4,291	auxin-activated signaling pathway-transmembrane transport (GO:0009926)	Auxin signaling pathway, auxin polar transport (GO:0009926)
		TraesCS1B02G269400	3,006	protein self-association-unfolded protein binding(GO:0009651), hydrolase activity, hydrolyzing O-glycosyl compounds (GO:0005886)	response to heat-response to reactive oxygen species (GO:0009651), response to cold (GO:0009409)
		TraesCS1B02G272000	2,745	water channel activity(GO:0009414)	response to water deprivation(GO:0009414), response to cold (GO:0009409)
	2A	TraesCS2A02G144900	1,511	heme binding-metal ion binding-peroxidase activity(GO:0009505), chlorophyll binding (GO:0009628)	response to environmental stresses(GO:0009505), response to abiotic stimulus (GO:0009628)
		TraesCS2A02G145000	1,181	chlorophyll binding (GO:0009628)	light harvesting in photosystem I-response to light stimulus (GO:0009628) peroxidase activity-environmental stress (GO:0004601)
	2B	TraesCS2B02G409800	1,306	actin-dependent ATPase activity-actin filament binding-ATP binding-	actin filament organization-root hair elongation-vesicle transport along actin filament-root hair cell differentiation (GO:0048765)

				(GO:0048765), voltage-gated ion channel activity (GO:0009913)	
		TraesCS2B02G410400	4,291	protein self-association-unfolded protein binding (GO:0006950)	response to heat- response to reactive oxygen species-response to salt stress - response to stress (GO:0006950)
	4B	TraesCS4B02G259600	3,639	ion channel binding(GO:1903959), protein-macromolecule adaptor activity(GO:0040008)	regulation of anion transmembrane transport (GO:1903959),response to starvation-positive regulation of cell growth (GO:0040008)
	5A	TraesCS5A02G551700	939	ATPase activity- ATP binding -unfolded protein binding(GO:0034605), DNA-binding transcription factor activity-sequence-specific DNA binding(GO:0009751)	cellular response to heat (GO:0034605), hyperosmotic salinity, and hormone response(GO:0009751)
pRAD	7A	TraesCS7A02G064700	3,204	hydrolase activity-methyl jasmonate esterase activity-methyl salicylate esterase activity(GO:0009694), transcription regulatory region DNA binding	cellular response to auxin stimulus (GO:0071365), jasmonic acid-mediated signaling pathway (GO:0009864)
	7B	TraesCS7B02G432200	3,706	potassium ion leak channel activity(GO:0016021)	potassium ion transmembrane transport-stabilization of membrane potential(GO:0016021) , response to light intensity (GO:0009642)
pNRT	1A	TraesCS1A02G295400	629	water channel activity(GO:0009414), chlorophyll-binding (GO:0009579), hydrolase activity, hydrolyzing O-glycosyl compounds(GO:0005886), potassium ion leak channel activity (GO:0005774)	response to water deprivation (GO:0009414), photosynthesis, light harvesting in photosystem I-response to the light stimulus (GO:0009579), stabilization of membrane potential (GO:0005774)
		TraesCS1A02G295500	261	protein self-association-unfolded protein binding(GO:0006950)	response to heat-response to hydrogen peroxide-response to reactive oxygen species-response to salt stress-response to stress (GO:0006950)
		TraesCS1A02G295700	522	water channel activity(GO:0009414), potassium ion leak channel activity (GO:0065007), hydrolase activity, (GO:0005886)	response to water deprivation(GO:0009414),), potassium ion transmembrane transport-stabilization of membrane potential(GO:0065007),
		TraesCS1A02G296300	5,040	actin-dependent ATPase activity-(GO:0048765, ATP binding-protein serine/threonine kinase activity-transforming growth factor-beta receptor activity, type I(GO:0004675)	root hair cell differentiation and root hair elongation (GO:0048765) , lateral root development (GO:0048527), cellular response to growth factor stimulus (GO:0004675)
	3A	TraesCS3A02G039000	4,478	ATP binding-protein serine/threonine kinase activity (GO:0005819)	response to auxin-response to ethylene-response to gibberellin(GO:0009733), photosynthesis, light harvesting in photosystem I-response to the light stimulus (GO:0009941)

	4B	TraesCS4B02G259600	3,639	ion channel binding (GO:1903959), sodium-independent organic anion transmembrane transporter activity (GO:0098656), protein-macromolecule adaptor activity(GO:0040008), potassium ion leak channel activity(GO:0005774), voltage-gated chloride channel activity(GO:0008308)	cellular response to starvation-positive regulation of cell growth-positive regulation of protein serine/threonine kinase activity-regulation of cell size-regulation of growth (GO:0040008) , potassium ion transmembrane transport-stabilization of membrane potential-vacuolar membrane (GO:0005774), voltage-gated chloride channel activity(GO:0008308)
		TraesCS4B02G260200	2,261	potassium ion leak channel activity(GO:0016021), abscisic acid binding-protein phosphatase inhibitor activity-signaling receptor activity (GO:0050896)	potassium ion transmembrane transport-stabilization of membrane potential (GO:0016021), response to stimulus (GO:0050896)
	5A	TraesCS5A02G551700	939	hydrolase activity(GO:0005886), ATPase activity, (GO:0034605)	phenotypic switching (GO:0036166), cellular response to heat (GO:0034605) , hyperosmotic salinity response, response to auxin (GO:0009733)

The abbreviation: pTRL, plasticity of total root length; pRAD; plasticity of root average diameter; pNRT, plasticity of number of root tips; Chr, chromosome and GO, gene ontology.

Our results were similar to those of a previous study on water-deficit stress conditions, showing that plants increase the root length to enter into the deep soil layers to better explore the soil and is accompanied by drought tolerance (Wasaya et al. 2018; Friedli et al. 2019). Our results also indicated that the RAD decreased during water shortage, whereas TRL was increased (Table 1). These results revealed that during water-deficit stress, increased TRL with reduced RAD might be the candidate for improving plant adaptation to the drought. Reduced root diameter with greater root length has been established as a trait involving the enhancement of plant productivity during drought (Wasson et al. 2012). A narrow root diameter is beneficial for plants that can efficiently increase hydraulic conductance to minimise the root apoplastic barrier for entering water into the xylem (Hernández et al. 2010; Comas et al. 2012; Comas et al. 2013). Conversely, we found that the RSA and RV of the root were found to be decreased under drought conditions at the complete flowering stage (Table 1). Similarly, recent studies also reported that wheat genotypes under drought showed differential responses of root traits due to their growth stages, such as the increased RSA during the anthesis stage but reduced at the maturity stage (Sun et al. 2020), which may indicate that the RSA and RV of the root responses vary with plant growth stages. However, the NRF and NRC are also crucial traits showing a better adaptation of the plant during water-deficit stress conditions (Ibrahim et al. 2012). We observed that wheat genotypes increased the NRT under drought conditions than in the control condition (Table 1). Increasing the lateral root number helps plants to improve the water transport to sustain the drought stress condition and for rapid access to soil moisture (Ruiz et al. 2020; Putnik-Delic et al. 2018). Pearson's product-moment correlation heat-map showed that TRL was negatively correlated with RAD and positively correlated with NRT, NRF and NRC (Fig. S1). Similarly, a study on bread wheat indicated that the TRL, NRT and NRF were positively correlated under drought stress to assist plants toward an improved adaptation level (Chen et al. 2020).

Before performing a GWAS, fulfilling the requirements of individuals with high genetic diversity is essential for obtaining more allelic variations (Milner et al. 2019). In our GWAS, an MLM, including the PC and kinship matrix, enabled us to avoid false MTAs (Kang et al. 2010). Following these approaches, a total of 25 significant SNPs harbouring 235 putative candidate genes were detected for the trait associated with plasticities, such as pTRL, pRAD and pNRT and drought-treated RSA, NRF and RV after a successful FDR correction (Table 2 and 3), although NRC did not yield any significant SNPs. These results indicate those root traits were controlled by a diverse set of genes to adapt to drought (Courtois et al. 2009). A total of 235 plausible candidate loci were identified across wheat chromosomes, which were associated with root trait responses during drought stress. (Tables 2 and 3). The majority of the SNP plasticity was located on chromosomes 1A, 2A and 5A associated with a better response for

plasticity traits under water-deficit stress (Figs. 1-3). The abundant genomic regions in wheat for drought and root-related traits are detected on chromosomes 1A, 2A and 5A encompassing plausible genes upregulated during abiotic stresses (Soriano and Alvaro 2019).

The LD analysis detects neighbouring and associated SNPs based on the relationship of SNPs on the adjacent stretch of genomic regions within the population; thereby, LD explains genetic variations over the population (Bush and Moore 2012). The putative candidate genes were identified based on LD blocks harbouring significant SNP markers (Tables 3 and 4). The LD-based GWAS successfully delivers chromosomal regions underlying candidate genes affecting the plant adaptation to environmental stresses (Begum et al. 2020; Siddiqui et al. 2021b). Next, haplotype analysis was performed for plasticity traits, pTRL, pRAD and pNRT For the pTRL on chromosome 1A, two haplotype blocks, and 2A, and chromosome 3A in two haplotypes were abundantly observed under drought stress conditions (Figs. 1D-I). The pRAD contained four main haplotypes on chromosome 7B, which were associated with plasticity of RAD under drought conditions (Figs. 2D, E). Haplotype blocks of pNRT trait on chromosome 1A formed two haplotypes and on chromosome 5A three distinct haplotypes establishing those were widely dispersed on cultivars that may be related to the pNRT under drought conditions (Figs. 3D-G). Interestingly, all adaptive loci carrying major haplotypes were found to have larger contributions to the root phenotypic plasticity under droughts when compared with minor haplotypes (Figs. 1-3), suggesting that exchanging these haplotype alleles could greatly induce root phenotypic adaptation to drought conditions.

Candidate genes associated with pTRL under drought conditions showed biological functions on responses to heat and reactive oxygen species, water deprivation, environmental stress response and abiotic stimulus, cellular response to auxin signalling pathway, root hair elongation and lateral root development (Table 4). Another study showed that some genes can regulate the auxin signalling pathway under drought stress and assist in the lateral root formation or root elongation to access more water from its surrounding environments (Koevoets et al. 2016b). The putative candidate genes for pRAD were associated with the cellular response to auxin stimulus, jasmonic acid-mediated signalling pathway and stabilisation of membrane potential (Table 4). The genes were upregulate in response to drought for increasing cell division, tropisms, vascular differentiation and root meristem maintenance. Moreover, a jasmonic-acid responsive gene shows an interactive function for the plant resistance to abiotic stress conditions (Ali and Baek 2020).

The pNRT under water-deficit conditions was putatively controlled by multiple candidate genes (Table 4). Upregulations of genes responsible for root water deprivation and abscisic-acid biosynthesis associated with auxin transport to the root tips are major factors of drought stress tolerance (Grzesiak et al. 2019). Overall, we short-listed 25 plasticity candidate genes showing

highly putative relationships with drought (Table 4). *In silico* transcript expression analysis showed distinct expression levels of eight candidate genes in root under drought treatments in multiple root growth stages (Fig. 4). This result confirms that these eight candidate genes are particularly associated with drought stress adaptation underlying the root growth plasticity.

Conclusion

In this study, root phenotypic traits were quantified in the global collection of wheat cultivars with and without water supply in the field environment. Substantial genetic variation revealed for all of the traits in response to drought and plasticity that determines the phenotypic responses to water availability. Further, the identified MTAs and candidate genes, especially for root phenotypic plasticity, will be useful for further functional studies in improving the wheat root systems to better withstand plants in water-deficit soils. Our study also provides additional insights into the drought-induced natural root system variations conferring within diverse wheat germplasms. However, further in-depth investigation is crucial to better understand the genetic relationships of phenotypic plasticity among the individual root architectural traits underlying drought adaptation, which may result in efficient breeding to develop adaptive wheat cultivars better suited to water scarcity-prone agro-ecosystems.

Acknowledgements

We are highly grateful to the German Academic Exchange Service (DAAD) for providing a fellowship to MNS. We are also acknowledged to Mohammad Kamruzzaman, Marissa B. Barbossa, Patrice Koua and Karin Woitol for their help during root harvesting and phenotyping. We extend acknowledgement to the staff of Campus Klein-Altendorf to take care the field experiments.

References

Ahmed MA, Zarebanadkouki M, Meunier F, Javaux M, Kaestner A, Carminati A (2018) Root type matters: measurement of water uptake by seminal, crown, and lateral roots in maize. J Exp Bot 69: 1199–1206.

Alahmad S, El Hassouni K, Bassi FM, Dinglasan E et al (2019) A major root architecture QTL responding to water limitation in durum wheat. Front Plant Sci 10: 436.

Alaux M, Rogers J, Letellier T et al (2018) Linking the International Wheat Genome Sequencing Consortium bread wheat reference genome sequence to wheat genetic and phenomic data. Genome Biol 19 111.

Ali M, Baek KH (2020) Jasmonic acid signaling pathway in response to abiotic stresses in plants. Int J Mol Sci 21(2): 621.

Alizadeh MR, Adamowski J, Nikoo MR, AghaKouchak A, Dennison P, Sadegh M (2020) A century of observations reveals increasing likelihood of continental-scale compound dry-hot extremes. Sci Adv 6(39): eaaz4571.

Ballesta P, Mora F, Del Pozo A (2020) Association mapping of drought tolerance indices in wheat: QTL-rich regions on chromosome 4A. Sci Agric 77: e20180153.

Barrett JC, Fry B, Maller J, Daly MJ (2005) Haploview: analysis and visualization of LD and haplotype maps. Bioinformatics 21: 263–265.

Begum H, Alam MS, Feng Y, Koua P et al. (2020). Genetic dissection of bread wheat diversity and identification of adaptive loci in response to elevated tropospheric ozone. Plant Cell Environ 43(11): 2650-2665.

Bush WS, Moore JH (2012) Chapter 11: Genome-Wide Association Studies. PLoSComput Biol 8: e1002822.

Cericola F, Jahoor A, Orabi J, Andersen JR, Janss LL, Jensen J (2017) Optimizing training population size and genotyping strategy for genomic prediction using association study results and pedigree information. A case of study in advanced wheat breeding lines. PLOS ONE 12: e0169606.

Chen X, Robinson DG, Storey JD (2019) The functional false discovery rate with applications to genomics. Biostatistics kxz010.

Chen Y, Palta J, Prasad PV, Siddique KH (2020) Phenotypic variability in bread wheat root systems at the early vegetative stage. BMC Plant Biol 20(1): 1-16.

Christopher J, Christopher M, Jennings R et al (2013) QTL for root angle and number in a population developed from bread wheats (*Triticum aestivum*) with contrasting adaptation to water-limited environments. Theor Appl Genet 126: 1563–1574.

Comas LH, Becker SR, Cruz VMV, Byrne PF, Dierig DA (2013) Root traits contributing to plant productivity under drought. Front Plant Sci 4.

Comas LH, Mueller KE, Taylor LL, Midford PE, Callahan HS, Beerling DJ (2012) Evolutionary patterns and biogeochemical significance of angiosperm root traits. Int J Plant Sci 173: 584–595.

Courtois B, Ahmadi N, Khowaja F et al (2009) Rice root genetic architecture: meta-analysis from a drought QTL database. Rice 2: 115–128.

Crespo-Herrera LA, Crossa J, Huerta-Espino J et al (2017) Genetic yield gains in CIMMYT'S international elite spring wheat yield trials by modeling the genotype× environment interaction. Crop Sci 57: 789–801.

Cui F, Zhang N, Fan X et al (2017) Utilization of a Wheat 660K SNP array-derived high-density genetic map for high-resolution mapping of a major QTL for kernel number. Sci Rep 7: 3788.

Dadshani S, Mathew B, Ballvora A et al (2021) Detection of breeding signatures in wheat using a linkage disequilibrium-corrected mapping approach. Sci Rep 11: 5527.

Daryanto S, Wang L, Jacinthe PA (2016) Global synthesis of drought effects on maize and wheat production. PLOS ONE 11: e0156362.

Fenta B, Beebe S, Kunert K, Burridge J, Barlow K, Lynch J, Foyer C (2014) Field phenotyping of soybean roots for drought stress tolerance. Agronomy 4: 418–435.

Friedli CN, Abiven S, Fossati D, Hund A (2019) Modern wheat semi-dwarfs root deep on demand: response of rooting depth to drought in a set of Swiss era wheats covering 100 years of breeding. Euphytica 215: 85.

Gabriel SB (2002) The structure of haplotype blocks in the human genome. Science 296: 2225–2229.

Giraldo P, Benavente E, Manzano-Agugliaro F, Gimenez E (2019) Worldwide research trends on wheat and barley: A bibliometric comparative analysis. Agronomy 9: 352.

Gitonga VW, Koning-Boucoiran CF, Verlinden K et al (2014) Genetic variation, heritability and genotype by environment interaction of morphological traits in a tetraploid rose population. BMC Genet 15: 146.

Grzesiak MT, Hordyńska N, Maksymowicz A, Grzesiak S, Szechyńska-Hebda M (2019) Variation among spring wheat (*Triticum aestivum* L.) genotypes in response to the drought stress. II—Root system structure. Plants 8: 584.

Hernández EI, Vilagrosa A, Pausas JG, Bellot J (2010) Morphological traits and water use strategies in seedlings of Mediterranean coexisting species. Plant Ecol 207: 233–244.

Ibrahim SE, Schubert A, Pillen K, Léon J (2012) QTL analysis of drought tolerance for seedling root morphological traits in an advanced backcross population of spring wheat. Int J Agric Sci 2: 619-629.

Jaganathan D, Thudi M, Kale S et al (2015) Genotyping-by-sequencing based intra-specific genetic map refines a ‘‘QTL-hotspot” region for drought tolerance in chickpea. Mol Genet Genomics 290: 559–571.

Kadam NN, Tamilselvan A, Lawas LM et al (2017) Genetic control of plasticity in root morphology and anatomy of rice in response to water deficit. Plant Physiol 174(4): 2302-2315.

Kano-Nakata M, Gowda VR, Henry A, Serraj R, Inukai Y et al (2013) Functional roles of the plasticity of root system development in biomass production and water uptake under rainfed lowland conditions. Field Crops Res 144: 288-296.

Kang HM, Sul JH, Service SK, Zaitlen NA, Kong SY et al (2010) Variance component model to account for sample structure in genome-wide association studies. Nat Genet 42: 348– 354.

Kevei Z, Ferreira SDS, Casenave CMP et al (2022) Missense mutation of a class B heat shock factor is responsible for the tomato *bushy root-2* phenotype. Mol Horticulture 2: 4.

Khan MA, Gemenet DC, Villordon A (2016) Root system architecture and abiotic stress tolerance: current knowledge in root and tuber crops. Front Plant Sci 7: https://doi.org/10.3389/fpls.2016.01584

Khan MA, Korban SS (2012) Association mapping in forest trees and fruit crops. J Exp Bot 63: 4045–4060.

Koevoets IT, Venema JH, Elzenga J, Theo M, Testerink C (2016) Roots withstanding their environment: exploiting root system architecture responses to abiotic stress to improve crop tolerance. Front Plant Sci 07: https://doi.org/10.3389/fpls.2016.01335

Lehmensiek A, Bovill W, Wenzl P, Langridge P, Appels R (2009) Genetic mapping in the Triticeae, in: Muehlbauer, G.J., Feuillet, C. (Eds.), Genetics and Genomics of the Triticeae. Springer US, New York, NY, pp. 201–235.

Li L, Peng Z, Mao X, Wang J, Chang X, Reynolds M, Jing R (2019) Genome-wide association study reveals genomic regions controlling root and shoot traits at late growth stages in wheat. Ann Bot 124: 993–1006.

Liu W, Wang J, Wang C et al (2018) Root growth, water and nitrogen use efficiencies in winter wheat under different irrigation and nitrogen regimes in North China Plain. Front Plant Sci 1798.

Shahbandeh M (2019) Grain production worldwide by type, 2018/19 [WWW Document]. Statista. URL https://www.statista.com/statistics/263977/world-grain-production-by-type/ (accessed 3.21.20).

Macharia G, Ngugi BN, Arshad MS, Anjum FM, Sohaib M (2017) Wheat Improvement, Management and Utilization.

Milner SG, Jost M, Taketa S, Mazón ER et al (2019) Genebank genomics highlights the diversity of a global barley collection. Nat Genet 51: 319–326.

Mwadzingeni L, Shimelis H, Dube E, Laing MD, Tsilo TJ (2016) Breeding wheat for drought tolerance: Progress and technologies. J Integr Agric 15: 935–943.

Nguyen VL, Stangoulis J (2019) Variation in root system architecture and morphology of two wheat genotypes is a predictor of their tolerance to phosphorus deficiency. Acta Physiol Plant 41: 109.

Nkambule LL (2020) gwaRs: an R shiny web application for visualizing genome-wide association studies data. bioRxiv. https://doi.org/10.1101/2020.04.17.044784

Nouraein M, Mohammadi SA, Aharizad S, Sadeghzadeh B (2013) Evaluation of drought tolerance indices in wheat recombinant inbred line population. Ann Biol Res 4(3): 113-122.

Oyiga BC, Palczak J, Wojciechowski T, Lynch JP, Naz AA, Léon J, Ballvora A (2020) Genetic components of root architecture and anatomy adjustments to water-deficit stress in spring barley. Plant Cell Environ 43: 692–711.

Prince SJ, Murphy M, Mutava RN, Durnell LA, Valliyodan B, Shannon JG, Nguyen HT (2017) Root xylem plasticity to improve water use and yield in water-stressed soybean. J Exp Bot 68(8): 2027-2036.

Putnik-Delic M, Maksimovic I, Nagl N, Lalic B, Antonio C (2018) Plant, abiotic stress and responses to climate change.

Qaseem MF, Qureshi R, Muqaddasi QH, Shaheen H, Kousar R, Röder MS (2018) Genome-wide association mapping in bread wheat subjected to independent and combined high temperature and drought stress. PLOS ONE 13: e0199121.

R Core Team R (2018) R: A language and environment for statistical computing.Ray DK, Ramankutty N, Mueller ND, West PC, Foley JA (2012) Recent patterns of crop yield growth and stagnation. Nat Commun 3: 1293.

Rieger M, Litvin P (1999) Root system hydraulic conductivity in species with contrasting root anatomy. J Exp Bot 50: 201-209.

Ruiz S, Koebernick N, Duncan S et al (2020) Significance of root hairs at the field scale – modelling root water and phosphorus uptake under different field conditions. Plant Soil 447: 281–304.

Salazar-Henao JE, Vélez-Bermúdez IC, Schmidt W (2016) The regulation and plasticity of root hair patterning and morphogenesis. Development 143: 1848–1858.

Sallam A, Alqudah AM, Dawood MFA, Baenziger PS, Börner A (2019) Drought stress tolerance in wheat and barley: advances in physiology, breeding and genetics research. Int J Mol Sci 20: 3137.

Schneider HM, Klein SP, Hanlon MT, Nord EA, Kaeppler S, Brown KM, Warry A, Bhosale R, Lynch JP (2020) Genetic control of root architectural plasticity in maize. J Exp Bot 71: 3185–3197.

Siddiqui MN, Léon J, Naz AA, Ballvora A (2021a) Genetics and genomics of root system variation in adaptation to drought stress in cereal crops. J Exp Bot 72: 1007-1019.

Siddiqui MN, Teferi TJ, Ambaw AM et al (2021b) New drought-adaptive loci underlying candidate genes on wheat chromosome 4B with improved photosynthesis and yield responses. Physiol Plant 173 (4): 2166-2180.

Soriano JM, Alvaro F (2019) Discovering consensus genomic regions in wheat for root-related traits by QTL meta-analysis. Scientific Reports, 9(1), 1-14.

Sukumaran S, Lopes M, Dreisigacker S, Reynolds M (2018) Genetic analysis of multi-environmental spring wheat trials identifies genomic regions for locus-specific trade-offs for grain weight and grain number. Theor Appl Genet 131: 985–998.

Sun Y, Zhang S, Chen W (2020) Root traits of dryland winter wheat (*Triticum aestivum* L.) from the 1940s to the 2010s in Shaanxi Province, China. Sci Rep 10(1): 1-13.

Trachsel S, Kaeppler SM, Brown KM, Lynch JP (2011) Shovelomics: high throughput phenotyping of maize (*Zea mays* L.) root architecture in the field. Plant Soil 341(1): 75-87.

Ueda Y, Frimpong F, Qi Y, Matthus E, Wu L, Höller S, Kraska T, Frei M (2015) Genetic dissection of ozone tolerance in rice (*Oryza sativa* L.) by a genome-wide association study. J Exp Bot 66: 293–306.

Voorrips RE (2002) MapChart: software for the graphical presentation of linkage maps and QTLs. J Hered 93(1): 77-78.

Voss-Fels KP, Stahl A, Wittkop B et al (2019) Breeding improves wheat productivity under contrasting agrochemical input levels. Nat Plants 5(7): 706-714.

Waples RK, Albrechtsen A, Moltke I (2019) Allele frequency-free inference of close familial relationships from genotypes or low-depth sequencing data. Mol Ecol 28: 35–48.

Wasaya A, Zhang X, Fang Q, Yan Z (2018) Root phenotyping for drought tolerance: A review. Agronomy 8: 241.

Wasson AP, Richards RA, Chatrath R, Misra SC, Prasad SV, Rebetzke GJ, et al (2012) Traits and selection strategies to improve root systems and water uptake in water-limited wheat crops. J Exp Bot 63: 3485–3498.

Ye H, Roorkiwal M, Valliyodan B, Zhou L, Chen P, Varshney RK, Nguyen HT (2018) Genetic diversity of root system architecture in response to drought stress in grain legumes. J. Exp. Bot. 69, 3267–3277. York LM, Slack S, Bennett MJ, Foulkes MJ (2018) Wheat shovelomics I: A field phenotyping approach for characterising the structure and function of root systems in tillering species. BioRxiv 280875.

Zhang L, Dong C, Chen Z et al (2020) WheatGmap: a comprehensive platform for wheat gene mapping and genomic studies. Molecular Plant 14: 187–190.

Zhu Y, Weiner J, Yu M, Li F (2019) Evolutionary agroecology: Trends in root architecture during wheat breeding. Evol Appl 12: 733–743.

Title: *NPF2.12*, a convergently selected nitrate transporter that coordinates root growth and nitrate-use efficiency in wheat and barley

Md. Nurealam Siddiqui[1], Kailash Pandey[1], Suzan Kumer Bhadhury[1], Bahman Sadeqi[1], Michael Schneider[2], Miguel Sanchez-Garcia[3], Benjamin Stich[2], Jens Léon[1], and Agim Ballvora[1*]

[1]Institute of Crop Science and Resource Conservation (INRES)-Plant Breeding, University of Bonn, Katzenburgweg 5, D-53115 Bonn, Germany

[2]Institute for Quantitative Genetics and Genomics of Plants, Heinrich Heine University, Düsseldorf, Germany

[3]Biodiversity and Crop Improvement Program, International Center for Agricultural Research in the Dry Areas (ICARDA), Rabat 10101, Morocco

[*]**Corresponding author**: Dr. Agim Ballvora: ballvora@uni-bonn.de

Manuscript under revision (New Phytologist)

Key message: We identified a convergently selected low-affinity nitrate transporter, *NPF2.12* using a genome-wide scan between wheat and barley, and its variation in alleles can potentially transactivates *NIA1* encoding nitrate reductase activity that induces nitric oxide biosynthesis resulting a better root growth and nitrate-use efficiency to limited nitrogen availability.

Abstract

Understanding the genetic and molecular function of nitrate transport across crop species will accelerate breeding of cultivars with improved nitrogen (N)-use efficiency (NUE). The extent of nitrate transport convergence on a genome-wide scale between wheat and barley is very limited. Here, we performed a genome-wide scan using wheat and barley accessions characterized under low and high N inputs that uncovered a syntenic gene, *NPF2.12* for low-affinity nitrate transport. Phylogenetic analysis revealed that *NPF2.12* encodes a specific MAJOR FACILITATOR SUPERFAMILY domain-containing protein highly identical between wheat and barley with nitrate transporter activity. Further, we showed that the variation in *NPF2.12* promoter positively affected root growth and root-to-shoot nitrate transport by decreasing its expression under low nitrate availability. Further, loss-of-function mutant *npf2.12* specifically transactivates nitrate reductase *NIA1* gene at low nitrate concentrations resulted an elevated levels of nitric oxide production leading to higher root growth and nitrate transportation compared to wild-type. Notably, multiple field trails revealed that the elite allele *TaNPF2.12*^{TT} significantly enhanced N-uptake efficiency, N-transport in leaves and grains and subsequently increased NUE under minimum N. Our data indicate that *NPF2.12* serve as a convergently selected nitrate transporter candidate in wheat and barley and *NPF2.12-NIA1* cascade provides a new route to improve NUE underlying root growth to limited N availability.

Keywords: cereals, genetic variation, genome-wide association mapping, nitrate transport, nitrogen-use efficiency, root system architecture, candidate genes

Introduction

During the last decades, the breeding of cereals and other major crops has been concentrated on selection for increasing grain yield under high-input cropping systems, which are directly responsible for ecological imbalances and cost penalties (Foley et al. 2011; Garnet et al. 2013; Voss-Fels et al. 2019). Nitrogen (N) is the primary driver in agriculture and significantly increase crop yield. However, applying excess amounts of N leads to yield losses by limiting the N-use efficiency (NUE) of crops (Vitousek et al. 2009; Wang et al. 2014). It has been documented that only 33-40% of the applied N can be transformed into grain yield. As a result, remaining N is lost through nitrate (NO_3^-) leaching into the environment (Hirel et al. 2011; Dhital and Raun, 2016; Yang et al. 2019). In contrast, low soil N availability is also one of the limiting factors for crop yield in many countries of the world, including sub-Saharan Africa and Latin America (Dixon and Flores Velazquez, 2007). Therefore, there is increasing interest in utilizing NO_3^- transporter genes to develop high-NUE varieties to minimize the excess costs to farmers and detrimental impacts on ecosystems (Chen et al. 2014; Tang et al. 2019). However, improved NUE under N-limited conditions is influenced by efficient NO_3^- transporter genes (O'Brien et al. 2016; Li et al. 2016; Jia et al. 2019). Expanding our knowledge on convergently regulated NO_3^- transporter genes across crops and their interconnections with the processes of root growth, NO_3^- sensing, uptake as well as of transport and assimilation will speed up the breeding of NUE in all species.

NO_3^- is the most predominant sources of N in natural as well as agricultural ecosystems (von Wirén et al. 2000). Plants uptake NO_3^- by roots and using NO_3^- transporters. In the next step, NO_3^- is then distribute within the whole plant, or it can be conjugated with carbon molecules to generate amino acids through assimilation prior to being redistributed (Miller et al., 2007; Xu et al., 2012). In spite of having its role as an essential nutrient, NO_3^- also acts as a signalling molecule that coordinates the NO_3^--induced gene expressions to regulate plant growth and development, especially root growth and development (Vidal and Gutierrez, 2008; Krouk et al. 2010; Alvarez et al. 2012). In higher plants, NO_3^- uptake and transport systems consists of the low-affinity transport system (LATS) and the high-affinity transport system (HATS) and their transport nature largely depends on availability of cellular energy and proton electrochemical gradient (Siddiqi et al. 1990; Miller et al. 2007). Over the last two decades, at least four transporter families involved in NO_3^- transport have been identified in plants. The major plant NO_3^- transporter has been identified in *Arabidopsis thaliana*, *nitrate-transporter 1* (*NRT1*) (Tsay et al. 1993) or *peptide transfer* (*PTR*) gene family together known as NPF family (Léran et al. 2014). The NPF family encompasses a wide range of genes, which can be further classified into 8-10 sub families. This family has 53 and 93 members in Arabidopsis and rice, respectively (Léran et al. 2014; von Wittgenstein et al. 2014). The NPF members are reported

to act as the main components of the LATS at high NO_3^- concentrations. Few of them, like NRT1.1 in Arabidopsis (Liu and Tsay, 2003) and MtNRT1.3 in *Medicago truncatula* (Morère-LePaven et al. 2011), function as dual-affinity transporters associated with both HATS and LATS. *NPF* genes play important functions in N utilization (Wang et al. 2018). Alterations in amino acid sequences of NPF proteins in rice have been delineated to affect the NO_3^- transport and NUE by integrating a regulatory network (Hu et al. 2015; Tang et al. 2019).

Comparative genome-wide association studies (GWAS) using multiple species has been recently flourishing as a powerful tool to dissect genetic architecture within species and to identify candidate genes conserved in related species that reflect the natural variations of RSA in cereals (Klein et al. 2020; Zheng et al. 2020). Among cereals, wheat and barley are both economically most valuable crops, ranked second and fourth, respectively in terms of their global production, food demands, and human nutrition (https:// faostat.fao.org/). These two species considerably diverged since evolved from a common ancestor around 10-14 million years ago. In-depth genetic mapping and structural genomic investigations have revealed that both genomes are largely conserved (Devos and Gale 1997; Schreiber et al. 2009). Even barley chromosomes can be swapped for wheat chromosomes (Islam et al. 1981). Comparative transcriptome analysis in Triticeae indicated that highly expressed genes in wheat and barley tend to be evolutionarily conserved (Schreiber et al. 2009). Therefore, convergent orthologues between related species are more likely to maintain steady functional patterns of gene regulation and expression (Davidson et al. 2012). However, no studies are available so far that reported a comparative GWAS between wheat and barley to unravel shared regulators of NO_3^- transport and to analyse their allelic variations related to root growth and NUE in respect to heterogeneous N availability.

Here we perform a genome-wide scale using diverse panels of winter wheat and spring barley to analyze root phenotypes under extreme N input levels in field and controlled conditions. We identify several marker-trait associations (MTAs) colocalizing with candidate genes that are involved in N transport and metabolisms and prioritize a convergently selected NO_3^- transporter between wheat and barley. We report that the *NPF2.12* natural alleles diverge in regulatory elements establish distinct haplotype (Hap) differences. The rare natural allele of *NPF2.12* significantly enhanced root growth and NO_3^- transport in both crops at low NO_3^-. Further, root transcriptome analysis revealed that *npf2.12* mutant allele induces *NITRATE REDUCTASE 1* (*NIA1*) encoding nitrate reductase (NR), thereby increases root growth, NO_3^- uptake and root-to-shoot transport leading to a robust NUE at limited N availability.

Results

N-induced divergence of root phenotypes in wheat and barley populations

The winter wheat panel comprised 221 cultivars registered in Europe from 1963 to 2013 was used in this study. The majority of cultivars were of German origin (60%), while the remaining originated from 25 different countries. This diversity panel has previously been used for several GWAS (Voss-Fels et al. 2019; Begum et al. 2020; Koua et al. 2021; Siddiqui et al. 2021a). For this study, we acquired phenotypic data for 21 root system-related traits (Table S1) under two contrasting environments: no additional N fertilizer (LN) and 220 kgN ha^{-1} (HN). We found that no fertilizer application significantly increased root morphological traits such as total root length (TRL), root surface area (RSA), root volume (RV), number of root tips (NRT) (Table S2 and S3). We also found that additional N-supply (HN) significantly decreased most of the anatomical traits, except some ratio-based anatomical traits such as percentage of main shoot and tiller nodal root cross section occupied by stele (mSDP) and (tSDP), respectively, while all of the traits showed significant genotype-treatment interactions (Table S2). Under increased N-supply, all 21 root-related traits exhibited a decreasing phenotypic variability, and their coefficients of variations were greater than 20% and 10% for morphological and anatomical traits, respectively (Table S2). The broad-sense heritability (H^2) of root traits under higher N-supply were found low ranges between 56 to 81% when compared with lower N-supply grown plants (Table S3).

The barley diversity panel was phenotyped in transparent plastic boxes placed in a growth chamber and supplied with high (10 mM) and low NO_3^--N (0.5 mM). Root phenotyping was carried out 14-days after imposing the treatment. The data showed that at low NO_3^- supply, root morphological attributes, importantly rooting depth (RD), TRL, number of tips, forks and crossings were significantly increased compared to high NO_3^- supply. For RSA, RAD and RV showed decreasing trends upon low NO_3^- supply when compared with high NO_3^- supply (Table S4). The coefficient of variations among all of the measured root traits were more than 15%, and ranged between 15 to 64%. Heritability (H^2) ranged from 23 to 68% among morphological traits under low NO_3^-, which was higher than in the high NO_3^- environment (Table S4). This trend indicated that both wheat and barley association panels may harbor substantial natural variations of root traits that confers them with efficient N-uptake and transport under low LN availability.

Candidate genes involved in root growth variations and N responses

To identify genetic factors involved in the variation of the above described root phenotypic traits in wheat and barley, we carried out a GWAS using an MLM that corrects for the confounding effects of population structure and family relatedness. We used the significance threshold of –

log10 (*P*) > 4.0, as a significant MTAS, as defined by a previous study using the same association panel (Siddiqui et al. 2021a). A total of 70 MTAs were identified for root architectural and anatomical traits under different levels of N such as HN, LN and LN/HN conditions across the wheat genome (Table S5). To unravel the candidate genes underlying these MTAs, we identified 37 LD blocks with 340 plausible candidate genes (data not shown). A total of 38 of them had an annotation in responses to N metabolisms, sensing, assimilation and transport systems (Table S6). Notably, we detected a hotspot on chromosome 3B that carries several candidate genes related to N and NO_3^- responses (Table S6).

Using the same significance threshold (–log10 (*P*) > 4.0), a total of 43 MTAs were identified across all the barley chromosomes except 4H and 7H under various NO_3^- treatments (Table S7). The analyses of the genomic regions of the 43 MTAs revealed that the most of them overlapped with the genes related to transporter families and domain-containing transcription factors (Table S7). Out of them, one gene belonged to NO_3^- transporter protein NRT family (Table S7).

Comparative genome-wide scan between wheat and barley uncovers a convergently selected gene associated with NO_3^- transport

Due to the conserved relationship between wheat and barley genomes (Salse et al. 2009; Schreiber et al. 2009; Siddiqui et al. 2021b), as well as the shared patterns of the root system development (Brenchley and Jackson, 1921), we hypothesize that both species may have a convergent regulation of root growth and NO_3^- transport. To test this hypothesis, we conducted a comparative analysis between the chromosomal intervals harboring the MTAs for root system traits of wheat and barley. Overlapping genes were detected within 20-kb windows surrounding respective SNPs in wheat and barley, respectively. Based on the FDR threshold ≤ 0.01, three pairs of overlapping genes were identified on chromosome 3 (Table S8). A permutation analysis revealed that the overlapping genes more likely than by chance (*P* = 1e-04). For instance, *TraesCS3B02G454000*, was annotated in wheat as low-affinity NO_3^- transporter (GO: 0080054), NO_3^- transporter (GO: 0015706), and NO_3^- assimilator (GO: 0042128), is located within centre position of a SNP that was significantly associated with RV under LN/HN conditions. Its orthologue in barley, *HORVU3Hr1G092870*, was annotated as low-affinity NO_3^- transmembrane transporter (Protein NRT1/ PTR FAMILY 2.13) and was detected by a SNP for TRL at low/high NO_3^- conditions (Fig. 1a). We defined this convergently selected gene pair as *TaNPF2.12* in wheat and *HvNPF2.12* in barley based on its unique homologs in *A. thaliana*. The alleles with minor frequency (*n*= 49 in wheat and 33 in barley) of both shared markers across wheat and barley showed significantly higher RV and TRL than the major alleles, respectively (Figs. 1b, c). Interestingly, all of the identified convergently

selected genes between wheat and barley were associated with root morphological traits, and in a unique environment, LN/HN (Table S8).

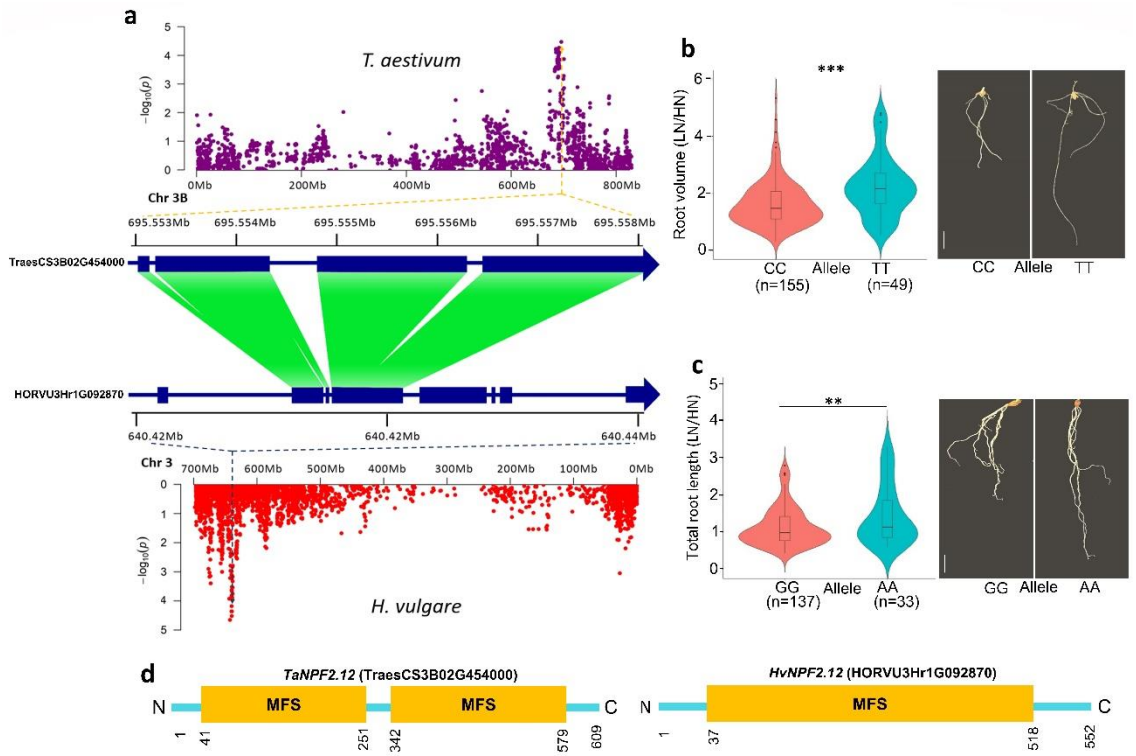

Fig.1: Comparative GWAS between wheat and barley for root volume (RV) and total root length (TRL) at LN/HN. **a**, Manhattan plots of chromosome 3 from SNP-based GWAS for RV of wheat (top) and TRL of barley (bottom) revealed a pair of convergently selected NO_3^- transporter genes; homologous sequences are highlighted in green. **b**, Allelic distribution and effect of wheat (left) and wheat root phenotypes (right); Anthus (CC) and Oakley (TT) alleles of the SNPs associated with RV. **c**, Allelic distribution and effect of barley (left) and barley root phenotypes (right); Gada (GG) and Harmal-02 (AA) alleles of the SNPs associated with TRL. **d**, Schematic depiction of wheat TaNPF2.12 (TraesCS3B02G454000) protein and barley HvNPF2.12 (HORVU3Hr1G092870) protein sequences representing a relevant protein domains of MFS (major facilitator superfamily). Numbers denote the length of amino acid. Student's t test; $^{**}P < 0.01$ and $^{***}P < 0.001$, respectively. LN, low nitrogen/NO_3^-; HN, high nitrogen/NO_3^-. Scale bars, 1 cm.

Next, we performed a phylogenetic analysis to determine the sequence similarities of the *TaNPF2.12* and *HvNPF2.12*. Phylogenetic analyses with 32 NPF/NRT proteins from different plant species, including cereal species revealed that the barley NPF/NRT protein (KAE8800431.1) was highly similar compared to the wheat protein (KAF7025301.1) (Fig. S1a), and both NPF proteins in wheat and barley share a conserved domain structure. Namely, Major Facilitator Superfamily (MFS) in the N-terminus and a C-terminal were the strongest specific hits (Figs. 1d, S1b). To further confirm the predicted protein interactions of NPF, *in silico* protein-protein network analysis was conducted using Arabidopsis protein NRT1.6 (possessing the unique sequence of *NPF2.12*) as an input. Remarkably, five out of the top ten

and seven of the potential interacting proteins (score> 0.6) of NRT1.6 were MFS transporter (NO_3^- transporter) and high-affinity NO_3^- transporter (Fig. S1c). This data indicate that *TaNPF2.12* and *HvNPF2.12* are convergently selected, and encode for specific proteins with NO_3^- transporter activities.

Natural allelic variations at the *NPF2.12* promoter modulates root growth and NO_3^- transportation to NO_3^- availability

To validate the involvement of *TaNPF2.12* in root growth and NO_3^- transport in wheat, the full-length promoter and coding regions of 20 NO_3^--tolerant (higher RV under low/high NO_3^-) and 20 NO_3^--sensitives (lower RV under low/high NO_3^-) wheat cultivars were sequenced and compared (Table S9). Two distinct Hap groups were observed in the promoter sequence among these 40 cultivars, with 18 and 22 cultivars as Hap1and Hap2, respectively (Fig. 2a). The Hap2 had the allelic variations at -1299, -1282, -1275, -1267, -1266, -1264 and -88 bp of *TaNPF2.12* when compared with Hap1 (Fig. 2a), whereas no variations were observed in the coding regions. The majority of the selected NO_3^--sensitive cultivars belong to the Hap1. We observed highly significant differences (*P*=3.16e-11, Student's t test) in RV between inbreeds carrying Hap1 and Hap2; the average RV of Hap1 was <1.0, while the average RV of Hap2 was >3.0 (Fig. 2b). In contrast, genotypes with Hap2 showed significantly higher TRL, RSA, RV and NRT and root-to-shoot NO_3^- transport compared to Hap1 at low NO_3^-, while varying responses were observed at high NO_3^- concentration (Figs. 2c-h; Figs. S2a, b). Further, we selected two cultivars with Hap1 carrying CC allele of *NPF2.12* and two cultivars with Hap2 harbouring TT allele (Table S9) to examine the levels of gene expression. The expression levels of *TaNPF2.12* were significantly higher for Hap1 allele (CC) of *TaNPF2.12* than for Hap2 allele (TT) under low NO_3^- conditions, whereas almost similar expression levels were observed under high NO_3^- between two Hap groups (Fig. 2c).

To estimate the allelic variations of *HvNPF2.12* in barley, the full-length coding and promoter region in 40 barley genotypes were sequenced (Table S10). Alike wheat, two Hap groups were observed specifically for the promoter region. Fifteen NO_3^--sensitive genotypes (lower TRL under low/high NO_3^-) carried Hap1 and 25 NO_3^--tolerant genotypes (higher TRL under low/high NO_3^-) Hap2 (Fig. 3a). In comparison with Hap1, Hap2 had variations at upstream of the start codon (Fig. 3a). The average TRL of genotypes carrying Hap2 was >1.75, while the average TRL of inbreeds carrying Hap1 was significantly lower with 0.75 at low/high NO_3^- conditions (Fig. 3b). In the next step, we tested *HvNPF2.12* expressions in two barley genotypes carrying Hap1 allele and two with Hap2 allele (Table S10). At low NO_3^- availability, higher levels of expressions of *HvNPF2.12* were recorded for Hap1 genotypes than for genotypes carrying Hap2 (Fig. 3c). The Hap2 allele (AA) had significantly lower expression

under low NO_3^- than high NO_3^- conditions (Fig. 3c). Notably, Hap2 allele (AA) showed higher root growth-related traits and root-to-shoot NO_3^- transport at low NO_3^- when compared with the Hap1 allele (Figs. 3c-h; Figs. S2c, d). Our results in wheat and barley suggest that Hap2 allele had lower expression levels of *TaNPF2.12* and *HvNPF2.12* compared to Hap1 allele which might lead to increased root growth and NO_3^- transport in response to low NO_3^- availability. Further, we hypothesize that NO_3^--induced *NPF2.12* transcription might contribute to root growth and NO_3^- transport.

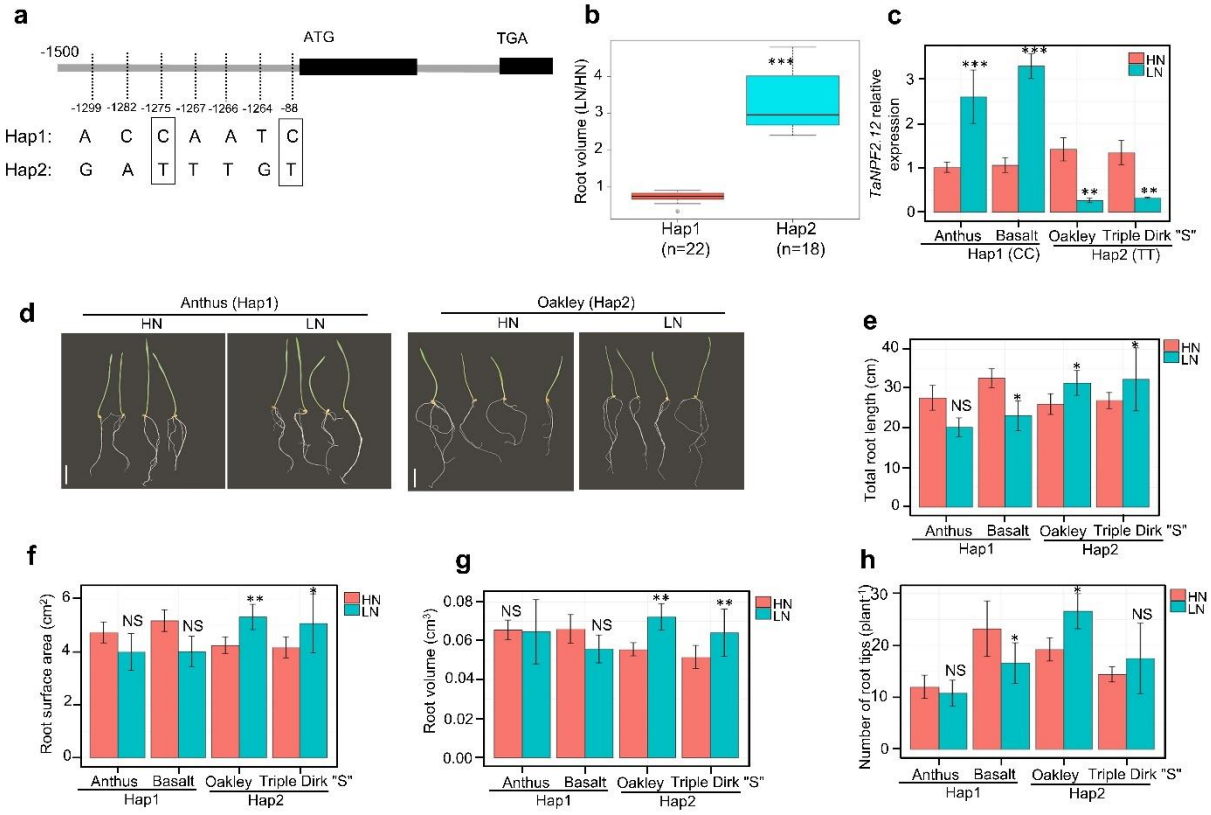

Fig.2: Haplotype, relative expression and root growth analyses of *TaNPF2.12* in wheat. **a,** Schematic graph reveals the allelic variation in the promoter regions of *TaNPF2.12* gene and the corresponding two haplotypes, Hap1 and Hap2. **b,** Boxplot of root volume ratio for two identified haplotype groups. Statistical significance (***P < 0.001) of the difference between two haplotypes was obtained by Student's t test. **c,** Relative expression of *TaNPF2.12* in two wheat cultivars from Hap1 (CC) and two from Hap2 (TT) alleles response to contrasting NO_3^- levels. The relative expression of *TaNPF2.12* in wheat roots at 14-days after NO_3^- imposition at low NO_3^- (0.5 mM NO_3^--N) and was quantified by qRT-PCR, using *TaEf-1a* and *TaEf-1b* as the internal control genes and the corresponding samples under 10 mM NO_3^--N supply as controls. Data illustrate the mean ± standard error of three replicates. **d-h,** Phenotypic differences of root systems. **e,** total root length. **f,** root surface area. g, root volume and **h.** number of root tips of Hap1 (CC) and Hap2 (TT) alleles plants grown at high and low NO_3^- availability. Bars represent means ± standard error (n = 06 independent biological replicates). Student's t test; *P < 0.05, **P < 0.01 and ***P < 0.001, respectively based on one-way ANOVA. Scale bars, 1 cm. HN, high NO_3^- (10 mM) and LN, low NO_3^- (0.5 mM) and NS, not significant.

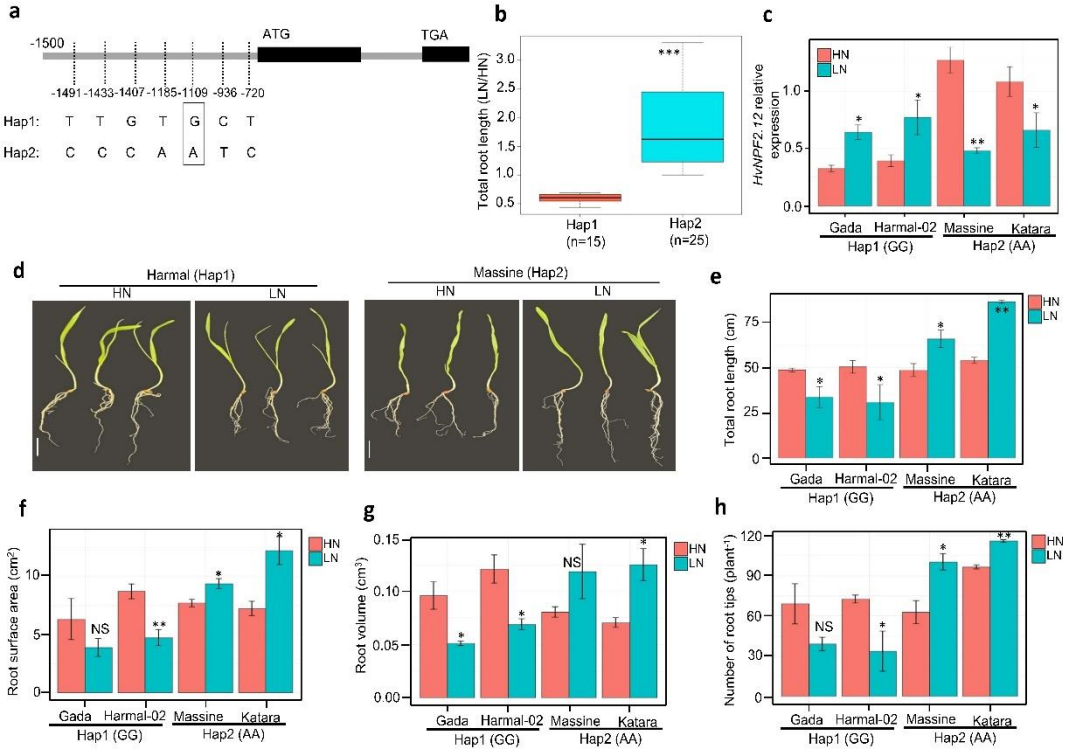

Fig.3: Haplotype, relative expression and root growth analyses of *HvNPF2.12* in barley. **a,** Schematic graph reveals the allelic variation in the promoter regions of *HvNPF2.12* gene and the corresponding two haplotypes, Hap1 and Hap2. **b,** Boxplot of total root length ratio for two identified haplotype groups. Statistical significance (***P < 0.001) of the difference between two haplotypes was obtained by Student's t test. **c,** Relative expression of *HvNPF2.12* in two barley genotypes from Hap1 (GG) and two from Hap2 (AA) alleles response to contrasting NO_3^- levels. The relative expression of *HvNPF2.12* in barley roots at 14-days after NO_3^- imposition at low NO_3^- (0.5 mM NO_3^--N) and was quantified by qRT-PCR, using *Ef-1a* as the internal control gene and the corresponding samples under 10 mM NO_3^--N supply as controls. Data illustrate the mean ± standard error of three replicates. **d-h,** Phenotypic differences of root systems. **e,** total root length. **f,** root surface area. g, root volume and **h.** number of root tips of Hap1 (GG) and Hap2 (AA) alleles plants grown at high and low NO_3^- availability. Bars represent means ± standard error (n = 05 independent biological replicates). Student's t test; *P < 0.05, **P < 0.01 and ***P < 0.001, respectively based on one-way ANOVA. Scale bars, 1 cm. HN, high NO_3^- (10 mM) and LN, low NO_3^- (0.5 mM) and NS, not significant.

Transcriptome analysis reveals the up-regulation of multiple genes involved in NO_3^- transport and metabolism between wild-type and *npf2.12* plants

To obtain insights into *TaNPF2.12* transcriptional responses and signaling pathways to NO_3^- availability, we utilized an *npf2.12* mutant developed by ethyl methanesulfonate (EMS) approach in a tetraploid Kronos wild-type (WT) variety (Kronos4652). One base-pair alteration was located at the 496 site of *NPF2.12*, which causes a premature termination codon in the fourth exon that disrupts its transcriptional activation domain (Fig. 4a). An Illumina HiSeq 6000

platform was utilized to perform high-throughput RNA-seq analysis of both WT and *npf2.12* mutant roots harvested after 14-days of high and low NO_3^- treatments. Differentially expressed genes (DEGs) between WT and *npf2.12* plants under two NO_3^- treatments were identified based on FDR adjusted *P*-value < 0.05 and a log_2fold change threshold. RNA-seq analysis revealed a total of 106,914 DEGs, of which 826 genes were upregulated in the WT (details in supplementary method; Fig. S3). The mutant line was characterized by 255 and 345 up-regulated DEGs, while WT revealed 418 and 435 upregulated genes in high and low NO_3^-, respectively (Table S15). Further analysis of DEGs in a comparison of WT and mutant (high to high and low to low NO_3^-), identified the significant up-regulations of 6 among 599 NO_3^- transporter genes by WT, five of these under high NO_3^- conditions (Table S15). Contrastingly, only one NRT1 family protein (5.5) was upregulated in high NO_3^- by the mutant plants when compared with WT (*P*-value <0.0001, log_2Fold = 6). However, a high-affinity nitrate transporter and an NRT1 family protein (2.1) were up-regulated in WT compared to mutant under low NO_3^- treatment (Table S16). To better understand the potential functions and biological processes of these DEGs, the ShinyGO enrichment tool was applied for up-regulated genes (Supplementary method). The nutrient transport pathways were found to be the most enriched pathways, followed by different molecules biosynthetic or metabolic pathways (Figs. S4). The NO_3^- transport and response pathways were the significantly enriched pathways in WT allele under high NO_3^- environment and a high-affinity NO_3^- transporter gene *NAR2.1* was involved in these pathways (Fig. 4b; Table S16). The NO biosynthesis and metabolic pathways were the most significant and enriched pathways found in *npf2.12* allele plants under low NO_3^- treatment, where *NIA1* was specifically associated with these pathways (Fig. 4c, Table S16). Hence, we further hypothesize that *NIA1* regulates NO production underlying activities of NR in *npf2.12* allele that might be candidate modulating root growth and NO_3^- transport under partial NO_3^- supply.

Next, to gain an overview of *NIA1*-dependent NO biosynthesis under NO_3^- availability, we compared *NIA1* transcript expression, activities of NR and NO production capacity between WT and *npf2.12* mutant plants. *NIA1* transcript expression was significantly (*P* <0.001) increased in mutant plants in response to low NO_3^- compared to WT (Fig. 4d). Accordingly, under low NO_3^- treatment, the mutant allele showed significantly higher NR activities and NO production levels than the WT (Fig. 4e, f). These results indicate that upon low NO_3^- inputs, when *NPF2.12* transcription is inactive, the *NIA1* transcription is highly activated to confer NR-mediated NO homeostasis.

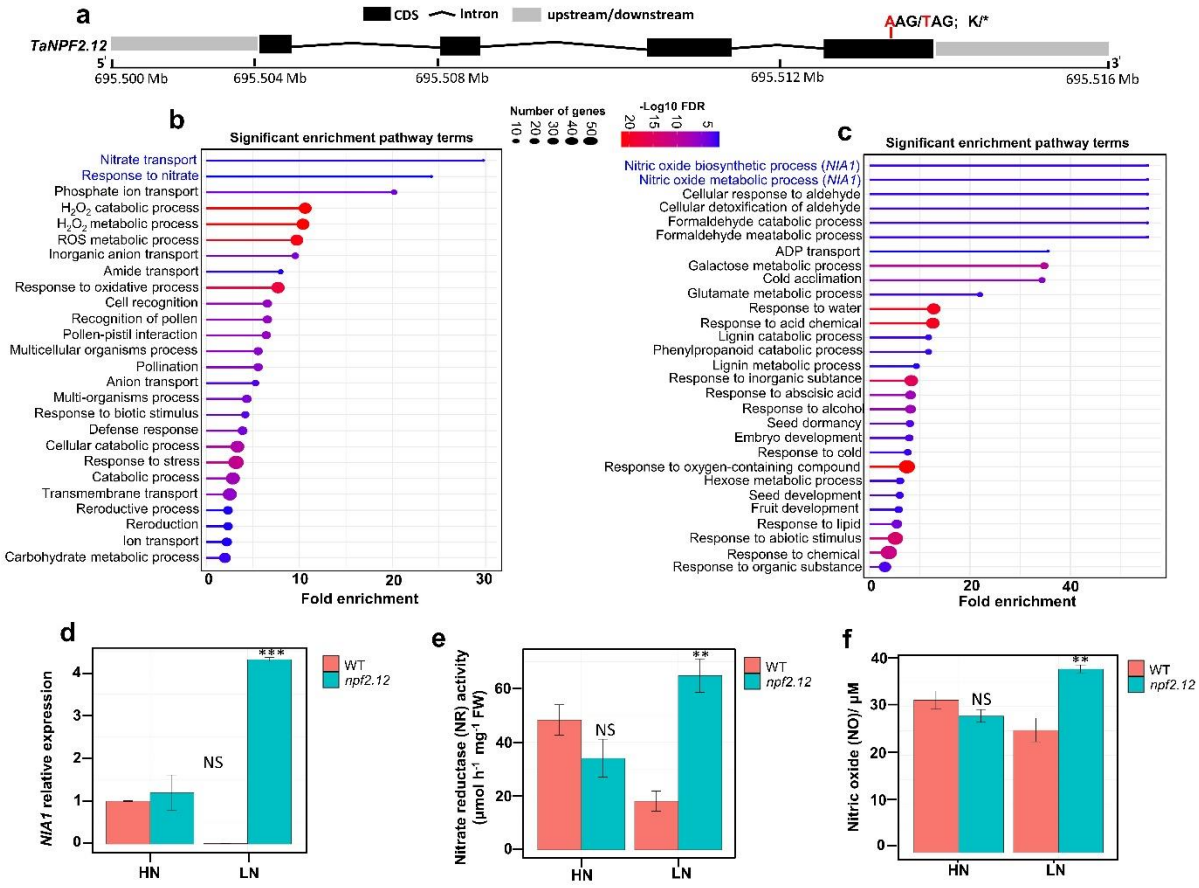

Fig. 4: RNA sequencing, *NIA1* expression, NR activity and NO content analyses of the *TaNPF2.12* wild-type and mutant allele after 14-days exposed to high and low NO_3^-. **a,** Gene structure of *TaNPF2.12* and mutant site. **b,** gene ontology and the 26 most significantly enriched pathways in WT allele under high NO_3^- treatment. **c,** gene ontology and the 29 most significantly enriched pathways in *npf2.12* mutant allele under low NO_3^- treatment analysed by ShinyGO enrichment tool. **d,** comparison of transcript expression levels of *NIA1* by qRT-PCR. **e,** NR activity and **f,** NO contents between WT and mutant plants. We considered differentially expressed genes when on average more than two normalized reads across all three replicates were recognized. Bars represent means ± standard error (n = 06 independent biological replicates). Student's t test; **P* < 0.05, ***P* < 0.01 and ****P* < 0.001, respectively based on one-way ANOVA. HN, high NO_3^- (10 mM) and LN, low NO_3^- (0.5 mM) and NS, not significant.

Loss-of-function of *npf2.12* allele mediates root growth and NO_3^- transport

To verify the loss-of-function of candidate *npf2.12* allele relation to root growth and NO_3^- transport, we phenotyped root growth and NO_3^- accumulation in root and shoot of the *npf2.12* mutant and WT under high (10.0 mM) and low NO_3^- (0.5 mM) treatments. The *npf2.12* mutant plants demonstrated increased root growth performances under low NO_3^- conditions compared to the WT after both 7- and 14-days of NO_3^- treatments (Figs. 5b, c). At high NO_3^- availability, the WT plant exhibited increased root growth compare to *npf2.12* mutant (Figs. 5b, c). Furthermore, qRT-PCR analysis in roots revealed significantly abundant *NPF2.12* transcript

levels in the 14-days old of wild-type at low NO_3^- compared to mutant seedlings, but no significant variations observed under high NO_3^- (Fig. 5d), predicting that *NPF2.12* is a NO_3^--dependent transporter in wheat. Subsequently, a root phenotyping experiment exhibited that root morphological traits, particularly TRL, RSA and RV were significantly increased in *npf2.12* mutant at low NO_3^- compared to WT (Figs. 5e-h). These results implied that the WT allele reduced root growth under low NO_3^- conditions. To estimate whether *NPF2.12* contributes to the divergence of NO_3^- uptake by root and transport to shoot, the mutant and WT seedlings were grown in a solution containing contrasting level of NO_3^- inputs. The NO_3^- contents in root and shoot were decreased in mutant plants compared to the WT seedlings at high NO_3^- conditions, but their accumulation was significantly increased in *npf2.12* plants at low NO_3^- conditions (Figs. 5i, j). Taken together, the *npf2.12* mutant allele strongly influences root growth, NO_3^- uptake and transport to low NO_3^- concentrations than the allele of WT (Figs. 5i, j).

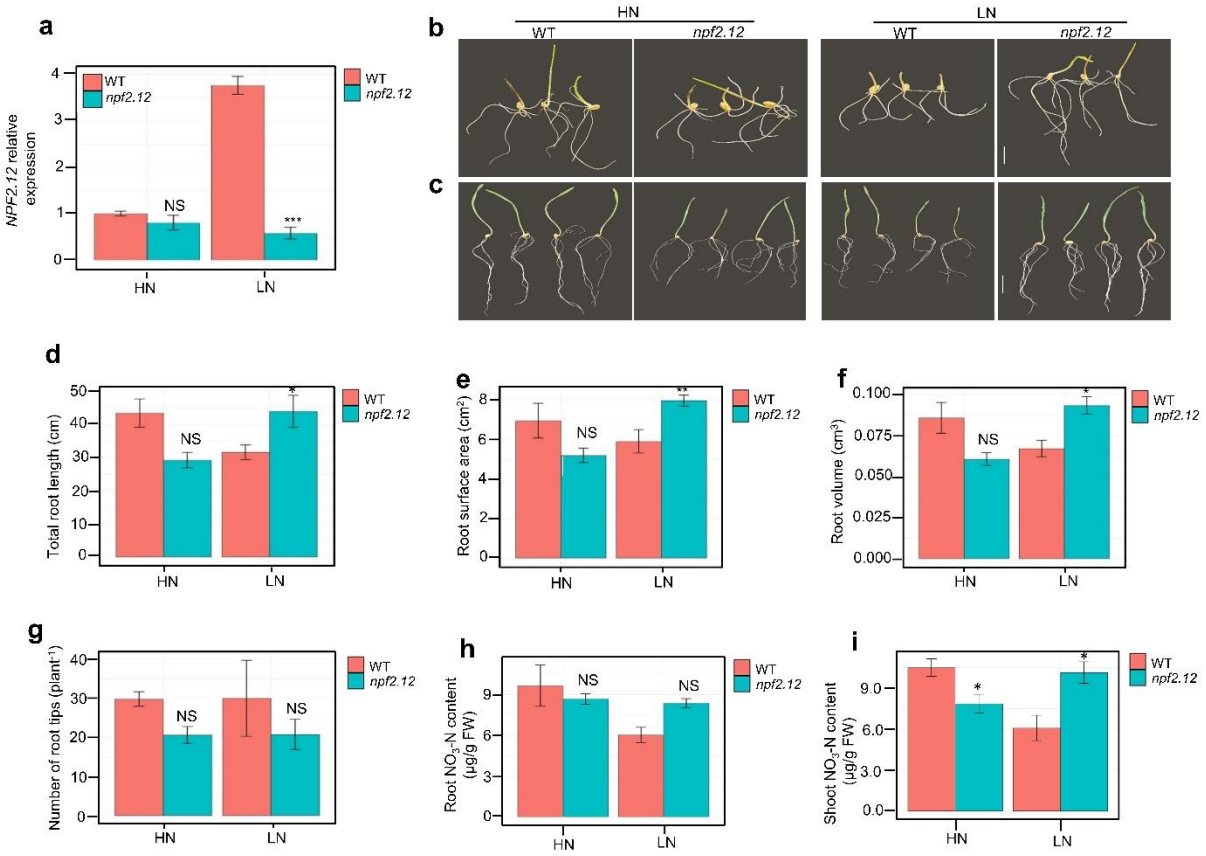

Fig. 5: Relative expression, root phenotypes and NO_3^--N content in root and shoot of *TaNPF2.12* EMS wheat mutant and wild-type (Kronos) under 10 mM and 0.5 mM NO_3^--N conditions. **a,** Relative expression of *NPF2.12* in *npf2.12* mutant and wild-type alleles response to contrasting NO_3^- levels. The relative expression of *NPF2.12* in mutant and wild-type seedling roots at 14-days after NO_3^- imposition at low NO_3^- (0.5 mM NO_3^--N) and was quantified by qRT-PCR, using *TaEf-1a* and *TaEf-1b* as the internal control genes and the corresponding samples under 10 mM NO_3^--N supply as controls. Data illustrate

the mean ± standard error of three replicates. **b-g,** Phenotypic differences of root growth. **b,** Root growth phenotypes of *npf2.12* mutant and wild-type plants after 7-days exposure to NO_3^- treatments. **c,** Root growth phenotypes of *npf2.12* mutant and wild-type plants after 14-days exposure to NO_3^- treatments. **d,** total root length. **e,** root surface area. **f,** root volume **g.** number of root tips **i,** NO_3^--N content in root. **j.** NO_3^--N content in shoot of mutant and wild-type plants grown at high and low NO_3^- availability. Bars represent means ± standard error (n = 06 independent biological replicates). Student's t test; **P* < 0.05, ***P* < 0.01 and ****P* < 0.001, respectively based on one-way ANOVA. Scale bars, 1 cm. HN, high NO_3^- (10 mM) and LN, low NO_3^- (0.5 mM) and NS, not significant.

The natural allele of *TaNPF2.12* enhances N-uptake and NUE under field conditions

Field experiments were performed to analyse the allelic effects of *TaNPF2.12* on NUE-related traits. The cultivars harbouring CC (Hap1) and TT (Hap2) alleles were grown in the field supplied with HN (220 kgN ha^{-1}) and LN (0 kgN ha^{-1}) levels over three consecutive cropping seasons. The N content in leaves of plants carrying the TT allele significantly increased by 7.30% in 2017-2018 and non-significantly increased by 6.17% in 2019-2020 as compared to the CC allele under LN input level,, while no significant differences in N-content were observed under LN supply in 2018-2019 (Figs. 6a-c). No significant changes in N content were observed between the *TaNPF2.12* alleles under HN input levels (Figs. 6a-c). Correspondingly, the N content in grains of the genotypes carrying the TT allele was consistently increased under LN input levels over three years compared to the cultivars carrying the CC allele (Figs. 6d-f). The wheat cultivars harboring the TT allele of *TaNPF2.12* exhibited significantly higher N uptake efficiency (NUpE) compared to the allele of CC under LN supply in 2018-2019 and 2019-2020, while no significant changes in NUpE were observed under HN over the three growing seasons (Figs. 6g-i). Importantly, the cultivars possessing the TT allele of *TaNPF2.12* significantly increased NUE in all three trials as compared to the CC cultivars at LN conditions (Figs. 6j-k). These results illustrate that the presence of wheat allele of $TaNPF2.12^{TT}$confers enhanced levels of N content in leaves and grains, which ultimately resulted in robust NUE under limited N availability over three successive field trials.

Discussion

The trait values observed for all of the root traits in both wheat and barley were significantly reduced by higher N-supply, which is an agreement with previous reports (Li et al. 2015; Xin et al. 2021). For 21 root traits in wheat and 9 in barley, the GWAS identified 70 and 43 SNPs that are in proximity of 341 and 38 candidate genes related to N responses and root growth across wheat and barley chromosomes, respectively. Using a comparative GWAS between wheat and barley, three pairs of convergently selected genes were identified, which includes

one NO_3^- transporter gene *TraesCS3B02G454000 (TaNPF2.12)*/*HORVU3Hr1G092870* (*HvNPF2.12*) on chromosome 3. In previous studies, several NO_3^- transporter NPF genes have been reported in hexaploid wheat and barley, which are mainly abundant on the chromosome 3 (Guo et al. 2020; Wang et al. 2020). However, comparative GWAS provides a conserved architecture on chromosome 3 in both wheat and barley containing a high number of candidate genes related to NUE. Next, phylogenetic analysis revealed a conserved and unique domain of MFS in both *TaNPF2.12* and *HvNPF2.12*. This shared MFS domain specifically encodes a protein with NO_3^- transporter activity. The MFS domain-containing proteins comprises of 12 transmembrane regions. The MFS transporters are single-polypeptide secondary transporters competent to carrying small solutes in relation to chemiosmotic ion gradients that functions as uniporters, symporters or antiporters (Marger and Saier 1993; Pao et al 1998); therefore, the function of *TaNPF2.12* and *HvNPF2.12* were examined in more detail.

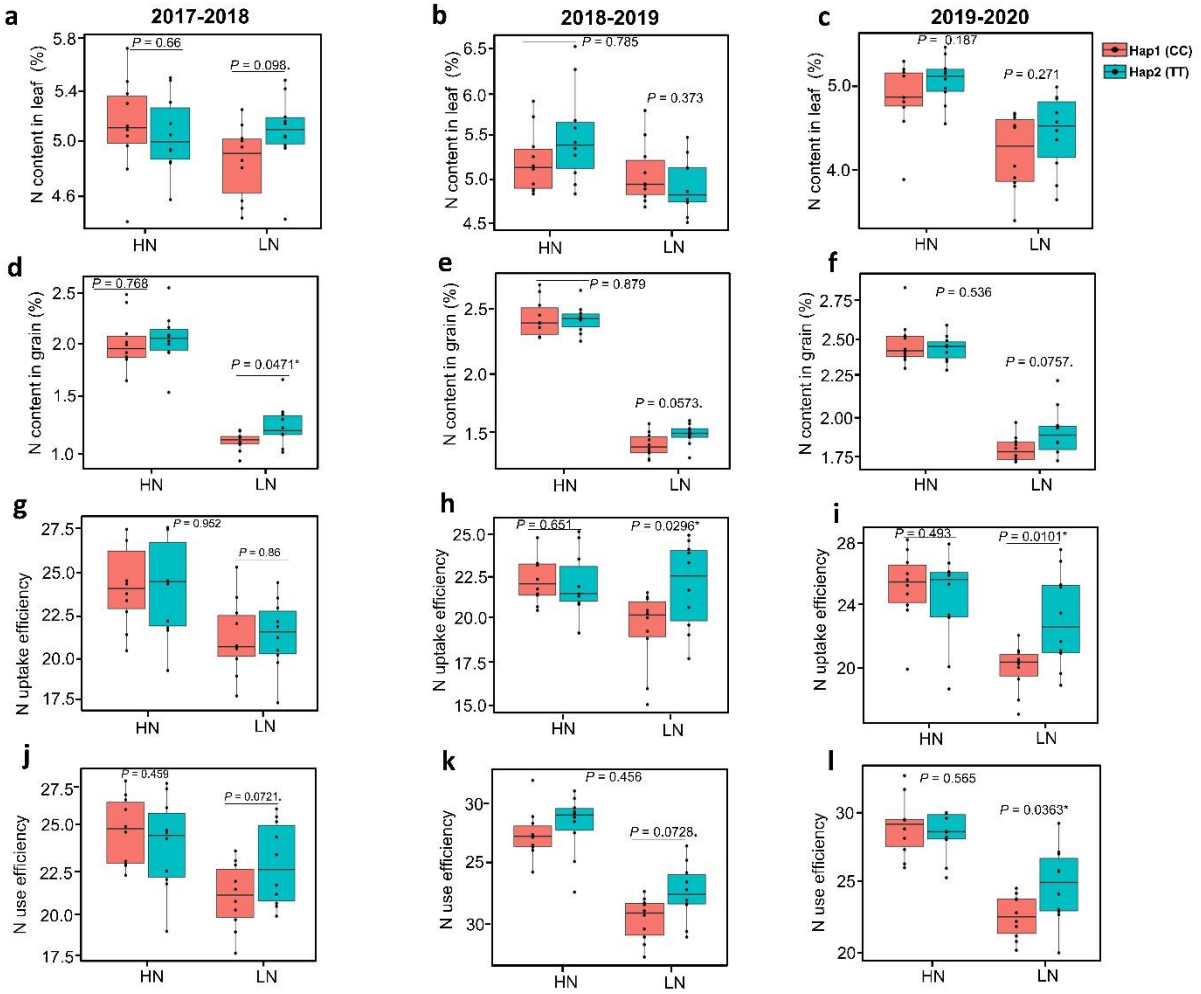

Fig. 6: Field-based evaluation of N-use efficiency related traits in wheat plants carrying TT and CC alleles of *TaNPF2.12* grown under 220 kg N ha^{-1} and 0 kg N ha^{-1} conditions in three growing seasons (2017-2018,-2018-2019 and 2019-2020). **A**, N content in leaf (%) in 2017-2018; **b,** N content in leaf in

2018-2019; **c,** N content in leaf in 2019-2020; **d,** N content in grain (%) in 2017-2018; **e,** N content in grain in 2018-2019; **f,** N content in grain in 2019-2020; **g,** N uptake efficiency (ratio) in 2017-2018; **h,** N uptake efficiency in 2018-2019; **i,** N uptake efficiency in 2019-2020; **j,** N use efficiency (ratio) in 2017-2018; **k,** N use efficiency in 2018-2019; **l,** N use efficiency in 2019-2020. The mean value was obtained from 10 cultivars of each allele from two independent plots as replication for each treatment. Statistical significance was calculated based on one-way ANOVA with $^{\cdot}P < 0.1$ and $^{*}P < 0.05$, respectively. HN, high nitrogen and LN, low nitrogen.

Sequence analysis of the coding and promoter elements of this gene of 40 wheat and 40 barley NO_3^- contrasting genotypes demonstrated that only the promoter region of *TaNPF2.12* and *HvNPF2.12* had consistent allelic variations among wheat but also barley genotypes. The results implied that the majority of tolerant genotypes, i.e. with higher RV and TRL belong to Hap2, while most of the sensitive genotypes, i.e. lower RV and TRL under LN/HN conditions belong to Hap1. Consistently, root phenotyping and NO_3^- assay also indicated that the Hap2 promoters of *TaNPF2.12* and *HvNPF2.12* were significantly associated with better root growth and NO_3^- transport capacity than Hap1 under low NO_3^-, explaining that the Hap2 promoter is more active to low NO_3^- availability.

To verify our hypothesis that variations at coding elements of *NPF2.12* integrate a signaling networks that might contribute to root growth, NO_3^- uptake and transport to shoot systems, an *npf2.12* EMS mutant was used to perform comparative transcriptome analysis. This analysis found that *NIA1* transcript levels highly increased by *npf2.12* allele in response to low NO_3^-, thus further elicited NR activity and NO homeostasis. It has been well established that the NR-defective *nia1* mutant reduces the endogenous NO levels (Zhao et al. 2009). When plant sense NO_3^-, multiple NO_3^- assimilation pathway genes, importantly *NIA* is induced within minutes to serve as NO_3^- enhancer (Wang et al. 2010). The NR is a key enzyme involved in the first step of NO_3^- assimilation, encoded by two genes, *NIA1* and *NIA2* (Wilkinson and Crawford, 1993), and *NIA1* is a major constituent underlying NR-dependent NO production (Zhao et al. 2009). Next, NO_3^--induced expression patterns of *npf2.12* mutant was compared with its WT under 0.5 and 10 mM NO_3^- treatments, and we did not observe expression differences at 10 mM NO_3^-, while treatment with 0.5 mM NO_3^- confirmed that the mutant allele was very low responsive to availability of the NO_3^- balance compared to WT allele. Further, root phenotyping under contrasting NO_3^- input levels showed that the TRL, RSA and RV of mutant plants were significantly higher than that of the WT at low NO_3^- concentration, indicating that lower expressions of *npf2.12* contributes better root growth. The NO_3^--N content in roots and shoots of *npf2.12* plants were greater than those in the WT to low NO_3^-, suggesting that loss-of-function allele may candidate for efficient NO_3^- transport from root-to-shoot. Overall, these results imply that *npf2.12* allele under low NO_3^- can potentially activate *NIA1* expressions in

promotion of NR-dependent NO production (Bright et al. 2006; Zhao et al. 2009), which in turn contributed better root growth phenotypes, NO_3^- uptake by root and transport to shoot (Neill et al. 2003; Sun et al. 2015).

As we observed the expression levels of *TaNPF2.12* and *HvNPF2.12* decreased at limited NO_3^- supply, which may affects the root growth and NO_3^- transport efficiency of their natural alleles. The *TaNPF2.12*^{TT} allele may thus lead to increased N-uptake, resulting in enhanced accumulation of N in leaf and grain as well as higher NUE at LN supply compared to *TaNPF2.12*^{CC} allele. In rice, a NPF family NO_3^- transporter *OsNPF6.1* varies in both protein and promoter sequences, and its rare natural allele enhances NUE under field trials (Tang et al. 2019). The NPF family comprised by both low-affinity and peptide transporters sharing high sequence homology and a conserved structural domains (Tsay et al. 2007; Léran et al. 2014). Recently, genetic modification of an NO_3^- assimilation gene *OsNR2* encoding NR activity showed NUE enhancement in rice (Yu et al. 2021). Therefore, the identified *NPF2.12* may encompass a regulatory networks, which perform one of the coordination with *NIA1* encoding NR activity that contributed better root growth, N-uptake and transport and subsequently develop high-NUE to LN availability.

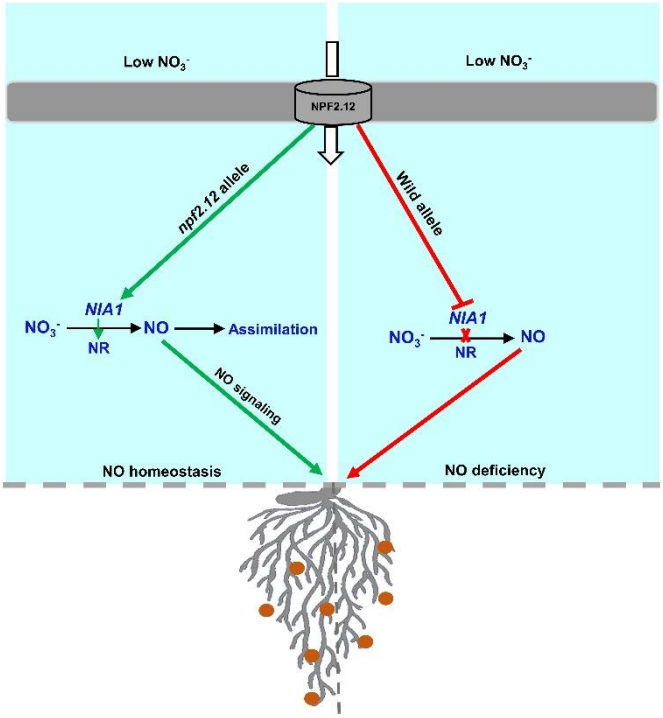

Fig. 7: Depiction of a proposed model of the regulatory pathways of *TaNPF2.12* in response to low NO_3^- availability. Under low NO_3^-, the loss-of-function *npf2.12* mutant allele up-regulated *NIA1* transcript expressions that elicited NR activity and ultimately NO homeostasis. This NO homeostasis and signaling might lead to enhanced root growth phenotypes underlying NO_3^- transport. Under low NO_3^-, the wild-type allele suppressed *NIA1* transcripts expression that caused inhibition of NR activity and NO production. This reduced levels of NO might be associated with stunted root growth and NO_3^- transport.

The brown colour round shapes indicates NO_3^-. *NIA1*; *NITRATE REDUCTASE 1*; NR, nitrate activity and NO, nitric oxide.

In summary, we first provide an experimental evidence that *NPF2.12* is a convergently selected low-affinity NO_3^- transporter candidate in wheat and barley, and its variant allele transactivates *NIA1* expression to elevate NR-mediated NO biosynthesis that finally confers root growth underlying NO_3^- transport at limited N availability. So, it is critically important to exploit natural allelic variants of *NPF2.12*, or developing de novo variants by genome editing may thus enable breeders to utilize this gene in breeding programs. This study also evident that genetic control of *NPF2.1-NIA1* signaling cascade as a potential strategy towards the breeding of high-NUE. Further efforts focusing on the regulatory networks of *NPF2.12* with other convergent orthologues across cereal species could largely accelerate breeding of improved NUE.

Materials and methods

Plant materials

The genetic material used in the present study is a global collection of 221 winter wheat (*Triticum aestivum* L.) cultivars (Table S11). These were selected from an association panel developed in the BRIWECS (breeding innovations in wheat for resilient cropping systems) consortium in Germany as previously described by Voss-Fels et al (2019).

For barley (*Hordeum vulgare* L.), a total of 200 spring barley inbreeds that consisted of advanced breeding lines, cultivars, and landraces developed by the International Center for Agricultural Research in the Dry Areas (ICARDA) were evaluated (listed in Table S12). This diverse panel of barley genotypes was selected from the stress inputs barley breeding programs (stress in terms of limited fertilizer and moisture) of ICARDA (Amezrou et al. 2018).

Field and controlled experiments

This diversity panel was evaluated in Campus Klein-Altendorf research facilities of Bonn University under natural field conditions in three consecutive growing seasons from 2017-2018, 2018-2019 and 2019-2020, under high dose N (220 kgN ha^{-1}, fertilizer adjusted based on soil mineral nitrogen, N_{min}) and no artificial nitrogen-supply as low dose (0 kgN ha^{-1}) conditions, where the experiments were performed in different fields. The experimental design and management practices were followed as previously described by Voss-Fels et al. (2019), except fungicide application. Fertilizer and lime applications were made following the soil test results to adjust the nutritional levels previously described (Table S13). At flowering stage

(BBCH65), root systems of at least three representative plants from each plot were harvested using the "*Shovelomics*" approach (Trachsel et al. 2011; Oyiga et al. 2020).

Sixteen seeds of each barley inbreed, were placed in transparent plastic boxes (29×22.5 cm) containing blotting paper (ALBET Lab Science, Dassel, Germany) soaked in 50 mL of a solution containing two levels of NO_3^- as N Ion Chromatography Standard [H_2O, NO_3 (-) as N: 1000µg/mL], supplied with either 10 mM (high NO_3^-) or 0.5 mM (low NO_3^-). The plastic box was kept in dark conditions at 4°C for 48 h to stimulate the germination process and then placed in a growth chamber (bronson CLIMATE) with white fluorescent light (600 µmol m^{-2} s^{-1}; 14 h light/10 h dark) at 23 ± 1°C, and relative humidity of 65 ± 8%. The experiment was repeated at least two times so that a total of 8 uniform plants were obtained per genotype per NO_3^- level. The 14-day-old seedlings of identical size for each barley genotype were harvested, and roots were carefully separated from shoot. The rooting depth was determined using a meter scale from root-shoot junction to root apex. After that, root samples were preserved in plastic pot containing 60% alcohol (v/v) for further root phenotyping.

Root phenotyping

The preserved root samples were properly placed in the scanner tray and adjusted vertically on scanning plates to avoid overlapping roots. Next to a ruler, an eight-bit gray scale image was generated using a high-resolution EPSON scanner (Perfection LA24000) maintaining a resolution of 600 dots per inch (Kadam et al. 2017). Root morphological traits were quantified by analyzing the root images with WinRHIZO analysis system (version 2020a, Regent Instruments Inc., Quebec, Canada).

To investigate the root anatomical structures, well cleaned and preserved root samples from main shoot and tiller nodal roots were free-hand sectioned using a razor blade (Apollo, HERKENRATH Solingen, Germany) at 1 cm position from root-shoot junction (Oyiga et al. 2020). Two root images from three individual plants per replicate were acquisited by the digital microscope (Keyence's VHX-1000D, Germany) with 50× and 100× magnification. The ratio of image pixels to the scale bar length was adjusted during image analysis by *ImageJ* (v1.52a) software. The diameter of the whole cross-section, the cortical cell, the stele, and the metaxylem vessels were measured to convert the pixel counts to diameter (µm) (Schneider et al. 2012; Kadam et al. 2017). The water conductance parameter in terms of axial hydraulic conductivity was measured as described by Kadam et al. (2015). The list of all traits with description is provided in Table S1.

SNP genotyping

For wheat, 24,216 single nucleotide polymorphisms (SNP) markers were obtained by extracting DNA from the 221 wheat cultivars and those genome-wide SNP markers as described by Voss-Felds et al. (2019) and Dadshani et al. (2021). For barley, a total of 23,805 SNPs were obtained using 23K iSelect SNP array based on Illumina's Inifinium Assay (Illumina, San Diego, CA, USA) (Amezrou et al. 2018). Both wheat and barley SNPs data were curated before data imputation using TASSEL (version 5.2.61), where SNP loci and individuals with <10% missing values and rare SNPs with <5% minor allele frequencies (MAF) were excluded from the data following Voss-Fels et al. (2019).

Comparative GWAS between wheat and barley

The SNPs involved with the alteration in root system traits induced by N levels were identified by adopting GWAS mixed linear model (MLM-PK, Stich et al. 2008). Here root traits were considered as phenotypes, whereas the confounding effects of population stratification in both panels were employed by incorporating population structure (P-matrix principal component analysis) and kinship (K-matrix) as covariates (Kang et al. 2010). The P- and K-Matrix were assembled using TASSEL (version 5.2.61). GWAS was also conducted in TASSEL (version 5.2.61), using the model: $y = X\beta + Zu + e$, where y considered as the vector of phenotypic traits; X is the corresponding SNP vector; β is the coefficient factors for SNP effect, Z represents the corresponding design matrix; u indicates random effects computing for populations structure and kinship; and e is a vector of random error (Kang et al. 2010). The false discovery rate (FDR) adjusted p-value (q-value) of 0.01 was calculated using the q-value package (Storey et al. 2019). Significant MTAs were considered when FDR q-values below the FDR ≤ 0.01 threshold were noticed. Manhattan and Quantile-Quantile (Q-Q) plots were generated in R using the 'qqman' package', based on TASSEL summary statistics.

To obtain wheat candidate genes, we additionally performed linkage disequilibrium (LD) analysis based on significant SNPs identified by GWAS using Haploview (version 2.4) as described by Siddiqui et al. (2021a). Parameter r^2 value was considered to determine the degree of LD (Li et al. 2016). All the associated significant SNPs in high chromosomal LD region with each other were defined to be linked (SNP-clusters). The LD blocks containing significant SNPs were considered as candidate loci. The significant SNPs that did belongs to LD blocks, were treated differently. All candidate genes within ± 1Mbp of the corresponding SNPs were annotated using the International Wheat Genome Sequencing Consortium (IWGSC) RefSeq v1.0 in the URGI wheat database (https://wheat-urgi.versailles.inra.fr; Alaux et al. 2018). For barley, core sequences of the significant markers were BLAST searched using the public Barley Genome Gene-set database (EnsemblPlants; https://plants.ensembl.org). Top gene hits were determined by considering scores of >80% similarity and e-values <1e-70

(Oyiga et al. 2020). The annotated high confidence (HC) genes [genes with known annotation and verified positions on the WGS assembly of cv. Morex (IBGC, 2012)] were searched in the IPK Barley Genome database (https://apex.ipk-gatersleben.de/apex/f?p=284:41:::NO:RP:P41_GENE_CHOICE:2). The candidate genes with functional annotations related to nutrient and ion transport systems, transmembrane transporter activity, hormonal signalling, root development, and response to stress were listed in Table S7. Wheat and barley syntenic genes were curated following the methods of Zhang et al. (2017) adopting the reference genomes IWGSC RefSeq v1.0 for wheat and IBSC_v2 for barley in EnsemblPlants database (https://plants.ensembl.org).

Phylogenetic and protein-protein interaction network analysis

The NPF2.12 protein domains were analyzed using blastp (protein-protein BLAST). The full-length protein sequences of *NPF2.12* orthologs in the Arabidopsis genus were sequenced from BLAST search online database. The multiple-sequence alignment and phylogenetic tree were constructed by ClustalW2 (https://www.ebi.ac.uk/Tools/msa/clustalw2/) (Larkin et al. 2007). The predicted protein-protein interaction network was carried out by Search Tool for the Retrieval of Interacting Genes (STRING, https://string-db.org/), using the Arabidopsis as input organisms and combined score >0.9 (Jin et al. 2021). The Cytoscape (https://cytoscape.org/) software was used to visualize the network.

Candidate gene sequence analysis

Whole genomic DNA of selected genotypes (Table S10 and S11) was extracted from leaves using a peqGOLD Plant DNA Mini Kit (VWR Life Science, USA). An approximately 1.5-kb region upstream from the start codon ATG of *TaNPF2.12* and *HvNPF2.12* was considered as promoter region (Muzammil et al. 2018). Primers (Table S16 and S17) were designed and synthesized by Sigma-Aldrich (Merck KGaA, Darmstadt, Germany). The region of interest was amplified by polymerase chain reaction (PCR) following reaction conditions: 12.5 µL of One *Taq* 2X Master Mix (NEW ENGLAND, BioLabs), 0.5 µL of each primer (10 µM), 8.5 µL of PCR-graded water, and 3.0 µL of genomic DNA (total volume 25 µL). The following cycling conditions were employed for amplification: 95 °C for 2 min and 40 cycles of 95 °C for 30 s, 57/59 °C for 50 s, and 68 °C for 40 s, ended by an additional 68 °C extension for 5 min. The amplified PCR products were purified by a FastGene Gel/PCR Extraction Kit (Nippon Genetics, Tokyo, Japan). DNA sequences were aligned and compared using DNASTAR 'SeqMan Pro' version 12.0.0 (www.dnastar.com) to detect possible polymorphic sites.

Isolation of RNA and RT-qPCR analysis

Total RNA isolation from the harvested root samples of wheat and barley plants were performed after 14-days in high NO_3^--N (10 mM) and low NO_3^--N (0.5 mM) conditions using Monarch Total RNA Miniprep Kit (BioLab) according to the manufacturer's guidelines. The RT-qPCR reaction mixture (20 µL) consisted of 10 µL master mix and 1 µL enzyme mix (supplied in the kit), 0.8 µL each of forward and reverse gene-specific primers (primers list in Table S16 and S17), 5.4 µL nuclease-free water, and 2 µL template RNA. The Luna Universal One-Step RT-qPCR Kit (NEB #E3005L) was used for the analysis. The PCR reactions were performed using cycler 7500 Sequence Detection System (Applied Biosystems) using following conditions: 10 mins at 55^0C (reverse transcription), 60 s at 95^0C (initial denaturation), 10 s at 95^0C (denaturation) and 30 s at 60^0C (extension) for 40 cycles. The gene expression levels were calculated using ΔΔCt values and expressed as fold change relative to the stably expressed two internal control genes, *TaEf-1a* and *TaEf-1b* (Unigene accession: Ta659) for wheat and *Ef1-a* for barley.

Transcriptome analysis

The *npf2.12* mutant of durum wheat (*Triticum turgidum*) were purchased from a TILLING population generated in tetraploid cv. Kronos background (Krasileva et al. 2017). The TILLING line (Kronos4652) possessed premature termination codons in the *npf2.12* homologous coding sequences of *TraesCS3B02G454000* (Fig. 4a). The mutated seeds were selfed to F_5 to fix the mutations. The *npf2.12* mutant and WT seedlings were grown in transparent plastic boxes (29×22.5 cm) with blotting paper and irrigated with the solution containing 10 (high) and 0.5 (low) mM NO_3^--N weekly. The roots of the *npf2.12* mutant and WT plants were collected after 14 days of NO_3^--N impositions. Total RNA was extracted using the Monarch Total RNA Miniprep Kit (BioLab). The library preparation and sequencing were conducted by NGS Core Facility at the University of Bonn, Germany (https://btc.uni-bonn.de/ngs). RNA sequencing reaction performed using the QuantSeq 3´-mRNA-Seq Kit from Lexogen and sequenced on an Illumina NovaSeq 6000 platform. Three biological replicates for each treatment were used and for each replicate 14 million reads were sequenced. The transcriptome data analysis was performed following the steps illustrated in the supplementary method file.

Quantification of NO, NR activity and NO_3^--N contents

The WT and mutant lines were grown in transparent plastic boxes containing blotting paper in a growth chamber applied either high or low NO_3^--N as mentioned above. The NO contents and NR activity were determined in the fresh root samples harvested after 14-days of NO_3^--N treatments using NO Assay Kit from Abnova (Cat. No. KA1641) and NR Assay Kit from Biorbyt (Cat. No. 0rb219870), respectively following the manufacturer's protocols.

For NO_3^--N determination, freshly harvested root and shoot were homogenized using 5 mL of boiling water to 0.1 g tissue samples and then tubes were boiled in a water bath for 10 min. An aliquot of 0.2 mL extract were mixed with 0.8 mL of 5% salicylic acid in concentrated H_2SO_4 and then incubated for 20 min. In the following step, 19 mL of 2M NaOH were added and then absorbance was taken in a spectrophotometer at 410 nm. NO_3^- determination were performed as previously described by Catldo et al. (1975). Total NO_3^--N concentrations in root and shoot were represented as µmol NO_3^--N per g fresh weight (ppm).

Evaluation of NUE-related traits of *TaNPF2.12* alleles under field conditions

The ten wheat cultivars containing *TaNPF2.12*^{CC} and *TaNPF2.12*^{TT} from each allele group (Table S9) were grown in field conditions across three cropping systems in 2017-2018, 2018-2019 and 2019-2020. The seeds of each genotype were sown in a plot (7 × 3 meters) distributed as split plot design with two replications (organized in randomized block design). The selected cultivars were grown under two different N levels (HN and LN) as mentioned above for wheat cultivation previously described by Voss-Fels et al. (2019), except fungicide application. After harvest, N uptake was determined by ratio of the amount of N at the shoot by the total N availability per hectare. The N content in dry grinded leaves and grain was determined using the near-infrared spectrometer (NIRS) with Diode Array 7250 NIR analyzer (Perten Instruments, Inc., USA) as described by Koua et al. (2021). NUpE was determined by the ratio of the total aboveground N at the by the total N available in soil and NUE was estimated by the ratio of total grain yield to applied N fertilizer as defined by Moll et al. (1982).

Statistical analysis

For descriptive statistics, two-way analysis of variance (ANOVA) was performed using MLM, where genotypic and treatment effects were considered as fixed effects with their interaction, and block and replications were treated as random effects (Siddiqui et al. 2021a). The broad-sense heritability (H^2) was calculated following the equation by Johnson et al. (1955). Binary comparisons of data were statistically analysed following Student's *t* test (P<0.05 and P<0.01). For multiple comparisons between WT, mutant and haplotype lines, one-way ANOVA followed by post-hoc Tukey's test at P< 0.05 and P<0.01. All statistical analyses were conducted in R (R Foundation for Statistical Computing, 2013, 2014).

Acknowledgement

We are grateful to the NGC core facility by Medical Faculty at University of Bonn. We are grateful to the DAAD (German Academic Exchange Service) for financial support to MNS. We are grateful to Professor Dr. Annaliese Mason for providing lab facilities. We also acknowledge

to Mohammad Kamruzzaman, Marissa B. Barbosa, Patrice Koua, Said Dadshani and Karin Woitol for their help during root harvesting under field experiments. We also extend acknowledgement to the campus Klein-Altendorf staff for their supports to take care field experiments. We also highly grateful to the International Center for Agricultural Research in the Dry Areas (ICARDA), Rabat for providing us barley association panel. We acknowledge to the Breeding Innovations in Wheat for Resilient Cropping Systems (BRIWECS) project funded by the German Federal Ministry of Education and Research (BMBF), PTJ for funding with the grant 031A354 for necessary financial supports.

References

Alaux, M. et al. Linking the International Wheat Genome Sequencing Consortium bread wheat reference genome sequence to wheat genetic and phenomic data. Genome Biol 19, 111 (2018).

Alvarez, J. M., Vidal, E. A. & Gutiérrez, R. A. Integration of local and systemic signalling pathways for plant N responses. Curr Opin Plant Biol 15, 185–191 (2012).

Amezrou, R. et al. Molecular and phenotypic diversity of ICARDA spring barley (*Hordeum vulgar*e L.) collection. Genet Resour Crop Evol 65, 1–15 (2018).

Begum, H. et al. Genetic dissection of bread wheat diversity and identification of adaptive loci in response to elevated tropospheric ozone. Plant Cell Environ 43, 2650–2665 (2020).

Brenchley, W. E. & Jackson, V. G. Root development in barley and wheat under different conditions of growth. Ann Bot 35, 533–556 (1921).

Bright, J., Desikan, R., Hancock, J.T., Weir, I.S., Neill, S.J. ABA-induced NO generation and stomatal closure in Arabidopsis are dependent on H_2O_2 synthesis. Plant J 45, 113–122 (2006).

Cataldo, D. A., Maroon, M., Schrader, L. E. & Youngs, V. L. Rapid colorimetric determination of nitrate in plant tissue by nitration of salicylic acid. Commun Soil Sci Plan 6, 71–80 (1975).

Chen, X. et al. Producing more grain with lower environmental costs. Nature 514, 486–489 (2014).

Dadshani, S., Mathew, B., Ballvora, A., Mason, A. S. & Léon, J. Detection of breeding signatures in wheat using a linkage disequilibrium-corrected mapping approach. Sci Rep 11, 5527 (2021).

Davidson, R. M. et al. Comparative transcriptomics of three Poaceae species reveals patterns of gene expression evolution. Plant J 71, 492–502 (2012).

Devos, K. M. & Gale, M. D. Comparative genetics in the grasses. Plant Mol Biol 35, 3–15 (1997).

Foley, J. A. et al. Solutions for a cultivated planet. Nature 478, 337–342 (2011).

Foulkes, M. J. et al. Identifying traits to improve the nitrogen economy of wheat: recent advances and future prospects. Field Crops Research 114, 329–342 (2009).

Garnett, T. et al. Sustainable intensification in agriculture: Premises and policies. Science (New York, N.Y.) 341, 33–4 (2013).

Gibbon, D., Dixon, J. & Velázquez, D. Beyond drought tolerant maize: study of additional priorities in maize. Report to Generation Challenge Program (2007).

Guo, B. et al. Characterization of the Nitrate Transporter gene family and functional identification of HvNRT2.1 in barley (*Hordeum vulgare* L.). PLOS ONE 15, e0232056 (2020).

Hirel, B., Tétu, T., Lea, P. J. & Dubois, F. Improving nitrogen use efficiency in crops for sustainable agriculture. Sustainability 3, 1452–1485 (2011).

Hu, B. et al. Variation in NRT1.1B contributes to nitrate-use divergence between rice subspecies. Nat Genet 47, 834–838 (2015).

International Barley Genome Sequencing Consortium et al. A physical, genetic and functional sequence assembly of the barley genome. Nature 491, 711–716 (2012).

Islam, A. K. M. R., Shepherd, K. W. & Sparrow, D. H. B. Isolation and characterization of euplasmic wheat-barley chromosome addition lines. Heredity 46, 161–174 (1981).

Jia, Z., Giehl, R. F. H., Meyer, R. C., Altmann, T. & von Wirén, N. Natural variation of BSK3 tunes brassinosteroid signaling to regulate root foraging under low nitrogen. Nat Commun 10, 2378 (2019).

Jin, T. et al. Natural variation in the promoter of GsERD15B affects salt tolerance in soybean. Plant Biotechnol J 19, 1155–1169 (2021).

Kadam, N. N. et al. Genetic control of plasticity in root morphology and anatomy of rice in response to water deficit. Plant Physiol 174, 2302–2315 (2017).

Kadam, N. N., Yin, X., Bindraban, P. S., Struik, P. C. & Jagadish, K. S. V. Does morphological and anatomical plasticity during the vegetative stage make wheat more tolerant of water deficit stress than rice? Plant Physiol 167, 1389–1401 (2015).

Kang, H. M. et al. Variance component model to account for sample structure in genome-wide association studies. Nat Genet 42, 348–354 (2010).

Klein, S., Reeger, J., Kaeppler, S., Brown, K. & Lynch, J. Shared genetic architecture underlying root metaxylem phenotypes under drought stress in cereals. (2020). doi:10.1101/2020.11.02.365247.

Koua, A. P., Oyiga, B. C., Baig, M. M., Léon, J. & Ballvora, A. Breeding driven enrichment of genetic variation for key yield components and grain starch content under drought stress in winter wheat. Front Plant Sci 12, (2021).

Krasileva, K. V. et al. Uncovering hidden variation in polyploid wheat. Proc Natl Acad Sci U S A 114, 913–921 (2017).

Krouk, G., Crawford, N. M., Coruzzi, G. M. & Tsay, Y.-F. Nitrate signaling: adaptation to fluctuating environments. Curr Opin Plant Biol 13, 266–273 (2010).

Larkin, M. A. et al. Clustal W and Clustal X version 2.0. Bioinformatics 23, 2947–2948 (2007).

Léran, S. et al. A unified nomenclature of NITRATE TRANSPORTER 1/PEPTIDE TRANSPORTER family members in plants. Trends Plant Sci 19, 5–9 (2014).

Li, L. et al. Loci and candidate gene identification for resistance to Phytophthora sojae via association analysis in soybean [*Glycine max* (L.) Merr.]. Mol Genet Genom 291, (2016).

Li, P. et al. A genetic relationship between nitrogen use efficiency and seedling root traits in maize as revealed by QTL analysis. J Exp Bot 66, 3175–3188 (2015).

Li, Y. et al. Disruption of the rice nitrate transporter OsNPF2.2 hinders root-to-shoot nitrate transport and vascular development. Sci Rep 5, 9635 (2015).

Liu, Kun-Hsiang, and Yi-Fang Tsay. Switching between the two action modes of the dual-affinity nitrate transporter CHL1 by phosphorylation. EMBO J 22, 1005–1013 (2003).

Marger, M. D. & Saier, M. H. A major superfamily of transmembrane facilitators that catalyse uniport, symport and antiport. Trends Biochem Sci 18, 13–20 (1993).

Miller, A. J., Fan, X., Orsel, M., Smith, S. J. & Wells, D. M. Nitrate transport and signalling. J Exp Bot 58, 2297–2306 (2007).

Morère-Le Paven, M.-C. et al. Characterization of a dual-affinity nitrate transporter MtNRT1.3 in the model legume Medicago truncatula. J Exp Bot 62, 5595–5605 (2011).

Moll, R.H., Kamprath, E.J. & Jackson, W.A. Analysis and interpretation of factors which contribute to efficiency of nitrogen utilization. Agron J 74, 562–564 (1982).

Muzammil, S. et al. An Ancestral Allele of Pyrroline-5-carboxylate synthase1 Promotes Proline Accumulation and Drought Adaptation in Cultivated Barley. Plant Physiol 178, 771–782 (2018).

Nacry, P., Bouguyon, E. & Gojon, A. Nitrogen acquisition by roots: physiological and developmental mechanisms ensuring plant adaptation to a fluctuating resource. Plant Soil 370, 1–29 (2013).

Neill, S. J., Desikan, R., & Hancock, J. T. Nitric oxide signalling in plants. New Phytol 159(1), 11-35 (2003).

Ngwepe, M. R., Shimelis, H. & Mashilo, J. Estimates of the variance components, heritability and genetic gains of phenotypic traits in citron watermelon (*Citrullus lanatus* var. citroides). Plant Breed 140, 953–967 (2021).

O'Brien, J. A. et al. Nitrate transport, sensing, and responses in plants. Mol Plant 9, 837–856 (2016).

Oyiga, B. C. et al. Genetic components of root architecture and anatomy adjustments to water-deficit stress in spring barley. Plant Cell Environ 43, 692–711 (2020).

Pao, S. S., Paulsen, I. T. & Saier, M. H. Major facilitator superfamily. Microbiol Mol Biol Rev 62, 1–34 (1998).

Salse, J., Abrouk, M., Murat, F., Quraishi, U. M. & Feuillet, C. Improved criteria and comparative genomics tool provide new insights into grass paleogenomics. Brief Bioinform 10, 619–630 (2009).

Schneider, C. A., Rasband, W. S. & Eliceiri, K. W. NIH Image to ImageJ: 25 years of image analysis. Nat Methods 9, 671–675 (2012).

Schreiber, A. W. et al. Comparative transcriptomics in the Triticeae. BMC Genom 10, 285 (2009).

Siddiqi, M. Y., Glass, A. D., Ruth, T. J. & Rufty, T. W. Studies of the Uptake of Nitrate in Barley: I. Kinetics of NO (3) Influx. Plant Physiol 93, 1426–1432 (1990).

Siddiqui, M. N. et al. New drought-adaptive loci underlying candidate genes on wheat chromosome 4B with improved photosynthesis and yield responses. Physiol Plant 173, 2166–2180 (2021a).

Siddiqui, M. N., Léon, J., Naz, A. A. & Ballvora, A. Genetics and genomics of root system variation in adaptation to drought stress in cereal crops. J Exp Bot 72, 1007–1019 (2021b).

Storey, J. D., Bass, A. J., Dabney, A., Robinson, D. & Warnes, G. qvalue: Q-value estimation for false discovery rate control. (Bioconductor version: Release (3.14), 2022). doi:10.18129/B9.bioc.qvalue.

Sulochana Dhital & W. R. Raun. Variability in Optimum Nitrogen Rates for Maize. Agron J 108, 2165–2173 (2016).

Sun, H. et al. Nitric oxide generated by nitrate reductase increases nitrogen uptake capacity by inducing lateral root formation and inorganic nitrogen uptake under partial nitrate nutrition in rice. J Exp Bot 66(9), 2449-2459.

Tang, W. et al. Genome-wide associated study identifies NAC42-activated nitrate transporter conferring high nitrogen use efficiency in rice. Nat Commun 10, 5279 (2019).

Trachsel, Samuel, et al. Shovelomics: high throughput phenotyping of maize (*Zea mays* L.) root architecture in the field. Plant Soil 341(1), 75-87 (2011).

Tsay, Y. F., Schroeder, J. I., Feldmann, K. A. & Crawford, N. M. The herbicide sensitivity gene CHL1 of Arabidopsis encodes a nitrate-inducible nitrate transporter. Cell 72, 705–713 (1993).

Tsay, Y.-F., Chiu, C.-C., Tsai, C.-B., Ho, C.-H. & Hsu, P.-K. Nitrate transporters and peptide transporters. FEBS Lett 581, 2290–2300 (2007).

Vidal, E. A. & Gutiérrez, R. A. A systems view of nitrogen nutrient and metabolite responses in Arabidopsis. Curr Opin Plant Biol 11, 521–529 (2008).

Vitousek, P. M. et al. Agriculture. Nutrient imbalances in agricultural development. Science 324, 1519–1520 (2009).

von Wirén, N., Gazzarrini, S., Gojon, A. & Frommer, W. B. The molecular physiology of ammonium uptake and retrieval. Curr Opin Plant Biol 3, 254–261 (2000).

von Wittgenstein, N. J., Le, C. H., Hawkins, B. J. & Ehlting, J. Evolutionary classification of ammonium, nitrate, and peptide transporters in land plants. BMC Evol Biol 14, 11 (2014).

Voss-Fels, K. P. et al. Breeding improves wheat productivity under contrasting agrochemical input levels. Nat Plants 5, 706–714 (2019).

Wang, H. et al. Phylogeny and gene expression of the complete NITRATE TRANSPORTER 1/PEPTIDE TRANSPORTER FAMILY in *Triticum aestivum*. J Exp Bot 71, 4531–4546 (2020).

Wang, J. et al. Rice nitrate transporter *OsNPF7.2* positively regulates tiller number and grain yield. Rice 11, 12 (2018).

Wang, R., Guan, P., Chen, M., Xing, X., Zhang, Y., & Crawford, N. M. Multiple regulatory elements in the Arabidopsis *NIA1* promoter act synergistically to form a nitrate enhancer. Plant Physiol 154(1), 423-432 (2010).

Wang, S. et al. Characterization of polyploid wheat genomic diversity using a high-density 90,000 single nucleotide polymorphism array. Plant Biotechnol J 12, 787–796 (2014).

Wilkinson, J.Q. & Crawford, N.M. Identification and characterization of chlorate-resistant mutant of Arabidopsis thaliana with mutations in both nitrate reductase structural genes *NIA1* and *NIA2*. Mol Gen Genet 239, 289–297 (1993).

Xin, W. et al. Adaptation mechanism of roots to low and high nitrogen revealed by proteomic analysis. Rice 14, 5 (2021).

Xu, G., Fan, X. & Miller, A. J. Plant Nitrogen Assimilation and Use Efficiency. Annu Rev Plant Biol 63, 153–182 (2012).

Yang, J. T., Schneider, H. M., Brown, K. M. & Lynch, J. P. Genotypic variation and nitrogen stress effects on root anatomy in maize are node specific. J Exp Bot 70, 5311–5325 (2019).

Yu, J. et al. Enhanced OsNLP4-OsNiR cascade confers nitrogen use efficiency by promoting tiller number in rice. Plant Biotechnol J 19(1), 167-176(2021).

Zhang, H., Rong, H. & Pilbeam, D. Signalling mechanisms underlying the morphological responses of the root system to nitrogen in *Arabidopsis thaliana*. J Exp Bot 58, 2329–2338 (2007).

Zhang, Yang, et al. Differentially regulated orthologs in sorghum and the subgenomes of maize. Plant Cell 29 (8), 1938-1951 (2017).

Zhao, M. G., Chen, L., Zhang, L. L., & Zhang, W. H. Nitric reductase-dependent nitric oxide production is involved in cold acclimation and freezing tolerance in Arabidopsis. Plant Physiol 151(2), 755-767 (2009).

Zheng, Z. et al. Shared genetic control of root system architecture between *Zea mays* and *Sorghum bicolor*. Plant Physiol 182, 977–991 (2020).

General Discussion

Roots are the primary contact point of plants with the soil. Their capacity for soil exploration greatly contributes to improving water and N acquisition efficiency (Foulkes et al. 2009; Siddiqui et al. 2021a). In this study, novel genetic regulators and putative candidate genes, associated with root architectural adaptation to water-deficit stress, were summarized in cereals (Chapter 2) and explored in a winter wheat diversity panel (Chapter 3). Moreover, a syntenic loci involved in root growth variations and low-affinity nitrate transport systems was elucidated in wheat and barley (Chapter 4). Uncovering the genetic components and transporter genes related to root architecture traits for efficient water and N use are the prerequisite for successful marker-assisted breeding. Therefore, this study offers novel genetic resources for cereal improvements to save production costs and reduce environmental pollution, which can ultimately contribute to future food security.

5.1 Genetic mechanisms and syntenic loci for root phenotypic adaptation to water- and nitrogen-deficit conditions

Chapter 2 summarized the progress of quantitative genetic and genomic approaches in identifying natural genetic variations of root system architecture and their interplay with shoot architecture. For an in-depth understanding of root-mediated drought stress adaptation, we first highlighted how root system traits confer tolerance to drought stress by maintaining root-shoot balance. We identified adaptive root architectural traits, especially root angle and rooting depth and anatomical traits, such as xylem vessel size, as the most promising traits for drought adaptation. Then, we explored current studies to identify genetic variations and genomic loci related to drought stress responses. We compiled specific and syntenic QTLs/genes interlinked to root traits that show potential for resilience breeding. Finally, we established a microsynteny-based comparative genomic map of cereal species. This enabled us to identify a gene controlling rooting depth in rice (Uga et al. 2013) that showed syntenic relationships with wheat, barley and sorghum.

In Chapter 3, genomic loci for root phenotypic plasticity underlying drought adaptation in bread wheat were dissected by GWAS. For this, root phenotyping was performed on 200 wheat cultivars under control (natural field) and drought (rain-out shelter) conditions. The water supply was turned off from the tillering to the flowering stage. Upon drought, wheat cultivars showed significant root phenotypic variability, especially for root length, root average diameter, number of root crossings, forks and tips. Several reports established that these root traits are involved in conferring water stress tolerance by improving water absorption from the soil (Macharia et al. 2017; Wasaya et al. 2018; Friedli et al. 2019). A negative correlation was observed between root length and root diameter, while root length, number of root tips, forks

and crossings correlated positively, indicating that root length coordinates other traits to aid in improving drought adaptation (Chen et al. 2020).

Next, to identify promising alleles of SNPs/genes, we employed GWAS using a mixed linear model by correcting the principle components and kinship matrix that enabled us to avoid false marker-trait associations (MTAS) (Yu et al. 2006). Across wheat chromosomes, we identified 25 significant marker-MTAs that harboured 396 putative candidate genes for root system traits associated with phenotypic plasticity in response to drought treatment, such as root surface area, volume, length, average diameter and number of root forks and tips. The majority of the plasticity-related MTAs were found on chromosomes 1A, 2A and 5A. In wheat, genomic loci for drought and root-related traits are known to be abundant on chromosomes 1A, 2A and 5A and their causal genes are upregulated during abiotic stress (Soriano and Alvaro 2019). Further, linkage disequilibrium (LD) analysis was conducted to identify promising haplotypes carrying beneficial alleles that regulate root phenotypic plasticity traits and tolerance to drought (Siddiqui et al. 2021b). Interestingly, we found that all of the adaptive loci carrying major haplotypes showed greater contributions to the root phenotypic plasticity under drought stress compared to minor haplotypes. Exchanging the major haplotypes alleles with minor alleles could greatly induce root phenotypic adaptation to water-deficit conditions. Gene ontology analysis revealed that the candidate genes associated with root plasticity have biological functions in water deprivation response, water channel activity, abiotic stress pathways, cellular response to auxin signalling, root hair elongation and lateral root development. Finally, *in silico* transcript expression analysis uncovered that eight candidate genes are highly expressed in multiple root growth stages and under drought stress conditions. Upregulation of genes that are associated with root water deprivation, abscisic acid biosynthesis and auxin transport to the root tips are vital factors of water stress tolerance (Grzesiak et al. 2019). Taken together, in chapter 2 and 3 we provide novel loci and candidate genes that are particularly involved in the pathways related to water stress adaptation by modulating root architecture and plasticity.

Understanding the extent of convergent selection across crop species could greatly accelerate breeding programs (Chen et al. 2022). However, the molecular convergence of nitrate (NO_3^-) transport processes among crop species, especially between wheat and barley is very limited. Chapter 4 covers the results of a comparative genome-wide scan for characterized root architecture (morphology and anatomy) traits of 221 winter wheat and 200 spring barley accessions grown under high and low nitrogen (N)/nitrate (NO_3^-) input levels in both field and growth chamber conditions. For this, we phenotyped 21 root traits in wheat and 9 root traits in barley in response to contrasting N (220 and 0 kg ha^{-1}) and NO_3^- (10 and 0.5 mM) input levels. In both wheat and barley, all of the root trait values were significantly decreased by a higher

N/NO_3^- supply, which is well corroborated by previous studies (Li et al. 2015; Xin et al. 2021). The GWAS following a similar approach outlined in Chapter 3 identified 70 and 43 SNPs in wheat and barley, respectively. This yielded a total of 39 candidate genes related to N metabolism, sensing, assimilation and transport systems underlying root growth variations.

Our comparative genome-wide scan in wheat and barley revealed three pairs of genes that underwent convergent selection, including *TaNPF2.12*/*HvNPF2.12* on chromosome 3, which is associated with low-affinity NO_3^- transport systems. Several studies already identified NO_3^- transporter genes of the *NPF* family on chromosome 3 in wheat and barley (Guo et al. 2020; Wang et al. 2020). Further phylogenetic analysis uncovered a conserved and unique domain of the major facilitator superfamily (MFS), associated with NO_3^- transporter activity, in TaNPF2.12 and HvNPF2.12. The MFS is comprised of single-polypeptide secondary transporters that act as uniporters, symporters or antiporters (Marger and Saier 1993; Pao et al 1998). To determine the allelic variations in *NPF2.12* coding and promoter elements, sequence analysis was performed using 40 wheat and 40 barley genotypes. We found that only the promoter region of *TaNPF2.12* and *HvNPF2.12* showed consistent allelic variations that established two distinct haplotype differences. Furthermore, root phenotyping and NO_3^- assays indicated that the *Hap2* promoters of *TaNPF2.12* and *HvNPF2.12* were associated with significantly better root growth and NO_3^- transport capacity under low NO_3^- availability than *Hap1*, suggesting that the *Hap2* promoter allele is more active at low NO_3^- levels.

To identify *TaNPF2.12* regulatory networks involved in root growth, NO_3^- uptake and root-to-shoot transport, transcriptome profiles in response to contrasting NO_3^- levels of an *npf2.12* EMS mutant carrying a premature stop codon were dissected. We observed that *NIA1*, encoding a NO_3^- reductase (NR), was highly expressed by the *npf2.12* mutant in response to low NO_3^-, thereby increasing nitric oxide (NO) homeostasis. The NR-defective *nia1* mutant reduces the endogenous NO levels as demonstrated by Zhao et al. (2009). NR is a principle enzyme for NO_3^- assimilation and encoded by two genes, *NIA1* and *NIA2* (Wilkinson and Crawford, 1993). *NIA1* plays a major role in NR-dependent NO production (Zhao et al. 2009). Root scanning and qRT-PCR analyses of *npf2.12* revealed improved root architecture traits and decreased expression levels of the mutant allele compared to wild-type, especially after low NO_3^- treatment. At low NO_3^- levels, the NO_3^- content in roots and shoots of *npf2.12* plants were greater than in the WT, indicating that the loss-of-function allele may be a candidate for efficient NO_3^- transport from root-to-shoot. Taken together, we found that the *npf2.12* allele highly activates *NIA1* expressions in response to low NO_3^- levels in promotion of NR-dependent NO production (Bright et al. 2006; Zhao et al. 2009). This higher accumulation of NO contributes to better root growth, NO_3^- uptake and transport (Neill et al. 2003; Sun et al. 2015).

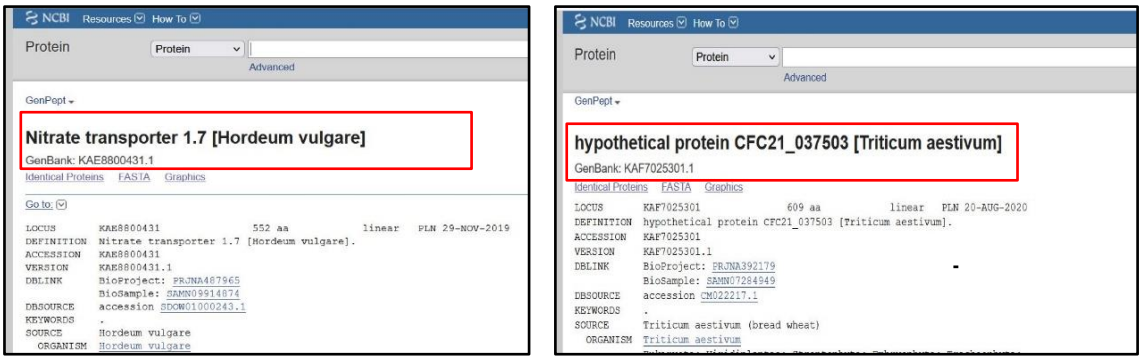

Figure 5-1: Comparing NPF2.12 protein activity between barley (*Hordeum vulgare*) and wheat (*Triticum aestivum*) curated from NCBI database using barley protein ID: KAE8800431.1 and wheat protein ID: KAF7025301.1.

Using the NCBI database, we found out our identified HvNPF2.12 protein has already been characterized as a NO_3^- transporter in *Hordeum vulgare*, while the TaNPF2.12 protein in *Triticum aestivum* is listed as a hypothetical protein (Figure 5-1). But we showed that TaNPF2.12 also serves as a low-affinity NO_3^- transporter in wheat. An NPF family NO_3^- transporter in rice, *OsNPF6.1*, varies in both protein and promoter sequences and its rare natural allele enhanced NUE in field trials (Tang et al. 2019). The NPF family genes constitute low-affinity and peptide transporters and share high sequence similarity and conserved structural domains (Tsay et al. 2007; Léran et al. 2014). Therefore, we also observed the minor allele of *TaNPF2.12* to increase N-uptake, accumulation of N in leaves and grains as well as NUE in low N conditions compared to the major allele.

Overall, this study provide novel genetic loci on a genome-wide scale and identifies *DRO1* and *NPF2.12* as syntenic genes regulating root architecture traits for efficient water use and NO_3^- transport in cereal crops, respectively.

5.2 Future perspectives

This PhD study improved the understanding of the extent of genetic and molecular convergence of root architecture adaptations to water- and N-deficit conditions and raised many interesting questions for future research. We identified crucial root traits, genomic regions and candidate genes related to water and N transport, including their syntenic relationships. Specifically, *DRO1,* a gene known to regulate rooting depth under drought conditions in rice that underwent convergent selection during cereal evolution. We first established orthologues of *DRO1* in wheat, barley, maize and sorghum using a genome-wide microsynteny map (Siddiqui et al. 2021a). Next, we identified several NO_3^- transporter genes, including *NPF2.12,* as convergently selected low-affinity NO_3^- transporters on a genome-wide scale in wheat and barley. Further, we provided insight into the *NPF2.12* regulatory networks with *NIA1*, a nitrate reductase (NR). At limited NO_3^- availability, the *NPF2.12-NIA1* cascade leads to elevated levels of nitric oxide through NR activity to confer NO_3^- transport efficiency. Based on our findings, we recommend the following future activities to enhance knowledge-driven cereal breeding.

- Genome-wide identification of the genes that showed convergent selection (*DRO1* and *NPF2.12*) across cereal species will definitely contribute in clarifying the evolution of cereal species as well as hasten the breeding process.

- In-depth functional characterization of the *NPF2.1-NIA1* signaling cascade could provide a potential route towards the breeding of high nitrogen use efficiency.

- Further validation of the orthologous genes could uncover insight into their functional involvement in specific pathways regulating traits which in turn could contribute to expanding knowledge-based crop breeding.

- Gene editing of orthologous genes could deliver a unique way to reshape the root system architecture in breeding lines for efficient water and nitrogen acquisition.

- Finally, our comparative genome-wide scan approach could pave the way to new breeding strategies for syntenic/convergently selected genes controlling root architecture traits related to high water and nitrogen use efficiency.

5.3 References

Bright, J., Desikan, R., Hancock, J.T., Weir, I.S., Neill, S.J. ABA-induced NO generation and stomatal closure in Arabidopsis are dependent on H_2O_2 synthesis. Plant J 45, 113–122 (2006).

Chen, W., Chen, L., Zhang, X., Yang, N., Guo, J., Wang, M.,.. Yang, X. Convergent selection of a WD40 protein that enhances grain yield in maize and rice. Science 375 (6587), eabg7985 (2022).

Chen, Y., Palta, J., Prasad, P.V., Siddique, K.H. Phenotypic variability in bread wheat root systems at the early vegetative stage. BMC Plant Biol 20(1), 1-16 (2020).

Foulkes, M. J. et al. Identifying traits to improve the nitrogen economy of wheat: recent advances and future prospects. Field Crops Res 114, 329–342 (2009).

Friedli, C.N., Abiven, S., Fossati, D., Hund, A. Modern wheat semi-dwarfs root deep on demand: response of rooting depth to drought in a set of Swiss era wheats covering 100 years of breeding. Euphytica 215, 85 (2019).

Grzesiak, M.T., Hordyńska, N., Maksymowicz, A., Grzesiak, S., Szechyńska-Hebda, M. Variation among spring wheat (*Triticum aestivum* L.) genotypes in response to the drought stress. II—Root system structure. Plants 8, 584 (2019).

Guo, B. et al. Characterization of the nitrate transporter gene family and functional identification of HvNRT2.1 in barley (*Hordeum vulgare* L.). PLOS ONE 15, e0232056 (2020).

Léran, S. et al. A unified nomenclature of NITRATE TRANSPORTER 1/PEPTIDE TRANSPORTER family members in plants. Trends Plant Sci 19, 5–9 (2014).

Li, P. et al. A genetic relationship between nitrogen use efficiency and seedling root traits in maize as revealed by QTL analysis. J Exp Bot 66, 3175–3188 (2015).

Macharia, G., Ngugi, B.N., Arshad, M.S., Anjum, F.M., Sohaib, M. Wheat improvement, management and utilization (2017).

Marger, M. D. & Saier, M. H. A major superfamily of transmembrane facilitators that catalyse uniport, symport and antiport. Trends Biochem Sci 18, 13–20 (1993).

Neill, S. J., Desikan, R., & Hancock, J. T. Nitric oxide signalling in plants. New Phytol 159(1), 11-35 (2003).
Pao, S. S., Paulsen, I. T. & Saier, M. H. Major facilitator superfamily. Microbiol Mol Biol Rev 62, 1–34 (1998).

Siddiqui, M. N. et al. New drought-adaptive loci underlying candidate genes on wheat chromosome 4B with improved photosynthesis and yield responses. Physiol Plant 173, 2166–2180 (2021b).

Siddiqui, M. N., Léon, J., Naz, A. A. & Ballvora, A. Genetics and genomics of root system variation in adaptation to drought stress in cereal crops. J Exp Bot 72, 1007–1019 (2021a).

Soriano, J.M., Alvaro, F. Discovering consensus genomic regions in wheat for root-related traits by QTL meta-analysis. Sci Rep 9(1), 1-14 (2019).

Sun, H. et al. Nitric oxide generated by nitrate reductase increases nitrogen uptake capacity by inducing lateral root formation and inorganic nitrogen uptake under partial nitrate nutrition in rice. J Exp Bot 66(9), 2449-2459.

Tang, W. et al. Genome-wide associated study identifies NAC42-activated nitrate transporter conferring high nitrogen use efficiency in rice. Nat Commun 10, 5279 (2019).

Tsay, Y.-F., Chiu, C.-C., Tsai, C.-B., Ho, C.-H. & Hsu, P.-K. Nitrate transporters and peptide transporters. FEBS Lett 581, 2290–2300 (2007).

Uga, Y., Sugimoto, K., Ogawa, S., Rane, J., Ishitani, M., Hara, N., ... & Yano, M. Control of root system architecture by DEEPER ROOTING 1 increases rice yield under drought conditions. Nat Genet 45(9), 1097-1102 (2013).

Wasaya, A., Zhang, X., Fang, Q., Yan, Z. Root phenotyping for drought tolerance: A review. Agronomy 8, 241 (2018).

Xin, W. et al. Adaptation mechanism of roots to low and high nitrogen revealed by proteomic analysis. Rice 14, 5 (2021).

Yu, J., Pressoir, G., Briggs, W.H., Vroh, Bi I., Yamasaki, M., Doebley, J.F., McMullen, M.D., Gaut, B.S., Nielsen, D.M., Holland, J.B., Kresovich, S., Buckler, E.S. A unified mixed-model method for association mapping that accounts for multiple levels of relatedness. Nat Genet 38 (2), 203-208 (2006).

Zhao, M. G., Chen, L., Zhang, L. L., & Zhang, W. H. Nitric reductase-dependent nitric oxide production is involved in cold acclimation and freezing tolerance in Arabidopsis. Plant Physiol 151(2), 755-767 (2009).

Appendix

Supplementary Data Chapter 3

Supplementary Data Chapter 4

Supplementary for Chapter 3

Title: Genetic dissection of candidate genes underlying root phenotypic plasticity for adaptation to drought in bread wheat

Md. Nurealam Siddiqui, Melesech T. Gabi, Abebaw M. Ambaw, Tesfaye J. Teferi, Said Dadshani, Jens Léon, Agim Ballvora

This file contain the following information:

Supplementary Figure S1: Pearson product-moment correlations coefficient between the drought responses of two variables under drought condition. The abbreviations indicate; total root length (TRL), number of root forks (NRF), root surface area (RSA), number of root tips (NRT), number of root crossing (NRC), root volume (RV), and root average diameter (RAD).

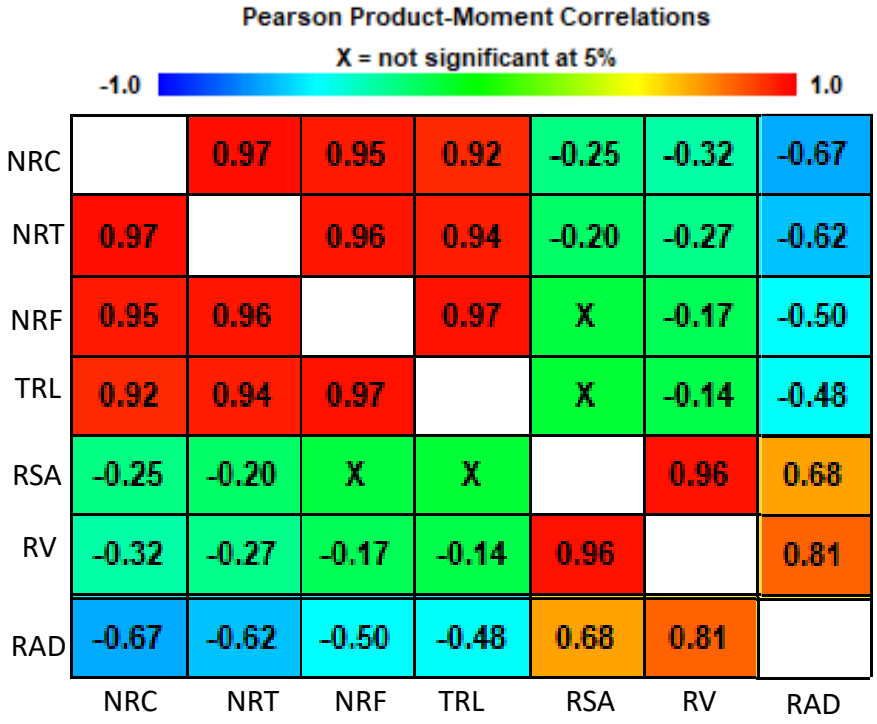

Supplementary Figure S2. Association mapping for root volume (RV) traits under drought conditions. (A) the histogram shows the frequency distribution of log-transformed data of RV traits and the blue and red color middle lines indicate the mean and median of the data set. (B) Quantile- Quantile plot of GWAS p values showing Y-axis: observed negative log 10(P-value) and X-axis expected negative log (p-value). (C) Rectangular Manhattan plot from association mapping of RV using a mixed linear model (MLM) considering the kinship and population structure, Y-axis: -$\log_{10}$ (*p*-value) and X-axis: the entire 21 chromosomes of the wheat genome**.** The red SNPs above the black line indicated the significant SNPs which passed the threshold level at $p \leq 0.0001$. The black SNPs above the dotted black line represented all the SNPs that did not reach the threshold level.

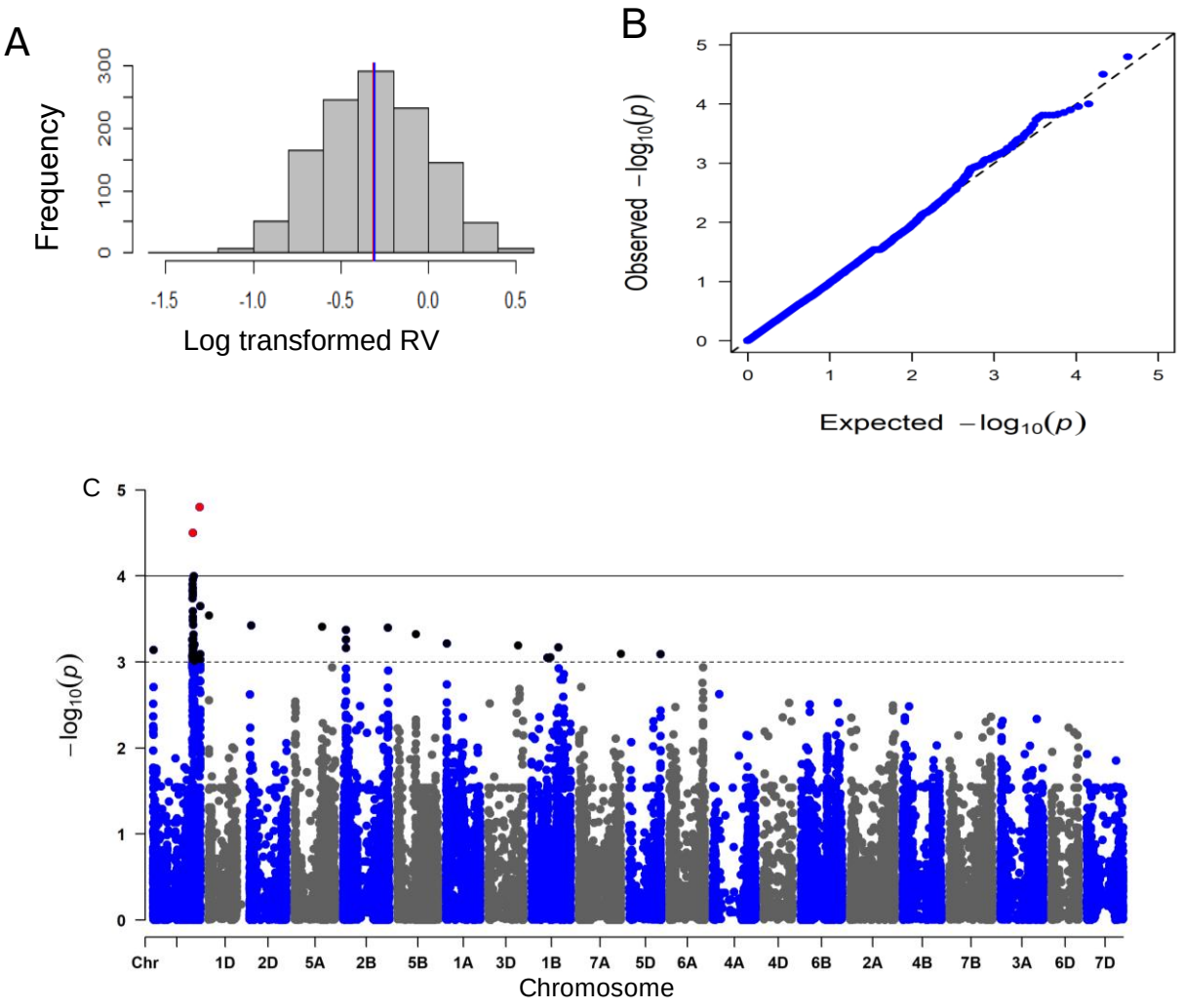

Supplementary Figure S3: Association mapping for root surface area (RSA) traits under drought. (A) the histogram shows the frequency distribution of log-transformed data of root fork (RF) and the blue and red color middle lines indicated the mean and median of the data set. (B) Quantile- Quantile plot of GWAS *p*-values showing Y-axis: observed -$\log_{10}$ (*p*-value) and X-axis expected -$\log_{10}$ (*p*-value). (C) Rectangular Manhattan plot from association mapping of RSA using a mixed linear model (MLM) considering the kinship and population structure, Y-axis: -$\log_{10}$ (*p*-value) and X-axis: the entire 21 chromosomes of the wheat genome**.** The red SNPs above the black line indicated the significant SNPs which passed the threshold level at *p*≤0.0001. The black SNPs above the dotted black line represented all the SNPs that did not reach the threshold level.

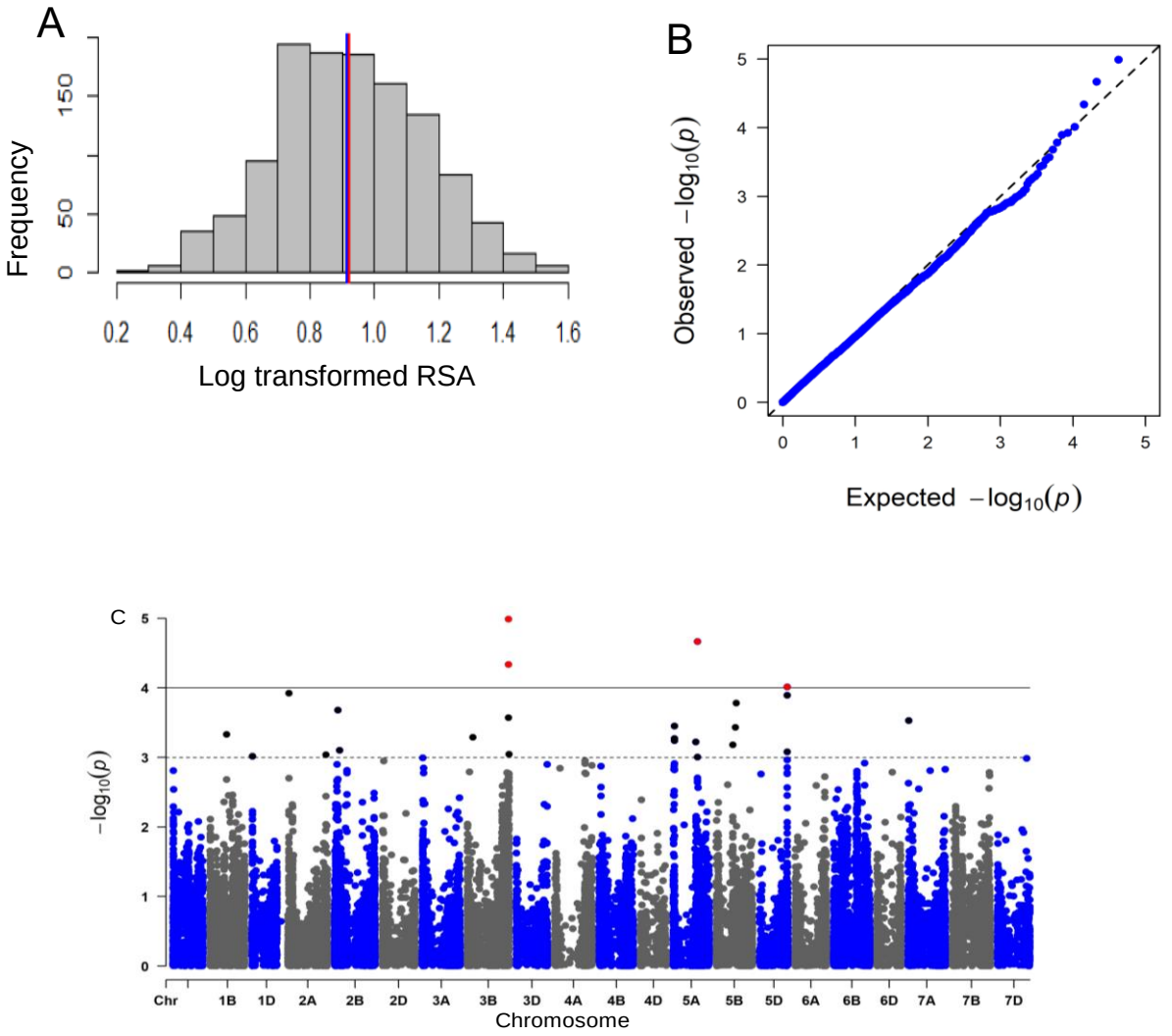

Supplementary Figure S4. Association mapping for the number of root forks (NRF) traits under drought. (A) The histogram shows the frequency distribution of log-transformed data of NRF and the blue and red color middle lines indicated the mean and median of the data set. (B) Quantile- Quantile plot of GWAS *p*-values showing Y-axis: observed -log 10 (*p*-value) and X-axis expected negative log (*p*-value). (C) Rectangular Manhattan plot from association mapping of NRF using a mixed linear model (MLM) considering the kinship and population structure, Y-axis: negative log10 (*p*-value) and X-axis: the entire 21 chromosomes of the wheat genome**.** The red SNPs above the black line indicated the significant SNPs which passed the threshold level at p≤0.0001. The black SNPs above the dotted black line represented all the SNPs that did not reach the threshold level.

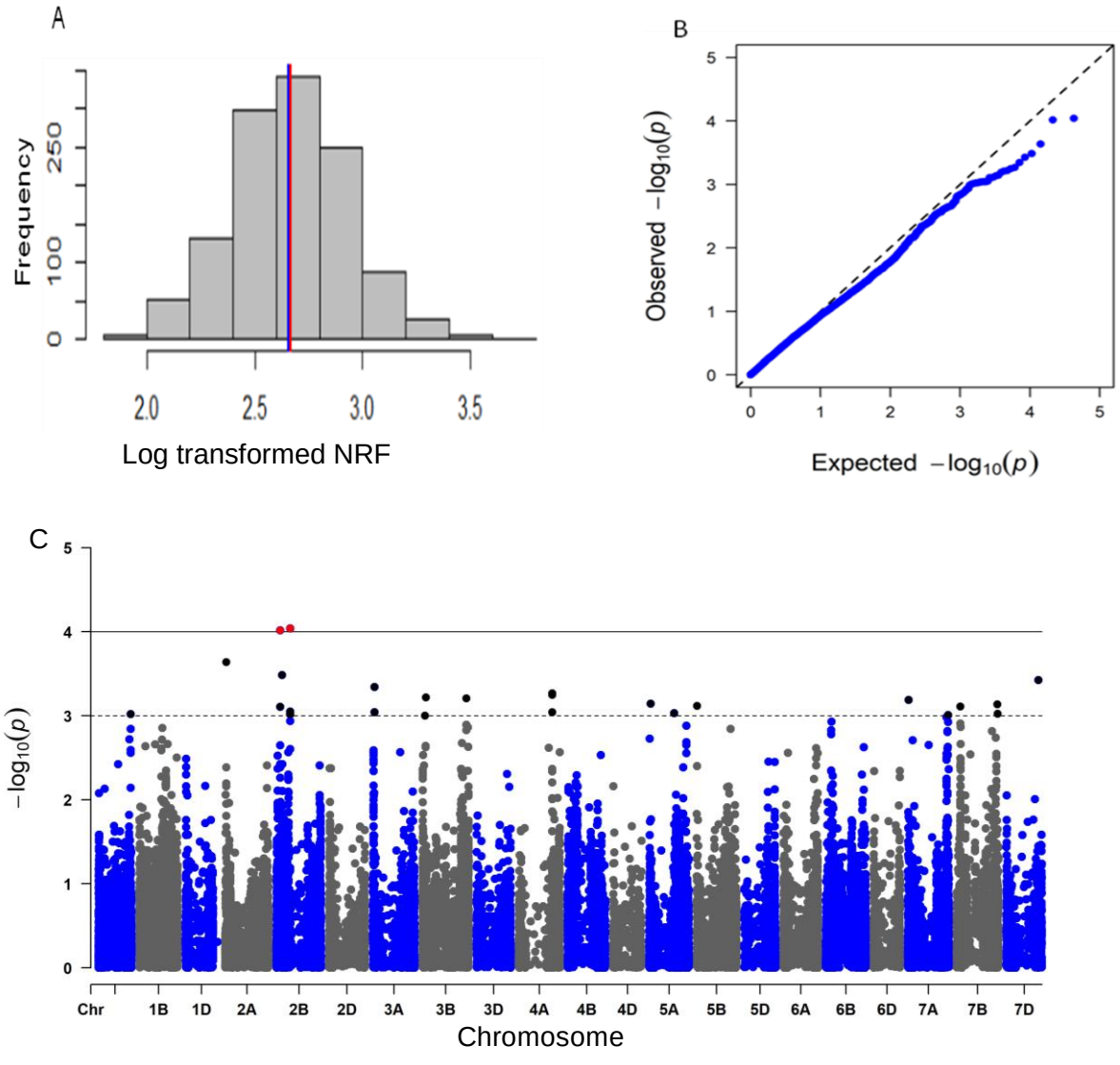

Supplementary Figure S5. Association mapping for the number of root crossing (NRC) traits under drought. (A)The histogram shows the frequency distribution of the log-transformed data number of root crossings (NRC). The blue and red color middle lines indicated the mean and median of the data set. (B) Quantile- Quantile plot of GWAS p values showing Y-axis: observed negative log 10(P-value) and X-axis expected negative log (*p*-value). (C) Rectangular

Manhattan plot from association mapping of RC using a mixed linear model (MLM) considering the kinship and population structure, Y-axis: negative log10 (*p*-value) and X-axis: the entire 21 chromosomes of the wheat genome**.** The red SNPs above the black line indicated the significant SNPs which passes the passes the threshold level at p≤0.0001. The black SNPs above the dotted black line represented all the SNPs that did not reach the threshold level.

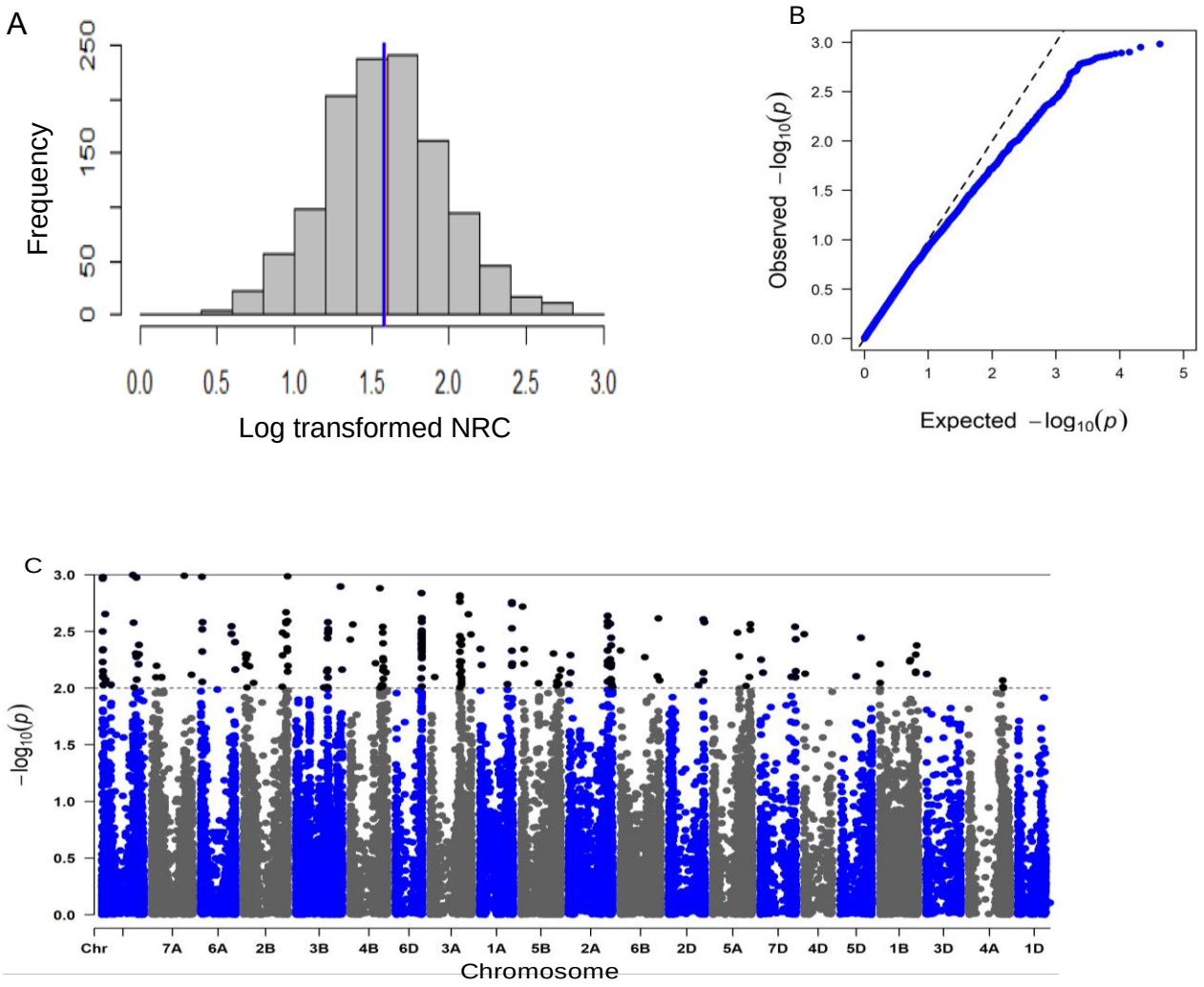

Supplementary Figure S6: Chromosomal location of the associated SNPs to the root architectural traits of wheat under drought stress condition. The name of the markers written on the left side of the chromosome and the right side of the chromosome indicated their position. The red-color markers indicated the significant SNPs markers on the chromosome.

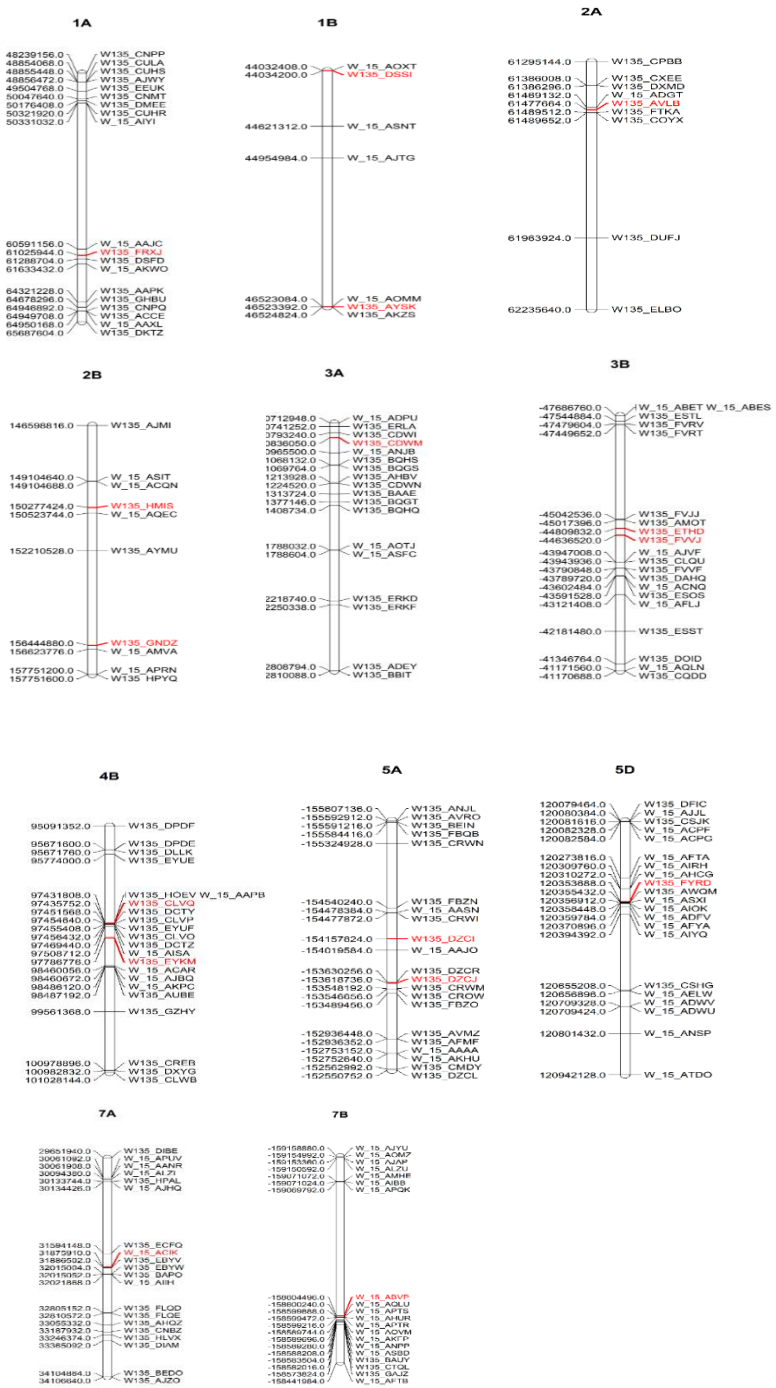

Supplementary Table S1. Annotation and ontology classification of candidate genes identified for root architectural traits in response to plasticity and drought stress.

Trait	Chr.	Gene ID	Gene (bp)	Gene ontology annotation	
				Molecular function	Biological function
TRL	1A (Block2)	TraesCS1A02G294000	3,703	abscisic acid binding- protein phosphatase inhibitor activity -signaling receptor activity(GO:0005488)	abscisic acid-activated signaling pathway -regulation of protein serine/threonine phosphatase activity(GO:0005488)
		TraesCS1A02G294500	3,731	potassium ion leak channel activity(GO:0016021), abscisic acid binding -protein phosphatase inhibitor activity -signaling receptor activity(GO:0031323)	potassium ion transmembrane transport -stabilization of membrane potential (GO:0016021), abscisic acid-activated signaling pathway -regulation of protein serine/threonine phosphatase activity (GO:0031323)
		TraesCS1A02G294100	2,178	abscisic acid binding-protein phosphatase inhibitor activity-signaling receptor activity(GO:0006464)	abscisic acid-activated signaling pathway-regulation of protein serine/threonine phosphatase activity(GO:0006464)
		TraesCS1A02G294600	1,359	hydrolase activity(GO:0006261), abscisic acid binding-protein phosphatase inhibitor activity-signaling receptor activity(GO:0050789)	DNA-dependent DNA replication -DNA repair (GO:0006261), abscisic acid-activated signaling pathway-regulation of protein serine/threonine phosphatase activity
		TraesCS1A02G294200	3,874	abscisic acid binding-protein phosphatase inhibitor activity-signaling receptor activity (GO:0050794), potassium ion leak channel activity (GO:0051179)	abscisic acid-activated signaling pathway-regulation of protein serine/threonine phosphatase activity(GO:0050794), stabilization of membrane potential(GO:0051179)
		TraesCS1A02G294300	4,020	potassium ion leak channel activity(GO:0065007)	potassium ion transmembrane transport -stabilization of membrane potential(GO:0065007)
		TraesCS1A02G294400	1,646	DNA binding-DNA-directed DNA polymerase activity- nucleotide binding (GO:0033554)	DNA replication- nucleic acid phosphodiester bond hydrolysis (GO:0033554)
		TraesCS1A02G294700	1,178	RNA polymerase II regulatory region sequence-specific DNA binding (GO:0006351)	Cell fate specification-negative and positive regulation of transcription by RNA polymerase II (GO:0006351)
		TraesCS1A02G294800	1,574	methyltransferase activity-RNA binding-tRNA (cytosine-5-)-methyltransferase activity(GO:0008168)	RNA methylation(GO:0008168)
		TraesCS1A02G294900	2,570	potassium ion leak channel activity(GO:0065007)	potassium ion transmembrane transport -stabilization of membrane potential(GO:0065007)

	TraesCS1A02G295100	1,591	potassium ion leak channel activity(GO:0006810), ion channel activity(GO:0019867)	potassium ion transmembrane transport -stabilization of membrane potential(GO:0006810), cation transport(GO:0019867)
	TraesCS1A02G295200	7,552	hydrolase activity, hydrolyzing O-glycosyl compounds (GO:0016020)	hydrolase activity, hydrolyzing O-glycosyl compounds(GO:0016020)
	TraesCS1A02G295300	2,911	potassium ion leak channel activity (GO:0005887), abscisic acid binding- signaling receptor activity (GO:0009738)	potassium ion transmembrane transport,stabilization of membrane potential(GO:0005887), abscisic acid-activated signaling pathway(GO:0009738), response to cold(GO:0009409)
	TraesCS1A02G295500	261	specific DNA binding(GO:0008283), DNA-binding transcription activator activity, RNA polymerase II-specific (GO:0009888)	cellular response to hormone stimulus -positive regulation of cell differentiation (GO:0008283) , tissue development- cell fate specification (GO:0009888)
	TraesCS1A02G295600	15,297	protein self-association -unfolded protein binding(GO:0009408)	response to heat -response to hydrogen peroxide-response to reactive oxygen species -response to salt stress(GO:0009408)
	TraesCS1A02G295700	522	hydrolase activity, hydrolyzing O-glycosyl compounds(GO:0005886)	carbohydrate metabolic process(GO:0005886)
	TraesCS1A02G295800	2,757	DNA binding-DNA topoisomerase activity (GO:0006139)	DNA topological change (GO:0006139)
	TraesCS1A02G295900	1,410	DNA-binding transcription activator activity, RNA polymerase II-specific(GO:0032502)	cell fate specification(GO:0032502)
	TraesCS1A02G296000	438	abscisic acid binding-protein phosphatase inhibitor activity-signaling receptor activity (GO:0023052), potassium ion leak channel activity(GO:0016021)	abscisic acid-activated signaling pathway-regulation of protein serine/threonine phosphatase activity-signaling (GO:0023052), potassium ion transmembrane transport-stabilization of membrane potential(GO:0016021)
	TraesCS1A02G296400	687	potassium ion leak channel activity(GO:0016021)	potassium ion transmembrane transport-stabilization of membrane potential(GO:0016021),
1B (Block1)	TraesCS1B02G268800	4,656	water channel activity (GO:0009414)	response to water deprivation (GO:0009414)
	TraesCS1B02G268700	4,154	DNA-binding transcription activator activity, RNA polymerase II-specific(GO:0032502)	cell fate specification(GO:0032502)

TraesCS1B02G269700	2,502	abscisic acid binding -signaling receptor activity (GO:0042221)	abscisic acid- regulation of protein serine/threonine phosphatase activity(GO:0042221)
TraesCS1B02G269600	3,713	translation elongation factor activity-Elongation factor (GO:0003746) , phospholipase A1 activity (GO:0009695)	Protein biosynthesis (GO:0003746), jasmonic acid biosynthetic process-lipid metabolic process(GO:0009695)
TraesCS1B02G270900	3,441	abscisic acid binding-protein phosphatase inhibitor activity-signaling receptor activity(GO:0050896)	abscisic acid-activated signaling pathway -regulation of protein serine/threonine phosphatase activity, response to stimulus (GO:0050896)
TraesCS1B02G271700	5,901	abscisic acid binding-protein phosphatase inhibitor activity-signaling receptor activity (GO:0050790)	abscisic acid-activated signaling pathway -regulation of protein serine/threonine phosphatase activity(GO:0050790)
TraesCS1B02G272300	999	abscisic acid binding -signaling (GO:0050794)	abscisic acid-regulation of protein serine/threonine phosphatase activity(GO:0050794)
TraesCS1B02G272500	1,284	DNA binding-zinc ion binding(GO:0009723)	response to auxin-response to ethylene-response to gibberellin-response to ethylene (GO:0009723)
TraesCS1B02G268900	927	abscisic acid binding-protein phosphatase inhibitor activity-signaling receptor activity(GO:0009725)	abscisic acid-activated signaling pathway-regulation of protein serine/threonine phosphatase activity-response to hormone (GO:0009725)
TraesCS1B02G269200	1,155	hydrolase activity, hydrolyzing O-glycosyl compounds(GO:0016020)	carbohydrate metabolic process(GO:0016020)
TraesCS1B02G269500	4,370	DNA helicase activity-single-stranded DNA binding(GO:0016787)	hydrolase activity (GO:0016787)
TraesCS1B02G269800	3,339	potassium ion leak channel activity(GO:0016021)	potassium ion transmembrane transport-stabilization of membrane potential (GO:0016021)
TraesCS1B02G269900	3,426	potassium ion leak channel activity(GO:0016021), sequence-specific DNA binding (GO:0009863)	stabilization of membrane potential (GO:0016021), hyper osmotic salinity-response to hormones(GO:0009863)
TraesCS1B02G270000	7,654	abscisic acid binding -signaling receptor activity(GO:0019222)	abscisic acid-regulation of protein serine/threonine phosphatase activity(GO:0019222)
TraesCS1B02G270300	2,889	potassium ion leak channel activity(GO:0016021)	potassium ion transmembrane transport-stabilization of membrane potential (GO:0016021)
TraesCS1B02G270100	5,416	hydrolase activity, hydrolyzing O-glycosyl compounds (GO:0005886)	carbohydrate metabolic process (GO:0005886)
TraesCS1B02G270300	2,889	potassium ion leak channel activity(GO:0016021)	potassium ion transmembrane transport-stabilization of membrane potential (GO:0016021)

TraesCS1B02G270200	1,313	potassium ion leak channel activity(GO:0016021), abscisic acid binding-signaling receptor activity (GO:0050896)	stabilization of membrane potential (GO:0016021), abscisic acid-activated signaling pathway-regulation of protein serine/threonine phosphatase activity-response to stimulus (GO:0050896)
TraesCS1B02G270400	4,077	potassium ion leak channel activity(GO:0065007)	potassium ion transmembrane transport-stabilization of membrane potential(GO:0065007)- tissue development (GO:0009888)
TraesCS1B02G270500	1,206	ATP binding(GO:0005524)	5-phosphoribose 1-diphosphate biosynthetic process- purine nucleotide biosynthetic process (GO:0005524)
TraesCS1B02G270600	6,014	NA	positive regulation of hydrolase activity (GO:0051345)
TraesCS1B02G270700	5,157	abscisic acid binding -signaling receptor activity (GO:0044267)	abscisic acid-regulation of protein serine/threonine phosphatase activity (GO:0044267)
TraesCS1B02G270800	3,493	protein self-association-unfolded protein binding(GO:0006950)	response to heat- response to reactive oxygen species-response to salt stress- response to stress (GO:0006950)
TraesCS1B02G271000	14,313	abscisic acid binding- signaling receptor activity(GO:0050789)	abscisic acid -regulation of protein serine/threonine phosphatase activity(GO:0050789)
TraesCS1B02G271100	7,518	abscisic acid binding -signaling receptor activity(GO:0050789)	abscisic acid -regulation of protein serine/threonine phosphatase activity(GO:0050789)
TraesCS1B02G271200	3,146	potassium ion leak channel activity(GO:0016021)	potassium ion transmembrane transport-stabilization of membrane potential- (GO:0016021)
TraesCS1B02G271300	4,924	abscisic acid binding -signaling receptor activity(GO:0009892)	abscisic acid -regulation of protein serine/threonine phosphatase activity(GO:0009892)
TraesCS1B02G271400	387	potassium ion leak channel activity(GO:0016021)	potassium ion transmembrane transport-stabilization of membrane potential (GO:0016021)
TraesCS1B02G271800	6,823	abscisic acid binding -signaling receptor activity (GO:0019222)	abscisic acid-regulation of protein serine/threonine phosphatase activity(GO:0019222)
TraesCS1B02G271900	1,832	potassium ion leak channel activity (GO:0065007)	potassium ion transmembrane transport-stabilization of membrane potential(GO:0065007)
TraesCS1B02G272200	4,753	potassium ion leak channel activity(GO:0016021)	potassium ion transmembrane transport-stabilization of membrane potential (GO:0016021)
TraesCS1B02G272600	2,336	abscisic acid binding-protein phosphatase inhibitor activity-signaling receptor activity (GO:0042221)	abscisic acid-activated signaling pathway-regulation of protein serine/threonine phosphatase activity (GO:0042221)
TraesCS1B02G272800	7,406	potassium ion leak channel activity(GO:0016021)	potassium ion transmembrane transport-stabilization of membrane potential (GO:0016021)

	TraesCS1B02G272700	2,215	potassium ion leak channel activity(GO:0006810)	potassium ion transmembrane transport-stabilization of membrane potential-transport (GO:0006810)
	TraesCS1B02G272400	2,297	potassium ion leak channel activity(GO:0016021)	potassium ion transmembrane transport-stabilization of membrane potential (GO:0016021)
2A (Block2)	TraesCS2A02G144600	243	RNA polymerase II regulatory region sequence-specific DNA binding(GO:0032502)	cell fate specification negative and positive regulation of transcription by RNA polymerase II-developmental process (GO:0032502)
	TraesCS2A02G144700	207	RNA polymerase II regulatory region sequence-specific DNA binding(GO:0031327)	cell fate specification negative and positive regulation of transcription by RNA polymerase II-developmental process(GO:0031327)
	TraesCS2A02G144800	3,488	translation elongation factor activity(GO:0003746)	Protein biosynthesis(GO:0003746)
	TraesCS2A02G145100	1,903	potassium ion leak channel activity(GO:0016021)	potassium ion transmembrane transport-stabilization of membrane potential (GO:0016021)
	TraesCS2A02G145200	5,318	hydrolase activity, hydrolyzing O-glycosyl compounds(GO:0016020)	carbohydrate metabolic process(GO:0016020)
2B (Block3)	TraesCS2B02G408800	8,275	abscisic acid binding -signaling receptor activity(GO:0032268)	abscisic acid-regulation of protein serine/threonine phosphatase activity(GO:0032268)
	TraesCS2B02G409100	2,072	amino acid transmembrane transporter activity-(GO:0015824)	amino acid transmembrane transport-proline transport (GO:0015824)
	TraesCS2B02G410400	4,291	abscisic acid binding-protein phosphatase inhibitor activity-signaling receptor activity(GO:0010033)	abscisic acid-activated signaling pathway -regulation of protein serine/threonine phosphatase activity(GO:0010033)
	TraesCS2B02G410600	8,832	chlorophyll binding (GO:0015979)	photosynthesis, light harvesting in photosystem I -response to light stimulus (GO:0015979)
	TraesCS2B02G409800	1,306	abscisic acid binding -signaling receptor activity-signal transduction (GO:0007165)	abscisic acid-regulation of protein serine/threonine phosphatase activity (GO:0007165)
	TraesCS2B02G410600	8,832	abscisic acid binding -signaling receptor activity-signal transduction (GO:0007165)	abscisic acid-regulation of protein serine/threonine phosphatase activity (GO:0007165)
	TraesCS2B02G410500	1,213	ubiquitin-protein transferase activity-zinc ion binding- (GO:0012501)	regulation of apoptotic process-programmed cell death (GO:0012501)
	TraesCS2B02G411500	1,188	ethylene binding-ethylene receptor activity (GO:0009873)	ethylene-activated signaling pathway (GO:0009873)
3A (Block3)	TraesCS3A02G039000	4,478	DNA binding-zinc ion binding(GO:0009733)	response to ethylene-response to gibberellin -response to auxin (GO:0009733)

	TraesCS3A02G039100	2,379	nitrate transmembrane transporter activity(GO:0010167) ,transporter activity (GO:0006826)	cellular response to nitrate- (GO:0010167) , transmembrane transport (GO:0006826)
	TraesCS3A02G039200	2,695	abscisic acid binding- -signaling receptor activity (GO:0007165), hydrolase activity (GO:0005886)	abscisic acid -regulation of protein serine/threonine phosphatase activity (GO:0007165) , carbohydrate metabolic process- plasma membrane (GO:0005886)
	TraesCS3A02G039800	1,623	potassium ion leak channel activity (GO:0016021)	potassium ion transmembrane transport-stabilization of membrane potential (GO:0016021)
	TraesCS3A02G039300	2,685	potassium ion leak channel activity (GO:0016021)	potassium ion transmembrane transport-stabilization of membrane potential (GO:0016021)
	TraesCS3A02G039400	3,624	potassium ion leak channel activity (GO:0016021)	potassium ion transmembrane transport-stabilization of membrane potential (GO:0016021)
	TraesCS3A02G039500	2,781	potassium ion leak channel activity (GO:0016021)	potassium ion transmembrane transport-stabilization of membrane potential (GO:0016021)
	TraesCS3A02G039600	1,885	transmembrane transporter activity- transporter activity (GO:0005783)	Transport (GO:0005783)
	TraesCS3A02G039700	6,584	abscisic acid binding-protein phosphatase inhibitor activity-signaling receptor activity(GO:0007165)	abscisic acid-activated signaling pathway-regulation of protein serine/threonine phosphatase activity- signal transduction (GO:0007165)
	TraesCS3A02G040100	3,151	potassium ion leak channel activity (GO:0016021)	potassium ion transmembrane transport-stabilization of membrane potential (GO:0016021)
4B (Block1)	TraesCS4B02G259900	2,400	potassium ion leak channel activity(GO:0065007)	potassium ion transmembrane transport-stabilization of membrane potential(GO:0065007)
	TraesCS4B02G260000	2,545	abscisic acid binding-protein phosphatase inhibitor activity-signaling receptor activity(GO:0050794)	abscisic acid-activated signaling pathway-regulation of protein serine/threonine phosphatase activity(GO:0050794)
	TraesCS4B02G260200	2,261	potassium ion leak channel activity (GO:0016021)	potassium ion transmembrane transport-stabilization of membrane potential (GO:0016021)
5A (Block1)	TraesCS5A02G551600	4,721	potassium ion leak channel activity (GO:0006810)	potassium ion transmembrane transport-stabilization of membrane potential-transport (GO:0006810)
	TraesCS5A02G551900	387	abscisic acid binding- signaling receptor activity(GO:0008289), potassium ion leak channel activity (GO:0016021)	abscisic acid-activated signaling pathway -regulation of protein serine/threonine phosphatase activity(GO:0008289),stabilization of membrane potential(GO:0016021)

		TraesCS5A02G552600	4,373	abscisic acid binding -signaling receptor activity(GO:0048519)	abscisic acid-regulation of protein serine/threonine phosphatase activity(GO:0048519)
RAD	2A (Block2)	TraesCS2A02G438800	8,465	abscisic acid binding- signaling receptor activity(GO:0009737),	auxin-activated signaling pathway-transmembrane transport (GO:0009734)-xylem development(GO:0010089), abscisic acid-activated signaling pathway -regulation of protein serine/threonine phosphatase activity(GO:0009737)
		TraesCS2A02G438900	6,573	sodium-independent organic anion transmembrane transporter activity(GO:0006820), abscisic acid binding-protein phosphatase inhibitor activity-signaling receptor activity(GO:0010427)	cellular response to cold (GO:0070417), developmental process (GO:0051452), regulation of ion transmembrane transport (GO:0034765), abscisic acid-regulation of protein serine/threonine phosphatase activity(GO:0010427)
		TraesCS2A02G439300	2,540	abscisic acid binding-protein phosphatase inhibitor activity-signaling receptor activity(GO:0050794)	intracellular protein transport-retrograde transport, endosome to Golgi (GO:0012505), abscisic acid-activated signaling pathway -regulation of protein serine/threonine phosphatase activity(GO:0050794)
		TraesCS2A02G439500	1,849	hydrolase activity, hydrolyzing O-glycosyl compounds (GO:0046658)	carbohydrate metabolic process (GO:0046658)
		TraesCS2A02G439800	2,093	potassium ion leak channel activity, oxidoreductase activity(GO:0016021) , acting on paired donors, with incorporation or reduction of molecular oxygen (GO:0004497)	potassium ion transmembrane transport-stabilization of membrane potential (GO:0016021) ,
		TraesCS2A02G440100	4,638	Receptor (GO:0006623)	Golgi to endosome transport-Golgi to vacuole transport-post -mediated transport (GO:0006623), intracellular protein transport-retrograde transport(GO:0005770)
		TraesCS2A02G440300	318	protein self-association-unfolded protein binding(GO:0043933) , transmembrane transporter activity(GO:0005783)	response to heat-response to hydrogen peroxide-response to reactive oxygen species-response to salt stress(GO:0043933),Transport(GO:0005783)
		TraesCS2A02G440700	1,228	peroxidase activity-thioredoxin peroxidase activity(GO:0045454)	cell redox homeostasis-cellular response to oxidative stress(GO:0045454)
	7A (no Block)	TraesCS7A02G062600	2,096	abscisic acid binding-protein phosphatase inhibitor activity-signaling receptor activity(GO:0023052)	cell wall organization-glucan catabolic process(GO:0005576), abscisic acid-regulation of protein serine/threonine phosphatase activity(GO:0023052)
		TraesCS7A02G062800	4,602	cation binding-hydrolase activity,(GO:0006112)	intracellular protein transport-photosystem II assembly-retrograde transport (GO:0005768) , glycogen biosynthetic process(GO:0006112)

		TraesCS7A02G063000	959	potassium ion leak channel activity (GO:0016021)	potassium ion transmembrane transport-stabilization of membrane potential (GO:0016021)
		TraesCS7A02G063700	6,709	potassium ion leak channel activity(GO:0000325)	potassium ion transmembrane transport-stabilization of membrane potential(GO:0000325)
		TraesCS7A02G064200	3,965	potassium ion leak channel activity (GO:0016021)	potassium ion transmembrane transport-stabilization of membrane potential(GO:0016021)
		TraesCS7A02G065600	1,959	cyclosporin A binding-peptidyl-prolyl cis-trans isomerase activity(GO:0070301)	cellular response to hydrogen peroxide, mitochondrial outer membrane permeabilization involved in programmed cell death,(GO:0070301)
RSA	3B (Block3)	TraesCS3B02G587900	9,933	ammonium transmembrane transporter activity-leak channel activity(GO:0072488)	ammonium transmembrane transport-cellular ion homeostasis(GO:0072488)
		TraesCS3B02G588000	4,328	abscisic acid binding -signaling receptor activity (GO:0050896)	abscisic acid-regulation of protein serine/threonine phosphatase activity-response to stimulus (GO:0050896)
		TraesCS3B02G588200	8,397	ATP binding-protein serine/threonine kinase activity(GO:0004672), abscisic acid binding-protein phosphatase inhibitor activity-signaling receptor activity(GO:0007165)	intracellular signal transduction- (GO:0004672), abscisic acid-regulation of protein serine/threonine phosphatase activity- signal transduction (GO:0007165)
		TraesCS3B02G588500	8,438	potassium ion leak channel activity (GO:0016021)	integral component of membrane (GO:0016021), potassium ion transmembrane transport-stabilization of membrane potential (GO:0016021)
		TraesCS3B02G588800	2,562	ammonium transmembrane transporter activity-leak channel activity(GO:0072488)	ammonium transmembrane transport-cellular ion homeostasis (GO:0072488)
		TraesCS3B02G588900	9,313	hydrolase activity, hydrolyzing O-glycosyl compounds (GO:0071944)	carbohydrate metabolic process (GO:0071944)
		TraesCS3B02G589100	7,214	ammonium transmembrane transporter activity-leak channel activity(GO:0072488)	ammonium transmembrane transport-cellular ion homeostasis(GO:0072488)
		TraesCS3B02G589300	5,221	ammonium transmembrane transporter activity-leak channel activity (GO:0072488)	ammonium transmembrane transport-cellular ion homeostasis-(GO:0072488)
		TraesCS3B02G589500	10,658	ATP binding-protein serine/threonine kinase activity (GO:0006468)	intracellular signal transduction-regulation of gene expression (GO:0006468)
		TraesCS3B02G589900	2,884	abscisic acid binding -signaling receptor activity (GO:0050794)	abscisic acid-regulation of protein serine/threonine phosphatase activity(GO:0050794)

		TraesCS3B02G590300	1,887	DNA-binding transcription factor activity-sequence-specific DNA binding (GO:0010014)	negative regulation of mitotic cell cycle-asymmetric cell division (GO:0010014)
		TraesCS3B02G590400	10,142	NA	intracellular protein transport-retrograde transport, endosome to Golgi(GO:0016482)
	5A (Block2)	TraesCS5A02G267400	1,242	abscisic acid binding- -signaling receptor activity(GO:0007154),selective channel activity-transmembrane signaling receptor activity(GO:0003008)	abscisic acid-regulation of protein serine/threonine phosphatase activity-cell communication (GO:0007154), -regulation of membrane potential-signal transduction (GO:0003008)
		TraesCS5A02G267200	2,563	protein serine/threonine kinase activity(GO:0032990), abscisic acid binding-protein phosphatase inhibitor activity-signaling receptor activity(GO:0044092)	establishment of cell polarity-intracellular signal transduction-cell part morphogenesis (GO:0032990), abscisic acid-regulation of protein serine/threonine phosphatase activity(GO:0044092)
		TraesCS5A02G267300	4,483	potassium ion leak channel activity(GO:0022857)	stabilization of membrane potential,transmembrane transporter activity (GO:0022857)
		TraesCS5A02G267800	417	abscisic acid binding -signaling receptor activity (GO:0050794)	abscisic acid-regulation of protein serine/threonine phosphatase activity(GO:0050794)
	5D (Block3)	TraesCS5D02G536600	857	potassium ion leak channel activity(GO:0016021)	potassium ion transmembrane transport-stabilization of membrane potential (GO:0016021)
NRF	2B (Block 1)	TraesCS2B02G104700	1,404	abscisic acid binding-signaling receptor activity(GO:0050896),hydrolase activity (GO:0048046)	abscisic acid-regulation of protein serine/threonine phosphatase activity-response to stimulus (GO:0050896), Hydrolase, apoplast (GO:0048046)
		TraesCS2B02G104800	3,323	amidase activity-glutaminyl-tRNA synthase (glutamine-hydrolyzing) activity(GO:0016879)	glutaminyl-tRNAGln biosynthesis via transamidation-mitochondrial translation(GO:0016879)
		TraesCS2B02G104900	1,085	abscisic acid binding-signaling receptor activity(GO:0007154)	abscisic acid-regulation of protein serine/threonine phosphatase activity-cell communication (GO:0007154)
		TraesCS2B02G105300	1,344	abscisic acid binding-protein phosphatase inhibitor activity-signaling receptor activity(GO:0038023)	abscisic acid binding-protein phosphatase inhibitor activity-signaling receptor activity-signaling receptor activity (GO:0038023)
		TraesCS2B02G237500	3,640	mRNA binding (GO:0003723)	posttranscriptional regulation of gene expression (GO:0003723)
		TraesCS2B02G237600	1,386	translation regulator activity(GO:0048522), potassium ion leak channel activity(GO:0016021)	positive regulation of mitochondrial translation (GO:0048522),stabilization of membrane potential- (GO:0016021)

TraesCS2B02G237800	1,361	serine-type carboxypeptidase activity(GO:0008236)	proteolysis involved in cellular protein catabolic process-serine-type peptidase activity (GO:0008236)
TraesCS2B02G237900	6,652	threonine-type endopeptidase activity (GO:0000502)	protein catabolic process (GO:0000502),regulation of unidimensional cell growth (GO:0051510)
TraesCS2B02G238000	2,895	metalloendopeptidase activity(GO:0008233), RNA polymerase II activating transcription factor binding(GO:0000977)	inducible membrane protein ectodomain proteolysis-peptidase activity (GO:0008233), cell fate specification-negative and positive regulation of transcription by RNA polymerase II(GO:0000977)
TraesCS2B02G238100	467	protein self-association-unfolded protein binding(GO:0006950) , abscisic acid binding-protein phosphatase inhibitor activity-signaling receptor activity(GO:0050794)	response to heat-response to hydrogen peroxide-response to reactive oxygen species-response to salt stress-response to stress (GO:0006950) , abscisic acid-regulation of protein serine/threonine phosphatase activity(GO:0050794)
TraesCS2B02G238200	2,473	DNA-binding transcription activator activity, RNA polymerase II-specific(GO:0035295)	cell fate specification-negative and positive regulation of transcription by RNA polymerase II-tube development (GO:0035295)
TraesCS2B02G238300	3,329	argininosuccinate lyase activity(GO:0006526)	arginine biosynthetic process via ornithine(GO:0006526)
TraesCS2B02G238400	1,668	abscisic acid binding-signaling receptor activity(GO:0007165)	abscisic acid binding-protein phosphatase inhibitor activity- signal transduction (GO:0007165)
TraesCS2B02G238600	3,646	RNA polymerase II-specific(GO:0035295), abscisic acid binding-protein phosphatase inhibitor activity-signaling receptor activity(GO:0060089)	cell fate specification-negative and positive regulation of transcription by RNA polymerase II-tube development (GO:0035295),auxin transport (GO:0010540),regulation of meristem growth (GO:0010075), positive gravitropism (GO:0009958),response to blue light (GO:0009637), abscisic acid binding-protein phosphatase inhibitor activity (GO:0060089)
TraesCS2B02G238500	3,991	aminoacyl-tRNA hydrolase activity(GO:0004045)	aminoacyl-tRNA hydrolase activity (GO:0004045)
TraesCS2B02G238700	372	abscisic acid binding-signaling receptor activity(GO:0050896),	abscisic acid binding -response to stimulus (GO:0050896), intracellular protein transport-retrograde transport, (GO:0005829)
TraesCS2B02G238800	2,662	abscisic acid binding -signaling receptor activity-(GO:0019222)	abscisic acid-regulation of protein serine/threonine phosphatase activity-regulation of metabolic process(GO:0019222)
TraesCS2B02G238900	10,331	heat shock protein binding (GO:0005844), translation regulator activity(GO:0019898),	cellular response to unfolded protein (GO:0005844), positive regulation of mitochondrial translation- extrinsic component of membrane (GO:0019898)

		TraesCS2B02G239000	4,064	potassium ion leak channel activity(GO:0016021), D-xylulose reductase activity-zinc ion binding(GO:0055114)	potassium ion transmembrane transport-stabilization of membrane potential(GO:0016021),oxidation-reduction process (GO:0055114)
		TraesCS2B02G239200	4,508	DNA helicase activity(GO:0016787), terpene synthase activity-transferase activity(GO:0016114)	hydrolase activity (GO:0016787), terpenoid biosynthetic process (GO:0016114)
		TraesCS2B02G239300	6,409	potassium ion leak channel activities(GO:0016021)	potassium ion transmembrane transport-stabilization of membrane potential (GO:0016021)
		TraesCS2B02G239400	4,706	abscisic acid binding -signaling receptor activity(GO:0007165), hydrolase activity, (GO:0016020)	abscisic acid-regulation of protein serine/threonine phosphatase activity-signal transduction (GO:0007165)
		TraesCS2B02G239500	6,550	RNA polymerase II regulatory region sequence-specific DNA binding (GO:0003700)	cell fate specification-negative and positive regulation of transcription by RNA polymerase II (GO:0003700)
		TraesCS2B02G239600	918	DNA helicase activity-single-stranded DNA binding (GO:0003677),nucleosomal DNA binding(GO:0006342)	nucleosome positioning-regulation of transcription, DNA-templated-chromosome condensation(GO:0006342)
		TraesCS2B02G239700	1,073	RNA polymerase II regulatory region sequence-specific DNA binding (GO:0000790)	cell fate specification-negative and positive regulation of transcription by RNA polymerase II (GO:0000790)
		TraesCS2B02G240000	1,197	response to red light(GO:0010114), photosynthesis activity(GO:0009767)	photosystem II assembly(GO:0009543), photosynthetic electron transport chain(GO:0009767)
		TraesCS2B02G240100	3,242	acyloxyacyl hydrolase activity (GO:0044247),electron transporter - photosynthesis activity (GO:0009523)	photosynthetic electron transport in photosystem II-protein-chromophore linkage(GO:0009523)
		TraesCS2B02G240200	2,983	oxidoreductase activity, oxygen as acceptor(GO:0009523)	photosynthetic electron transport in photosystem II-protein(GO:0009523), intracellular protein transport-retrograde transport,(GO:0005829), acyloxyacyl hydrolase activity(GO:0044247)
NRT	1A (Block2)	TraesCS1A02G294000	3,703	DNA helicase activity(GO:0005488),DNA topoisomerase type I (GO:0044237)	DNA topological change(GO:0044237)
		TraesCS1A02G294100	2,178	potassium ion leak channel activity(GO:0016021)	potassium ion transmembrane transport-stabilization of membrane potential (GO:0016021)
		TraesCS1A02G294200	3,874	potassium ion leak channel activity(GO:0016021)	potassium ion transmembrane transport-stabilization of membrane potential(GO:0016021)

TraesCS1A02G294300	4,020	abscisic acid binding- signaling receptor activity(GO:0016788)	abscisic acid-regulation of protein serine/threonine phosphatase activity-hydrolase activity(GO:0016788)
TraesCS1A02G294400	1,646	potassium ion leak channel activity(GO:0016021),DNA-directed DNA polymerase activity (GO:0033554)	potassium ion transmembrane transport-stabilization of membrane potential (GO:0016021),cellular response to stress (GO:0033554)
TraesCS1A02G294500	3,731	potassium ion leak channel activity(GO:0016021), translation regulator activity(GO:0048518), abscisic acid binding- signaling receptor activity (GO:0031323)	potassium ion transmembrane transport-stabilization of membrane potential (GO:0016021),positive regulation of biological process (GO:0048518), abscisic acid-regulation of protein serine/threonine phosphatase activity(GO:0031323)
TraesCS1A02G294600	1,359	potassium ion leak channel activity(GO:0016021), abscisic acid binding-protein phosphatase inhibitor activity-signaling receptor activity(GO:0050789), hydrolase activity (GO:0006261)	potassium ion transmembrane transport-stabilization of membrane potential (GO:0016021), abscisic acid-activated signaling pathway-regulation of protein serine/threonine phosphatase activity-regulation of biological process (GO:0050789),
TraesCS1A02G294700	1,178	RNA polymerase II regulatory region sequence-specific DNA binding(GO:0045892)	cell fate specification-negative and positive regulation of transcription by RNA polymerase II(GO:0045892),
TraesCS1A02G294800	1,574	potassium ion leak channel activity(GO:0016021), DNA helicase activity (GO:0016787), abscisic acid binding- -signaling receptor activity(GO:0006464)	potassium ion transmembrane transport-stabilization of membrane potential (GO:0016021),hydrolase activity (GO:0016787),abscisic acid-regulation of protein serine/threonine phosphatase activity (GO:0006464)
TraesCS1A02G294900	2,570	potassium ion leak channel activity(GO:0065007)	potassium ion transmembrane transport-stabilization of membrane potential- (GO:0065007)
TraesCS1A02G29500	1,549	abscisic acid binding-signaling receptor activity(GO:0023052), protein self-association (GO:0006950), potassium ion leak channel activity(GO:0016021)	abscisic acid -regulation of protein serine/threonine phosphatase activity- signaling (GO:0023052),response to heat- response to reactive oxygen species-response to salt stress-response to stress (GO:0006950),stabilization of membrane potential (GO:0016021)
TraesCS1A02G295100	1,591	potassium ion leak channel activity(GO:0006810), abscisic acid binding- signaling receptor activity (GO:0050789)	stabilization of membrane potential-transport (GO:0006810), abscisic acid -regulation of protein serine/threonine phosphatase activity-regulation of biological process (GO:0050789)
TraesCS1A02G295200	7,552	DNA helicase activity-single-stranded DNA binding(GO:0016787)	hydrolase activity (GO:0016787)

	TraesCS1A02G295300	2,911	potassium ion leak channel activity (GO:0005887), abscisic acid binding -signaling receptor activity (GO:0009738) , (GO:0009409)	stabilization of membrane potential- (GO:0005887), regulation of jasmonic acid mediated signaling pathway(GO:0009867), abscisic acid-regulation of protein serine/threonine phosphatase activity(GO:0009738), cellular response to light stimulus (GO:0009581), response to cold - Transport(GO:0009409)
	TraesCS1A02G295600	15,297	hydrolase activity, hydrolyzing O-glycosyl compounds(GO:0005886), potassium ion leak channel activity(GO:0005774), potassium ion leak channel activity(GO:0065007)	intracellular protein transport-retrograde transport, (GO:0012505), potassium ion transmembrane transport-stabilization of membrane potential(GO:0005774) ,response to high light intensity (GO:0009644), potassium ion transmembrane transport-stabilization of membrane potential-biological regulation (GO:0065007),response to heat-response to reactive oxygen species-response to salt stress-(GO:0042542)
	TraesCS1A02G295800	2,757	nucleic acid binding(GO:0010162), potassium ion leak channel activity	negative regulation of transcription, DNA-templated-seed dormancy process(GO:0010162), potassium ion transmembrane transport-stabilization of membrane potential(GO:0016021)
	TraesCS1A02G295900	1,410	abscisic acid-activated signaling pathway-regulation of protein serine/threonine phosphatase activity(GO:0050794),RNA polymerase II regulatory region sequence-specific DNA binding(GO:0032502)	abscisic acid binding-protein phosphatase inhibitor activity-signaling receptor activity (GO:0050794), cell fate specification-negative and positive regulation of transcription by RNA polymerase II(GO:0032502), retrograde transport, (GO:0012505)
	TraesCS1A02G296000	438	DNA helicase activity-single-stranded DNA binding(GO:0016787), abscisic acid-activated signaling pathway-regulation of protein serine/threonine phosphatase activity(GO:0023052), potassium ion leak channel activity (GO:0005773)	hydrolase activity (GO:0016787), abscisic acid binding- signaling receptor activity-signaling (GO:0023052), potassium ion transmembrane transport-stabilization of membrane potential(GO:0005773)
	TraesCS1A02G296200	4,331	potassium ion leak channel activity(GO:0005215)	potassium ion transmembrane transport-stabilization of membrane potential- transporter activity (GO:0005215)
	TraesCS1A02G296400	687	potassium ion leak channel activity(GO:0016021)	potassium ion transmembrane transport-stabilization of membrane potential integral component of membrane
2B	TraesCS2B02G407500	5,821	specific DNA binding-(GO:0009630)- hydrolase activity(GO:0005886)	cell fate specification-gravitropism(GO:0009630)- carbohydrate metabolic process(GO:0005886)

	TraesCS2B02G407600	1,755	RNA polymerase II regulatory region sequence-specific DNA binding(GO:0030154)	cell fate specification-negative and positive regulation of transcription by RNA polymerase II-cell differentiation (GO:0030154)
	TraesCS2B02G407700	2,483	potassium ion leak channel activity(GO:0016021),abscisic acid binding -signaling receptor activity(GO:0044267)	potassium ion transmembrane transport-stabilization of membrane potential (GO:0016021) abscisic acid -regulation of protein serine/threonine phosphatase activity(GO:0044267)
	TraesCS2B02G407800	1,604	potassium ion leak channel activity(GO:0016021)	potassium ion transmembrane transport-stabilization of membrane potential (GO:0016021)
	TraesCS2B02G407900	4,964	nucleic acid binding(GO:0048316), transmembrane transporter activity(GO:0034755)	negative regulation of transcription, DNA-templated-seed dormancy process-seed development (GO:0048316), transmembrane transport(GO:0034755)
	TraesCS2B02G408000	4,686	nucleic acid binding(GO:0048316), transmembrane transporter activity(GO:0034755)	transmembrane transport(GO:0034755)
	TraesCS2B02G408100	663	abscisic acid binding -signaling receptor activity(GO:0050794), protein self-association-unfolded protein binding(GO:0006950), hydrolase activity (GO:0005886)	abscisic acid-activated signaling pathway-regulation of protein serine/threonine phosphatase activity(GO:0050794),-response to heat-response to hydrogen peroxide-response to reactive oxygen species-response to salt stress- response to stress (GO:0006950),
	TraesCS2B02G408200	264	potassium ion leak channel activity(GO:0065008), abscisic acid binding- signaling receptor activity(GO:0048519), protein self-association-unfolded protein binding(GO:0006950)	stabilization of membrane potential(GO:0065008) , abscisic acid-activated signaling pathway-regulation of protein serine/threonine phosphatase activity(GO:0048519),response to heat-response to hydrogen peroxide-response to reactive oxygen species-response to salt stress-response to stress (GO:0006950)
	TraesCS2B02G408300	15,064	potassium ion leak channel activity-(GO:0065007), ATP binding-protein serine/threonine kinase activity(GO:0004672)	potassium ion transmembrane transport-stabilization of membrane potential-biological regulation (GO:0065007), intracellular signal transduction-regulation of gene expression- protein kinase activity (GO:0004672)
3A (Block3)	TraesCS3A02G038700	11,894	potassium ion leak channel activity(GO:0016021)	stabilization of membrane potential (GO:0016021), regulation of hydrogen peroxide (GO:0010310), salicylic acid mediated signaling pathway (GO:0009862), jasmonic acid mediated signaling pathway (GO:0009867)
	TraesCS3A02G038900	1,754	transporting ATP synthase activity, rotational mechanism(GO:0043531), D-xylulose reductase activity(GO:0055114)	ATP synthesis coupled proton transport(GO:0043531), - oxidation-reduction process (GO:0055114)

	TraesCS3A02G039100	2,379	potassium ion leak channel activity (GO:0016021), abscisic acid binding -signaling receptor activity(GO:0007165) , ATP binding-protein serine/threonine kinase activity(GO:0004674)	potassium ion transmembrane transport-stabilization of membrane potential (GO:0016021), abscisic acid-regulation of protein serine/threonine phosphatase activity (GO:0007165) , intracellular signal transduction-regulation of gene expression(GO:0004674)
	TraesCS3A02G039200	2,695	abscisic acid binding -signaling receptor activity(GO:0007165), potassium ion leak channel activity (GO:0016021)	abscisic acid-regulation of protein serine/threonine phosphatase activity-signal transduction (GO:0007165), potassium ion transmembrane transport-stabilization of membrane potential (GO:0016021)
	TraesCS3A02G039300	2,685	potassium ion leak channel activity (GO:0016021),protein serine/threonine kinase activity (GO:0004674)	potassium ion transmembrane transport-stabilization of membrane potential (GO:0016021), intracellular signal transduction-regulation of gene expression (GO:0004674)
	TraesCS3A02G039400	3,624	potassium ion leak channel activity (GO:0016021),protein serine/threonine kinase activity (GO:0004674)	potassium ion transmembrane transport-stabilization of membrane potential(GO:0016021), intracellular signal transduction-regulation of gene expression (GO:0004674)
	TraesCS3A02G039500	2,781	potassium ion leak channel activity (GO:0016021),protein serine/threonine kinase activity (GO:0004674)	potassium ion transmembrane transport-stabilization of membrane potential (GO:0016021), intracellular signal transduction (GO:0004674)
	TraesCS3A02G039600	1,885	potassium ion leak channel activity (GO:0016021),	potassium ion transmembrane transport-stabilization of membrane potential (GO:0016021), oxidation-reduction process (GO:0055114)
	TraesCS3A02G039700	6,584	abscisic acid binding-protein phosphatase inhibitor activity-signaling receptor activity	abscisic acid-activated signaling pathway-regulation of protein serine/threonine phosphatase activity-signal transduction (GO:0007165)
4B (Block2)	TraesCS4B02G259500	5,196	ATP binding-magnesium ion binding-ribose phosphate diphosphokinase activity(GO:0005524)	nucleoside metabolic process-nucleotide biosynthetic process-purine nucleotide biosynthetic process(GO:0005524)
	TraesCS4B02G259700	5,543	transferase activity, transferring alkyl or aryl (other than methyl) groups(GO:0005737)	isoprenoid biosynthetic process(GO:0005737), carbonate dehydratase activity-zinc ion binding(GO:0006730)
	TraesCS4B02G259800	3,000	potassium ion leak channel activity-biological regulation (GO:0065007), abscisic acid binding -signaling receptor activity- (GO:0051716), transmembrane transporter (GO:0015931)	potassium ion transmembrane transport-stabilization of membrane potential (GO:0065007), abscisic acid -regulation of protein serine/threonine phosphatase activity- cellular response to stimulus (GO:0051716)
	TraesCS4B02G259900	2,400	potassium ion leak channel activity(GO:0065007)	potassium ion transmembrane transport-stabilization of membrane potential(GO:0065007)

	TraesCS4B02G260000	2,545	serine-type peptidase activity(GO:0006626), abscisic acid binding -signaling receptor activity(GO:0023052)	protein targeting to mitochondrion (GO:0006626), abscisic acid-regulation of protein serine/threonine phosphatase activity(GO:0023052)
	TraesCS4B02G260100	3,877	hydrolase activity, hydrolyzing O-glycosyl compounds (GO:0005886)	carbohydrate metabolic process (GO:0005886)
	TraesCS4B02G260300	4,482	hydrolase activit,(GO:0009691), ATP binding-protein kinase activity(GO:0009506) ,potassium ion leak channel activity (GO:0005774)	cytokinin biosynthetic process (GO:0009691), plasmodesma (GO:0009506) , intracellular protein transport (GO:0005794),stabilization of membrane potential (GO:0005774)
	TraesCS4B02G260600	2,393	hydrolase activityGO:0005886), abscisic acid binding-signaling receptor activity(GO:0050789)	abscisic acid-activated signaling pathway-regulation of protein serine/threonine phosphatase activity-regulation of biological process (GO:0050789)
	TraesCS4B02G260400	6,220	potassium ion leak channel activity(GO:0034220)	potassium ion transmembrane transport-stabilization of membrane potential-ion transmembrane transport (GO:0034220)
	TraesCS4B02G260500	5,957	hydrolase activity(GO:0005886), abscisic acid binding -signaling receptor activity (GO:0044267)	carbohydrate metabolic process(GO:0005886), abscisic acid-activated signaling pathway-regulation of protein serine/threonine phosphatase activity(GO:0044267)
	TraesCS4B02G260700	825	abscisic acid binding-protein phosphatase inhibitor activity-signaling receptor activity(GO:0007165)	abscisic acid-activated signaling pathway-regulation of protein serine/threonine phosphatase activity,signal transduction (GO:0007165)
	TraesCS4B02G260800	6,172	protein self-association-unfolded protein binding(GO:0044085), RNA polymerase II regulatory region sequence-specific DNA binding(GO:0009888)	response to heat-response to hydrogen peroxide-response to reactive oxygen species-response to salt stress(GO:0044085), cell fate specification-negative and positive regulation of transcription by RNA polymerase II- tissue development (GO:0009888)
	TraesCS4B02G260900	1,736	DNA helicase activity-single-stranded DNA binding (GO:0016043), abscisic acid binding-protein phosphatase inhibitor activity-signaling receptor activity(GO:0050794)	abscisic acid-activated signaling pathway-regulation of protein serine/threonine phosphatase activity-regulation of cellular process (GO:0050794)
	TraesCS4B02G261000	1,479	potassium ion leak channel activity(GO:0016021), abscisic acid binding-protein phosphatase inhibitor activity-signaling receptor activity(GO:0009725)	potassium ion transmembrane transport-stabilization of membrane potential (GO:0016021), abscisic acid-activated signaling pathway-regulation of protein serine/threonine phosphatase activity-response to hormone (GO:0009725)
5A (Block1)	TraesCS5A02G551300	2,788	DNA helicase activity-single-stranded DNA binding(GO:0003824)	catalytic activity (GO:0003824)

		TraesCS5A02G551400	3,269	potassium ion leak channel activity(GO:0016021), abscisic acid binding -signaling receptor activity(GO:0007165)	potassium ion transmembrane transport-stabilization of membrane potential (GO:0016021), abscisic acid-regulation of protein serine/threonine phosphatase activity-signal transduction (GO:0007165)
		TraesCS5A02G551500	3,246	DNA-binding transcription activator activity, RNA polymerase II-specific(GO:0032502), abscisic acid binding-signaling receptor activity(GO:0007165)-potassium ion leak channel activity(GO:0016021),	cell fate specification-negative and positive regulation of transcription by RNA polymerase II-developmental process (GO:0032502), abscisic acid-regulation of protein serine/threonine phosphatase activity-signal transduction (GO:0007165)- potassium ion transmembrane transport-stabilization of membrane potential (GO:0016021),hydrolase activity (GO:0016787)
		TraesCS5A02G551600	4,721	abscisic acid binding- signaling receptor activity(GO:0007165), potassium ion leak channel activity(GO:0006810)	abscisic acid-activated signaling pathway-regulation of protein serine/threonine phosphatase activity-signal transduction (GO:0007165), potassium ion transmembrane transport-stabilization of membrane potential(GO:0006810)
		TraesCS5A02G551800	1,881	potassium ion leak channel activity(GO:0016021), abscisic acid binding- signaling receptor activity(GO:0050789)	potassium ion transmembrane transport-stabilization of membrane potential (GO:0016021), abscisic acid-activated signaling pathway-regulation of protein serine/threonine phosphatase activity-regulation of biological process (GO:0050789)
		TraesCS5A02G551900		growth factor activity(GO:0008284), protein self-association-unfolded protein binding(GO:0006950)	regulation of root meristem growth- positive regulation of cell population proliferation (GO:0008284), response to heat-response to hydrogen peroxide-response to reactive oxygen species-response to salt stress-response to stress (GO:0006950)
		TraesCS5A02G552500	708	potassium ion leak channel activity(GO:0016021)	potassium ion transmembrane transport-stabilization of membrane potential- (GO:0016021), regulation of cell communication (GO:0010646)
		TraesCS5A02G552600	4,373	potassium ion leak channel activity(GO:0016021), abscisic acid binding- signaling receptor activity(GO:0048519)	potassium ion transmembrane transport-stabilization of membrane potential (GO:0016021), abscisic acid-activated signaling pathway-regulation of protein serine/threonine phosphatase activity (GO:0048519)
		TraesCS5A02G552700	8,033	potassium ion leak channel activity(GO:0016021),	potassium ion transmembrane transport-stabilization of membrane potential (GO:0016021),
RV	3B (Block1)	TraesCS3B02G453100	6,031	potassium ion leak channel activity(GO:0016021	potassium ion transmembrane transport-stabilization of membrane potential (GO:0016021),

TraesCS3B02G453300	1,314	abscisic acid binding- signaling receptor activity(GO:0009737) ,protein self-association-unfolded protein binding (GO:0009651)	,cell differentiation (GO:0030154), abscisic acid-activated signaling pathway-regulation of protein serine/threonine phosphatase activity (GO:0009737), response to hormone (auxin, gibberellin)(GO:0009723), response to heat- response to reactive oxygen species (GO:0009651)
TraesCS3B02G453400	1,550	abscisic acid binding-protein phosphatase inhibitor activity-signaling receptor activity(GO:0070887)	abscisic acid-activated signaling pathway-regulation of protein serine/threonine phosphatase activity(GO:0070887)
TraesCS3B02G453700	3,957	5'-flap endonuclease activity-crossover junction endodeoxyribonuclease activity(GO:0090305)	double-strand break repair via homologous recombinationnucleic acid phosphodiester bond hydrolysis (GO:0090305)
TraesCS3B02G453200	1,840	hydrolase activity(GO:0016020), abscisic acid binding-protein phosphatase inhibitor activity-signaling receptor activity(GO:0050896)	carbohydrate metabolic process(GO:0016020), abscisic acid-activated signaling pathway-regulation of protein serine/threonine phosphatase activity-response to stimulus (GO:0050896)
TraesCS3B02G453500	3,245	peroxidase activity-thioredoxin peroxidase activity(GO:0045454), potassium ion leak channel activity(GO:0016021)	anatomical structure development (GO:0048856), cell redox homeostasis (GO:0045454), potassium ion transmembrane transport-stabilization of membrane potential (GO:0016021)
TraesCS3B02G453600	1,248	peroxidase activity-thioredoxin peroxidase activity(GO:0045454)	response to light intensity (GO:0009642),cell redox homeostasis (GO:0045454)
TraesCS3B02G453800	1,074	DNA-binding transcription activator activity, RNA polymerase II-specific(GO:0009888), potassium ion leak channel activity(GO:0016021)	cell fate specification-tissue development (GO:0009888),cell population proliferation (GO:0008283), stabilization of membrane potential (GO:0016021)
TraesCS3B02G454000	9,123	potassium ion leak channel activity(GO:0034220), hydrolase activity(GO:0005886)	stabilization of membrane potential (GO:0034220), transmembrane transport(GO:0006857), carbohydrate metabolic process(GO:0005886)
TraesCS3B02G454100	4,234	potassium ion leak channel activity(GO:0034220), potassium ion leak channel activity(GO:0016021)	stabilization of membrane potential (GO:0034220), transmembrane transport(GO:0006857), potassium ion transmembrane transport-stabilization of membrane potential (GO:0016021)
TraesCS3B02G454190	7,498	abscisic acid binding- signaling receptor activity (GO:0050794), DNA helicase activity-single-stranded DNA binding(GO:0009987), hydrolase activity (GO:0016020)	abscisic acid -regulation of protein serine/threonine phosphatase activity (GO:0050794), anatomical structure development (GO:0048856), developmental process (GO:0032502), carbohydrate metabolic process(GO:0016020)
TraesCS3B02G454200	1,767	5'-flap endonuclease activity-crossover junction endodeoxyribonuclease activity(GO:0004519)	leaf vascular tissue pattern formation (GO:0010305), phloem or xylem histogenesis (GO:0010087) ,cotyledon vascular tissue pattern formation (GO:0010588)

	TraesCS3B02G454300	6,301	protein self-association-unfolded protein binding(GO:0009651), DNA helicase activity-single-stranded DNA binding(GO:0016887)	response to heat-response to hydrogen peroxide-response to reactive oxygen species-response to salt stress-response to salt stress (GO:0009651), ATPase activity (GO:0016887)
	TraesCS3B02G454400	6,396	protein self-association-unfolded protein binding(GO:0009651)	response to heat-response to hydrogen peroxide-response to reactive oxygen species-response to salt stress(GO:0009651)
3B (Block3)	TraesCS3B02G588200	8,397	abscisic acid binding-protein phosphatase inhibitor activity-signaling receptor activity(GO:0007165)	abscisic acid-activated signaling pathway-regulation of protein serine/threonine phosphatase activity-signal transduction (GO:0007165)
	TraesCS3B02G588300	2,559	potassium ion leak channel activity(GO:0016021) , G protein-coupled photoreceptor activity (GO:0009581)	potassium ion transmembrane transport-stabilization of membrane potential (GO:0016021),plant-type hypersensitive response (GO:0009626), cellular response to light stimulus (GO:0009581)
	TraesCS3B02G588400	3,869	potassium ion leak channel activity(GO:0016021)	potassium ion transmembrane transport-stabilization of membrane potential (GO:0016021)
	TraesCS3B02G588600	885	potassium ion leak channel activity(GO:0016021)	potassium ion transmembrane transport-stabilization of membrane potential (GO:0016021)
	TraesCS3B02G588500	8,438	potassium ion leak channel activity(GO:0016021)	potassium ion transmembrane transport-stabilization of membrane potential (GO:0016021)
	TraesCS3B02G588700	9,254	potassium ion leak channel activity(GO:0016021)	potassium ion transmembrane transport-stabilization of membrane potential (GO:0016021)
	TraesCS3B02G588800	2,562	potassium ion leak channel activity(GO:0016021)	potassium ion transmembrane transport-stabilization of membrane potential (GO:0016021)
	TraesCS3B02G588900	9,313	DNA helicase activity- (GO:0016787),, potassium ion leak channel activity(GO:0016021),	hydrolase activity (GO:0016787), potassium ion transmembrane transport-stabilization of membrane potential (GO:0016021)
	TraesCS3B02G589000	7,383	potassium ion leak channel activity(GO:0016021)	potassium ion transmembrane transport-stabilization of membrane potential (GO:0016021)
	TraesCS3B02G589400	1,143	potassium ion leak channel activity(GO:0016021)	potassium ion transmembrane transport-stabilization of membrane potential (GO:0016021)
	TraesCS3B02G589500	10,658	potassium ion leak channel activity(GO:0016021)	potassium ion transmembrane transport-stabilization of membrane potential (GO:0016021)
	TraesCS3B02G589600	5,350	potassium ion leak channel activity(GO:0016021)	potassium ion transmembrane transport-stabilization of membrane potential (GO:0016021)
	TraesCS3B02G589700	11,881	potassium ion leak channel activity(GO:0016021)	potassium ion transmembrane transport-stabilization of membrane potential (GO:0016021)

TraesCS3B02G589900	2,884	potassium ion leak channel activity(GO:0016021)	potassium ion transmembrane transport-stabilization of membrane potential (GO:0016021)
TraesCS3B02G590100	1,326	potassium ion leak channel activity(GO:0016021)	potassium ion transmembrane transport-stabilization of membrane potential (GO:0016021)
TraesCS3B02G590400	10,142	hydrolase activity,(GO:0016020)	carbohydrate metabolic process(GO:0016020)
TraesCS3B02G590600	16,150	potassium ion leak channel activity(GO:0016021)	potassium ion transmembrane transport-stabilization of membrane potential (GO:0016021)
TraesCS3B02G590500	3,455	potassium ion leak channel activity(GO:0016021)	potassium ion transmembrane transport-stabilization of membrane potential (GO:0016021)

Candidate genes are located in linkage disequilibrium (LD) block embedded the significant single nucleotide polymorphism (SNP) markers. The significant SNPs which does not belong to an LD block, a 1Mbp window on either side of significant SNP was considered to search putative candidate genes. The available gene annotation and gene ontology(GO) was obtained from the wheat @URGI database(Alaux *et al*., 2018b). Abbreviation: **Car**, chromosome; TRL, total root length; RSA, root surface area; RAD, root average diameter; RV, root volume; NRT, number of root tips; NRF, number of root forks; and NA, not available.

Supplementary Table S2: Expression data of selected candidate genes in wheat within different tissues and development stages.

Genes	flag_leaf_1	flag_leaf_8	grain_10	leaf_105	root_apical_meristem_5	roots_10	roots_15	roots_20	roots_25	roots_35	roots_40	second_leaf_15	shoot_apical_meristem_5	shoots_25	spike_20
TraesCS1A02G295000	0.000	0.000	0.000	0.000	0.000	0.000	0.000	0.000	0.000	0.000	0.000	0.000	0.000	0.000	0.000
TraesCS1A02G295400	0.000	1.743	0.000	1.281	6.355	5.246	5.502	5.226	5.260	5.721	6.004	0.652	5.634	6.213	7.491
TraesCS1A02G296200	0.186	1.638	3.630	2.580	3.895	2.715	2.992	3.523	3.508	3.116	2.972	1.760	3.253	2.448	2.075
TraesCS1A02G296300	5.109	1.510	1.492	1.895	1.604	2.733	2.705	2.532	2.623	1.741	3.218	0.981	2.363	1.722	0.694
TraesCS1B02G269100	0.000	0.060	0.228	0.172	1.384	0.955	0.873	2.056	2.682	3.263	0.000	0.000	1.210	2.055	3.612
TraesCS1B02G272100	0.000	0.887	0.306	0.463	0.306	0.544	0.986	0.453	0.447	0.343	0.000	0.993	0.699	0.199	1.555
TraesCS1B02G272900	0.549	5.292	0.000	0.204	0.115	0.117	0.000	5.307	5.379	4.681	0.248	5.825	0.000	5.432	0.000
TraesCS1B02G269400	0.000	0.840	2.418	2.731	7.133	6.878	5.239	7.025	6.340	6.886	1.624	3.580	6.492	6.619	5.519
TraesCS1B02G272000	0.000	0.319	0.000	0.056	0.631	1.875	2.299	0.695	0.444	0.098	0.166	0.491	0.252	0.000	0.765
TraesCS2A02G144900	0.000	0.000	0.000	0.000	5.906	1.891	3.393	0.311	1.788	1.596	3.794	0.000	0.489	0.000	0.000

TraesCS2A02G145000	0.000	0.000	0.000	0.000	0.055	0.114	0.000	0.138	0.034	0.117	0.000	0.000	0.000	0.000	0.000
TraesCS2B02G409800	0.000	0.310	0.000	0.000	0.088	0.221	0.693	0.113	0.314	0.315	0.396	0.354	0.000	0.104	0.000
TraesCS2B02G410400	0.000	0.200	0.000	0.000	0.000	0.113	0.000	0.070	0.017	0.000	0.000	0.036	3.746	0.243	1.564
TraesCS4B02G259600	1.559	3.835	2.881	4.216	7.170	5.465	5.165	5.517	5.754	5.342	5.196	3.642	6.048	5.078	4.119
TraesCS5A02G551700	0.000	0.000	0.745	0.000	0.000	0.000	0.000	0.000	0.000	0.000	0.000	0.000	0.000	0.000	0.000
TraesCS7A02G064700	0.000	0.867	1.441	3.408	3.129	5.682	6.302	3.330	2.457	3.360	3.556	1.011	3.245	3.118	0.000
TraesCS7B02G432200	1.245	0.000	0.000	0.172	1.077	0.503	0.414	1.178	0.544	0.697	0.838	0.021	0.536	0.828	0.222
TraesCS1A02G295400	0.000	1.743	0.000	1.281	6.355	5.246	5.502	5.226	5.260	5.721	6.004	0.652	5.634	6.213	7.491
TraesCS1A02G295500	0.000	0.000	0.000	0.000	0.000	0.000	0.000	0.000	0.000	0.000	0.119	0.262	0.141	0.000	0.000
TraesCS1A02G295700	0.000	2.123	0.962	0.312	6.588	5.514	5.697	5.554	5.728	6.057	6.114	1.042	5.807	0.775	8.129
TraesCS1A02G296300	5.109	1.510	1.492	1.895	1.604	2.733	2.705	2.532	2.623	1.741	3.218	0.981	2.363	1.722	0.694

TraesCS3A02G039000	0.000	0.000	0.000	0.000	0.000	0.000	0.000	0.000	0.000	0.000	0.000	0.000	0.000	0.000	0.000
TraesCS4B02G259600	1.559	3.835	2.881	4.216	7.170	5.465	5.165	5.517	5.754	5.342	5.196	3.642	6.048	5.078	4.119
TraesCS4B02G260200	0.547	1.716	3.843	2.669	1.547	2.922	3.547	2.680	2.583	2.277	2.526	1.605	0.853	1.334	0.996
TraesCS5A02G551700	0.000	0.000	0.745	0.000	0.000	0.000	0.000	0.000	0.000	0.000	0.000	0.000	0.000	0.000	0.000

Supplementary Table S3: Expression data of selected candidate genes under 1 and 6 h (hours) of drought stress.

Genes	1 h of drought	6 h of drought
TraesCS1A02G295000	0.000	0.000
TraesCS1A02G295400	1.774	1.230
TraesCS1A02G296200	1.231	1.653
TraesCS1A02G296300	2.449	0.794
TraesCS1B02G269100	0.025	0.053
TraesCS1B02G272100	1.017	0.536
TraesCS1B02G272900	5.393	3.864
TraesCS1B02G269400	3.559	2.205
TraesCS1B02G272000	0.081	0.092
TraesCS2A02G144900	0.000	0.000
TraesCS2A02G145000	0.000	0.000
TraesCS2B02G409800	0.221	0.000
TraesCS2B02G410400	0.030	0.032
TraesCS4B02G259600	3.729	3.640
TraesCS5A02G551700	0.000	0.000
TraesCS7A02G064700	2.020	1.011
TraesCS7B02G432200	0.671	0.352
TraesCS1A02G295400	1.774	1.230
TraesCS1A02G295500	0.000	0.000
TraesCS1A02G295700	2.506	1.045
TraesCS1A02G296300	2.449	0.794
TraesCS3A02G039000	0.000	0.000
TraesCS4B02G259600	3.729	3.640
TraesCS4B02G260200	1.505	1.604

Supplementary for Chapter 4

Title: *NPF2.12*, a convergently selected nitrate transporter that coordinates root growth and nitrate-use efficiency in wheat and barley

Md. Nurealam Siddiqui, Kailash Pandey, Suzan Kumer Bhadhury, Bahman Sadeqi, Michael Schneider, Miguel Sanchez-Garcia, Benjamin Stich, Jens Léon, and Agim Ballvora

The following supporting data is available for Chapter 4:

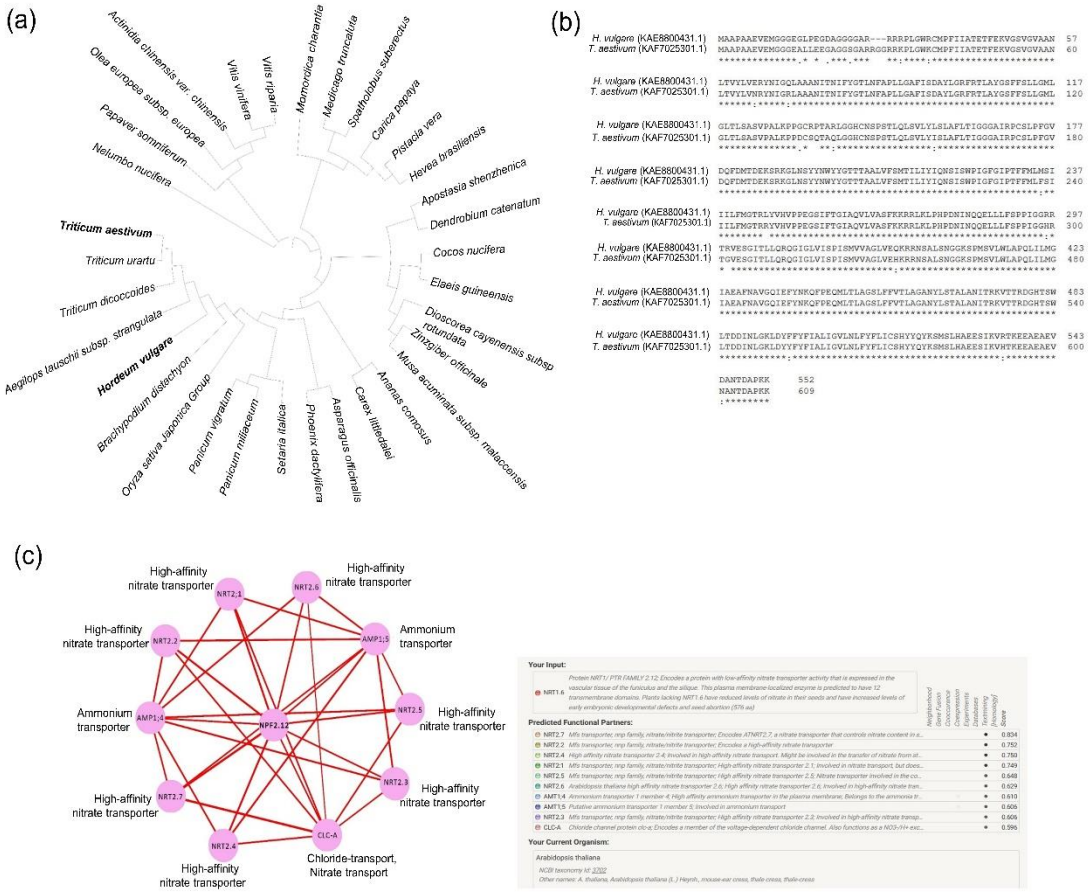

Supplementary Figure 1: Phylogenetic, sequence alignment and predicted protein-protein interaction analysis of the NPF2.12 proteins**.** a) Phylogenetic tree of NPF2.12 proteins. The 1000 bootstrap values are shown on the branches. (b) Sequence alignment of TaNPF2.12 (KAF7025301.1) and HvNPF2.12 (KAE8800431.1) proteins. (c) The predicted protein–protein interaction network of NPF2.12 using STRING database and Cytoscape software. Nodes represent proteins and edges represent interactions.

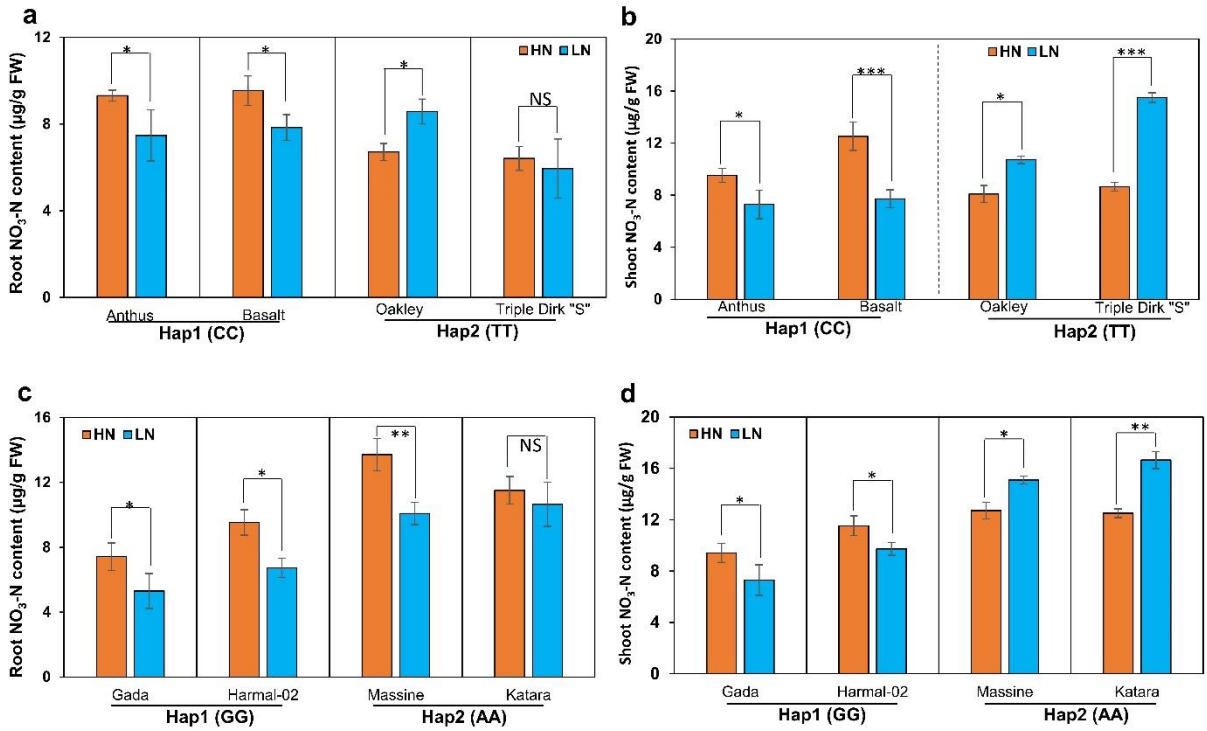

Supplementary Figure 2: NO_3^--N determination in root and shoot in wheat and barley haplotype (Hap) groups. **a.** NO_3^--N content in wheat root, **b.** NO_3^--N content in wheat shoot, **c.** NO_3^--N content in barley root, and **d.** NO_3^--N content in barley shoot at high and low NO_3^- availability. Bars represent means ± standard error (n = 03 independent biological replicates). Student's t test; **P* < 0.05, ***P* < 0.01 and ****P* < 0.001, respectively based on one-way ANOVA. Scale bars, 1 cm. HN, high NO_3^- (10 mM) and LN, low NO_3^- (0.5 mM).

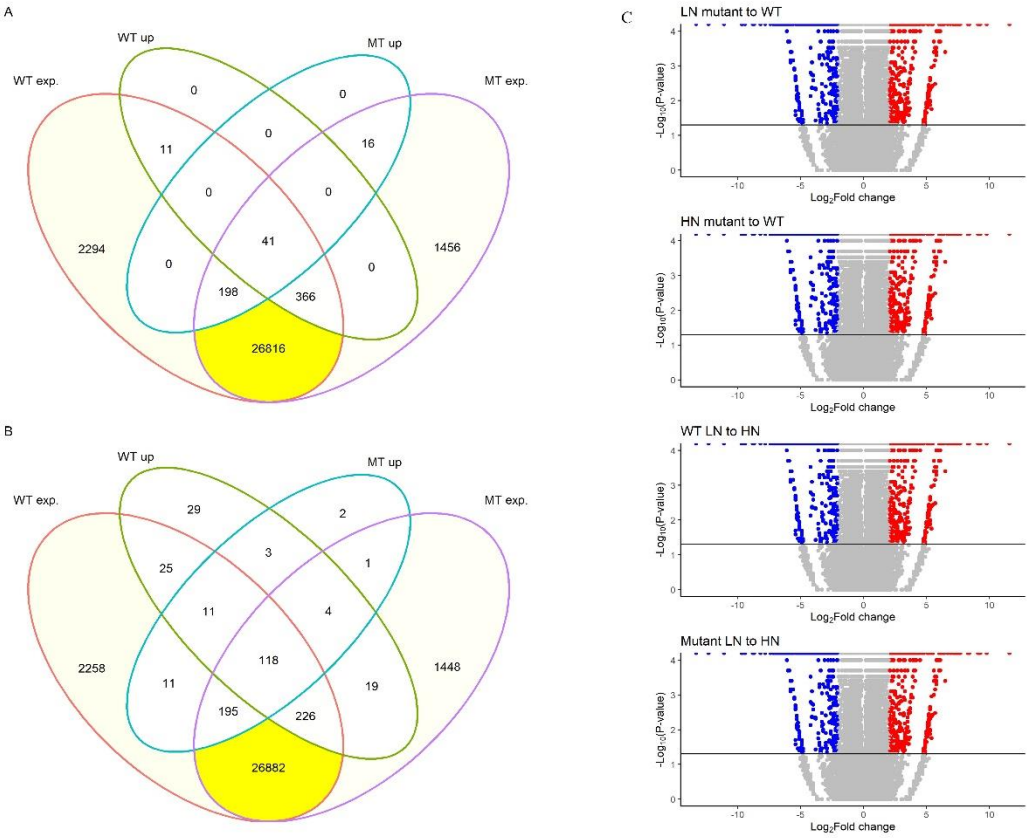

Supplementary Figure 3: Expression and overexpression observed in the sample comparison. **A** count of genes expressed and overexpressed in the HN environment. A pairwise comparison was performed genotype-wise (LN to HN) for mutant and wild-type separately. **B** similar to A, but for overexpressed genes in the LN environment. **C** volcano plots of the pairwise comparisons between the samples mentioned in the subfigure title. WT = wild-type; MT = mutant; LN = low nitrogen application; HN = high nitrogen application; up = significantly overexpressed in the environment; exp. = all genes with more than two normalized reads observed.

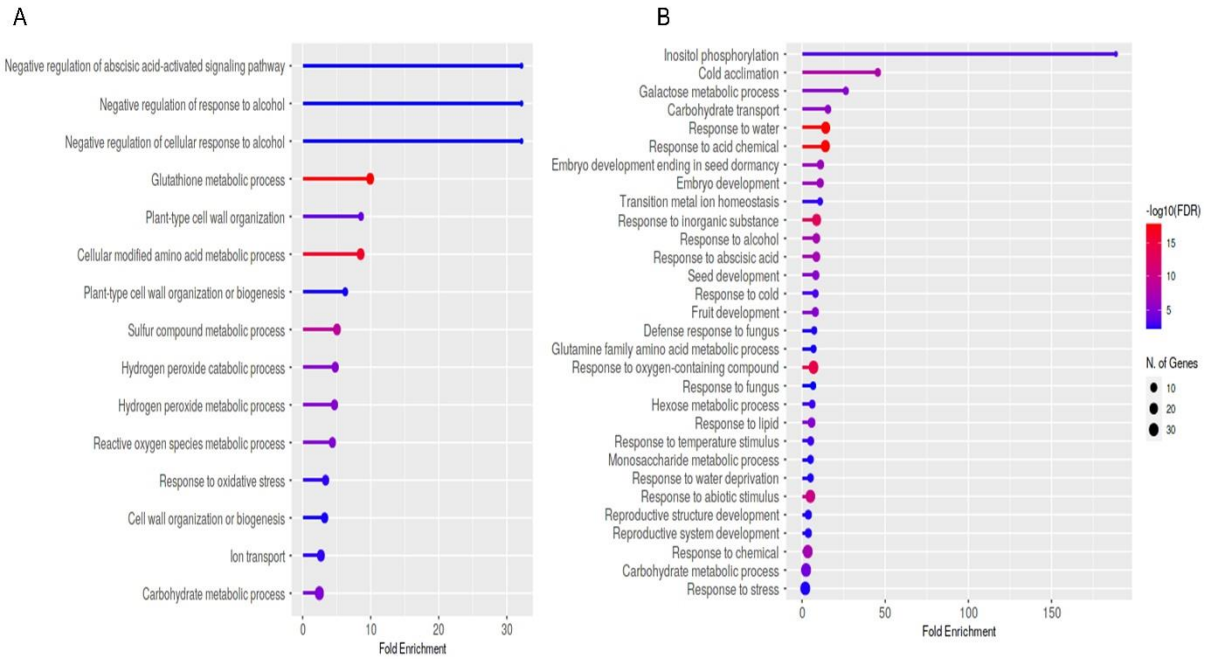

Supplementary Figure 4: RNA sequencing analyses of the *TaNPF2.12* wild-type and mutant allele after 14-days exposed to high and low NO_3^-. A**,** the 15 most significantly enriched pathways in *npf2.12* mutant allele under high NO_3^- treatment. **B,** the 30 most significantly enriched pathways in WT allele under low NO_3^- treatment analysed by ShinyGO enrichment tool.

Supplementary Table 1: Description of root system morphological and anatomical traits with trait acronyms and unit.

SL	Trait description	Trait acronym	Unit
Root morphological traits			
1.	Root to shoot ratio	R:S	ratio
2.	Rooting depth	RD	cm plant^{-1}
3.	Total root length	TRL	cm plant^{-1}
4.	Root surface area	RSA	cm^2 plant^{-1}
5.	Average root diameter	ARD	mm plant^{-1}
6.	Root volume	RV	cm^3 plant^{-1}
7.	Number of root tips	NRT	count
8.	Number of root forks	NRF	count
9.	Number of root crossings	NRC	count
Root anatomical traits			
10.	Main shoot nodal root cross sectional diameter	mRXD	µm
11.	Main shoot nodal root stele diameter	mSXD	µm
12.	Main shoot axis nodal root cortical diameter = mRXD - mSXD	mCXD	µm
13.	Number of main shoot nodal root metaxylem vessels	mMXN	count
14.	Main shoot nodal root metaxylem vessel diameter	mMXD	µm
15.	Percentage of main shoot nodal root stele diameter occupied by metaxylem vessel	mMXDP	%
16.	Percentage of main shoot nodal root cross section occupied by stele	mSDP	%
17.	Main shoot nodal root axial hydraulic conductivity	mAXMc	mg m MPa^{-1}s^{-1}
18.	Tiller nodal root cross sectional diameter	tRXD	µm
19.	Tiller nodal root stele diameter	tSXD	µm
20.	Tiller nodal root cortical diameter = tRXD - tSXD	tCXD	µm
21.	Number of tiller nodal root metaxylem vessels	tMXN	count
22.	Tiller nodal root metaxylem vessel diameter	tMXD	µm
23.	Percentage of tiller nodal root stele occupied by metaxylem vessel	tMXDP	%
24.	Percentage of tiller nodal root cross section occupied by stele	tSDP	%
25.	Tiller nodal root axial hydraulic conductivity	tAXMC	mg m MPa^{-1}s^{-1}

Supplementary Table 2: Descriptive statistics for investigated root morphology and anatomy traits in wheat association panel.

Traits	LN fertilisation				HN fertilisation				% C
	Min	Max	Mean	CoV	Min	Max	Mean	CoV	
Root morphological traits									
TRL	54.08	377.5	163.3	0.33	25.18	295.01	115.29	0.34	+42
RSA	14.94	99.16	44.61	0.32	6.86	83.17	29.60	0.33	+51
ARD	0.42	1.61	0.89	0.20	0.42	1.55	0.84	0.22	+6.0
RV	0.24	3.11	1.07	0.43	0.07	2.39	0.63	0.47	+70
NRT	98	1193	409.7	0.45	50	712	237.3	0.41	+73
Root anatomical traits									
mRXD	385.2	1510.6	983.97	0.24	342.8	1349.8	748.03	0.24	+31
mSXD	161.7	615.5	389.71	0.22	171.2	555.4	322.20	0.21	+21
mMXN	3.0	10.0	6.32	0.23	3.0	9.0	5.49	0.25	+15
mMXD	16.66	61.77	36.81	0.24	12.89	57.78	31.05	0.26	+18
mAXMC	0.002	0.31	0.062	0.32	0.001	0.27	0.033	0.27	+17
mCXD	183.2	1014.3	594.26	0.27	151.9	845.5	426.00	0.28	+39
mMXDP	4.48	15.68	9.58	0.19	4.13	16.73	9.74	0.22	-2
mSDP	29.11	52.87	40.01	0.10	29.48	59.06	43.52	0.11	-8
tRXD	410.4	1531.3	927.72	0.25	326.4	1289.7	699.04	0.25	+32
tSXD	154.0	601.6	371.22	0.23	159.8	548.3	304.71	0.23	+21
tMXN	3.0	10.0	6.00	0.23	3.0	9.0	5.17	0.27	+16
tMXD	16.25	61.44	35.16	0.25	12.00	55.78	29.02	0.28	+21
tAXMC	0.002	0.30	0.053	0.30	0.001	0.21	0.026	0.28	+19
tCXD	222.1	995.2	556.51	0.23	142.3	794.0	394.33	0.30	+41
tMXDP	5.00	16.83	9.59	0.19	3.66	17.01	9.63	0.23	-0.5
tSDP	29.61	54.18	40.47	0.10	29.52	61.87	44.13	0.12	-8

Supplementary Table 3: Analysis of variance (ANOVA) and broad-sense heritability (H^2) for investigated traits in wheat association panel.

Trait	Nitrogen (N)	Genotype (G)	G*T	Heritability (H^2)	
				LN	HN
Root morphological traits					
TRL	324.13***	7.09**	0.13^{ns}	0.68	0.67
RSA	463.57***	15.65***	0.65^{ns}	0.85	0.79
ARD	23.6***	4.53*	0.001^{ns}	0.71	0.81
RV	319.33***	15.72***	1.05^{ns}	0.80	0.79
NRT	417.69***	5.95*	0.07^{ns}	0.87	0.78
Root anatomical traits					
mRXD	3493.72***	22.91***	17.44***	0.95	0.71
mSXD	1877.20***	20.07***	16.10***	0.94	0.73
mMXN	417.46***	6.02***	6.04***	0.88	0.57
mMXD	636.68***	8.54***	8.06***	0.89	0.64
mAXMC	618.19***	8.88***	8.01***	0.83	0.57
mCXD	3171.60***	18.02***	13.43***	0.94	0.69
mMXDP	6.49*	4.82***	3.51***	0.73	0.59
mSDP	687.01***	5.61***	4.19***	0.79	0.57
tRXD	2898.87***	19.15***	14.05***	0.93	0.71
tSXD	1683.57***	18.18***	13.73***	0.92	0.73
tMXN	406.51***	6.05***	4.70***	0.86	0.61
tMXD	690.59***	9.14***	6.58***	0.87	0.68
tAXMC	710.37***	9.53***	6.47***	0.80	0.60
tCXD	2665.69***	15.13***	10.95***	0.91	0.68
tMXDP	0.20^{ns}	5.55***	3.28***	0.73	0.66
tSDP	584.55***	4.83***	3.10***	0.78	0.56

Supplementary Table 4: Descriptive statistics, ANOVA and broad-sense heritability (H^2) for investigated traits in barley association panel.

Trait	Low NO_3^- (0.5 mM)				High NO_3^- (10 mM)				ANOVA		
	Range	Mean	CoV	H^2	Range	Mean	CoV	h^2	G	T	G*T
R:S	0.43-2.08	1.09	0.28	28.60	0.47-2.09	1.00	0.27	43.89	***	***	***
RD	4.0 to 36.0	18.57	0.30	44.58	3.5-30.5	17.43	0.29	39.19	***	***	***
TRL	10.75-209.1	82.12	0.37	23.24	6.81-158.9	79.97	0.34	17.09	***	**	***
RSA	2.16-26.49	12.03	0.33	41.47	1.59-23.02	12.12	0.31	37.21	***	NS	***
ARD	0.34-0.79	0.48	0.15	39.66	0.32-1.18	0.50	0.16	21.90	***	***	***
RV	0.03-0.40	0.14	0.34	45.07	0.02-0.30	0.15	0.32	41.88	***	NS	***
NRT	27-845	248.61	0.57	67.50	13-828	209.53	0.56	30.21	***	***	***
NRF	23-688	218.10	0.47	30.31	14-544	203.11	0.49	26.29	***	***	***
NRC	0-97	17.68	0.64	24.55	0-67	16.34	0.66	15.14	***	*	***

Supplementary Table 5: List of identified significant marker-traits associations in wheat genome under different N input levels in wheat panel.

Trait	Treatment	Year	Chr.	Marker (SNP site)	Local LD Block	-log10(*P*)	Allele	MAF
RV	LN/HN	2020	3B	AX-695508890	692122909 -698423254	4.48	C:T	0.24
			3B	AX-691454854	689687872-691459943	4.28	G:A	0.231
			3B	AX-689685122	688385213-689686678	4.26	T:C	0.31
			3B	AX-685497264	685076934-685497299	4.24	A:G	0.237
			3B	AX-685220382	685076934-685497299	4.21	C:T	0.234
			3B	AX-689516169	686376435-689689324	4.21	T:C	0.234
			3B	AX-685473628	685076934-685497299	4.12	T:C	0.231
			3B	AX-691709229	691709194-691713932	4.11	T:C	0.244
mAXMC	LN/HN	2019	5B	AX-550338444	550151669-550749029	6.1	C:A	0.078
			5B	AX-550210239	550151669-550749029	6.02	A:C	0.082
			5A	AX-377327509	375375809-382326479	4.46	T:C	0.11
			5A	AX-359737052	347010867-370239164	4.42	C:A	0.114
			5A	AX-367602432	347010867-370239164	4.28	G:A	0.115
			5A	AX-358484677	347010867-370239164	4.24	T:C	0.119
			5A	AX-350541125	347010867-370239164	4.21	G:A	0.12
			6A	AX-600395131	600395166-600396587	4.68	G:A	0.081
			6A	AX-600396622	600395166-600396587	4.02	C:T	0.12
tAXMC	LN/HN	2019	7B	AX-630662592	629020321-632657336	6.95	C:T	0.056
			7B	AX-634141984	633246653-634834856	5.63	A:G	0.057
			7B	AX-633246653	633246653-634834856	5.32	A:G	0.072
			7B	AX-633922578	633246653-634834856	5.31	C:T	0.066
			7B	AX-634387709	633246653-634834856	5.31	C:T	0.066
			7B	AX-634553619	633246653-634834856	5.31	G:A	0.063
			7B	AX-633926462	633246653-634834856	5.27	A:G	0.064
			7B	AX-634465128	633246653-634834856	4.83	A:G	0.081
			7B	AX-634834856	633246653-634834856	4.83	C:T	0.08
			7B	AX-633927045	633246653-634834856	4.75	G:A	0.079
			2A	AX-410872829	383598264-438726330	5.03	G:A	0.07
			2A	AX-411124828	383598264-438726330	5.02	C:T	0.07
			2A	AX-448151721	448151721-469792854	4.84	G:A	0.07
			2A	AX-469792854	448151721-469792854	4.65	G:A	0.07
			2A	AX-501571322	498043625-502328982	4.5	G:A	0.109
			2A	AX-413487809	383598264-438726330	4.48	G:A	0.059
			2A	AX-500535694	498043625-502328982	4.34	G:T	0.107
			2A	AX-498044074	498043625-502328982	4.21	A:G	0.108
			2A	AX-498105776	498043625-502328982	4.17	A:G	0.111
			2A	AX-501850135	498043625-502328982	4.16	T:C	0.113
			1B	AX-627946404	627098767-628030486	4.21	C:T	0.061
			1B	AX-627946415	627098767-628030486	4.21	T:C	0.061
			1B	AX-628006420	627098767-628030486	4.21	C:T	0.061
NRT	HN	2020	7B	AX-17647040	17647040-17647040	4.58	G:A	0.151
			3B	AX-757883601	757872334-758877964	4.51	G:A	0.131
tAXMC	HN	2019	3B	AX-294401858	294401858-294401858	4.52	G:A	0.121
			3B	AX-803891765	803891730-804359562	4.43	C:A	0.119
			3B	AX-798462589	798462554-799207121	4.4	A:C	0.114

			3B	AX-806115107	806081287-807312155	4.34	T:C	0.12
			3B	AX-807341661	807341626-807341626	4.27	G:A	0.135
			3B	AX-804223163	803891730-804359562	4.16	T:C	0.127
			3B	AX-17988572	17862711-18025580	4.1	T:C	0.106
			3B	AX-807312120	806081287-807312155	4.08	T:C	0.145
mSXD	LN	2019	1A	AX-544139313	544055675-544170243	5.44	T:G	0.132
			1A	AX-544147405	544055675-544170243	5.02	A:G	0.134
			1A	AX-544139713	544055675-544170243	4.92	T:C	0.136
			1A	AX-544148374	544055675-544170243	4.8	C:T	0.138
mSDP	LN	2019	5A	AX-663765182	663724841-663947727	5.9	C:A	0.17
			5A	AX-663914530	663724841-663947727	5.73	G:A	0.165
			5A	AX-663948338	663948303-664550227	5.69	C:T	0.164
tMXDP	LN	2019	3A	AX-432857254	430524692-434820002	5.36	G:C	0.49
			3A	AX-141043562	141043597-144166270	5.22	A:C	0.495
			3A	AX-127368585	127368620-127368620	5.13	G:A	0.268
			3A	AX-124187670	124187705-124187705	4.83	A:C	0.454
			3A	AX-382355618	345371403-429545216	4.62	T:G	0.485
			3A	AX-144166305	141043597-144166270	4.59	G:A	0.466
			3A	AX-371612539	345371403-429545216	4.48	T:C	0.486
			3A	AX-384744757	345371403-429545216	4.34	A:G	0.483
			3A	AX-497710494	487458205-503027279	4.22	A:G	0.175
			3A	AX-480147334	479132629-480147334	4.12	T:C	0.176
			2B	AX-210259511	206117351-210259672	4.08	G:A	0.269
			3A	AX-490340674	487458205-503027279	4.07	T:C	0.202
			2B	AX-210259672	206117351-210259672	4.01	G:A	0.267

The trait description is provided in Table S1. Chr, chromosome; MAF, minor allele frequency

Supplementary Table 6: List of nitrogen associated genes in wheat and barley obtained by comparative GWAS.

Crop	Traits	LD Block (Position)	Chr	Gene ID	Gene annotation
Barley	TRL	640431682	3H	HORVU3Hr1G092870	Protein NRT1/ PTR FAMILY 2.13
Wheat	RV	692122909 - 698423254	3B	TraesCS3B02G454000	low-affinity nitrate transmembrane transporter activity (GO:0080054), nitrate assimilation (GO:0042128), cellular response to nitrogen levels (GO:0043562), nitrate transport (GO:0015706), integral component of membrane (GO:0016021), oligopeptide transport (GO:0006857), ion transmembrane transport (GO:0034220)
			3B	TraesCS3B02G454100	low-affinity nitrate transmembrane transporter activity (GO:0080054), nitrate assimilation (GO:0042128), cellular response to nitrogen levels (GO:0043562), nitrate transport (GO:0015706), integral component of membrane (GO:0016021), oligopeptide transport (GO:0006857), ion transmembrane transport (GO:0034220)
		689687872-691459943	3B	TraesCS3B02G450200	response to nitrate (GO:0010167), defense response (GO:0006952), nitrate transport (GO:0015706), integral component of membrane (GO:0016021),
		688385213-689686678	3B	TraesCS3B02G448600	cellular nitrogen compound metabolic process (GO:0034641)
		686376435-689689324	3B	TraesCS3B02G448000	response to nitrate (GO:0010167), auxin-activated signaling pathway (GO:0009734)
		686376435-689689324	3B	TraesCS3B02G448100	response to nitrate (GO:0010167), auxin-activated signaling pathway (GO:0009734)
	mAXMC	375375809-382326479	5A	TraesCS5A02G181800	response to nitrate (GO:0010167), nitrate transport (GO:0015706), cellular response to phosphate starvation (GO:0016036),
			5A	TraesCS5A02G181900	nitrogen compound metabolic process (GO:0006807), intracellular protein transport (GO:0006886), response to stimulus (GO:0050896), integral component of membrane (GO:0016021)
			5A	TraesCS5A02G182000	cellular nitrogen compound metabolic process (GO:0034641), integral component of membrane (GO:0016021)
			5A	TraesCS5A02G182400	cellular nitrogen compound metabolic process (GO:0034641), protein maturation by iron-sulfur cluster transfer (GO:0097428)
		347010867-370239164	5A	TraesCS5A02G163600	transport (GO:0006810), cellular nitrogen compound metabolic process (GO:0034641), cellular macromolecule metabolic process (GO:0044260), integral component of membrane (GO:0016021),

		5A	TraesCS5A02G165000	regulation of nitrogen compound metabolic process (GO:0051171), regulation of macromolecule metabolic process (GO:0060255)
		5A	TraesCS5A02G166600	nitrogen compound metabolic process (GO:0006807), response to oxidative stress (GO:0006979), cellular macromolecule metabolic process (GO:0044260), transaminase activity (GO:0008483), integral component of membrane (GO:0016021)
		5A	TraesCS5A02G168100	response to water (GO:0009415), meristem development (GO:0048507), cellular nitrogen compound metabolic process (GO:0034641), cellular component organization (GO:0016043), integral component of membrane (GO:0016021)
		5A	TraesCS5A02G174800	cellular nitrogen compound metabolic process (GO:0034641), cellular macromolecule metabolic process (GO:0044260)
tAXMC	629020321-632657336	7B	TraesCS7B02G366000	integral component of membrane (GO:0016021), response to stimulus (GO:0050896), nitrogen compound metabolic process (GO:0006807)
	383598264-438726330	2A	TraesCS2A02G262200	integral component of membrane (GO:0016021), intracellular transport (GO:0046907), cellular nitrogen compound metabolic process (GO:0034641)
		2A	TraesCS2A02G263300	transmembrane receptor protein kinase activity (GO:0019199), cellular nitrogen compound metabolic process (GO:0034641), integral component of membrane (GO:0016021)
		2A	TraesCS2A02G263700	cellular nitrogen compound metabolic process (GO:0034641)
		2A	TraesCS2A02G264300	calcium ion transport (GO:0006816), nucleotide transport (GO:0006862)

		2A	TraesCS2A02G264500	transmembrane transporter activity (GO:0022857), integral component of membrane (GO:0016021), oligopeptide transport (GO:0006857), nitrate assimilation (GO:0042128), abscisic acid transport (GO:0080168)
		2A	TraesCS2A02G264800	response to abscisic acid (GO:0009737), response to nitrate (GO:0010167), nitrate transport (GO:0015706), cellular response to endogenous stimulus (GO:0071495)
		2A	TraesCS2A02G266200	oxygen transport (GO:0015671), response to stimulus (GO:0050896), negative regulation of nitrogen compound metabolic process (GO:0051172)
	448151721-469792854	2A	TraesCS2A02G279700	amino acid transmembrane transport (GO:0003333), aromatic amino acid transport (GO:0015801, neutral amino acid transport (GO:0015804), amine transport (GO:0015837), amine transmembrane transporter activity (GO:0005275), aromatic amino acid transmembrane transporter activity (GO:0015173), active transmembrane transporter activity (GO:0022804)
	498043625-502328982	2A	TraesCS2A02G290500	nitrogen compound metabolic process (GO:0006807), abscisic acid signaling pathway (GO:0009738)
	627098767-628030486	1B	TraesCS1B02G396200	response to hypoxia (GO:0001666), amine biosynthetic process (GO:0009309), cellular amine metabolic process (GO:0044106)
NRT	757872334-758877964	3B	TraesCS3B02G516600	nitrogen compound metabolic process (GO:0006807), integral component of membrane (GO:0016021), macromolecule metabolic process (GO:0043170)
tAXMC	807341626-807341626	3B	TraesCS3B02G577400	nitrogen compound metabolic process (GO:0006807), methylglyoxal catabolic process to D-lactate via S-lactoyl-glutathione (GO:0019243)
tMXDP	430524692-434820002	3A	TraesCS3A02G232200	cellular nitrogen compound metabolic process (GO:0034641), cellular macromolecule metabolic process (GO:0044260)

381355212-383355212	3A	TraesCS3A02G212300	nitrate transport (GO:0015706), response to nitrate (GO:0010167), phenylpropanoid biosynthetic process (GO:0009699), systemic acquired resistance (GO:0009627)
141043597-144166270	3A	TraesCS3A02G151400	nitrate transport (GO:0015706), response to nitrate (GO:0010167), anion transmembrane transport (GO:0098656), regulation of anion transmembrane transport (GO:1903959), cellular amino acid biosynthetic process (GO:0008652), cellular ion homeostasis (GO:0006873), polyamine catabolic process (GO:0006598)
	3A	TraesCS3A02G151500	nitrogen compound metabolic process (GO:0006807), ubiquitin-protein transferase activity (GO:0004842), integral component of membrane (GO:0016021)
383744795-385733337	3A	TraesCS3A02G213300	cellular nitrogen compound metabolic process (GO:0034641), cellular macromolecule metabolic process (GO:0044260)
	3A	TraesCS3A02G213500	cellular nitrogen compound metabolic process (GO:0034641, response to chemical (GO:0042221), cellular transition metal ion homeostasis (GO:0046916)
496710680-498699316	3A	TraesCS3A02G270900	cellular nitrogen compound metabolic process (GO:0034641), macromolecule biosynthetic process (GO:0009059), regulation of cellular process (GO:0050794)
206117351-210259672	2B	TraesCS2B02G219000	cellular nitrogen compound metabolic process (GO:0034641), integral component of membrane (GO:0016021)
487458205-503027279	3A	TraesCS3A02G266300	nitrate assimilation (GO:0042128), cellular amine metabolic process (GO:0044106), response to ammonium ion (GO:0060359), ammonia assimilation cycle (GO:0019676), response to salt stress (GO:0009651),
	3A	TraesCS3A02G266600	cellular response to nitrogen starvation (GO:0006995), positive regulation of response to nutrient levels (GO:0032109), regulation of cellular response to stress (GO:0080135), positive regulation of cellular catabolic process (GO:0031331), positive regulation of cell communication (GO:0010647)

The trait description is provided in Table S1. LD, linkage disequilibrium; GO, Gene ontology

Supplementary Table 7: List of identified significant marker-traits association and underlying candidate genes in barley under different NO_3^- input levels.

Treatment	Trait	Marker	Chromosome	SNP Position	-log10(P)	Allele (major:minor)	Overlapping Gene	Gene annotation
LN/HN	RD	JHI-Hv50k-2016-283047	5H	16276890	4.181	T:C	HORVU5Hr1G007770	Tropinone reductase
LN/HN	RD	JHI-Hv50k-2016-419942	6H	549945453	4.027	T:G	HORVU6Hr1G082900	Tetratricopeptide repeat protein,G2/M transition of mitotic cell cycle, regulation of meristem structure
LN/HN	TRL	JHI-Hv50k-2016-283047	5H	16276890	5.509	T:C	HORVU5Hr1G007770	Tropinone reductase
LN/HN	TRL	SCRI_RS_192515	5H	14092391	5.493	A:T	HORVU5Hr1G007340	Leucine-rich repeat receptor-like protein kinase family protein
LN/HN	TRL	JHI-Hv50k-2016-351877	5H	641778099	5.064	C:G	HORVU5Hr1G113470	Undescribed protein
LN/HN	TRL	JHI-Hv50k-2016-206737	3H	642786210	4.623	T:G	-	-
LN/HN	TRL	JHI-Hv50k-2016-206418	3H	639795130	4.493	A:C	HORVU3Hr1G092690	B3 domain-containing transcription factor ABI3, response to auxin, response to abscisic acid, embryo development
LN/HN	TRL	JHI-Hv50k-2016-206382	3H	639696204	4.336	T:G	-	-
LN/HN	TRL	JHI-Hv50k-2016-206399	3H	639697374	4.336	T:C	-	-
LN/HN	TRL	JHI-Hv50k-2016-206584	3H	640431682	4.336	A:G	HORVU3Hr1G092880	RNA-binding protein 1
LN/HN	TRL	JHI-Hv50k-2016-206584	3H	640431682	4.336	A:G	HORVU3Hr1G092870	Protein NRT1/ PTR FAMILY 2.13
LN/HN	TRL	JHI-Hv50k-2016-206480	3H	640180244	4.157	A:G	HORVU3Hr1G092750	snRNA-activating protein complex subunit
LN/HN	R:S	JHI-Hv50k-2016-419942	6H	549945453	4.246	T:G	HORVU6Hr1G082900	Tetratricopeptide repeat protein,G2/M transition of mitotic cell cycle, regulation of meristem structural organization
LN/HN	NRT	JHI-Hv50k-2016-326307	5H	578550274	4.397	A:G	HORVU5Hr1G087380	Protein kinase superfamily protein, protein phosphorylation, recognition of pollen
LN/HN	NRT	JHI-Hv50k-2016-331120	5H	588124147	4.265	T:G	HORVU5Hr1G092310	Protein DYAD
LN/HN	NRC	JHI-Hv50k-2016-74875	2H	33900600	7.101	T:G	HORVU2Hr1G015260	Nascent polypeptide-associated complex subunit alpha-like protein 3
LN	RD	JHI-Hv50k-2016-145582	2H	761328427	4.655	T:G	-	-
LN	RD	BOPA1_1344-930	2H	758851064	4.397	A:G	HORVU2Hr1G124650	Inorganic pyrophosphatase

LN	RD	SCRI_RS_227525	2H	759290313	4.140	A:G	HORVU2Hr1G124860	ABC transporter G family member 5
LN	TRL	JHI-Hv50k-2016-89269	2H	153969048	4.261	T:C	HORVU2Hr1G035780	A-kinase anchor protein 17A
LN	TRL	JHI-Hv50k-2016-90193	2H	176961727	4.205	T:C	HORVU2Hr1G038120	BRICK1, L-phenylalanine catabolic process, cinnamic acid biosynthetic process
LN	TRL	JHI-Hv50k-2016-90193	2H	176961727	4.205	T:C	HORVU2Hr1G038110	Pentatricopeptide repeat-containing protein
LN	TRL	JHI-Hv50k-2016-216741	3H	671371379	4.048	T:G	HORVU3Hr1G106850	Integral component of membrane
LN	RSA	JHI-Hv50k-2016-145582	2H	761328427	4.412	T:G	-	-
LN	ARD	JHI-Hv50k-2016-213524	3H	663152662	4.481	C:G	HORVU3Hr1G100190	Jasmonate O-methyltransferase
LN	ARD	JHI-Hv50k-2016-213204	3H	662655004	4.231	C:G	HORVU3Hr1G099920	UV-stimulated scaffold protein A homolog
LN	RV	JHI-Hv50k-2016-66556	2H	13863264	5.413	T:C	HORVU2Hr1G006620	Unknown function
LN	RV	JHI-Hv50k-2016-125883	2H	718436658	5.400	A:G	HORVU2Hr1G109960	Endoribonuclease YbeY
LN	RV	JHI-Hv50k-2016-327139	5H	580834698	4.118	A:C	HORVU5Hr1G088140	Tumor susceptibility gene 101 protein
LN	RV	SCRI_RS_154288	5H	580511041	4.087	T:C	HORVU5Hr1G088060	Cytochrome P450 superfamily protein
LN	NRF	JHI-Hv50k-2016-216741	3H	671371379	4.083	T:G	HORVU3Hr1G106850	integral component of membrane
LN	NRC	JHI-Hv50k-2016-90193	2H	176961727	4.192	T:C	HORVU2Hr1G038120	BRICK1, L-phenylalanine catabolic process, cinnamic acid biosynthetic process
	NRC	JHI-Hv50k-2016-90193	2H	176961727	4.192	T:C	HORVU2Hr1G038110	Pentatricopeptide repeat-containing protein
HN	R:S	JHI-Hv50k-2016-380506	6H	28123263	4.073	T:C	HORVU6Hr1G013580	F-box domain containing protein
HN	R:S	SCRI_RS_167505	1H	289307338	4.002	A:G	-	-
HN	ARD	JHI-Hv50k-2016-351877	5H	641778099	11.704	C:G	HORVU5Hr1G113470	Undescribed protein
HN	ARD	SCRI_RS_192515	5H	14092391	8.384	A:T	HORVU5Hr1G007340	Leucine-rich repeat receptor-like protein kinase family protein
HN	ARD	JHI-Hv50k-2016-431960	6H	579597280	5.443	T:C	HORVU6Hr1G093490	579596730-579599433 Disease resistance protein

HN	ARD	JHI-Hv50k-2016-340642	5H	611226661	4.569	A:G	-	-	-
HN	ARD	JHI-Hv50k-2016-362796	5H	661158804	4.223	A:G	HORVU5Hr1G122000	661158565-661159811	Unknown function
HN	NRT	JHI-Hv50k-2016-60698	2H	3275282	6.544	T:G	HORVU2Hr1G001560	3274556-3277134	Undescribed protein
HN	NRT	JHI-Hv50k-2016-283618	5H	17682279	5.717	A:G	-	-	-
HN	NRC	JHI-Hv50k-2016-215504	3H	668420287	5.055	A:G	HORVU3Hr1G105400	668420181-668421708	Glucan endo-1,3-beta-glucosidase GV

The trait description is provided in Table S1. HN, high nitrate; LN, low nitrate; LD, linkage disequilibrium.

Supplementary Table 8: List of syntenic gene pairs that lies on chromosome 3 and highly associated with root system traits in both wheat and barley at LN/HN condition.

Wheat genes	Trait	Barley genes	Trait	Annotation
TraesCS3B02G454000 TraesCS3B02G454100	RV	HORVU3Hr1G092870	TRL	Protein NRT1/ PTR FAMILY 2.13, low-affinity nitrate transmembrane transporter activity.
TraesCS3B02G452200	RV	HORVU3Hr1G092690	TRL	B3 domain-containing transcription factor ABI3, response to auxin, response to abscisic acid activated signaling pathway.
TraesCS3B02G453100	RV	HORVU3Hr1G092750	TRL	snRNA-activating protein complex subunit, regulation of transcription, DNA-templated

Supplementary Table 9: Promoter sequence variation of *TaNPF2.12* from 40 different wheat cultivars. The position of the sequence variation is relative to the start codon (ATG), which is start from the right to left side. Highlighted allele our identified SNP marker allele in wheat (AX-695508890). RV, root volume; LN, low nitrogen and HN, high nitrogen.

Genotypes	Position from start codon (ATG)							SNP allele	RV (LN/HN)	Haplotype
	-1299	-1282	-1275	-1267	-1266	-1264	-88			
Oakley	G	A	T	T	T	G	T	TT	4.809	Hap2
Triple Drik "S"	G	A	T	T	T	G	T	TT	4.475	Hap2
Desamo	G	A	T	T	T	G	T	TT	4.250	Hap2
Pobeda	G	A	T	T	T	G	T	TT	4.024	Hap2
Capone	G	A	T	T	T	G	T	TT	3.477	Hap2
Aszita	G	A	T	T	T	G	T	TT	3.271	Hap2
Brilliant	G	A	T	T	T	G	T	TT	3.214	Hap2
Kobold	G	A	T	T	T	G	T	TT	2.985	Hap2
Robigus	G	A	T	T	T	G	T	TT	2.935	Hap2
Manager	G	A	T	T	T	G	T	TT	2.781	Hap2
Isengrain	G	A	T	T	T	G	T	TT	2.718	Hap2
Premio	G	A	T	T	T	G	T	TT	2.704	Hap2
Esket	G	A	T	T	T	G	T	TT	2.517	Hap2
Santiago	G	A	T	T	T	G	T	TT	2.515	Hap2
Renesansa	G	A	T	T	T	G	T	TT	2.414	Hap2
Forum	G	A	T	T	T	G	T	TT	2.400	Hap2
Carenius	G	A	T	T	T	G	T	TT	2.361	Hap2
Aquila	G	A	T	T	T	G	T	TT	2.348	Hap2
Patras	G	A	T	T	T	G	T	TT	2.288	Hap2
Helios	G	A	T	T	T	G	T	TT	2.287	Hap2
Kormoran	G	A	T	T	T	G	T	TT	2.215	Hap2
Schamane	G	A	T	T	T	G	T	TT	2.209	Hap2
Pantus	A	C	C	A	A	T	C	CC	5.337	Hap1
Arktis	A	C	C	A	A	T	C	CC	4.581	Hap1
Anthus	A	C	C	A	A	T	C	CC	0.303	Hap1
Basalt	A	C	C	A	A	T	C	CC	0.350	Hap1
Nelson	A	C	C	A	A	T	C	CC	0.537	Hap1
Zobel	A	C	C	A	A	T	C	CC	0.593	Hap1
Linus	A	C	C	A	A	T	C	CC	0.655	Hap1
Anapolis	A	C	C	A	A	T	C	CC	0.672	Hap1
Hermann	A	C	C	A	A	T	C	CC	0.681	Hap1
Phoenix	A	C	C	A	A	T	C	CC	0.697	Hap1
WW	A	C	C	A	A	T	C	CC	0.704	Hap1
Winnetou	A	C	C	A	A	T	C	CC	0.732	Hap1
Intro	A	C	C	A	A	T	C	CC	0.740	Hap1
Apollo	A	C	C	A	A	T	C	CC	0.743	Hap1
Genius	A	C	C	A	A	T	C	CC	0.761	Hap1
Cobalt	A	C	C	A	A	T	C	CC	0.828	Hap1
Carisuper	A	C	C	A	A	T	C	CC	0.831	Hap1
Topper	A	C	C	A	A	T	C	CC	0.831	Hap1

Supplementary Table 10: Promoter sequence variation of *HvNPF2.12* from 40 different barley genotypes. The position of the sequence variation is relative to the start codon (ATG), which is start from the right to left side. Highlighted allele our identified SNP marker allele in barley (HV-640431682). TRL, total root length; LN, low NO_3^- and HN, high NO_3^-.

Genotypes	Promoter position from start codon							SNP allele	TRL (LN/HN)	Haplotype
	-1491	-1433	-1407	-1185	-1109	-936	-720			
Katara	C	C	C	A	A	T	C	AA	3.30	Hap2
Massine	C	C	C	A	A	T	C	AA	3.14	Hap2
P. STO	C	C	C	A	A	T	C	AA	2.95	Hap2
IG 24770	C	C	C	A	A	T	C	AA	2.86	Hap2
CompCr229	C	C	C	A	A	T	C	AA	2.55	Hap2
IG 144107	C	C	C	A	A	T	C	AA	2.35	Hap2
Petunia1	C	C	C	A	A	T	C	AA	2.12	Hap2
Bermejo	C	C	C	A	A	T	C	AA	1.91	Hap2
Ataco	C	C	C	A	A	T	C	AA	1.85	Hap2
Orca-Bar	C	C	C	A	A	T	C	AA	1.78	Hap2
Rhn	C	C	C	A	A	T	C	AA	1.46	Hap2
Rhn-03	C	C	C	A	A	T	C	AA	1.40	Hap2
IPA-7	C	C	C	A	A	T	C	AA	1.35	Hap2
Madre Selva	C	C	C	A	A	T	C	AA	1.29	Hap2
Alanda	C	C	C	A	A	T	C	AA	1.28	Hap2
Penco	C	C	C	A	A	T	C	AA	1.18	Hap2
Aths	C	C	C	A	A	T	C	AA	1.13	Hap2
V Morales	C	C	C	A	A	T	C	AA	1.13	Hap2
Atahualpa	C	C	C	A	A	T	C	AA	1.10	Hap2
Trochu	C	C	C	A	A	T	C	AA	1.00	Hap2
Alanda 01	C	C	C	A	A	T	C	AA	0.93	Hap2
Rabat 071	C	C	C	A	A	T	C	AA	0.92	Hap2
IG 17007	C	C	C	A	A	T	C	AA	0.91	Hap2
Barque	C	C	C	A	A	T	C	AA	0.87	Hap2
Cerise	T	T	G	T	G	C	T	GG	2.57	Hap1
Brea	T	T	G	T	G	C	T	GG	2.59	Hap1
Legacy	T	T	G	T	G	C	T	GG	2.79	Hap1
Harmal-02	T	T	G	T	G	C	T	GG	0.43	Hap1
Gada	T	T	G	T	G	C	T	GG	0.47	Hap1
Msel	T	T	G	T	G	C	T	GG	0.50	Hap1
Melusine	T	T	G	T	G	C	T	GG	0.51	Hap1
Tissa	T	T	G	T	G	C	T	GG	0.53	Hap1
Chamico	T	T	G	T	G	C	T	GG	0.56	Hap1
Xena	T	T	G	T	G	C	T	GG	0.57	Hap1
WI3167	T	T	G	T	G	C	T	GG	0.59	Hap1
M104	T	T	G	T	G	C	T	GG	0.60	Hap1
Logan-Bar	T	T	G	T	G	C	T	GG	0.60	Hap1
P.STO	T	T	G	T	G	C	T	GG	0.61	Hap1
Gloria-Bar	T	T	G	T	G	C	T	GG	0.62	Hap1
Recla 60	T	T	G	T	G	C	T	GG	0.64	Hap1

Supplementary Table 11: List and description of winter wheat association panel comprising 221 diverse germplasms across worldwide collection.

Cultivar	Release Year	Country	Breeder
Einstein	2004	GB	Nickerson/Limagrain
Oakley	2008	UK	KWS UK Limited
Jafet	2008	DE	Sandra Senghaas-Kirschenlohr
Claire	1999	IE	Nickerson
Rebell	2013	DE	RAGT
Memory	2013	DE	Secobra Recherches
Kurt	2013	DE	LIMAGRAIN GmbH
Zappa	2009	DE	Ackermann Saatzucht
Chevalier	2005	EU	DSV
Gordian	2013	DE	Syngenta
Mentor	2012	DE	RAGT/Mellinger
Meister	2010	DE	RAGT/Mellinger
Santiago	2011	GB	KWS Lochow
Brigand	1979	GB	Plant Breeding International Cambridge
Profilus	2008	DE	RAGT/Mellinger
Durin	NA	FR	NA
Pius	2010	DE	KWS Lochow
Paroli	2004	DE	DSV
Estivus	2012	DE	Strube
Kronjuwel	1980	DE	Bayrische
Desamo	2013	DE	Syngenta
Carenius	2006	DE	Eger/Dieckmann
Mulan	2006	DE	Nordsaat
Kredo	2009	DE	Nordsaat
Nelson	2011	DE	Saatzucht
Patras	2012	DE	DSV
Götz	1978	DE	Bayrische
Robigus	2004	GB	KWS
Anapolis	2013	DE	NORDSAAT
Solstice	2001	GB	Limagrain
Biscay	2000	DE	Lochow-Petkus
Capone	2012	DE	LIMAGRAIN
Tabasco	2008	DE	Borris-Eckendorf
Kometus	2011	DE	Saatzucht
Cubus	2002	DE	Lochow-Petkus
Edward	2013	DE	Borries-Eckendorf
Famulus	2010	DE	DSV
Dekan	1999	DE	Lochow-Petkus
Topper	2002	NA	SW Seeds
Matrix	2010	DE	DSV
Jenga	2007	DE	Ackermann
Linus	2010	DE	RAGT/Mellinger

TJB	1980	GB	Plant Breeding International Cambridge
Forum	2012	EU	Nordsaat
Colonia	2011	EU	LIMAGRAIN
Transit	1994	DE	Saatzucht
Potenzial	2006	DE	DSV
Gaucho	1993	USA	USDA-ARS
Tarso	1992	DE	Saatzucht
Hermann	2004	DE	Limagrain-Nickerson
Glaucus	2011	DE	Strube
Tuareg	2005	DE	Nordsaat
Atomic	2012	DE	LIMAGRAIN
Tobak	2011	DE	W.v.Borries-Eckendorf
Pionier	2013	DE	Deutsche
Manager	2006	DE	Saatzucht
Gourmet	2013	DE	Secobra
Limes	2003	DE	Innoseeds
Ritmo	1993	DE	Cebeco
Kalahari	2010	EU	LIMAGRAIN
Intro	2011	DE	RAGT
Oxal	2010	DE	RAGT/Mellinger
Zobel	2006	DE	Syngenta
Event	2009	DE	Saatzucht
Joker	2012	DE	DSV
Global	2009	DE	RAGT/Mellinger
Elixer	2012	DE	Borris-Eckendorf
Fedor	2007	DE	W.
Türkis	2004	DE	Lantmaennen
Skagen	2006	DE	Borries-Eckendorf
Greif	1989	DE	Lochow-Petkus
Esket	2007	DE	RAGT/Mellinger
Primus	2009	DE	DSV
Skalmeje	2006	DE	KWS
Genius	2010	DE	Nordsaat
Enorm	2002	DE	Schweiger
Florian	2010	DE	Nordsaat
Skater	2000	DE	Limagrain-Nickerson
Brilliant	2005	DE	SW
Inspiration	2007	DE	Saatzucht
Apertus	2013	DE	Dr. Hermann Strube
Ellvis	2002	DE	Breun
Edgar	2010	DE	LIMAGRAIN
Maris	1975	DE	Nordsaat
Ferry	2012	DE	Syngenta
Landsknecht	2013	DE	Secobra
Sponsor	1994	FR	Unisigma

Impression	2005	DE	Saatzucht
Winnetou	2002	DE	Saatzucht
Toronto	1990	DE	Strengs
Torrild	2005	DE	Borris-Eckendorf
Contra	1990	DE	Saatzucht
Schamane	2005	DE	Saatzucht
Granada	1980	DE	Schweiger
Cobalt	2013	DE	KWS LOCHOW
Tommi	2002	DE	Nordsaat
Saturn	1973	DE	MPI
Severin	1980	NA	Bauer
Asano	2008	DE	Saatzucht Josef
Kerubino	2004	DE	Saatzucht
Arktis	2010	DE	DSV
Urban	1980	DE	Bauer
Orestis	1988	DE	Strube
Flair	1996	DE	Schweiger
Anthus	2005	DE	KWS Lochow
Bombus	2012	DE	Secobra
Lucius	2006	DE	Secobra
Herzog	1986	DE	Saatzucht
Sorbas	1985	DE	Strube
Tabor	1979	DE	Strube
Terrier	2001	DE	Nickerson
Magister	2005	DE	Bauer
Altos	2000	DE	Syngenta
Progress	1969	DE	Hege
Xanthippe	2011	DE	Sejet
Avenir	2013	DE	Saatzucht
Pantus	1966	DE	Streng
Drifter	1999	DE	Nickerson
Joss	1972	DE	Breustedt
Kranich	1969	DE	Lochow-Petkus
Sperber	1982	DE	Lochow-Petkus
Discus	2007	DE	Pflanzenzucht
Helios	1980	DE	Saatzucht
Obelisk	1987	NE	Dr. Strube
Magnus	2000	DE	Engelen
Disponent	1975	DE	Bayrische
Tambor	1993	DE	Semundo
Boxer	2013	DE	Ackermann
Sokrates	2001	DE	Saatzucht
Carisuper	1975	DE	Heidenreich
Rektor	1980	DE	Firlbeck
Alves	2010	DE	SW Seeds
NaturaStar	2002	DE	Saatzucht

Alidos	1987	DE	Saatzucht
Monopol	1975	DE	Firlbeck
Akratos	2004	DE	Strube
Knirps	1985	NA	Semundo
Bussard	1990	DE	Lochow-Petkus
Oberst	1980	DE	Engelen
Cappelle	NA	FR	NL
Tiger	2001	DE	Franck
Ibis	1991	DE	Lochow-Petkus
Batis	1994	DE	Strube
Topfit	1972	DE	Strube
Akteur	2003	DE	DSV
Ludwig	1998	DE	Franck
Asketis	1998	DE	Strube
Aristos	1997	DE	Strube
Zentos	1989	DE	Saatzucht
Diplomat	1966	DE	Firlbeck
Astron	1989	DE	Strube
Basalt	1980	DE	Hege
Kormoran	1973	DE	Lochow-Petkus
Aron	1992	DE	Semundo
Milaneco	2013	DE	KWS Lochow
Aszita	2005	DE	Getreidezüchtung
Kobold	1978	DE	Firlbeck
Carimulti	1975	DE	Heidenreich
Admiral	1968	DE	Firlbeck
Vuka	1975	DE	Franck
Benno	1973	DE	Bauer
Apollo	1984	DE	Saatzucht
Aquila	1979	EU	Nickerson
Kanzler	1980	DE	Engelen
Kraka	1982	DE	Petersen
Caribo	1968	DE	Heidenreich
Butaro	2009	DE	LandbauschuleDottenfelderhof
Konsul	1990	DE	Svaloef
Ares	1983	DE	Strube
Centurk	1971	USA	Nebraska
NS	1992	NA	NA
Benni	1980	USA	Purde University
Hope	NA	USA	S.Dakota
Vel	NA	USA	NA
Phoenix	1981	AUS	Agricultural Research Insititute Wagga
Mironovska	1963	exot	Mironovskii Institute Selekstii
Caphorn	2000	FR	RAGT
Cordiale	2003	GB	KWS UK Limited

Apache	1997	CZ	Nickerson>Limagrain
Premio	2006	FR	RAGT
Isengrain	1996	EU	Florimond
Alixan	2005	FR	Limagrain
Boregar	2007	FR	RAGT
Renesansa	1995	SRB	Institute
Tremie	1991	EU	Serasem>RAGT
Ferrum	2012	DE	KWS Lochow
Triple Drik "S"	NA	NA	NA
Cardos	1998	DE	Saatzucht
Soissons	1987	EU	Florimond
BCD	1983	NA	Goertzen Seed Research
Arlequin	2007	FR	Limagrain
Sonalika	1967	IND	Indian
Camp	1980	B	Unisigma
Cajeme	71	exot	CIMMYT
Avalon	1980	GB	Plant
Ivanka	1998	SRB	Institute
Pobeda	1990	SRB	Institute
NS	1992	NA	NA
Mexico	NA	MEX	BAZ Braunschweig Genetic Resources
Orcas	2010	DE	Secobra
Nimbus	1975	DE	Firlbeck
Muskat	2010	DE	DSV
Florida	1986	USA	NA
Rumor	2013	DE	Dr. Hermann Strube
Highbury	1968	GB	Plant Breeding International Cambridge
Siete Cerros	1966	MEX	Instituto Nacional
Kontrast	1990	DE	Saatzucht
WW	4180	NA	Saatzucht Josef Breun
INTRO	615	NA	NA
NS	1990	NA	NA
Mex.	NA	NA	CYMMIT
Labriego-Inia	1980	CHL	INIA Chillan
Pegassos	1994	EU	Strube Saatzucht
Hybred	2003	EU	Nordsaat
Hyland	2009	DE	Nordsaat
Hybery	2010	FR	Saaten Union Recherche
Hystar	2007	FR	Saaten Union Recherche
Hylux	2012	FR	Saaten Union Recherche
Piko	1994	DE	NORDSAAT
SUR	NA	NA	Saaten Union Recherche

Supplementary Table 12: List and description of spring barley association panel comprising 200 diverse germplasms across worldwide collection.

Ent	Pedigree
1	ATACO/BERMEJO//HIGO/3/CALI92/ROBUST/4/PETUNIA 1/5/PETUNIA 1/CHINIA/3/ATACO/BERMEJO//HIGO/6/ZIGZIG/3/M9846//CCXX14.ARZ3/PACO CBSS01M00763D-0TOPY-7M-2M-1Y-1M-0Y
2	MASSINE (INRA1705/5/NY65005-18/3/13929/NUM/ASSE/4/KBR)
3	BRS195/ND19098-1
4	TANGO-BAR/MALEBO
5	V Morales
6	LEGACY/4/TOCTE//GOB/HUMAI10/3/ATAH92/ALELI/5/CIRUELO
7	Rihane-03
8	LOGAN-BAR/MSEL//AZAF
9	Alanda 01
10	Katara//SLB34-65/Arar
	MSEL/LOGAN-BAR/CBSS03B00016S-0M-0Y-0M-0Y-1M-0Y
12	WI3180/4/ALISO/CI3909.2//HB602/3/MOLA/SHYRI//ARUPO*2/JET
13	STRIDER/3/GRIT/VALERIANA//GLORIA-BAR/COPAL
14	PENCO/CHEVRON-BAR//BREA/DL70
15	PETUNIA 1/RITA PELADA
16	AZAF/SCARLETT
17	ORCA-BAR/GUAYABA
18	M104/PFC 88210//DOÑA JOSEFA
19	CPOLO 9109/PETUNIA 2 M00053001 08/1G0035
20	80.5162/MSEL//GLORIA-BAR/IAR.H.485
21	P.STO/3/LBIRAN/UNA80//LIGNEE640/4/BLLU/5/PETUNIA 1/6/CHAMICO/TOCTE//CONGONA
22	CABUYA/MJA//PETUNIA1/5/PENCO/CHEVRON-BAR/3/ATACO/BERMEJO//HIGO/4/PETUNIA1
23	Alanda//Lignee527/Arar/3/Asal/4/AwBlack/Aths//Rhn-08/7/Man/4/Bal16/Pro//Apm/DwII-1Y/3/Api/CM67/5/Gas/OreS/6/Atahualpa
24	SHYRI/3/ZHEDAR#1/SHYRI//OLMO
25	IG 26731
26	ICARDA SN326
27	SICH84.80/BISON 129
28	BREA/DL70/M97.106
29	MSEL/FNC1
30	SVANHALS-BAR/MSEL//AZAF/GOB24DH/3/NE167/CLE176 CBSS05Y00056S-10Y-0M-0Y-0M-3AP
31	Alanda-01//Atahualpa/IraqiBlack
32	Rhn-03/Alanda
33	Alanda-01/Petunia1
34	CABUYA/MJA//PETUNIA 1/5/PENCO/CHEVRON-BAR/3/ATACO/ BERMEJO//HIGO/4/PETUNIA 1
35	TISSA (CalsbergII*inconnue)
36	ALELI/SCARLETT CBSS05M00148S-2M-0Y-0M-0AP-0TR
37	VMorales/6/ZIGZIG/4/EGYPT4/TERAN78//P.STO/3/QUINA CBSS04B00042S-0M-0Y-0M-0Y-1M-0AP

38	PFC9214//PENCO/CHEVRON-BAR
39	PENCO/CHEVRON-BAR/3/LEGACY//PENCO/CHEVRON-BAR CBSS04Y00048S-23Y-2M-0Y-0M-0Y-0AP
40	Carina/Moroc9-75//WI3257
41	H01063002 09/2S0009
42	BGCLM 157.MBV/ND20493
43	Alanda/5/Aths/4/Pro/TolI//Cer12/TolI/3/5106/6/Aths/7/Giza129
44	PENCO/CHEVRON-BAR
45	WI3167/6/ANCA/2469//TOJI/3/SHYRI/4/ATACO/5/ALELI/7/Arar/Lignee527//Zy/DL69
46	LEGACY/CHAMICO//ATAH92/GOB
47	IG 144107
48	IG 144146
49	P.STO/3/LBIRAN/UNA80//LIGNEE640/4/BLLU/5/PETUNIA 1/6/P.STO/3/LBIRAN/UNA80//LIGNEE640/4/BLLU/5/PETUNIA 1
50	ORCA-BAR/WC46310
51	P.STO/3/LBIRAN/UNA80//LIGNEE640/4/BLLU/5/PETUNIA 1/6/M9846//CCXX14.ARZ3/PACO/3/PALTON
52	PENCO/CHEVRON-BAR//GRIT
53	LIMON/BICHY2000/4/ALELI/3/ARUPO/K8755//MORA/5/MSEL
54	MSEL/ND19098-1//CANELA
55	IG 144015
56	BISON 217/3/SVANHALS-BAR/MSEL//AZAF/GOB24DH
57	IG 26051
58	Rihane-03
59	CANELA/Malt 2
60	P.STO/3/LBIRAN/UNA80//LIGNEE640/4/BLLU/5/PETUNIA 1/6/ZIGZIG/4/EGYPT4/TERAN78//P.STO/3/QUINA
61	Zanbaka/5/Pyo/Cam//Avt/RM1508/3/Pon/4/Mona/Ben//Cam/6/Mundah
62	PFC9202//LM 844/QUILMES PAMPA/3/CANELA
63	ATAH92/GOB/6/P.STO/3/LBIRAN/UNA80//LIGNEE640/4/BLLU/5/PETUNIA 1
64	CANELA/BICHY2000
65	ESMERALDA/LEGACY/6/P.STO/3/LBIRAN/UNA80//LIGNEE640/4/BLLU/5/PETUNIA 1
66	SICH84.80/BISON 216.4
67	Petunia1//Atahualpa/IraqiBlack
68	Mari/aths*2
69	ZIG ZIG/PUNGSANCHAPSSALBORI
70	P.STO/3/LBIRAN/UNA80//LIGNEE640/4/BLLU/5/PETUNIA 1/6/M111/7/LEGACY/3/SVANHALSBAR/MSEL//AZAF/GOB24DH
71	OPS 66/CANELA
72	AMIRA (WI2198/EMIR//ARAR/ESPERANCE)
73	ATACO/BERMEJO//HIGO/3/CALI92/ROBUST/4/PETUNIA1/5/PETUNIA/CHINIA/3/ATACO/ BERMEJO//HIGO/6/ZIGZIG/3/M9846//CCXX14.ARZ3/PACO
74	OPS 19/CANELA
75	CIRU/ZIGZIG
76	Arbayan/NK1272/6/CI01021/4/CM67/U.Sask.1800//Pro/CM67/3/DL70/5/Nacha2
77	H00010002 09/3H0006
78	PETUNIA 2/M111

79	IG 17007
80	MADRE SELVA/Barque
81	BISON 129/CANELA
82	ACUARIO T95/BCD12DH
83	SHYRI/3/SVANHALS-BAR/MSEL//AZAF/GOB24DH
84	ESMERALDA/3/SLLO/ROBUST//QUINA/4/M104
85	Harrington/Arta//Malt 1
86	ORW11/OPS 78
87	BBSC/CONGONA
88	MADRE SELVA/Malt 1
89	LEGACY/4/TOCTE//GOB/HUMAI10/3/ATAH92/ALELI/5/LEGACY/CHAMICO
90	STAB33/PASION
91	MSEL//DEFRA/CL128
92	IG 144149
93	SARA1-BAR/CAPUCHONA 20
94	IG 143951
95	PENCO/CHEVRON-BAR//ND20493
96	BICHY2000//GOB/HUMAI10
97	LEGACY/CHAMICO//TRADITION
98	FIRDAWS (NK/272/RM1508/NY65005-18/3/13929/NUM/ASSE/4/KBR)
99	Alanda//Lignee527/Arar/3/BF891M-617
100	MERIT,B/4/AZAF/3/ARUPO/K8755//MORA/5/MSEL
101	BRS195/SCARLETT
102	BREA/DL70//3*TOCTE/3/6B89.2027/CHAMICO
103	HB511/JAEGER H00056005 09/3H0078
104	MSEL/LA MOLINA 95
105	BBSC/CONGONA//FRESA CBSS05Y00126S-20Y-0M-0Y-0M-2AP
106	IG 24770
107	Coss/OWB71080-44-1H//Viringa'S'/3/WI3180
108	Atahualpa/DD-21//Malt 2
109	Arar/H.spont.19-15//Hml/3/H.spont.41-1/Tadmor/4/Tadmor//ER/Apm
110	6B89.2027/CHAMICO//TRADITION
111	CANELA/DEFRA
112	RWA.M54/3/K-247/2401-13//Vavilon/4/Meteor
113	H.spont.41-1/WI3257
114	MSEL/LOGAN-BAR
115	MADRE SELVA/Keel
116	P.STO/3/LBIRAN/UNA80//LIGNEE640/4/BLLU/5/PETUNIA 1
117	QUINA/MJA//SCARLETT
118	GADA/PYE//VADA
119	BREA/DL70//TOCTE/3/BREA/DL70//CABUYA/4/BREA/DL70//CABUYA
120	ARAMIR/COSSACK
121	CWB117-9-7/3/Roho//Alger/Ceres362-1-1/4/Pamir-147/Sonata
122	PETUNIA1/TITIRIBI
123	WI2269/Espe/3/WI2291/Bgs//Hml-02

124	RABAT 071
125	PENCO/CHEVRON-BAR//FEG53.16/3/LEGACY//PENCO/CHEVRON-BAR
126	BICHY2000/PRTL
127	Clipper//WI2291*2/WI2269/7/Hml-02/5/Cq/Cm//Apm/3/12410/4/Giza134-2L/6/Clipper/Volla/3/Arr/Esp//Alger/Ceres362-1-1/4/Hml
128	15UCM 64
129	15UCM 67
130	15UCM34
131	CC33MS/5/NY65005-18/3/13929/NUM/ASSE/4/KBR
132	GK58/3/Kc/MullersHeydla//Sls/4/Wieselbuger//Ahor1303-61//Ste/Antares
133	BICHY2000/SHENMAINO.3
134	CONDOR-BAR/3/PATTY.B/RUDA//ALELI/4/ALELI/5/DIAMALT
135	PENCO/CHEVRON-BAR/6/P.STO/3/LBIRAN/UNA80//LIGNEE640/4/ BLLU/5/PETUNIA 1
136	FRESA/PETUNIA 1/7/P.STO/3/LBIRAN/UNA80//LIGNEE640/4/ BLLU/5/PETUNIA 1/6/LEGACY//PENCO/CHEVRON-BAR
137	P.STO/3/LBIRAN/UNA80//LIGNEE640/4/BLLU/5/PETUNIA 1/6/TOCTE
138	CIRU/BGCLM 157.MBV
139	GLORIA-BAR/COPAL/6/P.STO/3/LBIRAN/UNA80 //LIGNEE640/4/BLLU/5/PETUNIA 1
140	RECLA 60/BICHY2000//LIMON/BICHY2000/3/ BCD12DH
141	BLLU/3/BREA/DL70//3*CABUYA
142	LBIRAN/UNA80//LIGNEE640/6/P.STO/3/LBIRAN/UNA80//LIGNEE640/4/BLLU/5/PETUNIA 1
143	Cerise/Shyri//Aleli/3/Mpyt169.1Y/Laurel//Olmo/4/Canela/5/DWRUB52
144	SLB15-05/4/H.spont.96-3/3/Roho//Alger/Ceres362-1-1/5/Roho/4/Zanbaka/3/ER/Apm//Lignee131
145	Moroc9-75//WI2291/WI2269/3/Nawair 1
146	Gloria'S'/Copal'S'//As46/Aths/3/Rhn-03/4/Lignee527/Aths//Lignee527/NK1272
147	Hma-02//11012-2/CM67/3/Alanda/5/Rhn-03//Lignee527/NK1272/4/Lignee527/Chn-01/3/Alanda/6/AwBlack/Aths//Rhn-08/3/Malouh
148	Gloria'S'/Copal'S'//As46/Aths/3/Rhn-03/5/QB813-2/5/Aths/Lignee686/4/Rhn-03/3/Bc/Rhn//Ky63-1294
149	Rihane-03/3/As46/Aths*2//Aths/Lignee686/4/Momtaz
150	Rhn-03/Eldorado/5/Rhn-03//Lignee527/NK1272/4/Lignee527/Chn-01/3/Alanda/6/Rihane-03/4/Lignee527//Bahtim/DL71/3/Api/CM67//Mzq
151	Hma-02//11012-2/CM67/3/Alanda/5/Rhn-03//Lignee527/NK1272/4/Lignee527/Chn-01/3/Alanda/6/Rhn//Bc/Coho/3/DeirAlla106//Api/EB89-8-2-15-4/5/CM67/3/Apro//Sv02109/Mari/4/Carbo
152	Baca'S'/3/AC253//CI08887/CI05761/4/Cen/Bglo'S'/5/Alanda-01/3/Alanda//Lignee527/Arar
153	Rhn-03/Eldorado/5/Rhn-03//Lignee527/NK1272/4/Lignee527/Chn-01/3/Alanda/6/Aths/Lignee686/4/Avt/Attiki//Aths/3/Giza121/Pue
154	CANELA//E.QUEBRACHO/W9338
155	Alanda//Ssn/Lignee640/3/QB813-2
156	Rhn-03//Lignee527/NK1272/3/Lignee527/Chn-01//Alanda/4/Eldorado
157	CIRU//BREA/DL70/3/SUMBARD400
158	TROCHU/VIVAR
159	TRADITION//PENCO/CHEVRON-BAR
160	MSEL//PENCO/CHEVRON-BAR
161	FRANKLIN-BAR//LIMON/BICHY2000
162	CHAMICO/TOCTE//CONGONA/3/LEGACY//PENCO/CHEVRON-BAR
163	PENCO/CHEVRON-BAR//FALCON-BAR
164	Rihane03/Atahualpa
165	CHAMICO

166	LIMON/BICHY2000//CANELA/3/MSEL
167	SC 36Z47-L2
168	CANELA//ND16680/ND13111
169	BISON 216.4/6/P.STO/3/LBIRAN/UNA80//LIGNEE640/4/BLLU/5/PETUNIA 1
170	LIMON/BICHY2000/3/ALELI/CANELA//GOB96DH/4/ASAHI 5/2*ALELI
171	BISON 136/CANELA
172	MSEL//LIMON/BICHY2000
173	Reem/TR05671
174	Xena/Nawair-01
175	MSEL/FNC1//Canela
176	Melusine/Aleli/3/Matico/Jet//Shyri/4/Canela/5/Canela
177	Melusine/Aleli/3/Matico/Jet//Shyri/4/Canela/5/MSEL//DEFRA/CL128
178	Xena/DWRUB52
179	ChiCm/An57//Albert/3/Alger/Ceres362-1-1/4/Arta/5/Hml
180	Hauran-3/MADRE SELVA
181	MADRE SELVA/4/Clipper/Volla/3/Arr/Esp//Alger/Ceres362-1-1/4/Hml
182	Cerise/Shyri//Aleli/3/Mpyt169-1Y/Laurel//Olmo/4/Canela/5/Leb71/CBB37//Leb71/CBB29/3/Lignee527/Chn-01
183	CompCr229//As46/Pro/3/Srs/4/RWA-M47/5/Carbo/Hamra/4/Rhn-08/3/DeirAlla106//DL71/Strain205
184	Rhn//Bc/Coho/3/DeirAlla106//Api/EB89-8-2-15-4/5/CM67/3/Apro//Sv02109/Mari/4/Carbo/6/Beecher
185	Rhn//Bc/Coho/3/DeirAlla106//Api/EB89-8-2-15-4/5/CM67/3/Apro//Sv02109/Mari/4/Carbo/6/IPA7
186	Aths/IPA7
187	Manal/6/P.STO/3/LBIRAN/UNA80//LIGNEE640/4/BLLU/5/PETUNIA 1
188	ATACO/COMINO//ALELI/6/P.STO/3/LBIRAN/UNA80//LIGNEE640/4/BLLU/5/PETUNIA 1
189	Giza132/Ishi
190	Momtaz/6/ESMERALDA/LEGACY/6/P.STO/3/LBIRAN/UNA80//LIGNEE640/4/BLLU/5/PETUNIA 1
191	P.STO/3/LBIRAN/UNA80//LIGNEE640/4/BLLU/5/PETUNIA 1/6/LACEY
192	Xena/3/MSEL//DEFRA/CL128
193	TRIUMPH-BAR/TYRA//ARUPO*2/ABN-B/3/CANELA/4/TOCTE//GOB/HUMAI10/3/ATAH92/ALELI/5/CANELA
194	BT554/MAHIGAN
195	RECLA 86/3/7085-B/ND4994.15//ND7556
196	Harmal-02/ArabiAbiad*2/4/Soufara-02/3/RM1508/Por//WI2269
197	WI2291//Apm/PI000046/3/Hml-02/4/WI3213
198	Tidone/8/Pld10342//Cr115/Por/3/Bahtim9/4/Ds/Apro/5/WI2291/6/WI2291/WI2269/7/WI2291/WI2269//WI2291/Bgs
199	WI2291//Apm/PI000046/3/Hml-02/4/Mzq/Gva//PI002917/3/WI2291/WI2269
200	Moroc9-75//WI2291/CI01387/3/H.spont.41-1

Ent means ‘Entry’.

Supplementary Table 13: Nmin amounts (based on ha) of soil samples at 0-30 cm, 30-60 cm, and 60-90 cm soil depth (average values).

Years	Site	P^H ($CaCl_2$)	N-min (kg/ha)			NO_3-N (kg/ha)			NH_4-N (kg/ha)			*P-value*[*]
			0-30 cm	30-60 cm	60-90 cm	0-30 cm	30-60 cm	60-90 cm	0-30 cm	30-60 cm	60-90 cm	
2018	KA-Bonn	6.8	13.7	23.9	46.2	14.3	25	45.4	< 1	< 1	< 1	
2019	KA-Bonn	6.8	13.6	23.7	46.4	13.8	25.5	45.8	< 1	< 1	< 0.9	ns
2020	KA-Bonn	6.7	13.8	24.0	46.9	14.5	24.8	45.9	<0.9	<0.9	<1	

The *p-value = 0.551*, as output of Krystal–Wallis test by rank between three years is not significant, which indicates, the differences between the yearly median value for all nitrogen (N) chemical compounds in the soil samples, are not statistically significant and the annual medians are equal, which indicates the homogeneity of soil properties is acceptable within and between N treated blocks.

Supplementary Table 14: Summary of RNA-seq analysis and list of high confidential (HC) genes and their up and down-regulation patterns.

ALL GENES			(bigger 2)	**Upregulated** (FDR < 0.05, log2Foldchange > abs(2), mean expression > 10)	
		Total number genes	*Total expressed*	*compared to the treatment (LN to HN)*	*compared to other genotype (WT to MT)*
Mutant	HN	106914	28893	255	215
	LN	106914	28996	345	198
Wildtype	HN	106914	29726	418	260
	LN	106914	29414	435	310

Expression statistics on the subset of NRT, NPF and Nitrate related genes

Nitrate related genes

		Total number genes	*Total expressed*	*compared to the treatment (LN to HN)*	*compared to other genotype (WT to MT)*
Mutant	HN	599	173	1	1
	LN	599	171	0	2
Wildtype	HN	599	177	5	1
	LN	599	181	1	2

logFold	**MT HN upregulation**	**MT LN upregulation**							
5.6	TraesCS3A01G383300	chr3A	466039627	*Protein*	*NRT1/*	*PTR*	*FAMILY*	*5.5*	
logFold	**WT HN up**	**WT LN up**							
2.5	TraesCS1A01G162500	chr1A	257960004	GRAM	domain-containing	protein	/	ABA-responsive	protein-related
2.8	TraesCS1A01G224800	chr1A	373766258	Ran-binding	protein	1	domain-containing		
2	TraesCS1B01G257800	chr1B	403541134	30S	ribosomal	protein	S18		
-2.7	TraesCS1B01G301900	chr1B	470910728	DNA	replication	and	repair	protein	RecF
2.4	TraesCS2A01G427600	chr2A	590636737	Methionine	aminopeptidase				
2.3	TraesCS3B01G578300	chr3B	652291889	Abscisic	stress-ripening	protein	1		

List of all significantly different genes from table 2, listed with their functional annotation

logFold	**WT to MT in LN, WT up**	WT to MT in LN, MT up							
3.7	TraesCS5D01G158500	chr5B	643650636	*Protein*	*NRT1/*	*PTR*	*FAMILY*	*2.1*	
4.1	TraesCS6B01G046600	chr6A	198178715	*High*	*affinity*	*nitrate*	*transporter*		
-2.4	TraesCS2B01G065800	chr2A	768541320	O-methyltransferase					
-2.2	TraesCS6D01G127200	chr6B	522639943	Hexosyltransferase					

logFold	**WT to MT in HN, WT up**	WT to MT in HN, MT up							
-6	TraesCS3A01G383300	chr3A	466039627	TraesCS3A03G0637200	Protein	NRT1/	PTR	FAMILY	5.5
2.2	TraesCS6B01G141400	chr6A	495152188	TraesCS6A03G0719000	Galactokinase				

Abbreviation: FRD, false discovery rate; MT, mutant; WT, wild-type; HN, high nitrate; LN, low nitrate

Supplementary Table 15: List of significantly enriched pathways of differentially expressed genes (DEGs) in wild-type and *npf2.12* mutant alleles under high and low nitrate treatments.

Enrichment FDR	No. Genes	Pathway Genes	Fold Enrichment	Pathway
3.04E-22	35	638	10.61115841	Hydrogen peroxide catabolic process
3.11E-22	35	652	10.38331145	Hydrogen peroxide metabolic process
1.93E-21	35	698	9.699024448	Reactive oxygen species metabolic process
6.94E-19	36	905	7.694304225	Response to oxidative stress
9.52E-12	54	3286	3.178642114	Response to stress
1.67E-09	41	2371	3.344781366	Cellular catabolic process
6.88E-08	43	2929	2.839648049	Catabolic process
5.55E-07	15	443	6.549421862	Recognition of pollen
5.55E-07	15	443	6.549421862	Cell recognition
6.32E-07	15	451	6.433245865	Pollen-pistil interaction
1.16E-06	43	3285	2.531911457	Transmembrane transport
3.07E-06	15	520	5.579603625	Pollination
3.07E-06	15	520	5.579603625	Multi-multicellular organism process
3.20E-05	16	716	4.322374503	Multi-organism process
4.81E-05	8	162	9.551914024	Inorganic anion transport
5.08E-05	17	841	3.909924379	Defense response
9.18E-05	5	48	20.14856865	Phosphate ion transport
0.001430254	11	509	4.180135263	Response to biotic stimulus
0.002612933	8	293	5.281263044	Anion transport
0.008840015	28	2732	1.982406754	Carbohydrate metabolic process
0.024090003	4	97	7.976340577	Amide transport
0.024207683	2	13	29.757886	Nitrate transport
0.024207683	16	1337	2.314749547	Reproductive process
0.024207683	16	1341	2.307844999	Reproduction
0.024207683	18	1592	2.186980315	Ion transport

0.035444372	2	16	24.17828237	Response to nitrate
List of significant enrichment pathways of DEGs in wild-type plants under low nitrate				
1.75E-18	25	336	14.03835109	Response to acid chemical
1.75E-18	25	332	14.20748785	Response to water
5.81E-15	32	875	6.900130326	Response to oxygen-containing compound
6.49E-14	25	540	8.734974009	Response to inorganic substance
5.54E-11	31	1168	5.007652908	Response to abiotic stimulus
1.52E-08	7	29	45.54234725	Cold acclimation
1.02E-07	33	1804	3.451379974	Response to chemical
1.02E-07	14	307	8.604091662	Response to alcohol
1.02E-07	14	307	8.604091662	Response to abscisic acid
3.77E-07	11	187	11.09855521	Embryo development ending in seed dormancy
4.05E-07	11	190	10.92331487	Embryo development
2.70E-06	8	97	15.56086092	Carbohydrate transport
4.90E-06	6	43	26.32680539	Galactose metabolic process
5.47E-06	11	251	8.268644719	Seed development
7.27E-06	11	260	7.982422402	Fruit development
8.72E-06	14	460	5.742295957	Response to lipid
7.44E-05	35	2732	2.417145077	Carbohydrate metabolic process
0.000889558	2	2	188.6754386	Inositol phosphorylation
0.000923876	7	164	8.05321994	Response to cold
0.001716659	8	247	6.11094538	Hexose metabolic process
0.002009069	9	327	5.19290198	Response to temperature stimulus
0.002755222	5	87	10.84341601	Transition metal ion homeostasis
0.004411983	8	296	5.099336178	Monosaccharide metabolic process
0.004411983	11	553	3.753037657	Reproductive structure development
0.004411983	6	155	7.303565365	Defense response to fungus
0.004411983	11	553	3.753037657	Reproductive system development
0.004411983	34	3286	1.952210868	Response to stress

0.004411983	8	297	5.082166696	Response to water deprivation
0.005165762	6	164	6.902759949	Glutamine family amino acid metabolic process
0.006052155	6	170	6.659133127	Response to fungus
List of significant enrichment pathways of DEGs in npf2.12 mutant plants under high nitrate				
4.04E-07	13	400	9.929580966	Glutathione metabolic process
1.25E-06	13	466	8.523245464	Cellular modified amino acid metabolic process
0.000313183	13	786	5.053221866	Sulfur compound metabolic process
0.004995596	10	652	4.685974972	Hydrogen peroxide metabolic process
0.004995596	10	638	4.788802009	Hydrogen peroxide catabolic process
0.006231402	22	2732	2.460308382	Carbohydrate metabolic process
0.006231402	10	698	4.377157137	Reactive oxygen species metabolic process
0.014469932	5	178	8.582178882	Plant-type cell wall organization
0.032875312	14	1592	2.686782635	Ion transport
0.032875312	10	905	3.375973129	Response to oxidative stress
0.039803074	10	944	3.236499663	Cell wall organization or biogenesis
0.039803074	5	244	6.26076984	Plant-type cell wall organization or biogenesis
0.042020307	2	19	32.16058612	Negative regulation of abscisic acid-activated signaling pathway
0.042020307	2	19	32.16058612	Negative regulation of response to alcohol
0.042020307	2	19	32.16058612	Negative regulation of cellular response to alcohol
List of significant enrichment pathways of DEGs in npf2.12 mutant plants under low nitrate				
2.50E-12	26	875	7.397275132	Response to oxygen-containing compound
1.03E-11	17	336	12.59552056	Response to acid chemical
1.03E-11	17	332	12.74727382	Response to water
1.54E-09	18	540	8.298225309	Response to inorganic substance
1.18E-08	24	1168	5.115344368	Response to abiotic stimulus
1.51E-07	28	1804	3.863918658	Response to chemical

1.39E-06	6	43	34.73675711	Galactose metabolic process
3.00E-05	10	307	8.10901496	Response to alcohol
3.00E-05	10	307	8.10901496	Response to abscisic acid
0.000251749	4	29	34.33748404	Cold acclimation
0.00085661	10	460	5.411886071	Response to lipid
0.004489133	6	187	7.987596554	Embryo development ending in seed dormancy
0.004519145	6	190	7.861476608	Embryo development
0.005725753	15	1235	3.023644849	Response to organic substance
0.009612701	6	247	6.047289699	Hexose metabolic process
0.009612701	2	9	55.32150206	Nitric oxide metabolic process
0.009612701	4	85	11.71514161	Phenylpropanoid catabolic process
0.009612701	4	85	11.71514161	Lignin catabolic process
0.009612701	2	9	55.32150206	Formaldehyde metabolic process
0.009612701	2	9	55.32150206	Formaldehyde catabolic process
0.009612701	6	251	5.950918548	Seed development
0.009612701	2	9	55.32150206	Cellular detoxification of aldehyde
0.009612701	2	9	55.32150206	Cellular response to aldehyde
0.009612701	3	34	21.96589052	Glutamate metabolic process
0.009612701	2	9	55.32150206	Nitric oxide biosynthetic process
0.009612701	5	164	7.589840221	Response to cold
0.011135131	6	260	5.744925214	Fruit development
0.014738297	4	107	9.306420907	Lignin metabolic process
0.019219154	2	14	35.56382275	ADP transport

Supplementary Table 16: Primers used for the DNA sequencing and expression analysis of *TaNPF2.12* in wheat cultivars.

Primers	Forward primer (5` to 3`)	Reverse primer (5` to 3`)	Purposes	Product size (bp)
Promoter seq-1	TTTTGCAGGGTTTAGCTGGG	GAGCAGCCATGTCTTCTGAA	Promoter sequencing	532
Promoter seq-2	AGGATCACTGACAGCTGGTT	GCGAGGAAAGGGAAGGTGAT	Promoter sequencing	866
TaNPF2.12-seq	GGTACGCTTCACAAGTTCACT	CCACGACCTGCTGCTAAGTA	cDNA sequencing	825
TaNPF2.12-seq	CGTGGGAGCTTTGCAGTATC	TGGGTTCCTCAGCATAGTGT	cDNA sequencing	765
TaNPF2.12-qPCR	TCAATGCAGTTGGTCAATTC	CGTCTGCGATCCAGCTAT	qRT-PCR analysis	177
NIA1-qPCR	TTGTACCATCCCACCTGCTT	GGAGGAGAAGAGGTCGAAGG	qRT-PCR analysis	127
TaEf-1a	CTGGTGTCATCAAGCCTGGT	TCCTTCACGGCAACATTC	Equalizing control	151
TaEf-1a	CAGATTGGCAACGGCTACG	CGGACAGCAAAACGACCAAG	Equalizing control	227

Supplementary Table 17: Primers used for the DNA sequencing and expression analysis of *HvNPF2.12* in barley genotypes.

Primers	Forward primer (5` to 3`)	Reverse primer (5` to 3`)	Purposes	Product size (bp)
Promoter seq-1	CCGTATGCCAAATTGTCCGT	GGCATTGCGTCTCTATCCTG	Promoter sequencing	706
Promoter seq-2	GGACCCATCAAGTGACCCTT	CCTGAACGCCTGGTCATACT	Promoter sequencing	779
HvNPF2.12-seq	TCTTTGCTATGAGAACAGGGGA	CCTGAACTGGGAAGTAAGTGG	cDNA sequencing	600
HvNPF2.12-qPCR	GCCCTGGTGTTCTCAATGAC	ATGCTTCCCTCTGGTGGTAC	qRT-PCR analysis	155
Ef1-a	CGAGGAGGACAAGAAAGCAG	AGAATCCAGCAGCAACAGGT	Equalizing control	375

Supplementary transcriptome methods

Illumina universal adapters were removed from 101 bp long single-end Illumina reads by *cutapt*[1]. No read trimming was performed (because the quality was already sufficient). Further, we used *bwa*[2] to align the short reads to the wheat reference genome (version 2.1[3]). The sorted aligned reads were annotated to the high confidential (HC) genes (version 2.1) using *featurecounts* from the *subread* package[4]. All reads with an average alignment quality score above 20 and multi-mapping reads were counted. Additionally, reads were extended by 30bp on both the 3' and 5' ends.

Subsequently, we performed pairwise expression level comparisons using *edgeR*[5]. We performed four pairwise comparisons. First, we compared the different levels of NO_3^- application (low and high NO_3^-) for both genotype (Wild-type and mutant) separately to each other. Further, the expression of both genotypes was compared on low and high NO_3^- levels, respectively. Differentially expressed genes (DEGs) were selected based on the following criteria – an average normalized expression in all six samples of more than 10; an adjusted *P*-value below 0.05 (FDR); and a Log_2Fold change of bigger 2 or smaller -2. We considered genes as expressed when on average more than two normalized reads across all three replicates were recognized.

The gene names of these significantly different genes were used in an enrichment analysis. Therefore, gene names were converted to version 1.2 and used to run a gene ontology enrichment in the ShinyGO[6] enrichment tool with default settings to determine biological process variations (v0.75).

References:

1. Martin, M. Cutadapt removes adapter sequences from high-throughput sequencing reads. EMBnet.journal 17, 10–12 (2011).
2. Li, H. & Durbin, R. Fast and accurate short read alignment with Burrows-Wheeler transform. Bioinformatics 25, 1754–1760 (2009).
3. Zhu, T. et al. Optical maps refine the bread wheat *Triticum aestivum* cv. Chinese Spring genome assembly. Plant J. 107, 303–314 (2021).
4. Liao, Y., Smyth, G. K. & Shi, W. The R package Rsubread is easier, faster, cheaper and better for alignment and quantification of RNA sequencing reads. Nucleic Acids Res. 47, (2019).
5. Robinson, M. D., McCarthy, D. J. & Smyth, G. K. edgeR: A Bioconductor package for differential expression analysis of digital gene expression data. Bioinformatics 26, 139–140 (2009).
6. Ge, S. X., Jung, D., Jung, D. & Yao, R. ShinyGO: a graphical gene-set enrichment tool for animals and plants. Bioinformatics 36, 2628–2629 (2020).

Acknowledgements

Almighty ALLAH had been so helpful in his blessings to give me this opportunity to successfully complete this PhD dissertation.

First of all, I would like to sincerely thank and gratitude to Prof. Dr. Jens Léon for providing me a great opportunity to work under his close supervision, as well as guiding me throughout the PhD tenure and exchanging scientific knowledge. I am grateful to him for his high level of trust, inspiration and professional support.

I am extremely grateful to my supervisor Dr. Agim Ballvora for allowing me to work in a nice project and delivering invaluable guidance and suggestions throughout this research. I have highly inspired for his vision, sincerity and motivational supervision. I would also like to sincerely thank to Prof. Dr. Frank Hochholdinger for serving as my co-supervisor. My sincere thanks also goes to Dr. Thomas Gaiser for accepting my request to be in the committee. I also would like to thank Prof. Dr. Florian M. W. Grundler for his support as the chairman of my PhD committee.

My sincere thank also goes to Prof. Dr. Annaliese Mason for providing me laboratory facilities. I am thankful to Prof. Dr. Ali A. Naz for his contribution by providing nice ideas, discussion and encouragements. Further, I am thankful to Prof. Dr. M. Afzal Hossain and Prof. Dr. Tofazzal Islam for their continuous inspiration and mental support.

I would like to express thank to my former and present lab mates: Dr. Said Dadshani, Dr. Bobby Mathew, Dr. Benedict Oyiga, Dr. Patrice Koua, Bahman Sadeqi, Dr. Michael Schneider, Dr. Diana Delgado, Dr. Hasina Begum, Md Kamruzzaman (Newton), Dr. Asis Shrestha, Dr. Salma Benaouda, Andreas Honecker, Carolyn Mukiri Kambona and Maisa Mohammed, for fruitful help during experiments and academic discussions. I am also giving thanks to my master and internship students; Tesfaye, Mele, Abebaw, Marissa, Mahmuda, Melisa, Walid, Suzan and Kailash for their enormous experimental supports.

Thanks are also extended to Karin Woitol, Anne Reinders, Martina Ruland and Karola Müller for their wonderful technical and administrative support. I also like to thank Karin Woitol and Jan Schoenenbach for editing thesis and translating the abstract. I would like to extend thank to the colleagues Campus Klein-Altendorf and Poppelsdorf greenhouse of Bonn University for their technical support.

I am highly grateful to the German Academic Exchange Service (DAAD) for providing me financial support (Personal ref. no. 91690550) to conduct my PhD smoothly and successfully.

I am also grateful to my home university Bangabandhu Sheikh Mujibur Rahman Agricultural University for granting study leave with necessary support.

Finally, endless thanks to my lovely sons Ayman and Ahnaf Siddiqui and sweet wife Mahmuda Akter for their hearty love, continuous support and great sacrifice. They were my courage to achieve this milestone achievements. I am forever indebted to my beloved mother, brothers and sisters for their love, blessings and support. My sincere gratitude to all of my friends, colleagues and well-wishers due to their supports and inspirations.

Peer-reviewed publications related to this thesis

Siddiqui, M. N., Léon, J., Naz, A. A., & Ballvora, A. (2021). Genetics and genomics of root system variation in adaptation to drought stress in cereal crops. ***Journal of Experimental Botany***, *72*(4), 1007-1019. DOI: 10.1093/jxb/eraa487

Siddiqui, M.N., Melesech, T. G., Abebaw, A.M., Tesfaye, J.T., Dadshani, S., Léon, J., & Ballvora, A. (2022). Genetic dissection of root architectural plasticity underlying candidate genes for adaptation to drought in bread wheat. ***Planta*** (Under revision).

Siddiqui, M.N., Pandey, K., Bhadhury, S.K., Sadeqi, B., Schneider, M., Stich, B., Léon, J., & Ballvora, A. (2022). *NPF2.12*, a convergently selected nitrate transporter that coordinates root growth and nitrate-use efficiency in wheat and barley. ***New Phytologist*** (Under revision).

Publications unrelated to this thesis

Siddiqui, M.N., Tesfaye, J.T., Abebaw, A.M., Melesech, T. G., Koua, P., Léon, J., & Ballvora, A. (2021). New drought-adaptive loci underlying candidate genes on wheat chromosome 4B with improved photosynthesis and yield responses. ***Physiologia Plantarum,*** 173 (4): 2166-2180. DOI: 10.1111/ppl.13566

Siddiqui, M.N., Schneider, M., Barbosa, M., Léon, J., & Ballvora, A. (2022). Long-term natural selection under conventional and organic cropping systems affect root architecture in spring barley. ***Scientific Reports*** (Under revision).

Kamruzzaman, M., Shrestha, A., **Siddiqui, M.N.**, Oyiga, B.C., Ballvora, A., Léon, J., Naz, A.A. 2022. Genetic mapping of candidate loci for drought-induced proline accumulation in bread wheat (*Triticum aestivum*). ***Plant Breeding*** (Under review).

Rsslan, M.A., **Siddiqui, M.N.,** Oyiga, B.C., Léon, J., & Ballvora, A. (2022). Uncovering QTL and their candidate operating genes related to salt tolerance in wheat (Under internal review).

Koua, A.P., **Siddiqui, M.N.,** Heß, K., Klag, N., Duarte-Delgado, D., Oyiga, B.C., Léon, J., & Ballvora, A. (2022). Genome-wide association study and *in silico* transcript abundance analysis identify candidate gene for drought tolerance and nitrogen-use efficiency in winter wheat (Under internal review).

Kamruzzaman, M., Beyene, M.A., **Siddiqui, M.N.**, Ballvora, A., Naz, A.A. 2022. Genetic dissection of genomic regions underlying proline and hydrogen peroxide variations among bread wheat cultivars under field condition (Under internal review).

Siddiqui, M.N., Léon, J., & Ballvora, A. (2022). Comparative genome-wide scan reveals root architectural and anatomical adaptation towards drought in wheat and barley (Under preparation).

Conference participation

Siddiqui, M.N., Léon, J., & Ballvora, A. (2022). A syntenic loci underpin nitrate transport and root system architecture in wheat and barley. German Plant Breeding Society (GPZ) main conference on September 12-14, 2022 in Düsseldorf, Germany (*Poster an*d *Oral Presentation*).

Siddiqui, M.N., Léon, J., & Ballvora, A. (2022). Nitrate-dependent dynamics of root system architecture: Uncovering its molecular regulators in winter wheat. 3rd international conference on "Climate Smart Agriculture: The Way towards Ecosystem Restoration" March 15-16, 2022 organized by University of Agriculture Multan, Punjab, Pakistan (*Oral Presentation*).

Siddiqui, M.N., Léon, J., & Ballvora, A. (2022). A syntenic loci tunes nitrate transport by regulating root system architecture between wheat and barley. International Conference on Sustainable Agriculture through Nuclear and Frontier Research, January 19-21, 2022 in Bangladesh Institute of Nuclear Agriculture (BINA), Bangladesh (*Oral Presentation*).

Siddiqui, M.N., Léon, J., & Ballvora, A. (2021). Natural variation in the promoter of *NPF2.12* is associated with nitrate-use efficiency and grain yield in wheat by tailoring root growth and development. 11th Symposium of the International Society of Root Research, May 24-28, 2021. University of Missouri, USA (*Poster Presentation*).